Polymers for Advanced Laundry Applications

Saskia Jane Boardman

Submitted in accordance of the requirements for the degree

of Doctor of Philosophy

The University of Leeds, School of Chemistry

July 2019

The candidate confirms that the work submitted is her own, except where work which has formed part of jointly authored publications has been included. The contribution of the candidate and the other authors to this work has been explicitly indicated below. The candidate confirms that the appropriate credit has been given within the thesis where reference has been made to the work of others.

In Chapter 4, Dr David Green performed the reported optical microscopy studies, in collaboration with Saskia Boardman. Additionally, in this chapter, Rajan Lad performed the UV-Visible spectroscopy studies of FITC-albumin loading and release. In Chapter 6, Jasmine Greenhalgh carried out the synthesis of two polymers reported. All polymer characterisation and analysis were carried out by Saskia Boardman. Also in Chapter 6, Algy Kazlauciunas performed scanning electron microscopy to obtain the images of the fabric samples.

Acknowledgements

There have been a number of people who have helped in the completion of this work, who I want to acknowledge and thank.

First and foremost, I wish to thank my supervisor Dr Paul Thornton for his advice and guidance over the course of my PhD. His support and expertise have been unrivalled, and I have no doubt I would not have completed a PhD without his supervision.

I also want to thank Dr Adam Hayward at Procter and Gamble for his advice and enthusiastic support over the years and Yvonne McMeekin for her help with the undertaking of consumer testing at the Newcastle Innovation Centre. I wish to thank Procter and Gamble and the EPSRC for funding this research.

I have had the help and friendship of many people who I have worked alongside in the lab, namely Dr Ana Garrote-Cañas, Dr Ellana Beard, Jason Rowley, Huayang Yu, David Martin, Simran Channa and Dr Andrew Booth. Additionally, two MChem students, Rajan Lad and Jasmine Greenhalgh, assisted in practical work in Chapters 4 and 6, respectively. I also wish to thank Dr David Green, for sharing his expertise in microscopy.

Finally, on a personal note I wish to thank my family, particularly my mum and dad, for their support and encouragement in the completion of all my studies which got me to this point.

Abstract

Dye transfer in the laundry occurs whereby dye molecules are removed from darker garments and deposit onto lighter garments. This results in greying and discolouration of the lighter coloured garments, shortening the lifespan of the clothing, or resulting in the need to separate washes into 'light' and 'dark' laundry loads. Therefore, dye transfer inhibitors are added to laundry detergent formulations to prevent dye transfer and preserve the appearance of consumer garments.

This thesis explores a variety of means to combat dye transfer, including biopolymeric particles and synthetic polymers which act in a variety of ways to preserve garment appearance. Firstly, biopolymeric hydrogels were investigated for their ability to adsorb dyes from aqueous solution. Chitosan hydrogels were found to be particularly effective, owing to the presence of free primary amine groups which may electrostatically attract anionic dye molecules. Therefore, microsphere biopolymer particles were explored for their ability to encapsulate dye molecules in simulated laundry wash loads to prevent dye transfer. It was found that dye transfer was reduced in the presence of anionic particles, suggesting the particles deposit onto the fabric and repel dye deposition.

Polymers which were designed to interact with the fabric and repel dye deposition were then researched, and methoxy-poly(ethylene glycol)-co-polyesters were found to be effective at preventing the deposition of indigo dye, alongside methoxy-poly(ethylene glycol)-co-poly(amino acid)s. Polymers based on γ-benzyl-L-glutamate were found to be most effective at preventing the deposition of indigo. The synthetic polymers therefore provide a large amount of scope for future detergent applications of dye transfer inhibition polymeric agents.

Table of Contents

List of Figures

List of Tables

List of Equations

Abbreviations

APC – Advanced Polymer Chromatography

BLGA - γ-benzyl-L-glutamic acid

CIE – Commission Internationale de l'Eclairage

cm - centimetre

CV - Crystal Violet

DB3 - C.I. Disperse Blue 3

DB22 - C.I. Direct Black 22

DLS - Dynamic Light Scattering

dm - decimetres

DMF - *N,N'*-Dimethyl formamide

DMSO - Dimethyl sulfoxide

DMT - Dimethyl terephthalate

DO3 - C.I. Disperse Orange 3

DO39 - C.I. Direct Orange 39

DTI - Dye Transfer Inhibitor/Inhibition

EDC - *N*-(3-diemethylaminopropyl)-*N'*-ethylcarbodiimide

FITC - Fluorescein isothiocyanate

FTIR - Fourier Transformed Infrared

g - grams

G' - Storage modulus

G'' - Loss modulus

Glu - Glutamic acid

GTAC - Glycidyl trimethylammonium chloride

kDa - kilo Daltons

Lys -Lysine

MB- Methylene Blue

mg - milligrams

min - minutes

mL - millilitres

mol - moles

MWCO - Molecular weight cut off

mV - milli volts

NCA - *N*-Carboxyanhydride

nm - nanometres

NMR - Nuclear Magnetic Resonance

Pa - Pascals

PDI - Polydispersity Index

PEG - Poly(ethylene glycol)

PET - Poly(ethylene terephthalate)

Phe – Phenylalanine

PPG- Poly(propylene glycol)

PVP - Poly(vinylpyrrolidone)

PVP-NO - Poly(vinylpyridine-*N*-oxide)

rad - radians

RB5 - C.I. Reactive Black 5

RB7 - C.I. Reactive Brown 7

ROP - Ring Opening Polymerisation

rpm - revolutions per minute

RR141 - C.I. Reactive Red 141

SB1 - C.I Sulfur Black 1

SDS – Sodium dodecyl sulfate

SRDW - Synthetic reactive dye wastewater

TEM- Transmission Electron Microscopy

THF - Tetrahydrofuran

TPP - Tripolyphosphate

UV-Vis - Ultraviolet-Visible spectroscopy

Z-Lys - *N*-ε-carboxybenzyl-L-lysine

µL - microlitres

ΔE - Colour change

Chapter 1. Introduction

1.1 Dye Transfer

Dye transfer occurs in the laundry process, whereby a 'fugitive' dye molecule detaches from one fabric and deposits on another garment.[1,2] This leads to the greying and discolouration of lighter garments. Dye bleeding is caused by a number of factors, including the pH of the aqueous medium, fabric agitation, washing time and temperature.[3] This problem is particularly noticeable for the non-reactive classes of dyes, which are non-covalently bound to the garment, that are used to colour fabrics such as cotton. These classes include direct, sulfur and vat dyes, which alongside reactive dyes account for 85% of the dyes that are used to colour cotton fabrics.[4,5] In addition, fibrillation of cellulosic fibres can occur, whereby mechanical damage is caused to the fibre that results in coloured fibrils detaching and depositing onto another garment, causing colour change.[6]

1.2 Fibre Types

Six of the main commercial fibre types used in modern clothing are: regenerated celluloses, cotton, nylon, polyester, acrylic and wool. These fibres will be investigated in this thesis, owing to their popularity.[7,8] The wide variety of fibre types and blends, together with their varied properties, provide a complex challenge to preventing dye transfer in the laundering process.

1.2.1 Cellulosic Fibres

Fibres such as acetate, modal, viscose and lyocell are regenerated cellulosic fibres.[9,10] These are differentiated by how cellulose pulp is processed to create the polysaccharidic fibre (Figure 1-1).[7,11] Cotton and linen, however, are naturally occurring cellulosic fibres, grown by plants with no chemical modification. Due to their high hydroxy content and irregular fibre structure, cellulosic

fibres are hydrophilic, and therefore absorb relatively large amounts of water.[12,13] By assessing the dye transfer onto regenerated cellulose and cotton, it is possible to predict the affinity of this class of fibres for dye deposition.

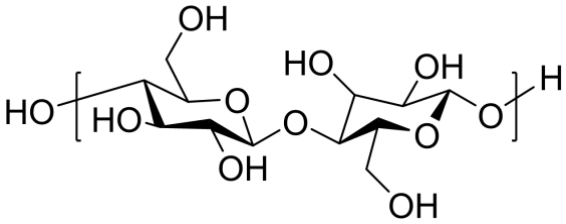

Figure 1-1. Structure of cellulose repeat unit.

1.2.2 Nylon

Nylons are a family of polyamides, whereby nylon-6,6 and nylon-6 are the two most commonly used fibres for garments, however many other varieties are available.[7,14] Nylon-6,6 and nylon-6 are aliphatic polyamides containing six carbon atoms in their respective monomers. There are two main routes to produce nylon fibres: through a polycondensation reaction between adipic acid, a six carbon dicarboxylic acid, and hexamethylene diamine to produce nylon-6,6 or; *via* ring opening of ε-caprolactam to produce nylon-6 (Figure 1-2).[15,16]

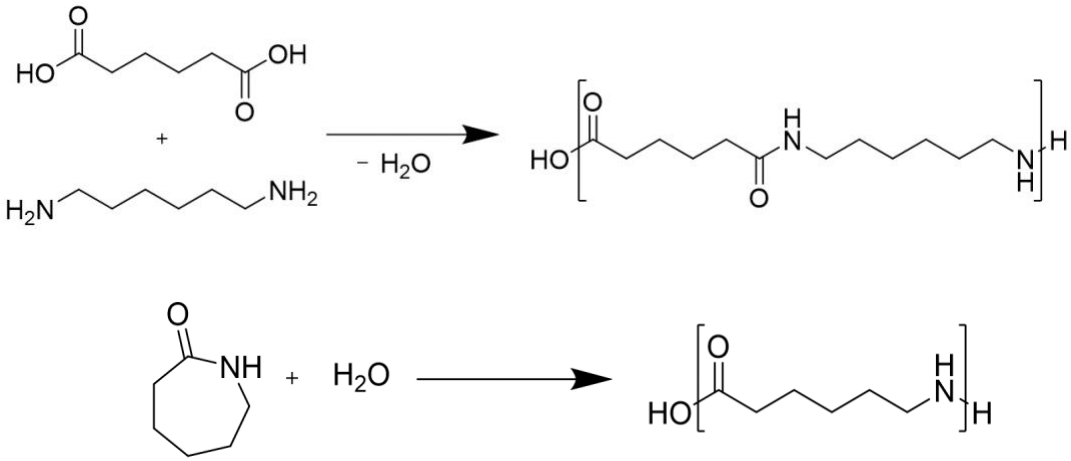

Figure 1-2 Top: Reaction of adipic acid with hexamethylene diamine to produce nylon-6,6. Bottom: Ring opening of ε-caprolactam to produce nylon-6.

Due to the amide groups generated in the polymerisations, both nylon-6 and nylon-6,6 contain hydrogen bond donors and acceptors. Due to the synthetic nature of the fibres, the polymers are

more crystalline than those of natural origin, and therefore have fewer sites available for the association of water, resulting in an hydrophobic fibre.[13] Nylon therefore may interact with dye molecules through either hydrogen bonding or through hydrophobic interactions.[17]

1.2.3 Polyester

Polyester fabric is formed from a synthetic, hydrophobic fibre of poly(ethylene terephthalate).[18,19] It is produced by the condensation of terephthalic acid or dimethyl terephthalate with ethylene glycol to produce an aromatic polymer (Figure 1-3).

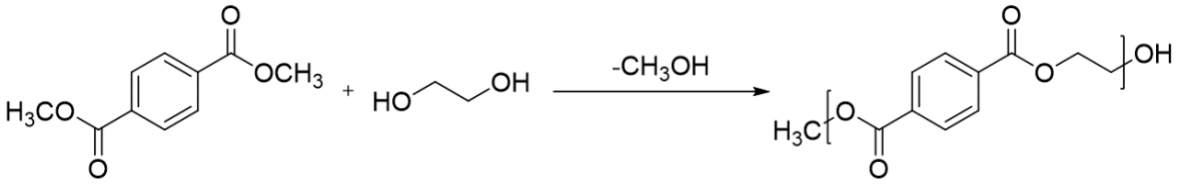

Figure 1-3 Condensation reaction between dimethyl terephthalate and ethylene glycol to produce PET.

Polyester-dye interactions may occur due to hydrogen bonding *via* the ester bond, π-π interactions due to the aromatic groups presented by the polymer, and hydrophobic interactions.

1.2.4 Acrylic

Acrylic fabrics are synthetic fibres composed of at least 85% acrylonitrile monomer (Figure 1-4), below this the fabric is termed 'modacrylic'.[20,21] The difference between the various types of acrylic fibres is due to the presence of a variety of comonomers such as vinylidene chloride, methyl acrylate, vinyl acetate, styrene, and methyl methacrylate, or the inclusion of grafted poly(vinyl pyrrolidone).[22] The inclusion of the various other monomer units causes significant variations in properties of the modacrylic class of fibres, therefore only acrylic fibres will be investigated in these studies.

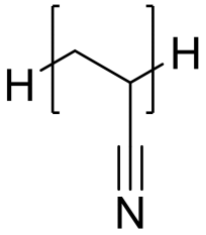

Figure 1-4 Repeat unit of polyacrylonitrile.

Polyacrylonitrile forms a *pseudo*-crystalline structure within the fibre, thereby meaning the fabric is less hydrophobic than other synthetic fibres as it is a less rigidly structured polymer than nylon and polyester, and so has a reduced degree of packing of polymer chains.[7] Additionally, the nitrile group provides the capability for a charged dye to interact *via* ion-dipole interactions.

1.2.5 Wool

Wool is formed from a naturally occurring protein, keratin, which is woven to produce wool fabrics. Wool is an hydrophilic fibre, able to absorb up to 200% its dry weight in water.[17] As it is a protein based fibre, the primary structure of wool contains a variety of amino acid residues, which have varying R groups, such as methyl groups in the amino acid alanine, acid groups in glutamic acid or amine groups in lysine (Figure 1-5). These R groups enable the keratin to form secondary and tertiary structures, and also provide binding sites for external species such as dyes or detergent additives.[23]

Wool provides a particularly complex problem for dye transfer, owing to its complex chemical composition and the rough, scaly structure of the fibre itself.

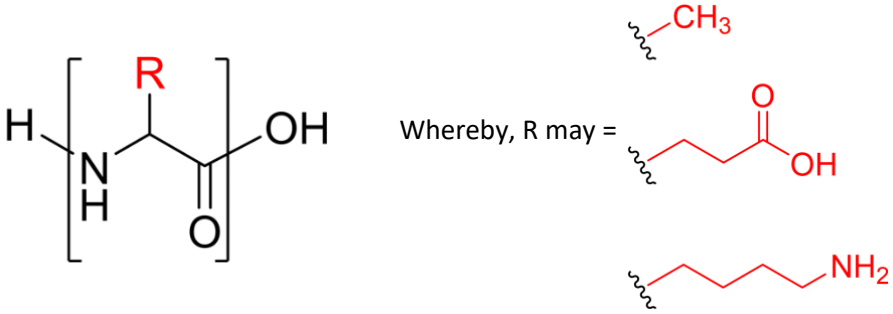

Figure 1-5 Generic structure of a polypeptide which can have various functional groups at the 'R' position (red) and the R groups of alanine, glutamic acid and lysine respectively.

Silk fibres are also naturally occurring protein fibres, however these fabrics are commonly dry cleaned, and therefore dye transfer onto silks in the wash is a less common issue.[13] Consequently, this fabric will not be investigated as part of this research.

1.3 Common Dye Classes

1.3.1 Direct Dyes

Direct dyes are anionic and commonly water-soluble.[24] They are considered to be easy to use, cost effective and provide a good colour range for cotton fabrics.[25,26] The dyeing of cotton with direct dyes occurs in two steps: adsorption of the dye to the surface of the fibre, followed by dye penetration into the fibre by diffusion. Because direct dyes are water-soluble and possess good substantivity for the cotton fibres, diffusion of the dye into the fibre often occurs rapidly.[27] This may result in a patchy, unlevel, dyed fabric. In order to control the levelness of the dyeing, a lower temperature may be used in the first instance to ensure that adsorption of the dye to the fibre occurs. Increasing the temperature and the pH then allows controlled dye diffusion into the fibre.[24] A high pH will reduce the charge barrier between anionic dyes and a fabric surface populated with hydroxy groups, such as cellulose. Additionally, auxillaries may be used in the dyeing process to reduce the diffusion rate, such as surfactants that encapsulate or complex the dye, allowing time for an evenly dyed effect to develop.[28]

Since cotton contains hydroxy groups which can deprotonate in water, anion-anion repulsion may occur between the dye and the cotton.[29] Because the dye is not fixed to the fibre by a covalent bond and experiences ionic repulsions, which can be interrupted by surfactants, direct dyes can give poor wash fastness.[30,31] The wash fastness may be improved with pre- or post-treatment of the cotton either to create cationic groups at the surface, reducing the ionic repulsion, or to fix the dye to the fibre.[29,32] However, this procedure is energy consuming, which alongside the environmental impact

of the use of auxiliaries and electrolytes, and the poor wash fastness of direct dyes, nullifies the benefits of low cost direct dyes. Therefore, attention has moved to other classes of dye for cotton dyeing.

1.3.2 Disperse Dyes

Disperse dyes are used to dye polyester, acrylic and nylon fabrics *via* a two-step process whereby the fabric is added to a dye bath at 140 °C, and then the excess dye is removed by the action of a reducing agent.[33] Disperse dyes are used for dyeing hydrophobic fabrics, such as polyester, and as such are non-ionic and aromatic in nature. The dye molecules therefore lack solubilising groups, and are typically smaller than other dye classes.[34] Due to this, auxiliary dispersion agents in the dye bath are required to enable the dissolution of the dyes at high temperatures, which then allows the adsorption of the dye onto the fibre surface, before finally becoming incorporated into the fibre structure.[35] The need to remove residual, unbound dye from the dye bath results in the potential for coloured, polluted effluents from the dye houses, as well as for surface residual dye to remain on the fabric and thus cause colour change on laundering of the finished garment with other clothes.[36]

1.3.3 Sulfur Dyes

Sulfur dyes possess superior wash fastness compared to direct dyes and have excellent colour properties for darker hues. For example C.I. Sulfur Black 1 (SB1) is the most widely used black dye for cotton.[37,38] However, the structures of commercial sulfur dyes are relatively unknown as the dye is brought about by addition of disulfur and sodium sulfide to nitro-substituted phenols to create sulfur linkages between the chromophores.[4,37] Therefore, the dye can have a varying extended

structure owing to different disulfide linkage positions and amounts.[38] For example, SB1 is formed from 2,4-dinitrophenol (Figure 1-6).[39]

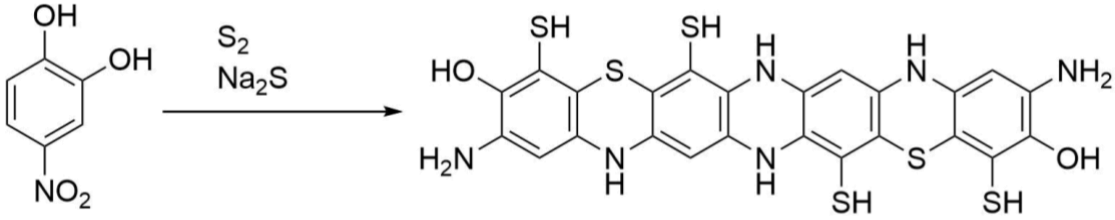

Figure 1-6 Conversion of 2,4-dinitrophenol into a proposed structure for C.I. Sulfur Black 1.

In dyeing cotton, sulfur dyes are reduced by cleavage of the disulfide bonds, using sodium sulfide as the reducing agent, to produce the water-soluble, *leuco* form of the dye, which can diffuse into the cotton fibre.[29,37,38] The dye is then oxidised to its water-insoluble, parent form and becomes trapped within the cotton fibre, giving the colour moderate wash fastness.[29,40] Thus the dye is mechanically entrapped within the fibre due to its insolubility in aqueous media.[27] However, the disulfide bonds render sulfur dye vulnerable to hydrolysis, resulting in colour fading with ageing and laundering of the garment.[37,40,41]

In a similar manner to direct dyes, sulfur dyes added to cellulosic fibres can undergo after-treatment using cationic fixing agents to improve wash fastness.[42] However, there are environmental concerns about the use of fixing agents and electrolytes, as well as unease surrounding the use of sodium sulfide as a reducing agent, since toxic hydrogen sulfide may be released.[6,38] Additionally, any dye left unoxidised is anionic and therefore more readily soluble in water, resulting in greater chance of colour change in the laundry upon liberation from the fabric.[31] The processing history of the fabric is a key issue in dye transfer, but is relatively unknown by clothing manufacturers.

1.3.4 Vat Dyes

Vat dyes are largely water-insoluble and, in a similar manner to sulfur dyes, must be reduced to their soluble *leuco* form using sodium dithionite, in order to penetrate cotton fibres.[43,44] The dye is then

oxidised, reforming the parent structure within the fibre. Vat dyes can be further reduced to their acid *leuco* form, which may be used for dyeing polyamide fibres, including nylon. The dyeing procedure of acid-*leuco* vat dyes combines the redox chemistry of vat dyeing, with the adsorptive characteristics of direct dyeing.[45] This indicates the applicability of vat dyes to many kinds of textile production. However, the large amount of sodium dithionite required to exhaust the dye onto the fibre raises serious environmental concern.

Vat dyes are more expensive than sulfur dyes, and have limited brightness and range of colours available.[4] However, they show improved light and wash fastness relative to sulfur and direct dyes.[4,43] Because of this, vat dyes are one of the more important classes of dyes in the textile industry; although their use declined with the advent of reactive dyes there is renewed interest in natural dyes such as indigo.[46,47] Indigo is one of the more commonly known and used vat dyes (Figure 1-7), used for dyeing denim fibres.

a 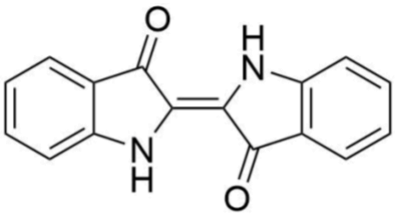 b 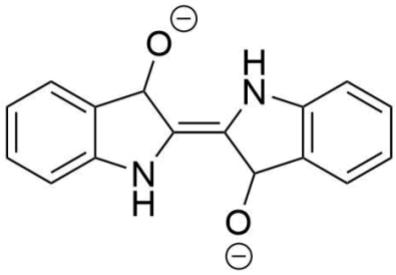

Figure 1-7 a). Structure of indigo and b). Structure of its alkali leuco form.

1.3.5 Reactive Dyes

Reactive dyes are anionic, water-soluble dyes that are unique to the other classes of dye because they are designed to covalently bind to cellulosic fibres. [48,49] This results in apparent good to excellent wash fastness, alongside other favourable properties such as ease of application and bright colour options.[4,50] As such, they have become widely used in the dyeing industry over the past two decades and are a popular class of dye.[51] There are a variety of types of reactive dyes, the most

common using a vinyl sulfone group to react with the hydroxy groups on cotton (Figure 1-8), as well as chlorotriazine reactive dyes.[52]

Since both the dye and the cellulosic fibre are anionic in the aqueous dye bath, large amounts of salts, such as sodium chloride, are used in the dyeing process to promote dyeing of the fibre.[53] Additionally, due to their reactivity towards hydroxy nucleophiles, reactive dyes are prone to hydrolysis in the dye bath, whereby the reactive terminus of the dye reacts with free hydroxy anions of deprotonated water, removing the reactivity of the dye irreversibly.[53] This can lead to highly coloured and often toxic effluent that cannot be used further for dyeing, combined with high concentrations of salt and other auxiliaries.[54] Alongside this, the fabric dyed may have unreacted or hydrolysed dye associated with it that is not covalently bound, which may lead to dye transfer problems on laundering.[54]

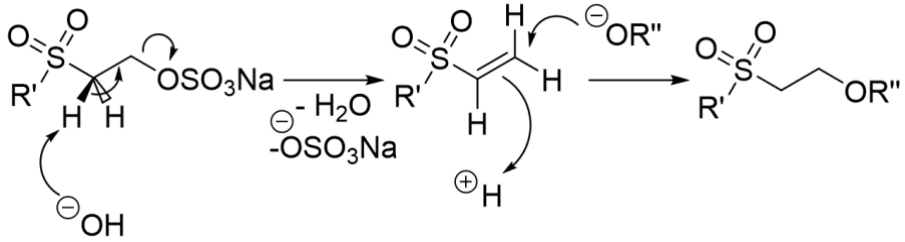

Figure 1-8 Covalent binding of a vinyl sulfone reactive dye to a hydroxy nucleophile.

The R' group shown in Figure 1-8 relates to the relevant chromophore for the desired dye, while R'' may be any hydroxy containing molecule such as cellulose, but also may be a hydroxy anion, resulting in the hydrolysis of the dye.

1.3.6 Acid Dyes

Acid dyes are used primarily for the dyeing of naturally occurring protein fibres such as wool and silk.[55] The dye molecules are water-soluble and contain carboxylate or sulfonate groups to create ionic bonds with the fibre, however this requires an acidic dye bath to protonate amine groups present in the fibre, in order to allow the ion-ion interaction.[56] Due to the reliance on weak

electrostatic interactions to dye the fibres, acid dyes have poor wash fastness. This may be improved by post treatment of the fibres with tannic acid which complexes with the protein fibre.[57]

1.3.7 Basic Dyes

Basic dyes are water-soluble, cationic dyes with affinity to cellulosic fibres such as cotton or paper, as well as wool, acrylic, nylon and polyeter.[58,59] Analogously to acid dyes, the fibre must be deprotonated to produce an anion capable of electrostatically interacting with the dye molecule, which contains amine groups that may be protonated, or cationic groups such as quaternary amines.[60] Due to the reliance on weak electrostatic interactions which do not penetrate the fibre surface, the dye molecules are gradually removed through subsequent washings and therefore exhibit poor wash fastness.[59]

1.4 Measuring Dye Transfer

The extent of dye transfer can be quantitatively analysed by colourimetry with a spectrophotometer using the Commission Internationale de l'Eclairage (CIE) L*a*b* system, based upon additive colour mixing of red, green and blue hues.[61] The CIE LAB three-dimensional colour space is able to provide coordinates for the measured colour, along the lightness axis (L*), the green to red axis (a*) and the blue to yellow axis (b*), whereby the lightness axis goes from dark to light (0 to 100). A schematic diagram of the three-dimensional axes is shown in Figure 1-9. This allows the determination of the CIE L*a*b* values for the colour of the garment, before and after washing.

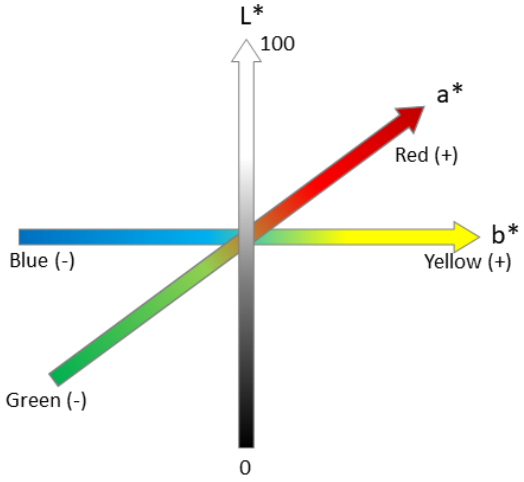

Figure 1-9 Schematic showing the CIE LAB axes.

The CIE LAB colour space is perceptibly uniform, whereby the perceptual difference to the human eye between two colour coordinates is related to a measure of Euclidean distance.[62,63] These coordinate points can then be compared before and after washing, and the change in colour (ΔE) can be calculated (Equation 1).[64]

Equation 1 Determination of ΔE using CIELAB 1976.

$$\Delta E = \sqrt{(\Delta L^*)^2 + (\Delta a^*)^2 + (\Delta b^*)^2}$$

1.5 Dye Transfer Inhibitors

Dye transfer inhibitors (DTIs) are added to laundry detergent formulations to prevent discolouration of lighter garments due to the transfer of fugitive dyes from darker coloured garments. There are three reported mechanisms of DTI action: degradation or adsorption of the dye once it is in the laundry liquor; prevention of the release of the dye from the donor fabric, and; prevention of the fugitive dye in the laundry liquor from depositing onto the fabric, *via* a blocking mechanism.[1,65]

1.5.1 Bleaching Agents as Dye Transfer Inhibitors

Bleaching and degradation of the fugitive dye allows for the decolouration of the wash liquor, and therefore preventing colour change caused by dye transfer. Since the rate of bleaching is significantly higher than the rate of dye adsorption by the acceptor fabrics, there is no risk of the dye depositing onto the fabric before it has been decoloured.[66] Hazenkamp *et al.* investigated three different manganese-salen oxidative catalysts (Figure 1-10) for the decolourisation of C.I. Reactive Black 5 (RB5) in aqueous solution to simulate a wash liquor.

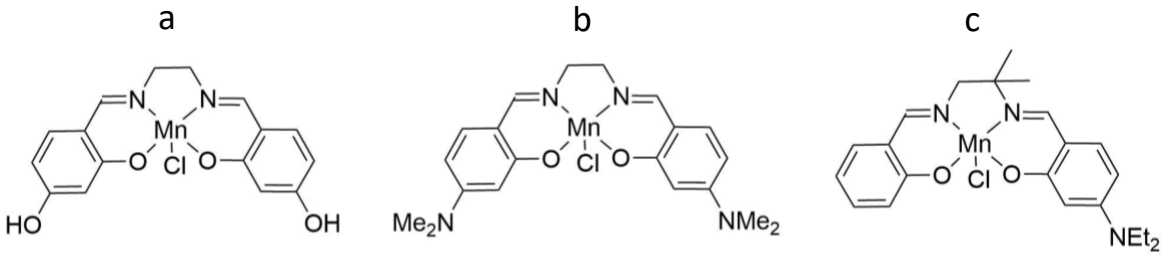

Figure 1-10 Structure of three manganese-salen complexes investigated for bleaching of laundry wash liquor.

Commonly, the use of a bleaching agent in a detergent causes the dye on the fabric to fade as well as damaging the fibres.[65,66] Additionally, the oxidising agent can interfere with the additional laundry detergent components, and are subject to degradation over the period of the wash.[67] Hazenkamp *et al.* found that of the three catalysts, **b** and **c** did cause garment fading, however, **a** was able to decolour the wash liquor without significantly affecting the colour of the garment.[66] Catalyst **a** is shown to have a slower rate of bleaching to the other two catalysts, at $2x10^{-3}$ s^{-1}, in comparison to $9x10^{-3}$ and $13x10^{-3}$ s^{-1} for catalysts **b** and **c** respectively, which may explain the reduced garment fading of catalyst **a**. However, this rate is sufficient to compete with the rate of dye adsorption onto the receiver fabric, and shows the fine-tuned balance between the rate of bleaching and the rate of dye adsorption that is required for bleaching-type DTIs to be effective. The authors do not provide

an explanation as to why one catalyst is more active than another, but the paper finds that the activity and stability are not mutually exclusive, and as such a finely-tuned catalyst can be produced.

While this is an encouraging result for DTI bleaching agents, the study only investigates RB5. This is therefore not representative of a wash load as a whole, and would require further investigation to observe the effects on other types of dyes. Additionally, the authors found that the activity of the catalyst reduced over the period of the wash, set at 30 minutes. Since many washes on a conventional UK washing machine are in excess of one hour, this is not a sufficiently long activity for the catalyst to act.

1.5.2 Dye Binding Dye Transfer Inhibitors

In order to prevent damage to the fibres of the garment, and to eliminate the reduced efficacy of a bleaching agent as the wash proceeds, polymers such as poly(vinyl pyrrolidone) (PVP) are commonly used to prevent dye transfer in the wash.[68,69,70] PVP complexes the dye molecules and prevents them from depositing onto the receiver fabric. However, DTIs that work by binding the dye in the wash liquor have also been found to remove the dye from the fabric, resulting in poorer wash fastness than is expected of the dye, and thus garment fading.[71]

Alternatively, the dye binding may occur on a physical substrate, typically a non-woven fabric swatch which can be incorporated into the laundry load and removed on completion of the wash, or may be a crosslinked PVP nanoparticle.[65,72,73] The swatch may contain polymeric dye adsorbants, such as PVP or chitosan, which attract the fugitive dye to the fabric and bind it.[67] However, this is inconvenient for the consumer as it results in the need to remove the swatch from the wash load once it is completed, and thus creates a waste product. Additionally, as the substrate cannot be uniformly mixed throughout the wash liquor, it cannot give a uniform DTI effect for the garments in

the wash. It therefore has reduced efficacy in comparison to a water-soluble DTI agent which can be dispersed evenly throughout the laundry liquor.

1.5.3 Dye Fixatives as Dye Transfer Inhibitors

The inclusion of a fixing agent in the detergent formulation, to prevent the dye from bleeding into the wash liquor, provides a method of reducing dye transfer without promoting dye loss. An example of this was reported by Clariant Produkte GmbH, whereby small molecule polyamines such as ethylenediamine, diethylenetriamine and triethylenetetramine were reacted with dicyandiamide and formaldehyde.[71] This creates a dicyandiamide-formaldehyde polymer, which are commonly used as flocculants as well as dye fixing agents (Figure 1-11).[74]

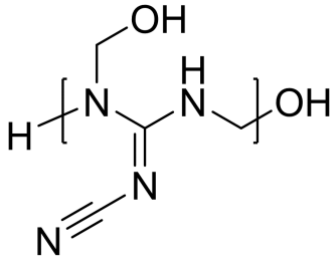

Figure 1-11 Generic structure of dicyandiamide-formaldehyde polymer.

The patent claims that the DTI molecules are also able to bind fugitive dye in the wash liquor, and thus prevent them from depositing onto receiver fabrics, giving the DTI molecule a secondary mode of action to further improve its efficacy. A white swatch of fabric was washed with a black swatch in the absence and presence of the DTI molecule. Without the DTI molecule, the ΔE was found to be 35.1. This value was reduced to 27.8 when the wash was conducted in the presence of the DTI, with a reduction in ΔE of 21%.

However, these DTI agents are for use in a detergent formulation that preferably includes a non-ionic surfactant, rather than an anionic surfactant.[71] This may be due to ion-ion interactions between the cationic DTI molecule and the anionic surfactant that would cause the DTI efficacy, as well as the surfactant cleansing efficacy, to be reduced. This is therefore not suitable for a

formulation which incorporates an anionic surfactant, such as those used in contemporary detergents formulations due to their superior cleaning properties.

Carbohydrates have been modified to contain cationic groups in order to protect the colour of the garments and prevent dye bleeding.[75,76] For example, imidazole modified cellulose was found to perform well for cotton dyed with three different direct dyes.[76] The reduced dye fading is attributed to the interaction of the carbohydrate with the fibre of the dyed garment, preventing the loss of the dye or pigment associated with the fibre.[75] These compounds are also able to reduce physical damage to the fibre caused by agitation in the wash, providing a secondary benefit.[77] However, this type of DTI additive is also not compatible with detergent formulations which contain anionic surfactants.[75]

1.5.4 Dye Blocking Type Dye Transfer Inhibitors

Henkel proposed water-soluble molecules and polymers that can interact with the fabric and block adsorption of the dye, without affecting the properties of the fabric after washing. An example of these DTIs are oligourea molecules.[78,79] These are formed by reacting a diisocyanate, such as toluene-2,4-diisocyanate, with a diamine, such as 2,4-diaminobenezenesulfonic acid, to produce an oligomer, capped by phenylisocyanate units (Figure 1-12).

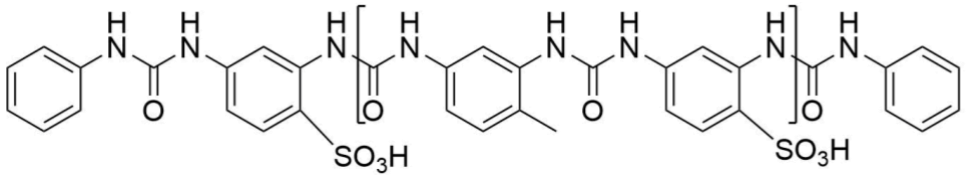

Figure 1-12 Structure of oligourea formed from the reaction of phenylisocyanate, 2,4-diaminobenezenesulfonic acid and toluene-2,4-diisocyanate.

The oligourea molecule was tested for its ability to prevent dye transfer onto a polyamide receiver fabric, against C.I. Acid Blue 113, C.I. Direct Orange 39 and C.I. Disperse Blue 79. The extent of staining was measured on a scale of one to five, one being the most stained, and five being the least stained.[79] It was found that in the absence of the oligourea compound, staining onto the polyamide fabric was found to be 1.8, 3.0 and 3.1 respectively for the three dyes. In the presence of the oligo(urea) however, the staining was reduced, giving staining values of 4.1, 4.6 and 4.1.[79] This shows a clear improvement in the dye transfer onto the polyamide fabric in the presence of these dyes. However, only three dyes in total, and no other receiver fabrics, were tested.

1.6 Summary, Aims and Objectives

It is clear that the wide variety of fabric types and dye classes creates a complex issue for preventing or reducing dye transfer in the laundering process of garments. The key properties of the fabrics discussed have been identified as hydrophilicity or hydrophobicity, and the chemical functionality of the fibres, which will be investigated for their effects in the prevention or promotion of dye transfer. A selection of dye classes has been identified and these will be assessed for their chemical properties. Comparisons will be drawn between these properties and the discolouration caused onto different fabric types. This will enable the essential features of a successful DTI to be elucidated and the DTI production and performance analysis to be conducted. Such a material must be compatible within a detergent formulation and effective against a variety of dye classes, for a variety of fibre types. A range of DTI polymer types will be investigated, and therefore each chapter in this thesis will examine the benefits of the polymer class, and the DTI mechanism it uses. Therefore, each chapter will individually explore the literature of the relevant DTI mechanism and polymer class and will then observe any DTI efficacy, and potential improvements, of the polymers examined.

1.7 References

[1] Uchiyama T., Kawauchi A. and DuVal D.L. Quick identification of polymeric dye transfer inhibitors in laundry detergents by pyrolysis-gas chromatography/mass spectrometry. *Journal of Analytical and Applied Pyrolysis*. 1998 **45** (2) 111–9

[2] Johnson K.A., Van Buskirk G. and Gillette S.M. Laundry article for preventing dye carry-over and indicator therefor. US005698476A. 1995

[3] Shih J.S., Srinivas B. and Hornby J.C. Water soluble dye complexing polymers. US5776879A. 1997

[4] Mohsin M., Rasheed A., Farooq A., Ashraf M. and Shah A. Environment friendly finishing of sulphur, vat, direct and reactive dyed cotton fabric. *Journal of Cleaner Production*. 2013 **53** 341–7

[5] Song Z., Mao J., Rohwer H. and Menge U. Laundry care products containing hydrophobically modified polymers as additives. EP2650353A2. 2003

[6] Soliman G., Carr C.M., Jones C.C. and Rigout M. Surface chemical analysis of the effect of extended laundering on C. I. sulphur black 1 dyed cotton fabric. *Dyes and Pigments*. 2013 **96** (1) 25–30

[7] Morton W.E. (William E., Hearle J.W.S. and Textile Institute (Manchester E. *Physical properties of textile fibres* (CRC Press)

[8] Anon. Society of Dyers and Colourists Enterprises Ltd ®.

[9] Wilkes A.G. and Bartholomew A.J. Cellulose fibre compositions. US6333108B1. 1995

[10] Colom X. and Carrillo F. Crystallinity changes in lyocell and viscose-type fibres by caustic treatment. *European Polymer Journal*. 2002 **38** (11) 2225–30

[11] Koh J., Soo Kim I., Soo Kim S., Sub Shim W., Pil Kim J., Yeop Kwak S., Wook Chun S. and Ku Kwon Y. Dyeing properties of novel regenerated cellulosic fibers. *Journal of Applied Polymer Science*. 2004 **91** (6) 3481–8

[12] Leppänen K., Andersson S., Torkkeli M., Knaapila M., Kotelnikova N. and Serimaa R. Structure of cellulose and microcrystalline cellulose from various wood species, cotton and flax studied by X-ray scattering. *Cellulose*. 2009 **16** (6) 999–1015

[13] Rowe C.D. and Rowe H.D. *Detergents, clothing and the consumer with sensitive skin* vol 30 (Blackwell Publishing Ltd Blackwell Publishing LtdOxford)

[14] Aelion R. Nylon 6 and Related Polymers. *Industrial & Engineering Chemistry*. 1961 **53** (10) 826–8

[15] Deng Y., Ma L. and Mao Y. Biological production of adipic acid from renewable substrates: Current and future methods. *Biochemical Engineering Journal*. 2016 **105** 16–26

[16] Arvanitoyannis I., Nakayama A., Kawasaki N. and Yamamoto N. Synthesis and properties of biodegradable copolyesteramides: Nylon 6,6/ϵ-caprolactone copolymers, 1. *Angewandte Makromolekulare Chemie*. 1994 **222** (1) 111–23

[17] Timár-Balázsy A. and Eastop D. *Chemical principles of textile conservation* (Butterworth-Heinemann)

[18] Deopura B.L. and Textile Institute (Manchester E. *Polyesters and polyamides* (Woodhead Pub. in association with the Textile Institute)

[19] Wróbel A.., Kryszewski M., Rakowski W., Okoniewski M. and Kubacki Z. Effect of plasma treatment on surface structure and properties of polyester fabric. *Polymer*. 1978 **19** (8) 908–12

[20] Matamá T., Carneiro F., Caparrós C., Gübitz G.M. and Cavaco-Paulo A. Using a nitrilase for the surface modification of acrylic fibres. *Biotechnology Journal*. 2007 **2** (3) 353–60

[21] Matamá T., Vaz F., Gübitz G.M. and Cavaco-Paulo A. The effect of additives and mechanical agitation in surface modification of acrylic fibres by cutinase and esterase. *Biotechnology Journal*. 2006 **1** (7–8) 842–9

[22] Causin V., Marega C., Schiavone S. and Marigo A. A quantitative differentiation method for acrylic fibers by infrared spectroscopy. *Forensic Science International*. 2005 **151** (2–3) 125–31

[23] Simpson W.S., Crawshaw G.H. and Textile Institute (Manchester E. *Wool : science and technology* (CRC Press)

[24] Chen K.-M., Lin L.-H., Wang C.F. and Hwang M.-C. Interactions between new multi-anionic surfactants and direct dyes and their effects on the dyeing of cotton fabrics. *Colloids and Surfaces A: Physicochemical and Engineering Aspects*. 2010 **356** (1–3) 46–50

[25] Burkinshaw S.. and Gotsopoulos A. Pretreatment of cotton to enhance its dyeability; Part 2. Direct dyes. *Dyes and Pigments*. 1999 **42** (2) 179–95

[26] Adeel S., Usman M., Haider W., Saeed M., Muneer M. and Ali M. Dyeing of gamma irradiated cotton using Direct Yellow 12 and Direct Yellow 27: improvement in colour strength and fastness properties. *Cellulose*. 2015 **22** (3) 2095–105

[27] Vickerstaff T. Reactive Dyes for Textiles. *Journal of the Society of Dyers and Colourists*. 2008 **73** (6) 237–45

[28] Eleftheriadis I.C., Pegiadou-Koemtzopoulou S.A. and Kehayoglou A.H. Colorimetric evaluation of the levelness of modified and unmodified cotton fabrics dyed with direct dyes with and without nonionic surfactants. *Journal of the Society of Dyers and Colourists*. 2008 **114** (4) 130–2

[29] Burkinshaw S.M. and Gotsopoulos A. The pre-treatment of cotton to enhance its dyeability—I. Sulphur dyes. *Dyes and Pigments*. 1996 **32** (4) 209–28

[30] Oakes J. Formulation of colour-care and heavy-duty detergents: A review. *Coloration Technology*. 2005

[31] Ghosh K. and Murch W.L. Method for treating laundry items. US20170159224A1. 2017

[32] Burkinshaw S.M. and Kumar N. Polyvinyl alcohol as an aftertreatment: Part 3 direct dyes on cotton. *Dyes and Pigments*. 2010 **85** (3) 124–32

[33] Szpyrkowicz L., Juzzolino C. and Kaul S.N. A Comparative study on oxidation of disperse dyes by electrochemical process, ozone, hypochlorite and fenton reagent. *Water Research*. 2001 **35** (9) 2129–36

[34] Chavan R.B. Environmentally friendly dyes. *Handbook of Textile and Industrial Dyeing*. 2011 515–61

[35] Carneiro P.A., Umbuzeiro G.A., Oliveira D.P. and Zanoni M.V.B. Assessment of water contamination caused by a mutagenic textile effluent/dyehouse effluent bearing disperse dyes. *Journal of Hazardous Materials*. 2010 **174** (1–3) 694–9

[36] Kim T.-H., Park C., Shin E.-B. and Kim S. *Decolorization of disperse and reactive dyes by continuous electrocoagulation process*

[37] Zhou W. and Yang Y. Improving the Resistance of Sulfur Dyes to Oxidation. *Industrial & Engineering Chemistry Research*. 2010 **49** (10) 4720–5

[38] Blackburn R.S. and Harvey A. Green chemistry methods in sulfur dyeing: application of various reducing D-sugars and analysis of the importance of optimum redox potential. *Environmental science & technology*. 2004 **38** (14) 4034–9

[39] Berenguer J., Domingo M.J. and Rocas J. Cationic dyes, their production and use. US5766269A. 1996

[40] Burkinshaw S.M. and Collins G.W. Aftertreatment to reduce the washdown of leuco sulphur dyes on cotton during repeated washing. *Journal of the Society of Dyers and Colourists*. 2008 **114** (5–6) 165–8

[41] Burkinshaw S.M. and Collins G.W. Aftertreatments to improve the wash fastness of sulphur dyeings on cotton. *Dyes and Pigments*. 1995 **29** (4) 323–44

[42] Burkinshaw S.M., Chaccour F.E. and Gotsopoulos A. The aftertreatment of sulphur dyes on cotton. *Dyes and Pigments*. 1997 **34** (3) 227–41

[43] Bhatti I.A., Adeel S. and Taj H. Application of Vat Green 1 dye on gamma ray treated cellulosic fabric. *Radiation Physics and Chemistry*. 2014 **102** 124–7

[44] Zhuo J. and Sun G. Antimicrobial Functions on Cellulose Materials Introduced by Anthraquinone Vat Dyes. *ACS Applied Materials & Interfaces*. 2013 **5** (21) 10830–5

[45] Burkinshaw S.M. and Collins G.W. The dyeing of conventional and microfibre nylon 6.6 with reactive disperse dyes. *Dyes and Pigments*. 1994 **25** (1) 31–48

[46] Hihara T., Okada Y. and Morita Z. Photo-oxidation and -reduction of vat dyes on water-swollen cellulose and their lightfastness on dry cellulose. *Dyes and Pigments*. 2002 **53** (2) 153–77

[47] Hossain M.D., Khan M.M.R. and Uddin M.Z. Fastness Properties and Color Analysis of Natural Indigo Dye and Compatibility Study of Different Natural Reducing Agents. *Journal of Polymers and the Environment*. 2017 **25** (4) 1219–30

[48] Hayashi T. and Thornton P.D. The synthesis and characterisation of thiol-bearing C. I. Disperse Red 1. *Dyes and Pigments*. 2015 **121** 235–7

[49] Khatri A. and White M. Sustainable dyeing technologies. *Sustainable Apparel*. 2015 135–60

[50] Elwakeel K.Z., Abd El-Ghaffar M.A., El-Kousy S.M. and El-Shorbagy H.G. Enhanced Remediation of Reactive Black 5 from Aqueous Media Using New Chitosan Ion Exchangers. *Journal of Dispersion Science and Technology*. 2013 **34** (7) 1008–19

[51] Eren Z. and Acar F.N. Adsorption of Reactive Black 5 from an aqueous solution: equilibrium and kinetic studies. *Desalination*. 2006 **194** (1–3) 1–10

[52] Clark M. *Handbook of textile and industrial dyeing. Volume 2, Applications of dyes* (Woodhead Pub)

[53] Khatri A., Peerzada M.H., Mohsin M. and White M. A review on developments in dyeing cotton fabrics with reactive dyes for reducing effluent pollution. *Journal of Cleaner Production*. 2015 **87** 50–7

[54] Chen L., Wang B., Ruan X., Chen J. and Yang Y. Hydrolysis-free and fully recyclable reactive dyeing of cotton in green, non-nucleophilic solvents for a sustainable textile industry. *Journal of Cleaner Production*. 2015 **107** 550–6

[55] Ujiie H. Fabric Finishing: Printing Textiles. *Textiles and Fashion*. 2015 507–29

[56] Babu K.M. and Babu K.M. The dyeing of silk. *Silk*. 2019 109–28

[57] Blackburn R.S. and Burkinshaw S.M. *Aftertreatment of acid dyes on conventional nylon 6.6 with a commercial syntan/cation system. Part 3: Improvements to the Fixogene AC system* vol 116

[58] Wang X.S., Zhou Y., Jiang Y. and Sun C. The removal of basic dyes from aqueous solutions using agricultural by-products. *Journal of Hazardous Materials*. 2008 **157** (2–3) 374–85

[59] Moser H. and Robinson T. Method for improving the fastness of dyeings with basic dyes on cellulosic substrates. US4439208A. 1982

[60] El Qada E.N., Allen S.J. and Walker G.M. Adsorption of basic dyes from aqueous solution onto activated carbons. *Chemical Engineering Journal*. 2008 **135** (3) 174–84

[61] Sangwine S.J. and Horne R.E.N. *The Colour Image Processing Handbook* (Springer US)

[62] López F., Valiente J.M., Baldrich R. and Vanrell M. Fast Surface Grading Using Color Statistics in the CIE Lab Space. *Iberian Conference of Pattern Recognition and Image Analysis* (Springer, Berlin, Heidelberg) pp 666–73

[63] Jin L. and Li D. A switching vector median filter based on the CIELAB color space for color image restoration. *Signal Processing*. 2007 **87** (6) 1345–54

[64] Robertson A.R. The CIE 1976 Color-Difference Formulae. *Color Research & Application*. 1977 **2** (1) 7–11

[65] Panandiker R.K., Aouad Y.G., Randall S.L. and Wertz W.C. Laundering aid for preventing dye transfer. US6833336B2. 2001

[66] Hazenkamp M.F., Bachmann F., Dannacher J.J. and Schlingloff G. Kinetic aspects of dye-transfer inhibition by catalytic oxidation. *Journal of Surfactants and Detergents*. 2001 **4** (1) 65–73

[67] Hood D.K. and Kamin S. Visually perceivable image-forming dye scavenging article. US9290721B2. 2011

[68] Fredj A., Johnston J.P., Thoen C.A.J., MacCorquodale F., Busch A., Hardy F.E. and Willey A.D. Detergent compositions inhibiting dye transfer. US005633225A. 1993

[69] Fox D.J., Pergament N. and Hsu F. Dye transfer inhibiting fabric softener compositions. US005964939A. 1997

[70] Fredj A., Johnston J.P. and Thoen C.A.J. Surfactant-containing dye transfer inhibiting compositions. US005458809A. 1993

[71] Lang F.P., Berenbold H. and Wessling M. Laundry detergents and laundry treatment compositions comprising dye-transfer-inhibiting dye fixatives. US7091167B2. 2002

[72] Orlandi V., Agostini A., Orlandini F.M., Curi P. and Meregalli R. Dye scavenging and water softening product. US8075635B2. 2006

[73] Detering J., Schade C., Perner J. and Jager H.U. Dye transfer inhibitors for detergents. US5830844A. 1995

[74] Meng X.-L., Nie Y., Sun J., Cheng W.-G., Wang J.-Q., He H.-Y. and Zhang S.-J. Functionalized dicyandiamide–formaldehyde polymers as efficient heterogeneous catalysts for conversion of CO_2 into organic carbonates. *Green Chem.* 2014 **16** (5) 2771–8

[75] Lambert F. and Orizet C. Protection of the coloration of textile fibers by cationic polysaccharides. WO2011157505A. 2010

[76] Oberlin A. and Partain E.M. Imidazole-modified carbohydrate polymers as laundry dye transfer inhibitors. US20170275562A1. 2015

[77] Wang J., Washington N.M., Hunter K.B. and Boyer S.L. Laundry detergent compositions with cellulosic polymers to provide appearance and integrity benefits to fabrics laundered therewith. US6833347B1. 1997

[78] Job M., Von Kathen A., Taylor J. and Lawrence A. Anti-grey detergent. WO2016062336A1. 2014

[79] Job M., Gluesen B., Taylor J. and Lawrence A. Colour protection detergent. US9404066B2. 2015

Chapter 2. Materials

2.12 Materials

All materials were used without further purification. Chemicals used are listed in Table 2-1 and Table 2-2. The solvents used have been listed in Table 2-3.

Table 2-1 A list of chemicals used in the experimental work.

Chemical	Supplier	Chemical	Supplier
Benzoylated dialysis tubing (Mw cut off 2 kDa)	Sigma-Aldrich	methoxy-PEG_{750}	Sigma-Aldrich
Butylated hydroxytoluene	Sigma-Aldrich	1,2-Propanediol	Sigma-Aldrich
Calcium chloride (>93%)	Sigma-Aldrich	Tartaric acid	Sigma-Aldrich
Chitosan powder (low molecular weight),	Sigma-Aldrich	Titanium(IV) isopropoxide	Sigma-Aldrich
C.I. Disperse Orange 3 (90%)	Sigma-Aldrich	HCl (*approx.* 37%)	Fisher Scientific
C.I. Reactive Black 5 (≥50%)	Sigma-Aldrich	NaOH pellets	Fisher Scientific
Dimethyl terephthalate	Sigma-Aldrich	α-Pinene	Fisher Scientific
Glycidyl trimethylammonium chloride (>98%)	Sigma-Aldrich	Microcrystalline cellulose	Aldrich
Glycerol	Sigma-Aldrich	methoxy-PEG_{5000}	Aldrich

Table 2-2 A list of chemicals used in the experimental work.

Chemical	Supplier	Chemical	Supplier
Anhydrous *N,N*'-dimethylformamide	Alfa Aesar	*N*-(3-diemethylaminopropyl)-*N*'-ethylcarbodiimide hydrochloride (98%)	Alfa Aesar
Alginic acid sodium salt	Alfa Aesar	Pentaerythritol	Alfa Aesar
2,2-Dimethyl-1,3-propanediol	Alfa Aesar	L-Phenylalanine	Alfa Aesar
Ethylene Glycol	Alfa Aesar	Triphosgene	Alfa Aesar
Methylene blue	Alfa Aesar	Tris(hydroxymethyl)aminomethane	Alfa Aesar
methoxy-PEG_{22}-NH_2 (M_W: 1000 g mol^{-1})	Alfa Aesar	2-Amino-2-methyl-1,3-propanediol	ACROS Organic
methoxy-PEG_{113}-NH_2 (M_W: 5000 g $mol^{-1)}$	Alfa Aesar	Citric acid monohydrate	ACROS Organic
methoxy-PEG_{295}-NH_2 (M_W: 13000 g mol^{-1})	Alfa Aesar	Crystal violet	ACROS Organic
methoxy-PEG_{13000}	Alfa Aesar	N-ε-carboxybenzyl-L-lysine	ACROS Organic
γ-Benzyl-L-glutamic acid	Fluorochem	methoxy-PEG_{500}	ACROS Organic
C.I. Disperse Blue 3	ChemCruz	Nanocellulose gel	Borregaard
Sodium tripolyphosphate	Sigma		

Table 2-3 A list of solvents used in the experiments.

Chemical	Supplier
d_6-DMSO	Euriso-top
d-$CDCl_3$	Sigma-Aldrich
Chloroform	Sigma-Aldrich
Diethyl ether	Sigma-Aldrich
Tetrahydrofuran	Sigma-Aldrich
Hexane	Sigma-Aldrich
Ethyl acetate	VWR International
Acetone (reagent grade)	VWR International
Ethanol	VWR International
Anhydrous ethyl acetate	Fisher Scientific
Anhydrous tetrahydrofuran	Fisher Scientific

2.13 Dye Bleeding Fabrics

Indigo (310 g m^{-2}), C.I. Sulfur Black 1 (420 g m^{-2}) and C.I. Direct Orange 39 (90 g m^{-2}) dye bleeding fabrics were purchased from Swissatest Testmaterialien AG (Switzerland). C.I. Reactive Red 141 (180 g m^{-2}), C.I. Reactive Brown 7 (90 g m^{-2}), C.I. Reactive Black 5 (180 g m^{-2}) and C.I. Direct Black 22 (90 g m^{-2}) were supplied by the Centre for Test Materials BV (Netherlands). Dye bleeding fabrics were cut to 5x10 cm swatches for each wash. Multifibre swatches (5x10 cm) were supplied by SDC Enterprises (Bradford, UK).

Chapter 3. Analysis of Dyes for Dye Transfer Inhibition Studies

Abstract

Poly(vinyl pyrrolidone) is a commonly used dye transfer inhibitor in commercial laundry detergent formulations. The capability of poly(vinyl pyrrolidone) to prevent the dye transfer of six key dyes, that were identified by Procter and Gamble as causing a high level of discolouration when washed with lighter coloured garments, was determined. To confirm that fabric discolouration caused by the particular dye molecule of interest, a swatch of fabric dyed with one of each of the key dyes was washed with plain water, and the extract characterised by FTIR spectroscopy and UV-Visible spectroscopy. In each case, the dye was found to be the expected compound, except in the case of indigo which was found to be anionic and water-soluble. The dyed fabrics were washed with PVP alongside a multifibre swatch to observe any colour change caused by the dye onto six receiver fabric types, and to determine the effectiveness of poly(vinyl pyrrolidone) as a dye transfer inhibitor.

3.1 Introduction

Several key dyes were identified in-house at the Procter and Gamble (P&G) Newcastle Innovation Centre as causing particularly noticeable dye transfer in the laundry. The identified dyes are outlined in Table 3-1.

Table 3-1 Six dyes identified by P&G for dye transfer testing.

Dye
Indigo
C.I. Sulfur Black 1
C.I. Direct Orange 39
C.I. Reactive Red 141
C.I. Reactive Black 5
C.I. Reactive Brown 7

In particular, indigo was identified by P&G as causing the worst discolouration, as well as being one of the most commonly used dyes in the fashion industry for the dyeing of denim. Indigo was therefore the focus of the studies for this thesis, and the first test for the efficacy of any dye transfer inhibitors (DTI) developed. The additional five dyes were also used as indicators of success of any DTIs developed in this research, once a positive result for indigo was obtained. This chapter analyses the dye solution created when the dyes bleed into the wash water. The colour change caused by the dye alone and in the presence of poly(vinyl pyrrolidone) (PVP), a commonly used DTI agent, is evaluated in order to assess the efficacy of PVP as a DTI.

3.1.1 Poly(Vinyl Pyrrolidone) for Dye Transfer Inhibition

PVP has been widely used as a dye transfer inhibitor in laundry detergent formulations (Figure 3-1).[1–3] This is due to the water-solubility of PVP and its ability to complex dyes.[4] The nitrogen atoms in PVP protonate and bind fugitive anionic dye molecules in the wash water, maintaining the dye in solution, thereby preventing deposition onto other garments.[5]

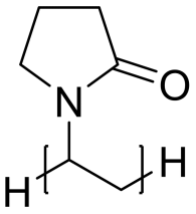

Figure 3-1 Repeat unit of poly(vinyl pyrrolidone).

However, PVP is affected by anionic surfactants present in the detergent formulation due to the surfactant competing with the dye to bind to PVP, thus reducing efficacy.[6] PVP is not affected by the presence of non-ionic surfactants, but, anionic surfactants are preferred in detergent formulations due to their superior cleaning qualities, processability into powdered forms and foaming qualities.[5,7–9] It is therefore necessary to develop new DTI polymers that can act on vat, sulfur and reactive dye classes, but do not strongly interact with anionic surfactants. These polymers may work by the adsorption or complexation of dyes. They may also deposit on the fabric to form a barrier, preventing dye deposition physically.[10]

Oakes and Dixon investigated PVP alongside four other water-soluble polymers: zwitterionic poly(4-vinylpyridine-*N*-oxide) (PVP-NO),poly(*N*-carboxymethyl-4-vinylpyridinium chloride) (PCM-VPy), cationic poly(diallyldimethyl ammonium chloride) (PDADMAC) and poly(vinyl imidazole) which, like PVP, can be protonated to become cationic (Figure 3-2).[3]

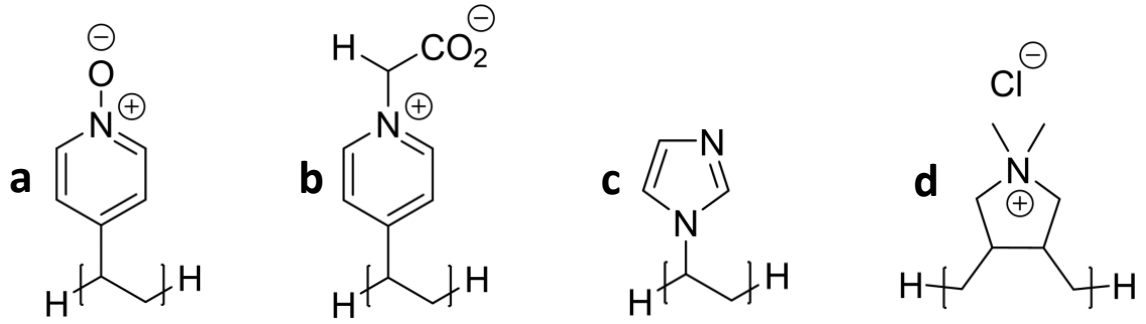

Figure 3-2 Repeat unit of a). Poly(vinylpyridine-N-oxide) (PVP-NO), b). Poly(N-carboxymethyl-4-vinylpyridinium chloride) (PCM-VPy) c) Poly(vinyl imidazole) and d). Poly(diallydimethyl ammonium chloride) (PDADMAC).

Several model dyes were tested for their deposition onto cotton, and the inhibition of dye deposition by the five polymers.[3] It was proposed that the dyes were preferentially adsorbed onto the polymers rather than to cotton, due to the ability of the polymer to 'wrap' around the dye. Additionally, the authors suggest that the dye is adsorbed by electrostatic interactions and hydrogen bonding rather than by hydrophobic interactions between the dye and the polymer, evidenced by the observed superior efficacy of PDADMAC as a DTI, followed by PVP-NO, PVP, PVI, and finally PCM-VPy as the least effective. This suggests that employing a cationic polymer is important for effective dye binding, rather than solely relying on dye encapsulation by hydrophobic interactions within surfactant micelles.

3.1.2 Effect of Anionic Surfactants on DTI Efficacy

The effect of the anionic surfactant sodium dodecyl sulfate (SDS) on the efficacy of the five DTI polymers stated in Section 3.1.1 was also investigated by Oakes and Dixon.[3] SDS is an amphiphilic molecule with a hydrocarbon chain attached to a sulfate head group. They found that the addition of SDS in sufficient concentrations caused PVP-NO to lose all efficacy as a DTI polymer against the dye C.I. Direct Red 80, with dye deposition being equivalent to that obtained without polymer addition.

Oakes and Dixon carried out a study to compare SDS to zwitterionic surfactant sulfobetaine, and non-ionic Synperonic A7, for their effect on the DTI PVP-NO. SDS was the most disruptive to the DTI efficacy of PVP-NO, followed by the zwitterionic surfactant.[3] The non-ionic surfactant did not affect DTI efficacy, indicating that dye-surfactant competition for binding to the polymer only occurs with ionic surfactants. This study indicates the many factors to be considered when designing a polymer as a DTI. However, only direct dyes were investigated, which are less common since the advent of reactive dyes.[11] Since other dyes, including vat dyes such as indigo, are known to redeposit, it is

important to examine the effects of PVP-type DTI polymers for their efficacy against a range of common dyes.

3.1.3 Dyes and Dye Transfer Assessment

The dyes identified by P&G were extracted from dye bleeding fabrics into water, and the aqueous dye solutions were analysed by UV-Vis, which were then lyophilised and the FTIR spectra of the dried samples were obtained. The dye bleeding fabrics are industry standards which are designed for wash fastness testing, and were supplied by Swissatest Testmaterialien AG (Switzerland) and the Centre for Test Materials BV (Netherlands). The analysis of the dye wash solutions was carried out to characterise the chemical dye species that is washed from the fabric and causes garment discolouration.

Additionally, in order to understand the interaction between the dyes, PVP DTI polymer and the fibres, a simulation wash of PVP solution and the dye bleeding fabric was performed. The simulated washes were in accordance with the British Standard ISO 105-C06:2010, which was performed using a James Heal GyroWash[2]. A swatch of the chosen dye bleeding fabric, 25 ball bearings and 50 mL of a polymer solution were all places into a stainless steel container alongside a swatch with six different adjacent fabrics (a 'multifibre swatch'). This was sealed and placed on a rotor in a water bath (the GyroWash) set to 40 °C, and the mixture was spun for 30 minutes at 40 rpm. The colour change onto the multifibre swatch was determined by spectrophotometry and compared to the colour change of a wash without polymer, in deionised water. This enabled the effectiveness of PVP as a DTI to be determined against a range of dyes.

3.2 Experimental

3.2.1 Fourier Transformed Infrared (FTIR) Spectroscopy

Infrared spectra were obtained on a Bruker Platinum FTIR-ATR spectrometer, using a diamond attenuated total reflectance (ATR) accessory, completing 32 scans in total. Bruker OPUS7.0 software was used to analyse the spectra. TRIOS software was used to plot and analyse the data.

3.2.2 Ultraviolet-Visible (UV-Vis) Spectrophotometry

UV-Vis readings were carried out on an Agilent Technologies Cary 100 UV-Vis spectrophotometer, whereby an absorbance scan from 190 to 750 nm was performed. Samples were analysed in a quartz 1 mL UV-Vis cuvette. The samples were in the deionised water the dye was extracted in.

3.2.3 Centrifugation, Sample Drying and Lyophilisation

Samples were separated by centrifuge with an MSE Mistral 3000i at 21 °C, 1000 rpm. A Buchi R-210 rotary evaporator and a FiStream vacuum oven were used to remove solvent and dry samples. Samples were lyophilised using a VirTis BenchTop Pro freeze dryer (SP Scientific).

3.2.4 GyroWash^2 Studies

Multifibre and dye bleeder washes were performed on a James Heal GyroWash^2 set at 40 °C, for 30 minutes at 40 rpm. The multifibre and dye bleeding fabrics were cut to 4x10 cm swatches and washed in deionised water (50 mL) or polymer solution (50 mL, 0.1 mg mL^{-1}), with 25 ball bearings. Colour changes were measured using a Spectraflash DataColor unit, which measured the L*, a* and b* coordinates, which can be compared to an unwashed sample to give a colour change (ΔE) value. Measurements were made under D65 lighting.

3.2.5 Dye Extraction

For each dye, a swatch of dye bleeding fabric (4x10 cm) was added to deionised water (50 mL) and washed on a James Heal Gyrowash^2 at 40°C for 30 minutes at 40 rpm. The resulting solution was analysed by UV-Vis spectroscopy, before lyophilisation. The resulting solid was analysed by FTIR spectroscopy.

3.2.6 Poly(Vinyl Pyrrolidone) Wash Studies

A swatch of dye bleeding fabric (4x10 cm) was added to an aqueous solution of PVP (50 mL, 0.1 mg mL^{-1}), alongside a multifibre swatch (4x10 cm) and 25 ball bearings. This was then washed using a James Heal Gyrowash^2 at 40°C for 30 minutes at 40 rpm. The multifibre swatch was then air dried and the L*a*b* coordinates measured.

3.3 Results and Discussion

The six key dyes outlined were extracted from their respective dye bleeding fabrics. The wash extract was then directly analysed by UV-Vis spectroscopy. The various dye solutions were then lyophilised to yield a solid that was analysed by FTIR.

3.3.1 Characterisation of Indigo

Indigo dye on cotton fabric was extracted and analysed to confirm the structure and properties of the dye moiety. Indigo is a vat dye with a known structure shown in Figure 3-3. The compound that was extracted may be compared and assessed for its similarity to the theoretical structure to confirm the form of the indigo that causes discolouration. As the extract was moderately water-soluble, when indigo itself is not, it was proposed that the dye may have been modified to improve solubility or may be present in its *leuco* form.

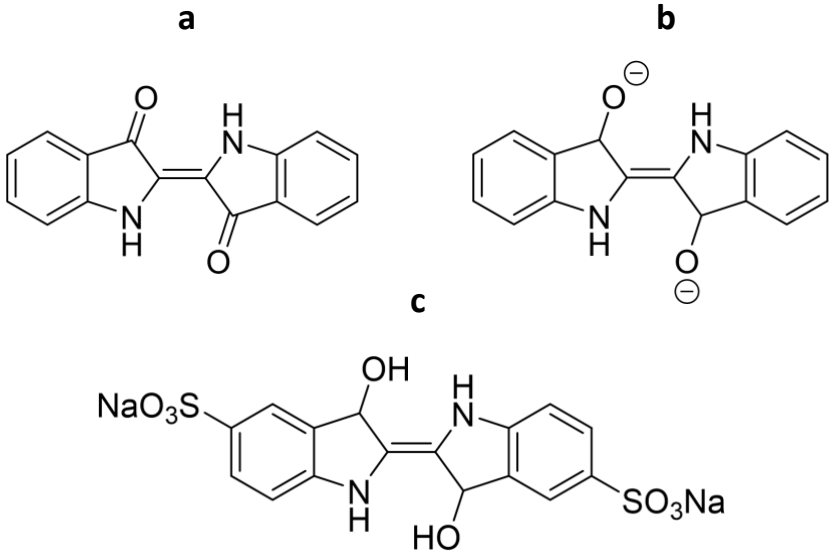

Figure 3-3 Structure of a). Indigo b). Leuco-indigo and c). Indigo carmine.

Firstly, the wash extract of indigo dye bleeding fabric was analysed by UV-Vis spectroscopy and the absorbance in the visible region observed (Figure 3-4).

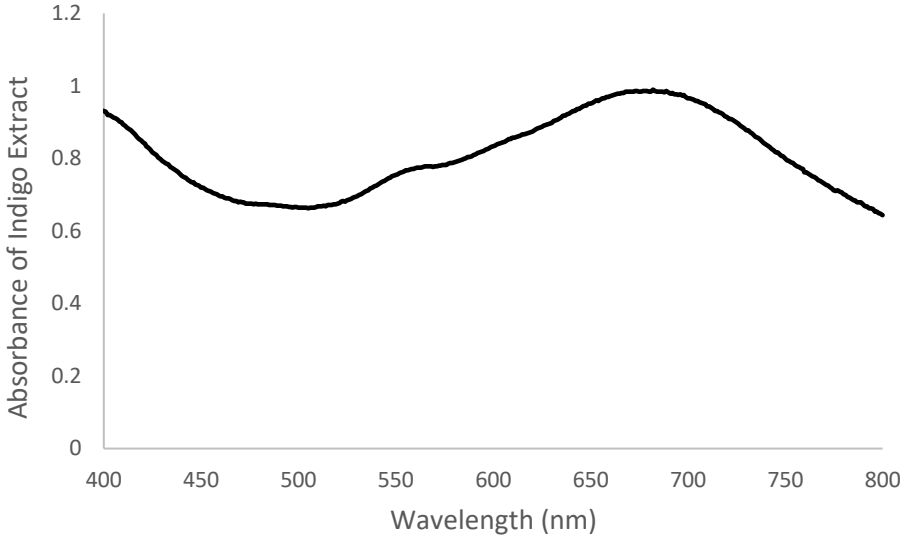

Figure 3-4 Visible region spectrum of indigo dye extract.

Figure 3-4 shows that the λ_{max} of the indigo dye wash extract is 695 nm, confirming that the dye transmits in the blue region. The literature λ_{max} of indigo is 682-6 nm, which shows that the λ_{max} value of the extract is of a longer wavelength.[12,13] The indigo dye extract was also analysed by FTIR (Figure 3-5)

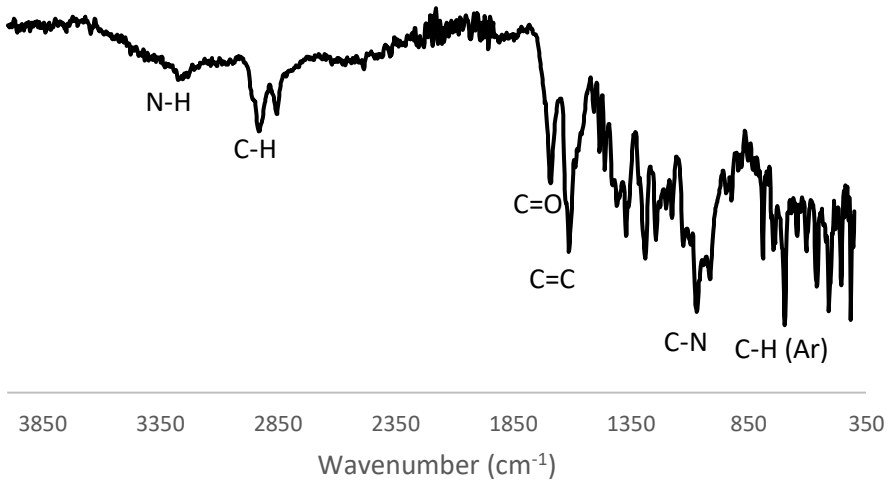

Figure 3-5 FTIR spectrum of indigo dye extract.

The FTIR in Figure 3-5 shows the presence of amine and aromatic groups, as expected within the known indigo structure. The absence of sulfonate groups indicates that it is not the water-soluble indigo carmine, and therefore provides further evidence the dye is in the *leuco* form, which enables water-solubility. The indigo dye bleeding fabric was then washed with PVP to assess the colour change caused in the presence of the DTI polymer (Figure 3-6).

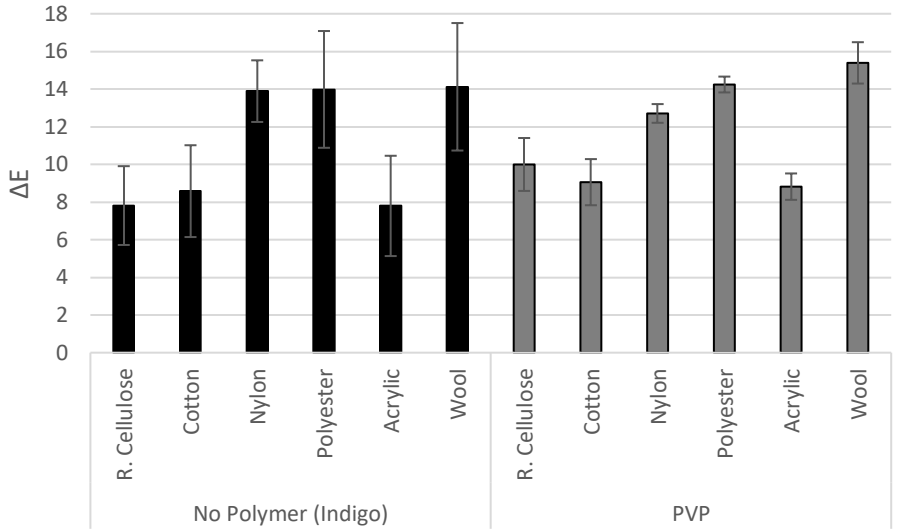

Figure 3-6 A comparison of the colour change caused by indigo in the absence of a DTI polymer, and in the presence of PVP.

From Figure 3-6, it can be seen that PVP has no effect on the colour change caused to the various fabrics by indigo. This is shown by the similar ΔE values between the multifibre swatch washed without polymer, and that washed with PVP, both with an indigo dye bleeding swatch.

3.3.2 Characterisation of C.I. Sulfur Black 1

C.I. Sulfur Black 1 (SB1) is a sulfur dye that has an inexact structure. However, the proposed structure contains a planar, aromatic scaffold and thiol, amine and hydroxy functional groups (Figure 3-7).

The *leuco* form of the dye is produced by the reduction of the SB1 molecule with Na_2S, in order to solubilise the dye to enable textile dyeing to occur.[14]

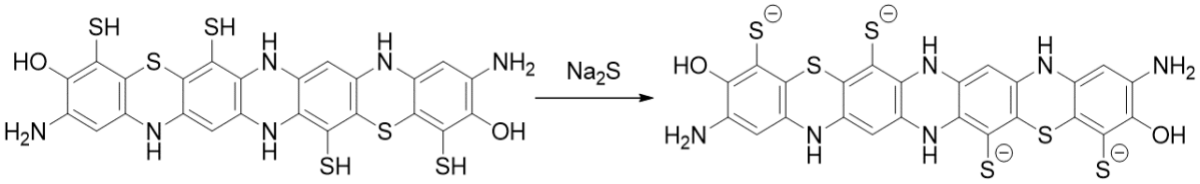

Figure 3-7 Proposed structure of C.I. Sulfur Black 1 and the formation of its leuco form.

The visible spectrum of SB1 wash extract was collected and analysed (Figure 3-8).

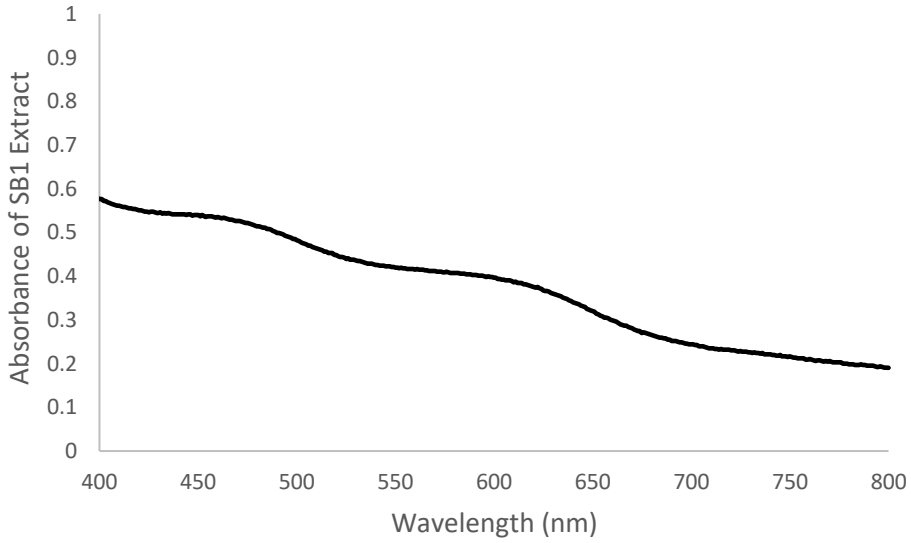

Figure 3-8 Visible spectrum of SB1 wash extract.

As SB1 is a black dye, it absorbs across the entire visible region, as indicated in Figure 3-8 where a discrete λ_{max} is not observable due to low level absorption across all wavelengths. The FTIR spectrum for the SB1 extract was obtained (Figure 3-9).

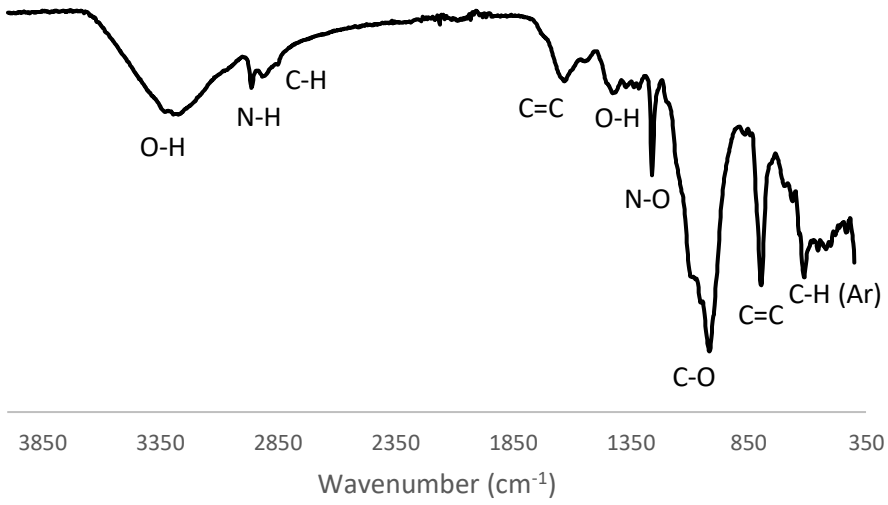

Figure 3-9 FTIR spectrum of SB1 dye extract.

The FTIR in Figure 3-9 shows the presence of an aromatic group, hydroxy groups and amine groups. However, a thiol group is not observable, confirming the inconsistency of commercial SB1. An SB1 dye bleeding fabric swatch was washed with PVP to assess the efficacy of the polymer as a DTI against SB1 (Figure 3-10).

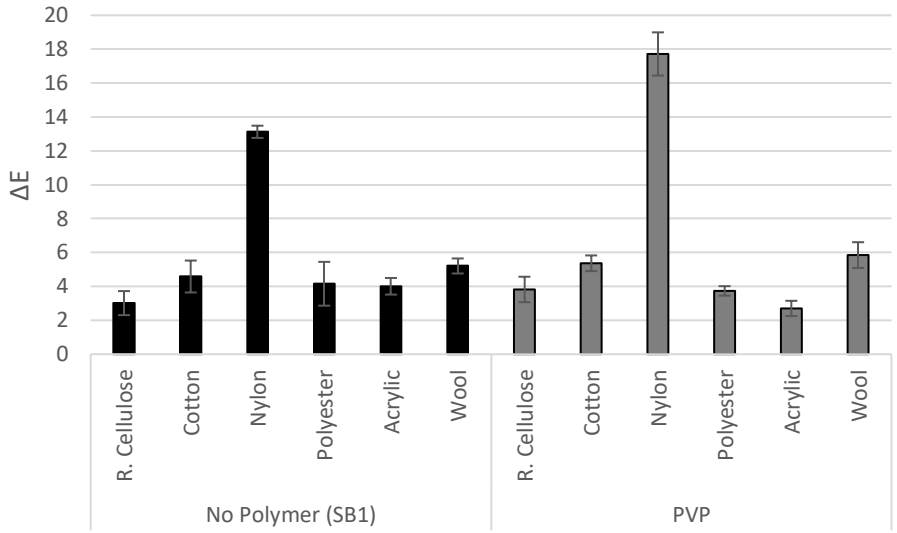

Figure 3-10 A comparison of the colour change caused by SB1 in the absence of a DTI polymer, and in the presence of PVP.

From Figure 3-10 it can be seen that PVP does not reduce the colour change caused by SB1. A worsened dye deposition is observed for nylon, whereby the colour change increases from 13.13 without polymer, to 17.72 in the presence of PVP, a 25.9% increase.

3.3.3 Characterisation of C.I. Direct Orange 39

C.I. Direct Orange 39 (DO39) on cotton fabric was extracted and characterised. The direct dye has a known structure, shown in Figure 3-11.

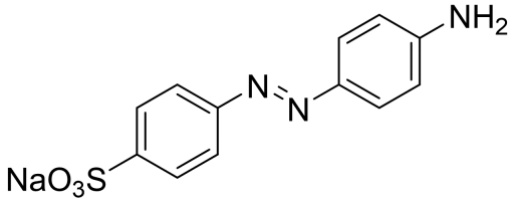

Figure 3-11 Structure of C.I. Direct Orange 39.

The dye extract was firstly analysed by visible spectroscopy (Figure 3-12).

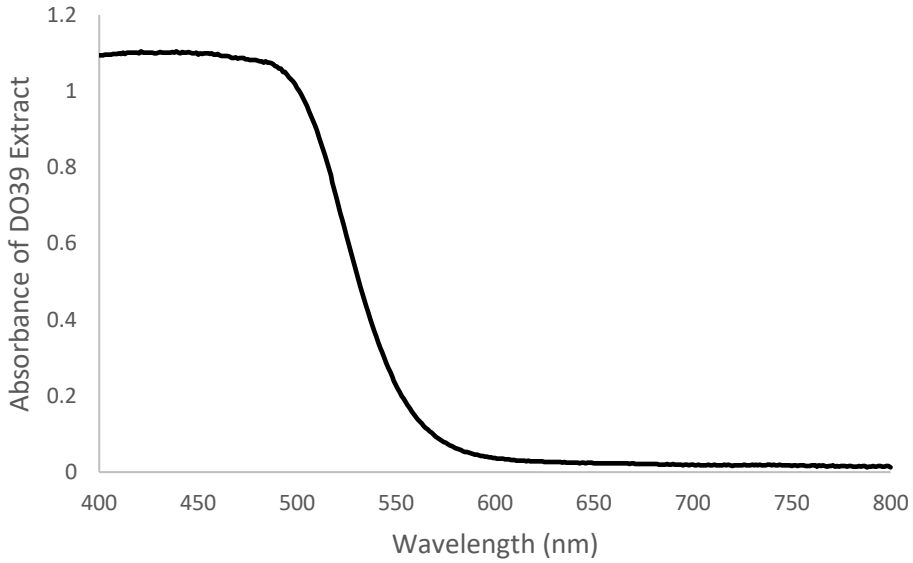

Figure 3-12 Visible region spectrum of DO39 dye extract.

Figure 3-12 shows that DO39 absorbs in the visible region across 400-500 nm, thereby transmitting an orange colour. This is in agreement with the literature value λ_{max} of 414 nm.[15] An FTIR spectrum of the DO39 dye extract was obtained (Figure 3-13).

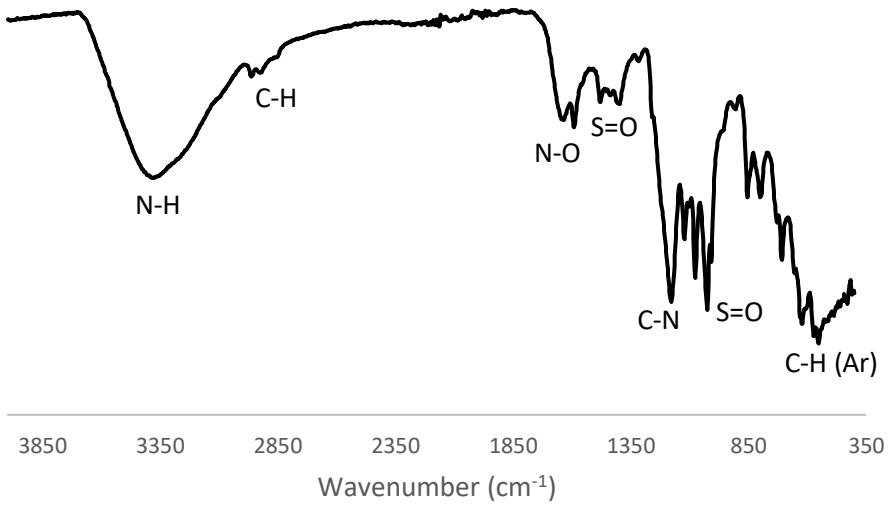

Figure 3-13 FTIR spectrum of DO39 dye extract.

The FTIR spectrum of DO39 in Figure 3-13 confirms the presence of amine, aromatic, and sulfonate groups. DO39 was then washed with PVP to observe any DTI effects (Figure 3-14).

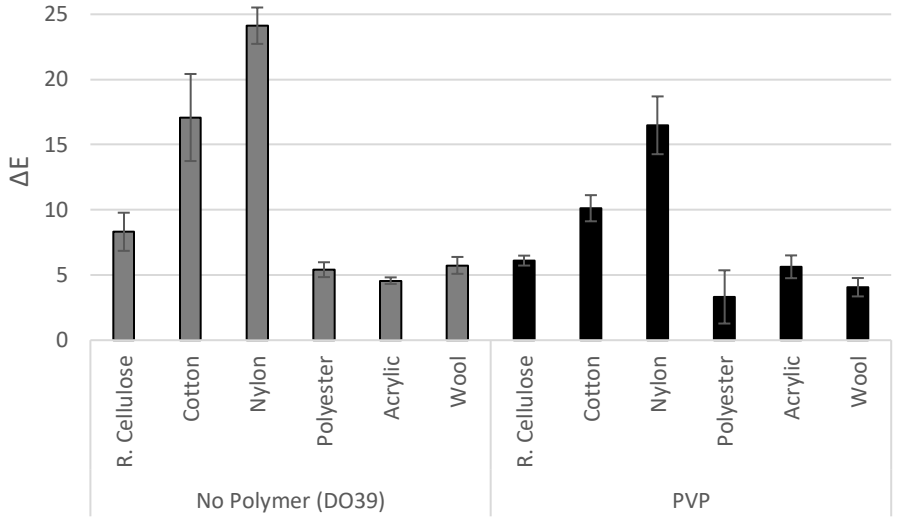

Figure 3-14 A comparison of the colour change caused by DO39 in the absence of a DTI polymer, and in the presence of PVP.

Figure 3-14 shows that PVP reduces the colour change caused by DO39. Cotton shows a 40.7% reduction in colour change, and nylon a 31.7% reduction. This is expected as PVP is designed to complex direct dyes *via* electrostatic interactions, and prevent them from depositing onto the fabric, reducing colour change.

3.3.4 Characterisation of C.I. Reactive Red 141

C.I. Reactive Red 141 (RR141) is a chlorotriazine reactive dye, the structure of which is shown in Figure 3-15.

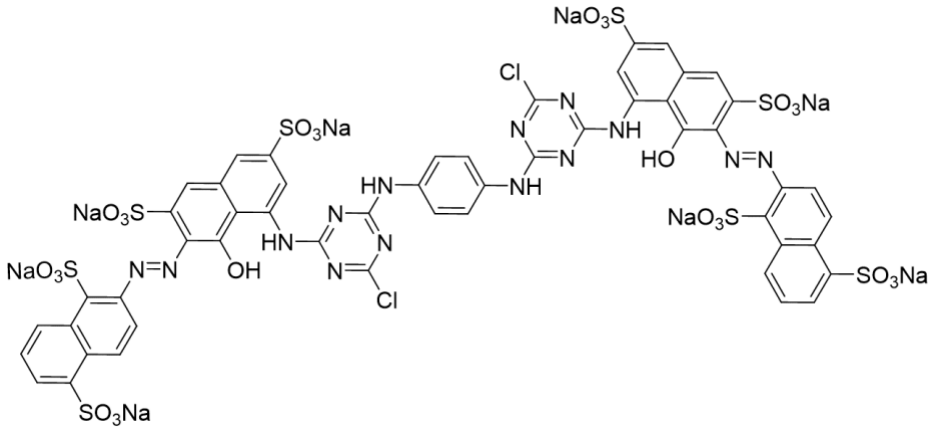

Figure 3-15 Structure of C.I. Reactive Red 141.

The extract was analysed by visible spectroscopy (Figure 3-16).

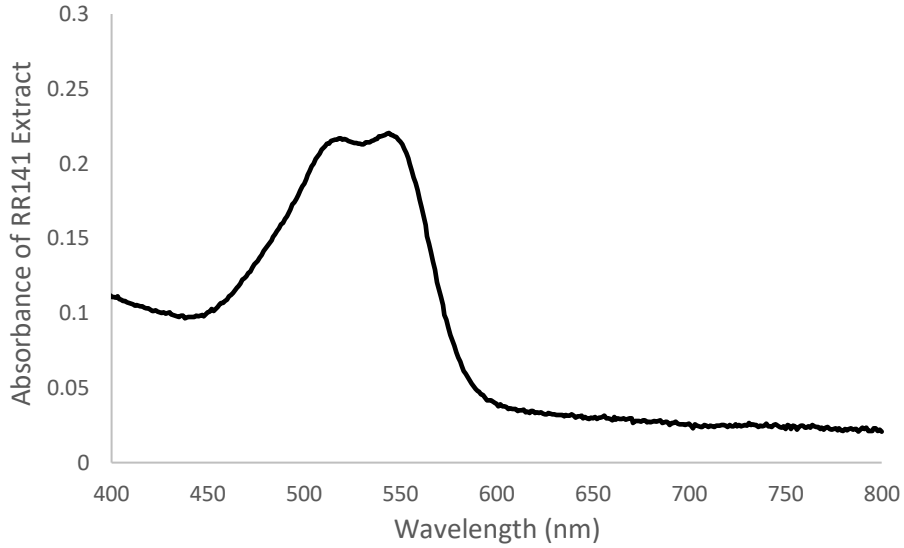

Figure 3-16 Visible region spectrum of RR141 dye extract.

From Figure 3-16 it can be seen that RR141 has a λ_{max} in the region of 523-555 nm. This value is in agreement with the literature value of 532 nm.[15] An FTIR spectrum of the dye extract was then assessed (Figure 3-17).

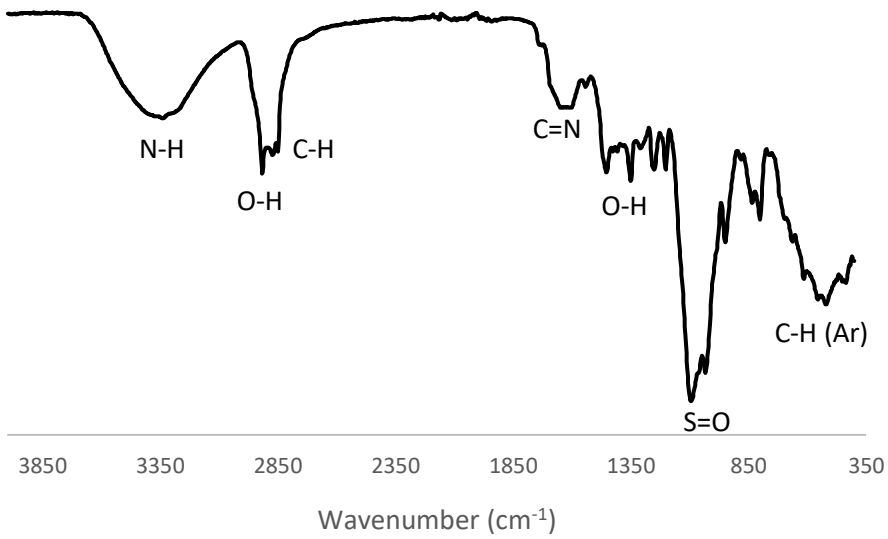

Figure 3-17 FTIR spectrum of RR141 dye extract.

From Figure 3-17 it can be seen that the dye extract from the RR141 dye bleeding fabric contains the expected groups attributed to the dye molecule, such imine, aromatic, and sulfonate groups. An RR141 dye bleeding fabric swatch was then washed with PVP and the colour change compared to that without polymer (Figure 3-18).

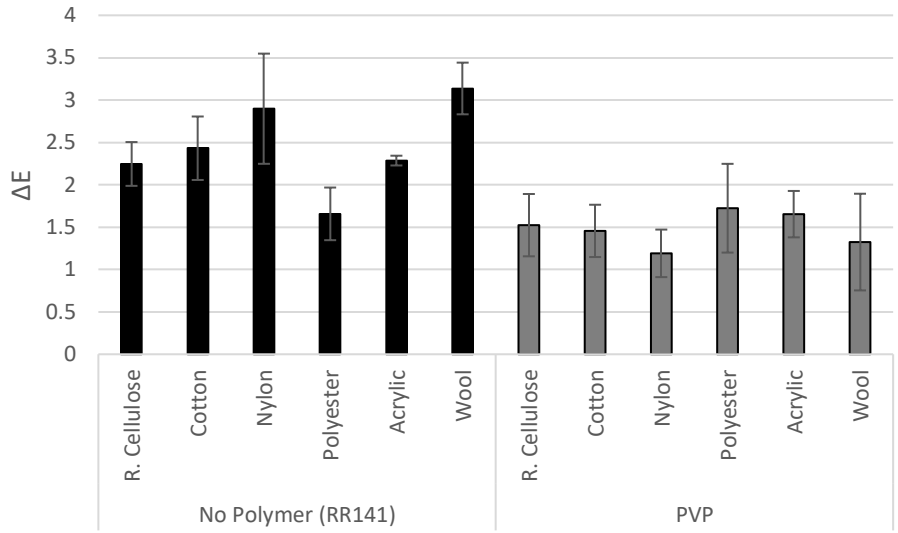

Figure 3-18 A comparison of the colour change caused by RR141 in the absence of a DTI polymer, and in the presence of PVP.

It can be seen from Figure 3-18 that PVP is effective at reducing colour change caused by RR141 onto most fabric types. For example, the colour change on nylon in the absence of polymer is 2.90, whereas in the presence of PVP is it reduced to 1.19, a 59.0% reduction in colour change. This shows that PVP type DTIs which complex the dye may be effective against RR141.

3.3.5 Characterisation of C.I. Reactive Black 5

The structure of C.I. Reactive Black 5 (RB5) is shown in Figure 3-19. The dye is a vinyl sulfone reactive dye.

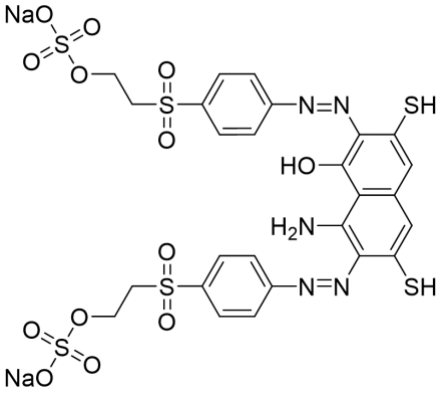

Figure 3-19 Structure of C.I. Reactive Black 5.

The visible spectrum of the dye extract was then analysed (Figure 3-20).

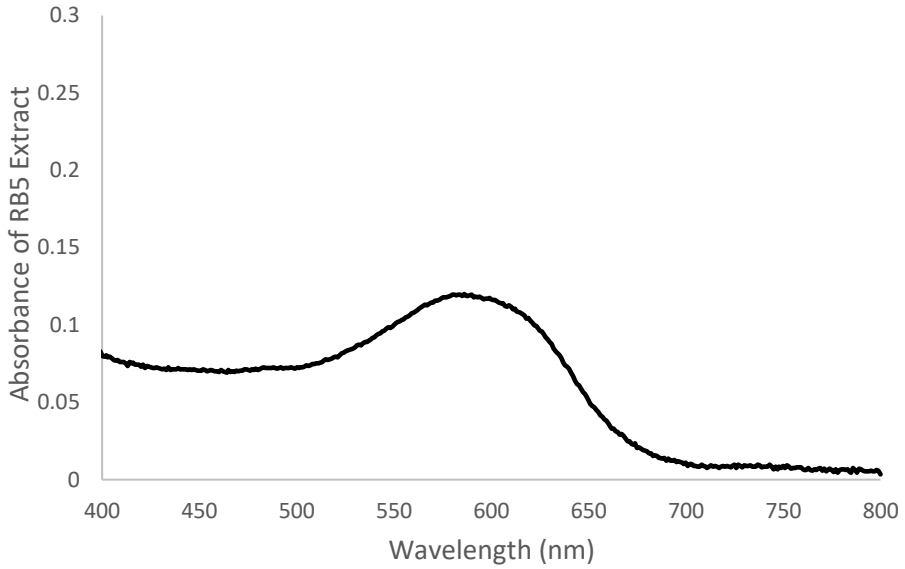

Figure 3-20 Visible region spectrum of RB5 dye extract.

RB5 is a blue coloured dye, which is confirmed in Figure 3-20 by a λ_{max} of 606 nm. This is in agreement with the reported literature value of 597 nm.[15] An FTIR spectrum of the RB5 dye extract was obtained (Figure 3-21).

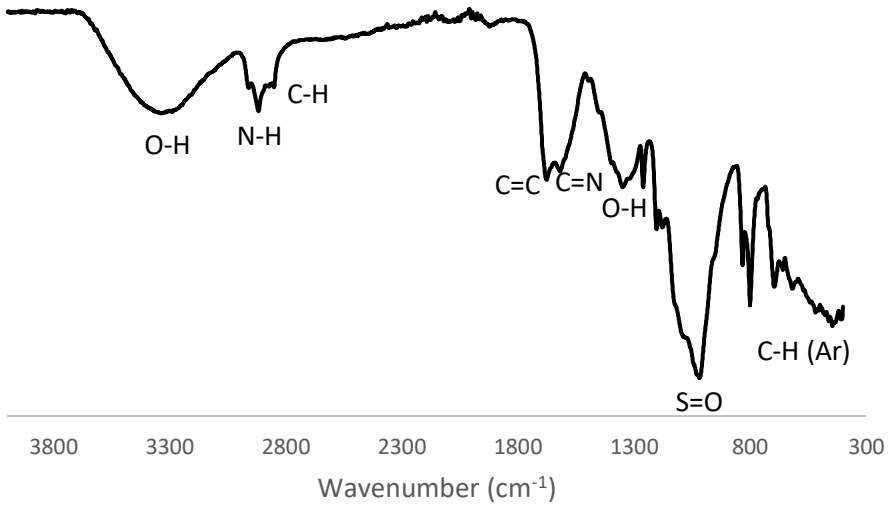

Figure 3-21 FTIR spectrum of RB5 dye extract.

The dye extracted from the dye bleeding fabric was found to contain the expected functional groups associated with RB5, such as sulfonate, hydroxy, amine and aromatic groups. The RB5 dye bleeding fabric was then washed with PVP to observe any DTI effects (Figure 3-22).

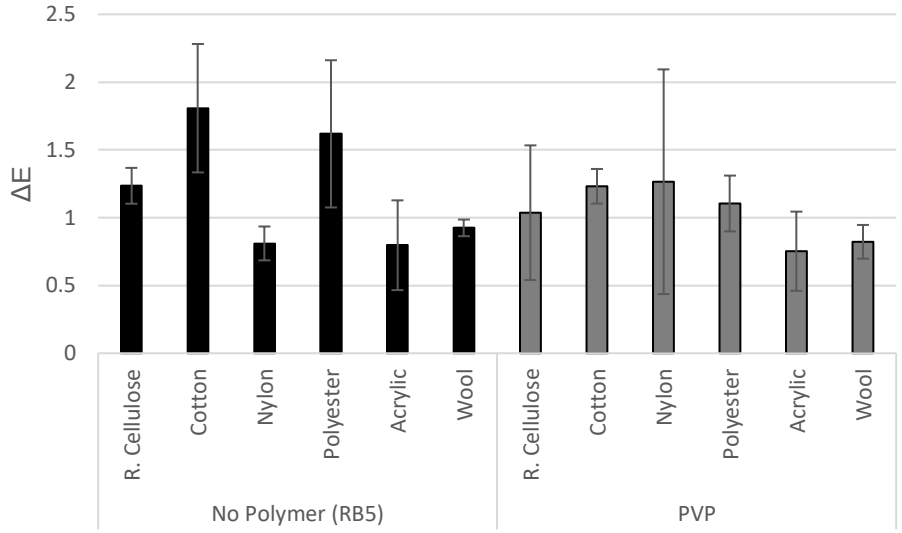

Figure 3-22 A comparison of the colour change caused by RB5 in the absence of a DTI polymer, and in the presence of PVP.

Overall, PVP does not reduce the colour change caused by RB5 except for cotton, which shows a 32.0% reduction in mean colour change, and polyester which shows a 31.7% reduction. This again shows that PVP is capable of complexing RB5, and reducing the colour change onto cotton, which RB5 is designed to dye and shows the highest level of discolouration in the absence of polymer. This may be due to the sulfonate groups in RB5, that may be capable of complexing with the amine groups in the PVP.

3.3.6 Characterisation of C.I. Reactive Brown 7

C.I. Reactive Brown 7 (RB7) is a chlorotriazine reactive dye, the structure of which is shown in Figure 3-23.

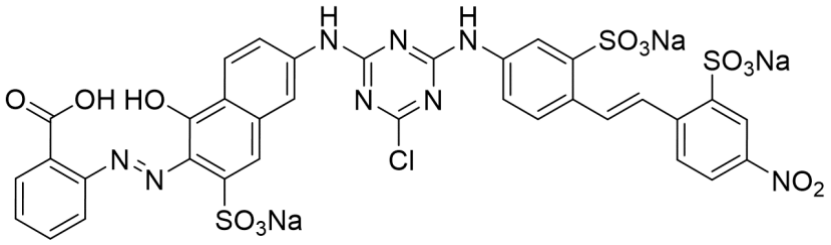

Figure 3-23 Structure of C.I. Reactive Brown 7.

The FTIR spectrum of the RB7 dye extract was then assessed (Figure 3-24).

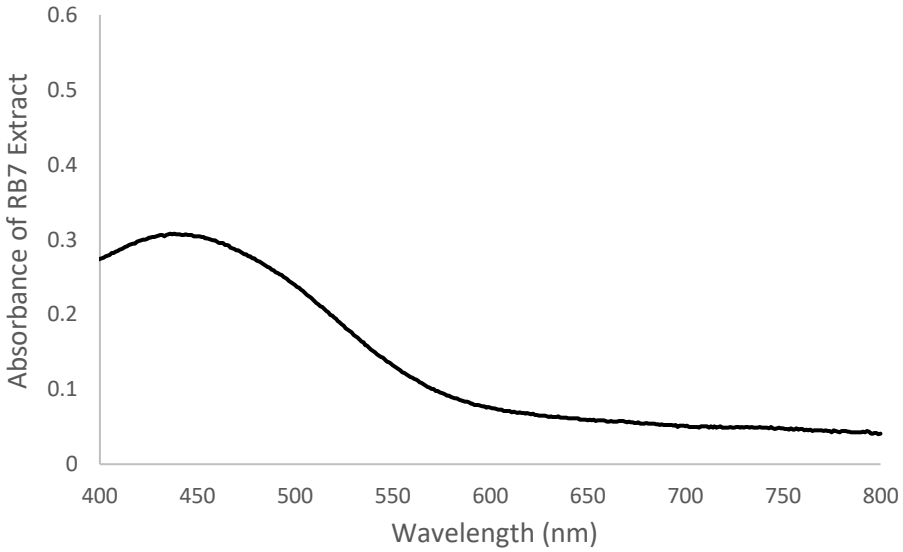

Figure 3-24 Visible region spectrum of RB7 dye extract.

RB7 is a brown dye, and the λ_{max} is found to be 457 nm, as shown in Figure 3-24. Brown light is absorbed across most wavelengths of light towards the red region. The spectrum shows that the dye is absorbing in the orange region specifically, rather than being a broad range across many wavelengths. The RB7 dye extract was also analysed by FTIR (Figure 3-25).

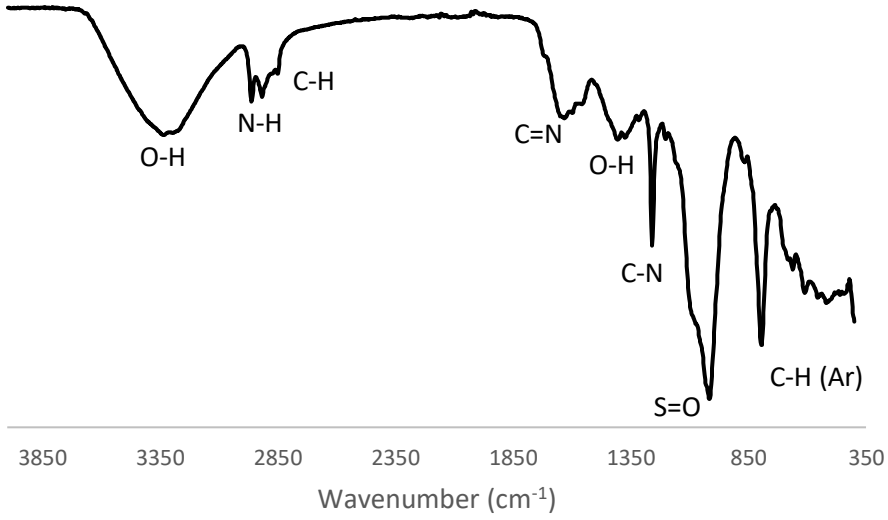

Figure 3-25 FTIR spectrum of RB7 dye extract.

The FTIR of RB7 dye extract in Figure 3-25 confirms the presence of hydroxy, amine, imine, aromatic and sulfonate functional groups, which are present in the RB7 known structure. This suggests the colourising moiety is the known structure of RB7. The RB7 dye bleeding fabric was then washed with PVP (Figure 3-26).

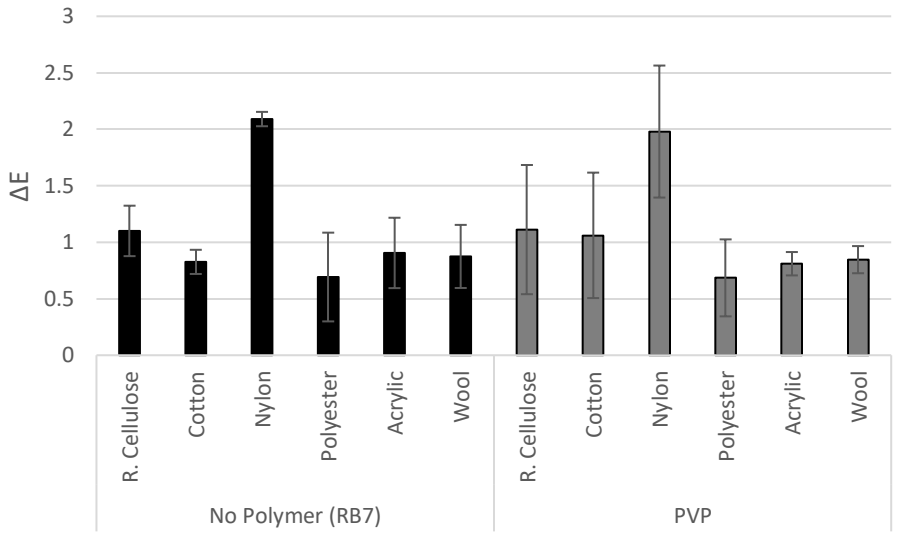

Figure 3-26 A comparison of the colour change caused by RB7 in the absence of a DTI polymer, and in the presence of PVP.

From Figure 3-26 it can be seen that PVP does not have an overall effect on the colour change caused by RB7. This is evidenced by the similar ΔE values in the absence of polymer and in the presence of

PVP for each fabric type. This is surprising as PVP was effective at preventing colour change caused by RR141 and RB5, two similar dyes, onto nylon in particular. This therefore highlights the need to develop new DTI polymers to prevent dye transfer of dyes that PVP is not effective against.

3.4 Conclusion

Six dyes were extracted from industry standard dye bleeding fabrics and individually characterised by UV-Vis, and FTIR. This was to confirm that the structure of the molecule causing colour change is the known dye structure. The analysis confirmed the structures to be those of the expected dye except in the case of indigo and SB1. Indigo was found to be moderately water-soluble, which may mean that the indigo dye released from the cotton contains solubilising groups, and SB1 has an unknown structure which cannot therefore be confirmed.

Dye bleeding fabrics were then washed with PVP and a multifibre swatch, which acts as a receiver fabric for the dye. The colour change of the multifibre swatch was compared between the wash with PVP and a wash in plain, deionised water. Overall, it was found that indigo, SB1 and RB7 were not affected by the presence of PVP. However, DO39 and RR141 showed a reduction in colour change, particularly onto nylon, in the presence of PVP. As all the dyes are anionic, it may be expected that PVP is able to complex with all the dyes and prevent them from discolouring the multifibre swatches. However, the two dyes which showed reduced colour change with PVP, RR141 and DO39, are extremely water-soluble dyes. Therefore, the efficacy of the complexation of the dye and PVP may be reliant on the hydrophilicity of the dyes. Additionally, dye molecule size was not found to affect the ability of PVP to complex it, as DO39 is a small molecule whereas RR141 is a large extended structure. These results confirm that PVP is ineffective as a DTI agent against a range of commercially-deployed dye molecules, and that new DTIs must be developed in order to reduce the dye transfer of many common dyes, including indigo, in laundry.

3.5 References

[1] Johnson L.M., Loughnane B.J., Hulskotter F., Scialla S. and Ludolph B. Cleaning compositions containing a cyclic amine and an encapsulated perfume. US2017/0015949A1. 2016

[2] Van Leeuwen P.J., Convents A.C., Busch A., Cachet T.L. and Joos C.E.A. Laundry detergent composition comprising substantially water-insoluble polymeric dye transfer inhibiting agent. US005912221A. 1995

[3] Oakes J. and Dixon S. Adsorption of dyes to cotton and inhibition by polymers. *Coloration Technology*. 2003 **119** (3) 140–9

[4] Johnson K.A., Van Buskirk G. and Gillette S.M. Laundry article for preventing dye carry-over and indicator therefor. US005698476A. 1995

[5] Oakes J. Formulation of colour-care and heavy-duty detergents: A review. *Coloration Technology*. 2005

[6] Shih J.S., Srinivas B. and Hornby J.C. Water soluble dye complexing polymers. US5776879A. 1997

[7] Zoller U. *Handbook of Detergents, Part E* ed U Zoller (CRC Press)

[8] Panandiker R.K., Wertz W.C. and Hughes L.J. Detergent compositions which provide dye transfer inhibition benefits. US005466802A. 1993

[9] Oakes J., Gratton P. and Dixon S. Solubilisation of dyes by surfactant micelles. Part 4: Influence of dye fixatives. *Coloration Technology*. 2004 **120** (6) 267–75

[10] Uchiyama T., Kawauchi A. and DuVal D.L. Quick identification of polymeric dye transfer inhibitors in laundry detergents by pyrolysis-gas chromatography/mass spectrometry. *Journal of Analytical and Applied Pyrolysis*. 1998 **45** (2) 111–9

[11] Carrion F.J. Influence of the dye transfer inhibitors for the washing of softened cotton fabric. *The Journal of The Textile Institute*. 2014 **105** (2) 150–5

[12] Dogan D. and Türkdemir H. Electrochemical oxidation of textile dye indigo. *Journal of Chemical Technology & Biotechnology*. 2005 **80** (8) 916–23

[13] Manu B. and Chaudhari S. Decolorization of indigo and azo dyes in semicontinuous reactors with long hydraulic retention time. *Process Biochemistry*. 2003 **38** (8) 1213–21

[14] Wang M., Yang J. and Wang H. Optimisation of the synthesis of a water-soluble sulfur black dye. *Dyes and Pigments*. 2001 **50** (3) 243–6

[15] Chen K.-C., Wu J.-Y., Liou D.-J. and Hwang S.-C.J. Decolorization of the textile dyes by newly isolated bacterial strains. *Journal of Biotechnology*. 2003 **101** (1) 57–68

Chapter 4. Biopolymeric Hydrogel Materials for Use as Dye Adsorbants

This chapter is based on work published as:

Boardman S. J., Lad R., Green D. C. and Thornton P. D. Chitosan hydrogels for targeted dye and protein adsorption. *Journal of Applied Polymer Science*. 2017 **134** (21)

Abstract

Polymer hydrogels were investigated for application in dye transfer inhibition in laundry, as well as dye bath clean-up of effluent from industrial dyeing. Biopolymer-based hydrogels were created owing to their ease of formation, low cost and low environmental impact. Chitosan hydrogels were found to be particularly effective for the adsorption of C.I. Reactive Black 5. However, C.I. Disperse Blue 3 and C.I. Disperse Orange 3 showed less significant adsorption to chitosan hydrogels, indicating the need for electrostatic interaction between the biopolymer and the dye. Alginate, chitosan and cellulose hydrogels were then tested for their ability to adsorb basic dyes, crystal violet and methylene blue. Cellulose was found to adsorb 83% of the crystal violet presented within 150 minutes.

4.1 Introduction

4.1.1 Reactive Dyes

Reactive dyes are unique to other classes of dye as they are designed to covalently bind to cellulosic fibres by an esterification reaction, which improves wash fastness.[1] They also possess favourable properties such as high water-solubility, ease of application and bright colour options.[2] As such they have become widely used in the dyeing industry over the past three decades and are a popular class of dye.[3] Procter and Gamble initially identified C.I. Reactive Black

5 as a key dye in causing dye transfer in the laundry process, as well as being highly popular, and therefore will be the main focus of this chapter.

4.1.2 C.I. Reactive Black 5

The extended aromatic structures of reactive dyes dictate that they are chemically stable.[3,4] This is a particular problem for C.I. Reactive Black 5 (RB5, Figure 4-1), which is a commonly used reactive dye but is toxic to aquatic life, deeming its environmental accumulation highly damaging to wildlife and ecosystems.[5] The reactive dye undergoes hydrolysis in the aqueous dye bath, meaning only 80% of the dye reacts with the fibre, creating a demand for dye-bath clean-up of the resulting coloured effluent.[6] The new found prevalence and unique properties of reactive dyes mean they are resistant to previously implemented dye bath clean-up methods such as biodegradation.[3] New methods must therefore be implemented to remove RB5 from dye bath waste water before its release into the environment, in order to prevent ecological harm. In addition, RB5 has an observed dye transfer effect in laundry that is caused by the removal of dye molecules from a garment before subsequent deposition onto alternative, often lighter garments, leading to greying of lighter clothing in the laundry cycle.[7]

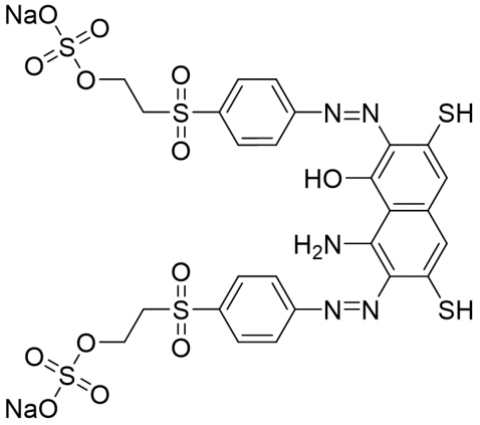

Figure 4-1 Structure of C.I. Reactive Black 5.

4.1.3 Dye Clean-Up

Highly-effective methods to adsorb RB5 are greatly sought after for application in dye clean-up and advanced laundry care applications.[8] A number of innovative approaches have been

reported to-date, including oxidation,[9] ion-exchange,[10] photocatalytic degradation[11] and membrane filtration.[12] In particular, the adsorption of RB5 molecules as an effective dye retrieval process has been investigated extensively, owing to its ease, speed and simplicity.[3,13–15] Activated carbon is an effective adsorbent for the removal of dyes and metal ions from waste water; however the materials produced are often deemed cost-prohibitive for use in dye clean-up.[16–19] Consequently, there is an urgent requirement for the development of cost-effective materials that are capable of effectual dye adsorption. Polymeric materials offer a particularly effective, easy and simple method of dye retrieval by adsorption.[20–22] The development of economically viable polymeric materials that efficiently adsorb and sequester dyes are therefore highly sought.

4.1.4 Chitosan

Chitosan boasts numerous advantageous features that make its use as a dye adsorbent suitable. Firstly, chitosan is produced by the deacetylation of the polysaccharide chitin, which is the second most abundant biopolymer, and a waste material from the food industry (Figure 4-2). Therefore, the economic case for using chitosan is highly compelling for this application.[4,14]

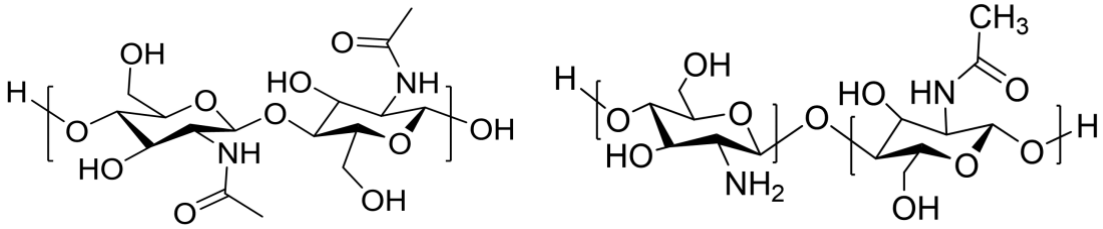

Figure 4-2 Left: Structure of chitin, and Right: Structure of chitosan, showing the deacetylated unit.

Secondly, chitosan exhibits extensive amine functionality. Primary amines may be exploited for chemical modification, but can also be used for the binding of groups by non-covalent interactions.[23] In solutions of pH levels lower than the pK_a value of the d-glucosamine unit of chitosan (6.5–7.0), electrostatic attraction between anionic RB5 and cationic chitosan enables

polymer-dye conjugation. However, chitosan-RB5 adsorption may also occur in aqueous solutions that have a pH level above pH 7 due to the formation of hydrogen bonds.[14]

4.1.5 Chitosan Beads and Flakes

Much research has been carried out concerning the use of chitosan as an adsorbent for reactive dyes such as RB5.[14,24,25] Chitosan beads and flakes have been at the forefront of this research, for example Ong and Seou investigated the effects of solution pH, time, RB5 concentration and agitation on RB5 adsorption by chitosan beads.[26] Through adsorption studies, the optimal solution pH for RB5 adsorption was found to be pH 6. However, the pH of zero charge for the chitosan beads was found to be pH 8, above which the surface charge becomes negative. Therefore, RB5 is still adsorbed at pH 8; the typical pH of a laundry detergent.

Sakkayawong *et al.* investigated the adsorptive properties of chitosan powder under caustic conditions using synthetic reactive dye wastewater (SRDW).[27] SRDW was adsorbed by chitosan at pH 6-11 by 96-98%, and by 99% at pH 2-5, therefore only showing a minor reduction in efficacy between optimal acidic conditions and in alkaline conditions. SRDW adsorption was deduced by infrared spectroscopy (IR) to be because of covalent bonding under caustic conditions between the reactive group of the dye and the hydroxy group of the chitosan, analogous to the dyeing process of reactive dyes to cellulosic fibres (Figure 4-3).[27,28] This suggests that it is not only the amine functional groups of the chitosan that serve to adsorb dyes, but also the hydroxy groups under alkaline conditions, making chitosan an ideal material for dye clean up. While this study does not detail RB5 specifically, it does observe generic reactive dye solution of SRDW therefore suggesting that RB5 would be included within this broad term.

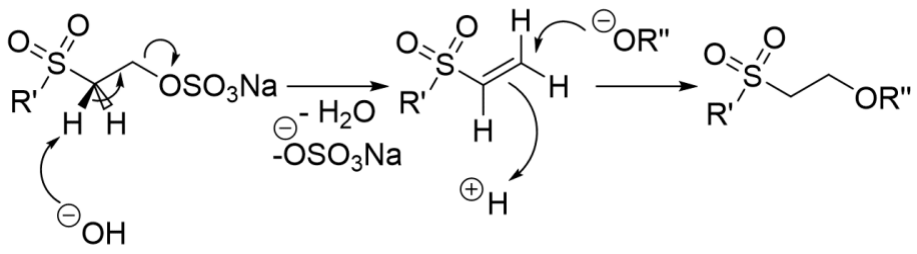

Figure 4-3 Vinyl sulfone dye reacting with hydroxy group of cellulose or chitosan.

4.1.6 Chemically Modified Chitosan

As a polyamine, chitosan provides many sites along the polymer backbone for functionalisation and chemical modification. This may be used advantageously for RB5 adsorption.

Elwakeel *et al*. investigated chitosan resins modified with 1,1,1,3,3,3-hexafloro-2-bis(3-amino-2-hydroxyphenyl)propane, 3-amino-1,2,4-triazole-5-thiol or melamine, all designed to chelate RB5 molecules.[2] They report that it is not only the charge on the chitosan backbone that affects uptake, but also the availability of the amine groups for electrostatic interaction with charged RB5 molecules. They found the less sterically hindered, but also most basic, amine groups were located on the chitosan modified with 1,1,1,3,3,3-hexafloro-2-bis(3-amino-2-hydroxyphenyl) propane (Figure 4-4). This showed the highest level of RB5 uptake, despite having the lowest nitrogen content, as observed *via* elemental analysis. Additionally, the study found that adsorption heavily relied on the solution pH. At solution pH below pH 3, the RB5 dye molecules do not readily dissociate to form a negatively charged species and therefore cannot electrostatically interact with the chitosan, however above pH 3, protonation of the chitosan begins to decrease. They therefore suggest that pH 3 is the optimum conditions for dye adsorption. For the intended application of chitosan to dye transfer inhibition pH 3 is too low, as laundry detergents are typically alkaline.

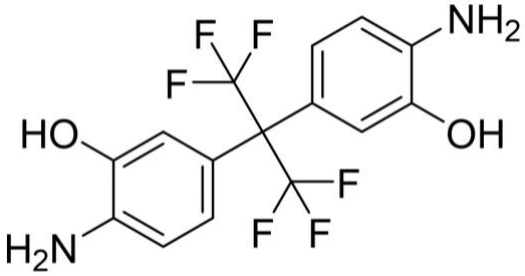

Figure 4-4 Structure of 1,1,1,3,3,3-hexafluoro-2-bis(3-amino-2-hydroxyphenyl) propane

Chitosan modified with poly(propylene imine) dendrimers attached to the backbone were investigated for their adsorption capacity of RB5.[29] The chitosan was first modified to *N*-carboxyethyl chitosan, and from the carboxylate group the dendrimer was added *via* an amide bond. This modification adds seven amine terminals, where previously there was only one. At

pH 2, RB5 uptake was 98.7%, however, at pH 6 RB5 uptake was limited to 55%. This may be due to the need for more acidic conditions to protonate the vastly increased number of amine groups, and indicates that this type of system is not suitable for the intended applications.

4.1.7 Chitosan Composites

Umpuch and Sakaew investigated the intercalation of chitosan with the mineral clay montmorillonite.[30] The intercalation of the chitosan with the clay provides chemical and mechanical stability to the adsorbent without the need to crosslink or graft to the polymer chain. The authors argue that because the amine sites become blocked on chemical modification of chitosan, its efficacy as an adsorbent is reduced as there are fewer protonated groups to interact with the RB5 dye molecules. Montmorillonite was selected for its high cationic exchange capacity; when chitosan was intercalated with the clay it exhibited an improved sorption capacity to montmorillonite alone. The sorption capacity was found to decrease with increasing pH, due to decreased protonation of the amine sites as expected. However, the range of adsorption occurred over a wide solution pH range of pH 2 – 10. Therefore, while adsorption may not be at its optimum, it still occurs at alkaline pH like those commonly used in laundry.

Additionally, a cellulose-chitosan composite was considered for its RB5 adsorbance by El-Zawahry *et al*.[6] Cellulose is the world's most abundant biopolymer, and can be extracted from plants including the *Eichhornia crassipes* which is considered to be a problematic weed in Egypt. Cellulose therefore provides comparable economic favourability to chitosan. A chitosan-cellulose composite was formed and TiO_2 nanoparticles were incorporated to improve hydrophilicity and dispersity of the cellulose chains. The composite reached a maximum RB5 adsorption at pH 2 of 95%, however at pH 8 there was 65% uptake. The authors argue that the observed adsorption occurring at high pH is evidence for hydrogen bonding between RB5 and the composite, as electrostatic interactions would be reduced due to the amine groups becoming deprotonated. Whilst this study does not compare the efficacy of the composite in

comparison to cellulose or chitosan alone, it is clear the role of the amine groups in chitosan is not the only factor to consider for adsorption of RB5.

4.1.8 Chitosan for Reactive Black 5 Degradation

As well as adsorption, RB5 degradation also provides a promising route to dye-bath clean up, as long as the products obtained are not harmful.[31] An alternative to chitosan as an adsorbant is its use as a support for the reversible immobilisation of laccase, as studied by Bayramroglu *et al.*[32] Laccase is a copper containing enzyme that oxidises organic compounds, such as dyes like RB5. Chitosan was selected as a support as it can be modified with itaconic acid, which then chelates the copper ion of the laccase, immobilising it. Chitosan was selected not just because of its high functionality for modification, but also due to its natural origin and biodegradability. The optimum solution pH for activity of the laccase enzyme was found to shift from pH 4 when a free enzyme to pH 5.5 on immobilisation. Enzyme activity was also found to occur over a broader solution pH range for the immobilised enzyme. The degradation of RB5 was found to be 19% without a chemical mediator, and 43% in the presence of the degradation mediator acetosyringone. The study compared three dyes: RB5, Methyl Orange and Cibacron Blue F3GA all of which have extended aromatic compounds and sulfonate groups. The latter two dyes were found to undergo more extensive degradation (87% and 69%, respectively) upon interaction with the acetosyringone mediator. However, this study strongly indicates the value of immobilised enzymes in decolourisation of waste dye water, either in industry or in a laundry medium.

In addition to the immobilisation of enzymes, chitosan has been used to create chitosan-Cu(II)-Fe(III) complexes in a 1:1:1 ratio as reported by Rashid *et al.*[31] in order to catalyse the degradation of RB5 and other azo dyes with hydrogen peroxide, in conjunction with dye adsorption. The chitosan bimetal complex with hydrogen peroxide was found to remove RB5 from solution by 88.6% within ten minutes, compared to chitosan alone which only removed

32.2% and chitosan with hydrogen peroxide which removed 38.5% in the same time. The sorption capacity of the complex was examined in the absence of hydrogen peroxide and was found to be 527 mg g^{-1} of the adsorbent, having reached equilibrium within ten minutes. This result indicates the value of the complex simply as an adsorbant without the catalytic degradation of the dye. At pH 8, approximately 70% dye removal was observed within ten minutes, highlighting the fast-acting nature of the adsorbent even at higher pH. However, the use of hydrogen peroxide may provide contamination dangers to the environment itself and is not suitable for a laundry application. The use of the complex purely as an adsorbent may provide an interesting possibility, however.

4.1.9 Chitosan Hydrogels

Chitosan hydrogels are a widely explored material in biomedical applications, such as wound dressings.[33,34] However, they are infrequently applied to dye bath clean up applications, despite the wide use of chitosan in this field. A hydrogel is defined as a cross-linked network with the ability to withhold a large amount of water in its structure, without dissolving.[35,36] This is brought about by the balance between the amount of hydrophilic groups on the polymer backbone, and its crosslinked nature resisting dissolution. This in turn, creates materials which can possess over 90% water content but do not flow like a liquid, providing interesting properties that may be exploited in many fields of chemistry. Polysaccharides, such as chitosan, are able to form physical hydrogels, whereby they do not require covalent crosslinking, but instead form non-covalent crosslinks between the polymer chains.

4.1.10 Alginate and Cellulose Hydrogels

Alginate and cellulose are biopolymers that are capable of forming hydrogels. Alginate is extracted from seaweed, and as such is widely available, meanwhile, cellulose is the most abundant biopolymer available.[37–39] As alginate contains acid groups (Figure 4-5), alginate hydrogels will provide an insight into the effects of the acid groups in comparison to the amine groups of chitosan. Alginate has been investigated for its ability to adsorb dyes in the form of beads, composite hydrogels with polyacrylamide and microcapsules with chitosan.[40–43] There is therefore scope to examine the efficacy of an alginate hydrogel for its ability to adsorb pollutant dyes. Cellulose only contains hydroxy groups (Figure 4-5) and therefore may allow for the observation of the benefits or drawbacks of the amine or acid functional groups in the hydrogels. Cellulose has been widely researched as an adsorbant for dyes, in particular chemically modified cellulose, as well as membranes, fibres and beads.[44–49]

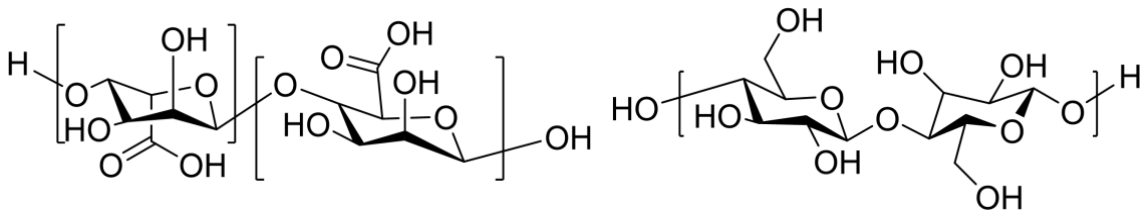

Figure 4-5 Structures of Left: Alginate Right: Cellulose.

4.1.11 Aims and Objectives

Chitosan hydrogels may provide a beneficial system which may be used for RB5 adsorption. The use of a physical chitosan hydrogels in unbuffered water for RB5 adsorption provides an economical, as well as ecological, route to dye uptake. Without chemical modification or addition, the risk of chemicals released to the environment is non-existent, and therefore is a credible option for ecological applications of the material. Additionally, hydrogels have a low chitosan content, usually less than 10% of the material weight, further adding to the economic benefits.

Physically crosslinked chitosan hydrogels were selected as a potential adsorbent for targeted RB5 uptake, and their ability to adsorb RB5 dye solution examined by UV-Visible spectroscopy. The hydrogels will also be applied to encapsulation and controlled release of protein molecules. This will be investigated by the hydrogel uptake of albumin, and pH-mediated protein release. This second function highlights the significant promise and versatility that the reported hydrogels have to be used as vehicles for the pH-mediated release of protein molecules for potential medicinal and personal care applications. Additional hydrogel-forming biopolymers alginate and cellulose will also be investigated for their ability to adsorb various dyes, alongside chitosan, and comparisons drawn between the three biopolymers.

4.2 Experimental

4.2.1 Ultraviolet-Visible Spectrophotometry

UV-Vis readings were carried out on an Agilent Technologies Cary 100 UV-Vis spectrophotometer, whereby an absorbance scan from 190 to 750 nm was performed. Samples were analysed in a quartz 1 mL UV-Vis cuvette. The uptake UV-Vis spectra were measured in deionised water, and the release studies were in ethanol.

4.2.2 Rheology Measurements

Rheological measurements were carried out at 25 °C using a stress-controlled AR 1500ex rheometer (TA instruments). The instrument was equipped with a steel-parallel plate geometry (40 mm in diameter) with the geometry gap distance maintained at 500 µm.

4.2.3 Optical Microscopy

A Nikon SMZ 1500 optical microscope imaged dye adsorption into chitosan hydrogels. Brightfield (illumination from fluorescent tube light box in transmission mode) image sequences were obtained using NIS-Advanced software-controlled operation of Nikon DS-Fi2 full colour CCD camera/DS-U3 controller system. Fluorescent microscopy for time-drive studies

of FITC-tagged albumin sequestration in chitosan hydrogels was conducted on Zeiss Observer Z1 with Zeiss LD A Pln 5x/0.15 Ph1 objective. Brightfield (full spectral illumination in transmission mode, intensity attenuated to avoid saturation) and fluorescence (filtered excitation light "GFP" centred at 488 nm, unfiltered emitted light detected in greyscale) image sequences were obtained using Zeiss Zen software-controlled operation of Zeiss Axiocam ICm1. Pixel intensity analysis was performed using ImageJ software.

4.2.4 pH Measurements

pH measurements were recorded using a Checker portable pH meter by Hanna Instruments.

4.2.5 Centrifugation, Sample Drying and Lyophilisation

Samples were separated by centrifuge with an MSE Mistral 3000i at 25 °C, 1000 rpm. A Buchi R-210 rotary evaporator and a FiStream vacuum oven were used to remove solvent and dry samples. Samples were lyophilised using a VirTis BenchTop Pro freeze dryer (SP Scientific).

4.2.6 Formation of Chitosan Hydrogels

Varying amounts of chitosan powder (Table 4-1) was added to deionised water (15 mL) with stirring. Concentrated HCl (0.3 mL) was then added, followed by ethanol (15 mL). This formed an off white, viscous liquid. The solution was placed in a vacuum oven for 24 hours at 30 °C. This solution was then added to aqueous NaOH solution (1 mol dm^{-3}, 75 mL) producing a white suspension, that was left for 24 hours at room temperature. The gel formed was separated from the remaining NaOH solution by centrifugation. The gels were then dialysed against water for 48 hours to decrease the solution pH to pH 7.

Table 4-1 Three chitosan hydrogels with their initial chitosan mass and water content.

Name	Chitosan Mass (g)	Mass of Gel Produced (g)	Water Content (%)
Hydrogel **1**	0.30	13.70	97.8
Hydrogel **2**	0.50	14.18	96.5
Hydrogel **3**	0.75	15.10	95.0

4.2.6.1 Chitosan Hydrogel Formation in the Presence of Reactive Black 5

The process described for Hydrogel **3** was then repeated, but RB5 (0.02 g) was included to form a hydrogel that contained RB5. Yield = 11.20 g

4.2.6.2 Adsorption of Reactive Black 5 by Chitosan Hydrogels

A sample of each chitosan hydrogel (0.5 g) was added to RB5 aqueous solution (4 mL, 0.1 mg mL^{-1}) and a sample of the supernatant was extracted (1 mL) at regular time intervals. The supernatant sample was immediately analysed by UV-Vis and the concentration of % dye uptake was determined using an RB5 calibration curve.

4.2.6.3 Release of Reactive Black 5 from Chitosan Hydrogels

Chitosan hydrogel formed in the presence of RB5 (0.5 g) was added to pH 3 Tris buffered aqueous solution. After 48 hours, no release of the dye was observed visually.

Hydrogel (0.5 g) loaded by an external solution of RB5 was incubated with various organic and aqueous solvents (5 mL) to assess the release of RB5. The solvents tested were: ethanol, methanol, ethyl acetate, water, DMF, THF, acetone, diethyl ether, phosphate buffered saline solution (pH 7.4), tris buffered pH 3 solution, Fairy detergent (1 mg mL^{-1}).

4.2.6.4 Adsorption of FITC-Albumin by Chitosan Hydrogels

Each hydrogel (0.5 g) was added to a FITC-albumin aqueous solution (2 mL, 0.5 mg mL^{-1}). At regular time intervals the absorbance of the external FITC-albumin solution was measured *via*

UV-Vis spectroscopy. The decreasing absorbance with time indicated the uptake of albumin by the hydrogel.

4.2.6.5 Release of FITC-Albumin from Chitosan Hydrogels

The hydrogels (0.5 g) were added to pH 5 and pH 3 solution (1 mL). The external solution was drained at regular time intervals for analysis and replaced with fresh solution (1 mL). The samples were analysed *via* UV-Vis spectroscopy to determine the extent of FITC-albumin release.

4.2.6.6 Adsorption of Disperse Dyes by Chitosan Hydrogels

Hydrogels 1, 2 and 3 were analysed for their ability to adsorb both C.I. Disperse Blue 3 and C.I. Disperse Orange 3. An aqueous solution of each dye (0.05 mg mL^{-1}, 2 mL) was added to each hydrogel (0.5 g). A sample of the external dye solution (0.5 mL) was analysed *via* UV-Vis spectroscopy at regular time intervals before being added back to the hydrogel to continue the adsorption study.

4.2.6.7 Release of Disperse Dyes from Chitosan Hydrogels

The hydrogels were washed with deionised water (20 mL) to remove surface dye. They were then added to ethanol (1 mL) which was removed after 30 seconds and replaced with fresh ethanol (1 mL). The UV-Vis spectrum of each sample of ethanol was measured and a cumulative absorbance was obtained.

4.2.6.8 Adsorption of Indigo and SB1 by Chitosan Hydrogel

Indigo dye bleeding fabric was washed at 40 °C for 30 minutes at 400 rpm in deionised water on a James Heal GyroWash[2]. The wash water containing Indigo dye (2 mL) was added to chitosan Hydrogel **3** (1 g). The same procedure was also carried out for C.I. Sulfur Black 1 (SB1) dye bleeding fabric.

4.2.7 Formation of Cellulose Hydrogel

Cellulose powder (0.5 g, Table 4-2) was suspended in 10% $NaOH_{(aq)}$ solution (12.5 mL) for 3.5 hours. This suspension was then frozen with $N_{2(l)}$ and left to thaw with stirring for 72 hours. This yielded a clear, viscous liquid. Yield = 14.45 g. pH 12. The liquids were then dialysed against deionised water for four days which formed a brittle, compact, white gel.

Table 4-2 Cellulose hydrogel with initial cellulose mass and water content.

Name	Cellulose Mass (g)	Mass of Gel Produced (g)	Water Content (%)
Hydrogel **4**	0.50	5.0	95.0

4.2.7.1 Adsorption of Reactive Black 5 by a Cellulose Hydrogel

Cellulose Hydrogel **4** (0.75 g) was injected with $RB5_{(aq)}$ solution (0.5 mL, 1 mg mL^{-1}). The gel did not appear to adsorb any dye initially. After 24 hours, the gel had completely turned blue however, the supernatant was also still coloured blue suggesting low level affinity for the dye by the cellulose.

4.2.7.2 Indigo and SB1 Adsorption by a Cellulose Hydrogel

Indigo dye bleeding fabric was washed at 40 °C for 30 minutes at 400 rpm in deionised water on a James Heal GyroWash[2]. The wash water containing indigo dye (2 mL) was added to cellulose Hydrogel **4** (1 g). The hydrogel was incubated for 24 hours in the dye extract solution.

4.2.8 Formation of Alginate Hydrogel

Alginic acid sodium salt powder (0.2 g) was dissolved in deionised water (10 mL). Calcium chloride solution of varying concentrations (Table 4-3) were added dropwise to the alginate solution to immerse the alginate. This mixture was then stored at 5 °C for 12 hours and then rinsed with deionised water to remove excess calcium chloride. This formed three alginate hydrogels.

Table 4-3 Three alginate hydrogels and the concentration of $CaCl_2$ used for crosslinking.

Name	Alginic Acid Mass (g)	$CaCl_2$ Concentration (g mol^{-1})	Mass of Gel Produced (g)	Water Content (%)
Hydrogel **5**	0.20	0.0150	6.3	98.36
Hydrogel **6**	0.20	0.0225	6.1	97.72
Hydrogel **7**	0.20	0.0300	5.2	96.15

4.2.9 Adsorption of Basic Dyes by Alginate, Cellulose and Chitosan Hydrogels

The hydrogels (0.5 g) were added to crystal violet or methylene blue solution (2 mL, 0.01 mg mL^{-1}). A sample was taken of the external dye solution at regular time intervals and a UV-Vis spectrum obtained. This was then returned to the solution the hydrogel was stored in to allow further adsorption to occur.

4.2.9.1 Release of Basic Dyes by Alginate Hydrogels

The hydrogels (0.5 g) were added to ethanol (1 mL). After 30 seconds the ethanol was removed and replaced with fresh ethanol. This was repeated until total release of the dye occurred. The removed ethanol solution aliquots were analysed by UV-Vis spectroscopy and the cumulative release determined.

4.3 Results and Discussion

A number of materials were produced that possess appropriate features to be considered suitable for use as dye adsorbents. Such features include having appropriate chemical properties for dye adsorption, ease of formation and the capability to produce the materials from renewable feedstock.

4.3.1 Chitosan Hydrogels

Initially, chitosan-based hydrogels were created with the rationale that the primary amine groups within the polymer structure may enable the material to participate in electrostatic interactions and/or hydrogen bonding with target dye molecules.

4.3.1.1 Chitosan Hydrogel Formation

The pK_a value of the d-glucosamine units of chitosan enables physical hydrogel formation as first reported by Ladet *et al.*[36] Dissolving chitosan in acidic solution, before returning the solution to neutral pH enabled the spontaneous formation of three different chitosan hydrogels.

4.3.1.2 Rheological Studies

The formation of the hydrogels was confirmed by a frequency sweep performed at 25 °C. This measures the storage modulus (G') and the loss modulus (G'') of the material in response to an applied frequency (Figure 4-6). The G' of an ideal gel dominates the G'', which indicates it will flow over a prolonged period of time.

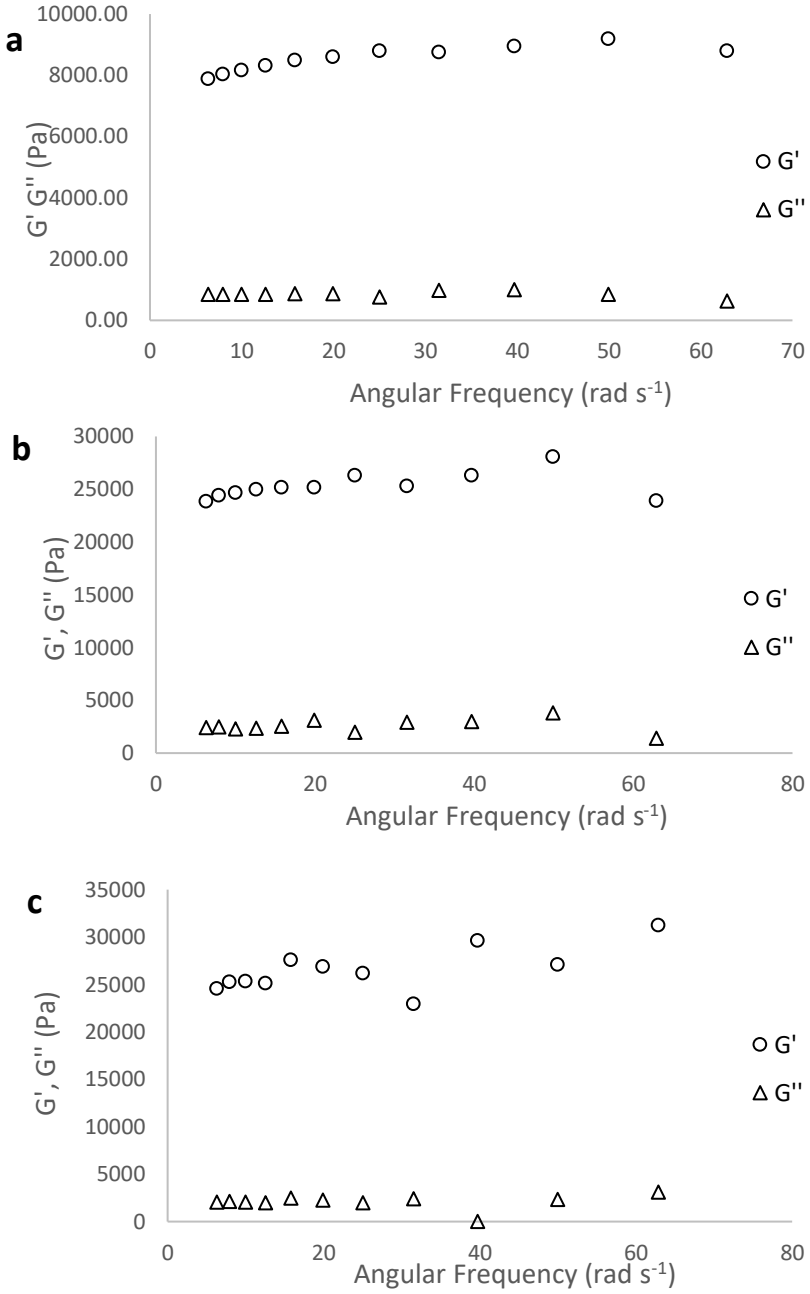

*Figure 4-6 Rheological analysis of chitosan hydrogels a). Hydrogel **1**, b). Hydrogel **2**, and c). Hydrogel **3.***

In Figure 4-6 it can be observed for all three chitosan hydrogels, that the G' value is larger than the G'' by an order of magnitude. The results of the rheological analysis therefore confirm the successful formation of hydrogels in each instance. The increasing amount of chitosan in the hydrogels increases the overall strength of the hydrogels. This is observable in the greater difference between the G' and G'' of Hydrogel **2** and **3** than that of Hydrogel **1**.

4.3.1.3 Adsorption of C.I. Reactive Black 5 by Chitosan Hydrogels

The zeta potential of chitosan at pH 7 was measured to be 12±4.5 mV, which is in agreement with reported values.[50] Consequently, chitosan possesses an overall positive charge under neutral conditions, and therefore electrostatic interactions may be used for the adsorption of anionic species, for instance RB5. Hydrogelation of chitosan provides a convenient physical form for the adsorption of RB5, avoiding the need for chemical modification of the chitosan, and the use of organic solvents in material production. As such, chitosan hydrogels provide an ideal material, created by relatively green chemistry, which may be applied to wastewater purification.

4.3.1.4 UV-Visible Spectroscopy Studies

The capability of Hydrogels **1, 2** and **3** to adsorb and withhold RB5 was investigated. The three hydrogels were added to aqueous RB5 stock solution and the absorbance at 598 nm by the external RB5 solution was periodically measured *via* UV-Vis spectroscopy (Figure 4-7).

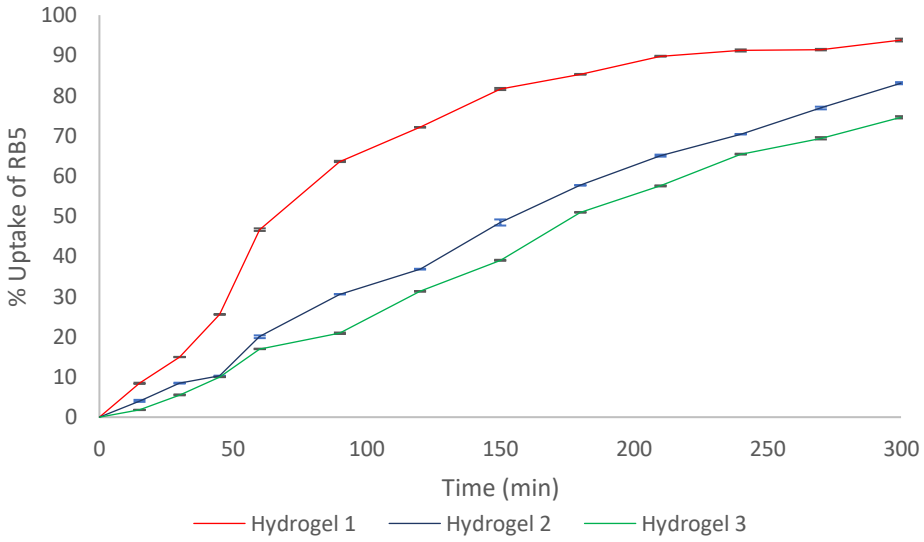

Figure 4-7 The uptake of RB5 solution by the three chitosan hydrogels.

In Figure 4-7, Hydrogel **1** shows the most rapid adsorption, with 93% absorption achieved within 300 minutes. However, the other two hydrogels are also effective adsorbants: Hydrogel **2** gives a dye uptake of 83% after 300 minutes and Hydrogel **3** shows 74% uptake.

4.3.1.5 Optical Microscopy

In order to monitor RB5 uptake visually, optical microscopy was employed to observe RB5 uptake from aqueous solution (0.1 mg mL^{-1}) by Hydrogel **2** over a period of 15 hours (Figure 4-8). ImageJ software can be used to analyse the mean pixel intensity of the images generated. It provides a tool for selecting an area of the hydrogel within the image, and determining the mean pixel intensity of this area. As such, the pixel intensity within the hydrogel can show the adsorption of the dye within it, and this data can be plotted against time to monitor dye adsorption by the hydrogel in real time (Figure 4-8).

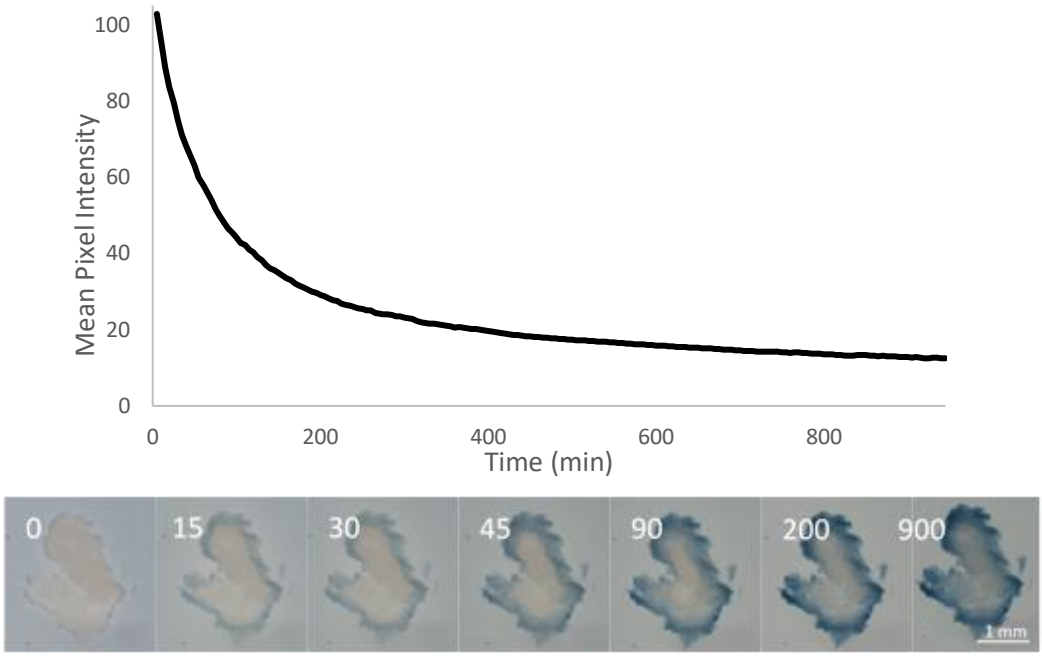

Figure 4-8 Top: ImageJ pixel intensity analysis within the hydrogel area. Bottom: Optical microscope image sequence of RB5 adsorption by Chitosan Hydrogel 2. The numbers represent the time (minutes) of hydrogel submersion within the dye solution.

The data in Figure 4-8 shows a decrease in pixel intensity of 77% over the first 300 minutes of incubation, before progression to 88% pixel intensity decrease after 945 minutes, thus signifying RB5 adsorption. This corresponds with the UV-Vis data produced, and further confirms the adsorption of RB5 by the chitosan hydrogel. Figure 4-8 also shows images of the chitosan hydrogel at 0 minutes (Left) and the same hydrogel following 900 minutes of immersion in RB5

solution (Right). After 22 hours the surrounding solution is colourless suggesting complete dye uptake by the hydrogel.

4.3.1.6 Reactive Black 5 Desorption

For the intended applications of waste dye adsorption and dye transfer inhibition, the hydrogel must not discharge the RB5 molecules back into solution. To test the capability of Hydrogel **3** to withhold RB5 molecules, the loaded hydrogel (0.38 mg in 0.5 g hydrogel) was stored in aqueous solutions of pH 3, 5, 7, 8 and pH 12 water (5 mL) for 24 hours without agitation at room temperature. Additional samples of Hydrogel **3** (0.5 g) were independently stored in a series of solvents (5 mL) at room temperature: chloroform, hexane, ethyl acetate, acetone, diethyl ether, ethanol and THF. The hydrogels were left for 24 hours to visually observe any release of the dye. Neither varying the solvent or the pH of aqueous solutions caused the dye to be released after 72 hours. This confirms the strong interaction between RB5 and the hydrogel, and the appropriateness of these materials for their intended applications.

4.3.1.7 Adsorption of FITC-Albumin by Chitosan Hydrogels

The chitosan hydrogels were then investigated for their ability to adsorb the model protein albumin *via* UV-Vis and fluorescence microscopy, which was possible due to the fluorescent tag, fluorescein isothiocyanate (FITC), conjugated to albumin (Figure 4-9). Hydrogels are particularly useful for the delivery of protein molecules that would otherwise need to be administered intravenously. Consequently, it is envisaged that the chitosan hydrogels produced may be used for the pH-triggered release of therapeutic protein guest molecules, which is of medicinal relevance, or may be employed as a dressing for chronic wounds. Chronic wounds show high levels of the protein elastase, which prevents wound healing.[51,52] Therefore, the adsorption and removal of proteins by polymeric hydrogel dressings has gained attention.[52–55]

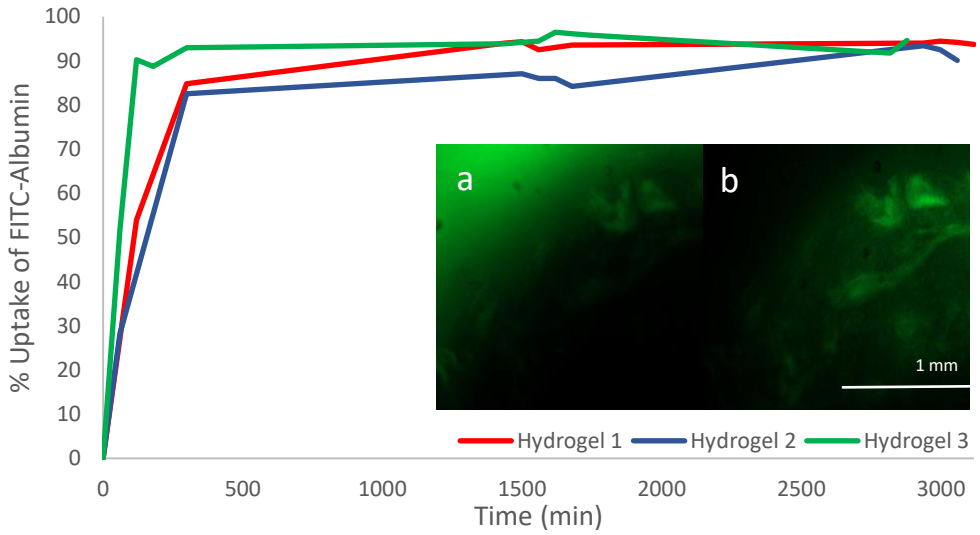

Figure 4-9 Main: Adsorption of FITC-albumin by three chitosan hydrogels; Insert: Fluorescence microscope image a). Before and b). After 12 hours incubation.

From Figure 4-9, it can be seen that the protein shows almost complete adsorption to the hydrogels after five hours. Hydrogel **2** plateaus at 85% uptake, whereas Hydrogel **3** shows the greatest amount of protein uptake of 95%. The fluorescence microscopy images show the albumin initially outside the hydrogel area (the hydrogel is the dark area in the bottom right corner of the image), and after 12 hours shows the preferential sequestration of the albumin within the hydrogel. Since the albumin is anionically charged, this rapid and almost complete adsorption further provides evidence for the significance of electrostatic intermolecular bonding for payload uptake by the chitosan hydrogels.

4.3.1.8 pH-Mediated Protein Release from Chitosan Hydrogels

In contrast to the hydrogels loaded with RB5, hydrogels loaded with FITC-labelled albumin were able to release the payload when stored in acidic solution (pH 3). This is due to the solution pH being below the isoelectric point of albumin (pH 4.3) and causing protein denaturation. The loss of the charge on the protein below its isoelectric point results in the loss of the electrostatic interactions between the chitosan and the protein, causing protein release. Washing of the FITC-albumin-loaded hydrogels with a series of solvents including ethanol, DMF, pH 7 solution and

pH 5 solution did not cause payload release. FITC-albumin may be released in its non-anionic form but cannot be released from chitosan hydrogels, by conventional washing methods, when it is present in its natural anionic form.

Protein release into acidic media was imaged by fluorescence microscopy over a 10 hour period, whereby the fluorescence is seen to be discharged from the hydrogel to the surrounding medium (Figure 4-10).

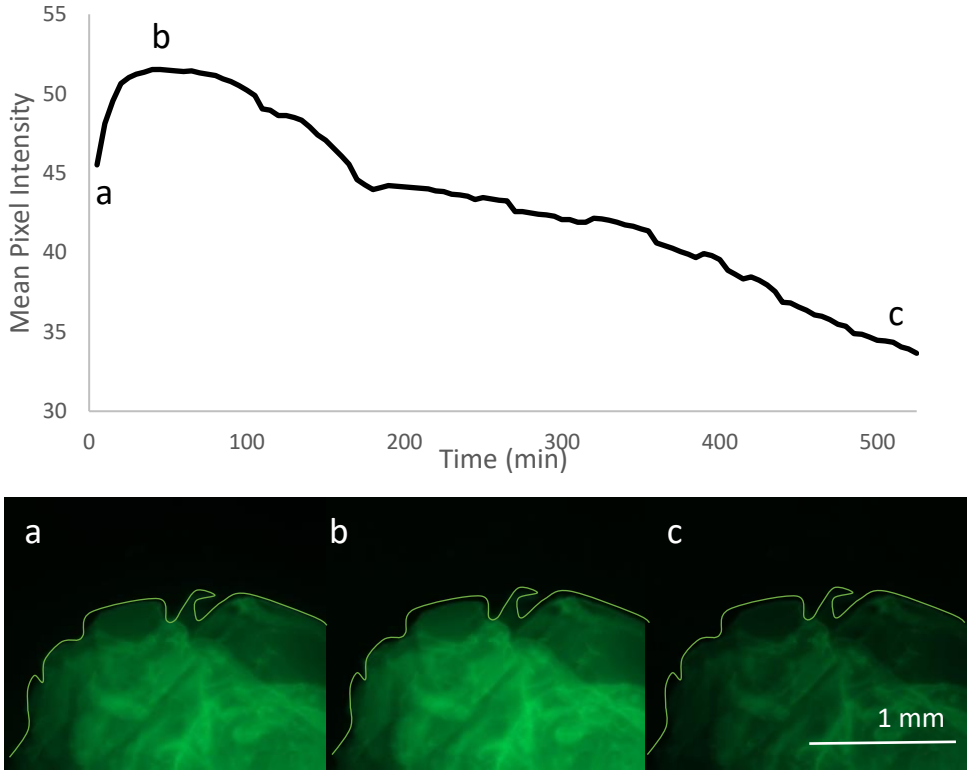

*Figure 4-10 Top: ImageJ pixel intensity analysis within hydrogel area. Bottom: Fluorescent microscope images a). At the start b). During and c). After FITC-albumin release from Chitosan Hydrogel **2**. The area of interest used for ImageJ analysis is the superimposed line in green on the hydrogel images.*

Figure 4-10 shows an initial increase and subsequent decrease in pixel intensity within the hydrogel. This may be due to the albumin travelling to the extremity of the hydrogel prior to release when first exposed to pH 3 solution. The pixel intensity then decreases below the original level, demonstrating that there is a reduced FITC-albumin concentration in the hydrogel, and thus the albumin has been released. As the microscope slide is a closed system the hydrogel is not totally decolourised after 10 hours, as an equilibrium between the hydrogel and the

surrounding solution is established. Nevertheless, FITC-albumin expulsion from the hydrogel is clearly observable.

4.3.1.9 Adsorption of C. I. Disperse Blue 3 and C. I. Disperse Orange 3 by Chitosan Hydrogels

Disperse dyes are sparingly water-soluble dyes, that are capable of dyeing synthetic fibres such as polyesters and acetate. During the dyeing process, some of the dye will deposit on the surface of the fibre, instead of undergoing fixation, and as such this can lead to dye redeposition in the laundry. Additionally, the dye bath effluent produced by the dyeing process is harmful to the environment. Therefore, chitosan hydrogels were investigated for their ability to adsorb two disperse dyes: C.I. Disperse Blue 3 (DB3) and C.I. Disperse Orange 3 (DO3) (Figure 4-11).

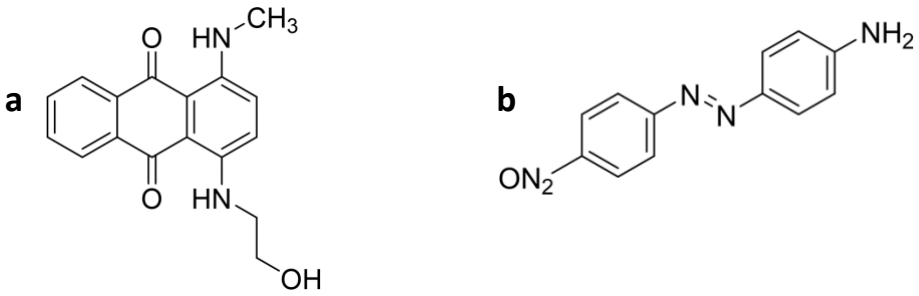

Figure 4-11 Structures of a). C.I. Disperse Blue 3 and b). C.I. Disperse Orange 3.

Unlike RB5, the two disperse dyes do not possess a charge, but are capable of hydrogen bonding with the chitosan.

The capability of the chitosan hydrogels to adsorb DB3 and DO3 was investigated *via* UV-Vis spectroscopy as 594 nm and 443 nm respectively (Figure 4-12).

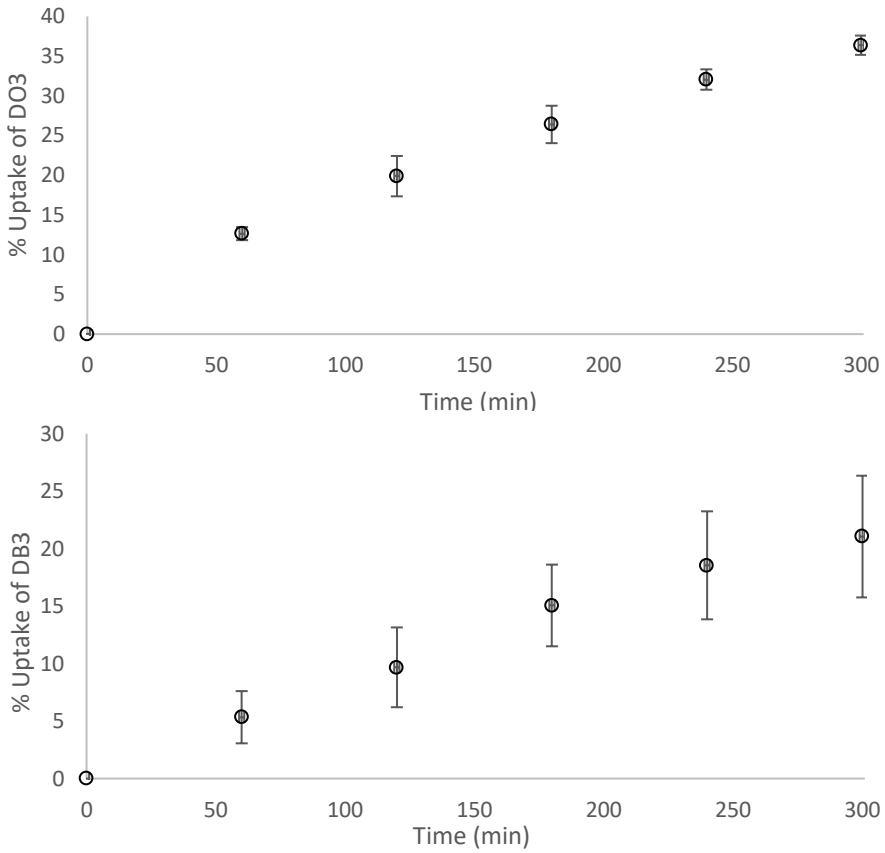

Figure 4-12 Top: Adsorption of DO3 at 443 nm; Bottom: Adsorption of DB3 at 594 nm.

Figure 4-12 shows that for DO3 adsorption, 36% dye uptake was achieved within 300 minutes, as assessed by UV-Vis spectroscopy, however DB3 adsorption was less effective, with 21% achieved in the same amount of time. Nevertheless, this result does serve to highlight that chitosan hydrogels are effective adsorbants for alternative dye classes to reactive dyes. Figure 4-13 shows the hydrogels loaded with DO3 (Left) and DB3 (Right).

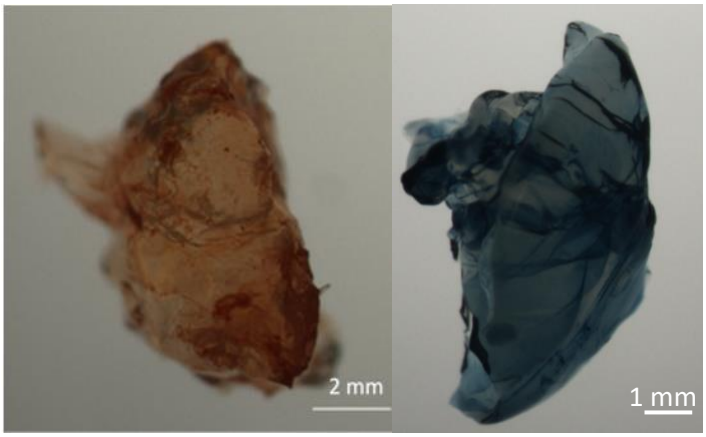

*Figure 4-13 Optical microscopy image of Hydrogel **2** loaded with Left: C.I Disperse Orange 3 and; Right: C.I. Disperse Blue 3.*

4.3.1.10 Release of Disperse Dyes by Chitosan Hydrogels

The release of the two disperse dyes, DO3 and DB3, from Hydrogel **2** was then investigated (Figure 4-14). The hydrogels did not show release of the dyes in water, therefore ethanol was used as a release medium owing to the superior solubility of the disperse dyes in ethanol compared to water. Release of the dyes in ethanol is particularly useful due to its low boiling point, allowing for easy recovery of the dye and the solvent.

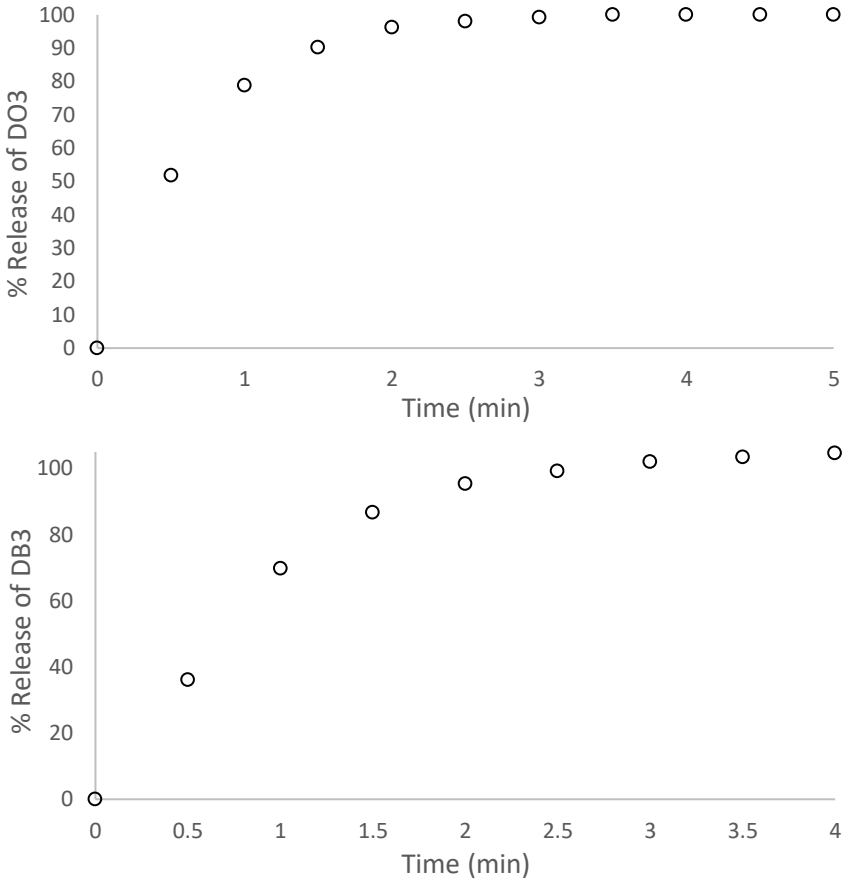

Figure 4-14 Top: Release of DO3 in ethanol at 443 nm; Bottom: Release of DB3 in ethanol at 594 nm.

Figure 4-14 shows that unlike for RB5, the two disperse dyes were rapidly released from the hydrogel when washed with ethanol. This demonstrates that the hydrogels may be recycled and used again when used to capture DB3 and DO3, an advantageous feature for adsorbents used in wastewater treatment.

4.3.1.11 Adsorption of Indigo by Chitosan Hydrogels

Indigo dye bleeding fabric was heated and agitated in water to extract Indigo dye. The capability of Chitosan Hydrogel **2** to adsorb and retain the extracted indigo was then assessed *via* UV-Vis spectroscopy at 603 nm (Figure 4-15).

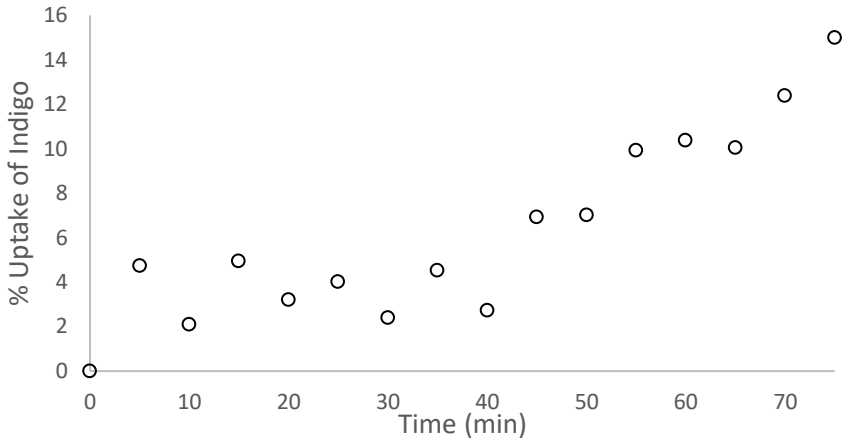

*Figure 4-15 Adsorption of indigo wash extract by Chitosan Hydrogel **2.***

In Figure 4-15, the chitosan hydrogel shows 15% absorbance of the indigo extract over 75 minutes of static incubation. The adsorption of indigo dye is not as rapid as that of RB5, however, it shows the hydrogel is capable of adsorbing this common dye to some extent.

4.3.1.12 Adsorption of C. I. Sulfur Black 1 by Chitosan Hydrogels

C.I. Sulfur Black 1 (SB1) was extracted from a dye bleeding fabric by agitation and heating in water. The affinity of the Chitosan Hydrogel **2** for SB1 was then assessed by UV-Vis spectroscopy at 599 nm (Figure 4-16).

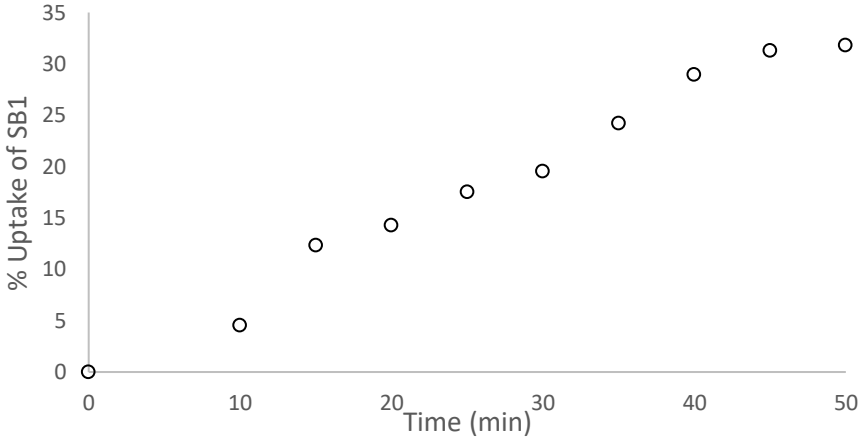

*Figure 4-16 Adsorption of SB1 wash extract by Chitosan Hydrogel **2.***

SB1 shows a fast rate of adsorption in Figure 4-16, reaching 31% uptake within 55 minutes. This may be due to anionic charge density provided by the nitro groups of SB1 that are able to electrostatically interact with the amine groups of chitosan.

4.3.2 Cellulose Hydrogels

Cellulose was selected as a hydrogelator owing to its abundance as a biopolymer, and the polar hydroxy groups which may form hydrogen bonds with appropriate target molecules. However, cellulose does not have amine groups as chitosan does, and so it is anticipated that the capability of cellulose hydrogels to adsorb anionic dye molecules such as RB5 would be limited, but their capability to adsorb cationic basic dyes may be investigated (Section 4.3.4.4)

4.3.2.1 Cellulose Hydrogel Formation

A cellulose hydrogel was produced using a freeze-thaw method. This was then investigated by rheological analysis to confirm production of a hydrogel (Figure 4-17).

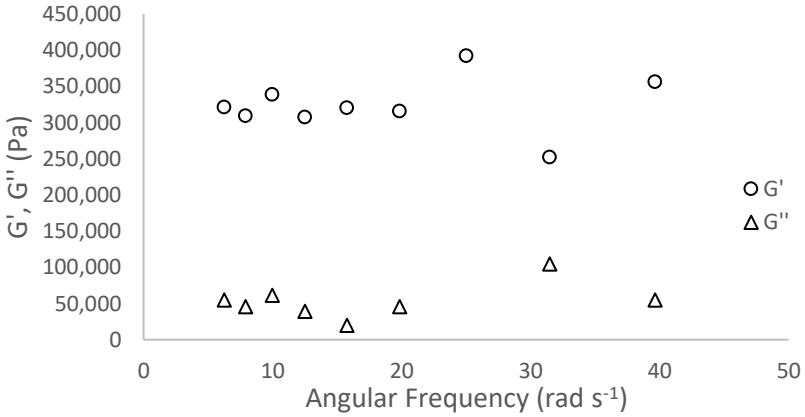

Figure 4-17 Rheological analysis of a cellulose hydrogel.

In Figure 4-17, the G' dominates the G'', thus indicating gelation has occurred successfully.

4.3.3 Alginate Hydrogels

4.3.3.1 Alginate Hydrogel Formation

Three alginate hydrogels were formed following the procedure described by Ko, Sfeir and Kumta, whereby alginic acid is dissolved in water and calcium chloride solution is added, creating Ca^{2+} physical crosslinks.[37] The rheological properties of the hydrogels were evaluated (Figure 4-18).

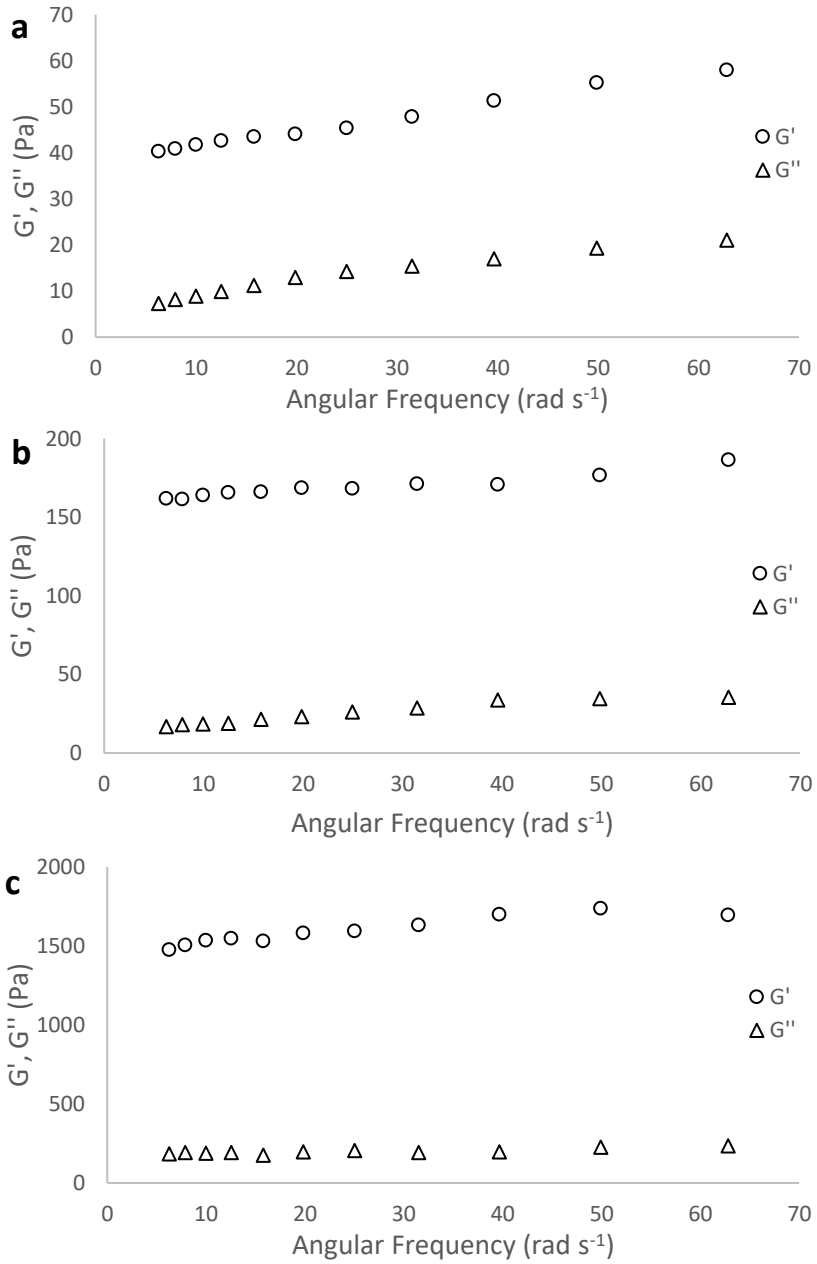

*Figure 4-18 Rheology studies for alginate hydrogels a). Hydrogel **5**, b), Hydrogel **6** and c). Hydrogel **7**.*

All three hydrogels in Figure 4-18 show a G' that dominates the G'', therefore indicating that a hydrogel has formed in each case.

4.3.4 Adsorption of Basic Dyes by Biopolymeric Hydrogels

Two cationic, basic dyes methylene blue (MB) and crystal violet (CV) were investigated for their ability to adsorb independently to alginate, chitosan and cellulose hydrogels (Figure 4-19).

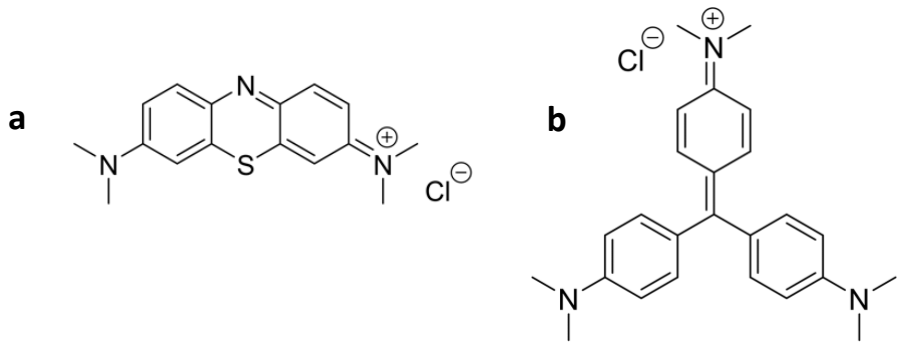

Figure 4-19 Structure of a). Methylene blue and b). Crystal violet.

Methylene blue and crystal violet are commonly used dyes for cellulose and silk colouration, as well as a biological staining, and both are gaining increasing interest as pharmaceuticals. However, they are both hazardous when released into the environment and must therefore be removed from aqueous effluents.

4.3.4.1 Adsorption by Alginate Hydrogels

The biopolymer alginate is anionic and as such it was expected to adsorb the cationic dyes in preference to the chitosan, which contains amines groups and would be expected to repel the dyes. Therefore, an alginate hydrogel was investigated for adsorption of crystal violet and methylene blue as analysed by UV-Vis at 590 nm and 670 nm respectively (Figure 4-20).

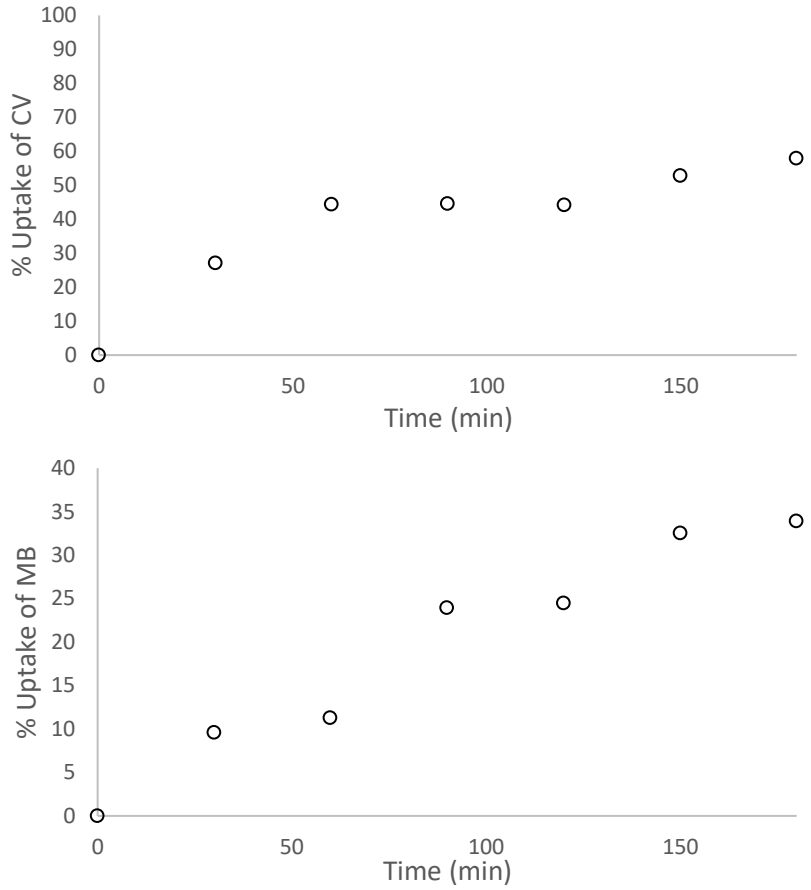

*Figure 4-20 Adsorption by alginate Hydrogel **6** of a). Crystal violet at 590 nm and b). Methylene blue at 670 nm.*

Alginate shows a far superior adsorption for crystal violet than for methylene blue in Figure 4-20, achieving 58% and 24% adsorption in 180 minutes respectively. Again, this may be due to the properties of the dyes, for example methylene blue is an extended, planar aromatic dye, unlike crystal violet which has more of a three-dimensional structure. This may mean crystal violet is less inclined to aggregate and is therefore more likely to penetrate the hydrogel.

4.3.4.2 Release of Basic Dyes by Alginate Hydrogels

Release of methylene blue and crystal violet was achieved by the introduction of ethanol, which the dyes are soluble in. The dye release rates were determined by UV-Vis spectroscopy (Figure 4-21).

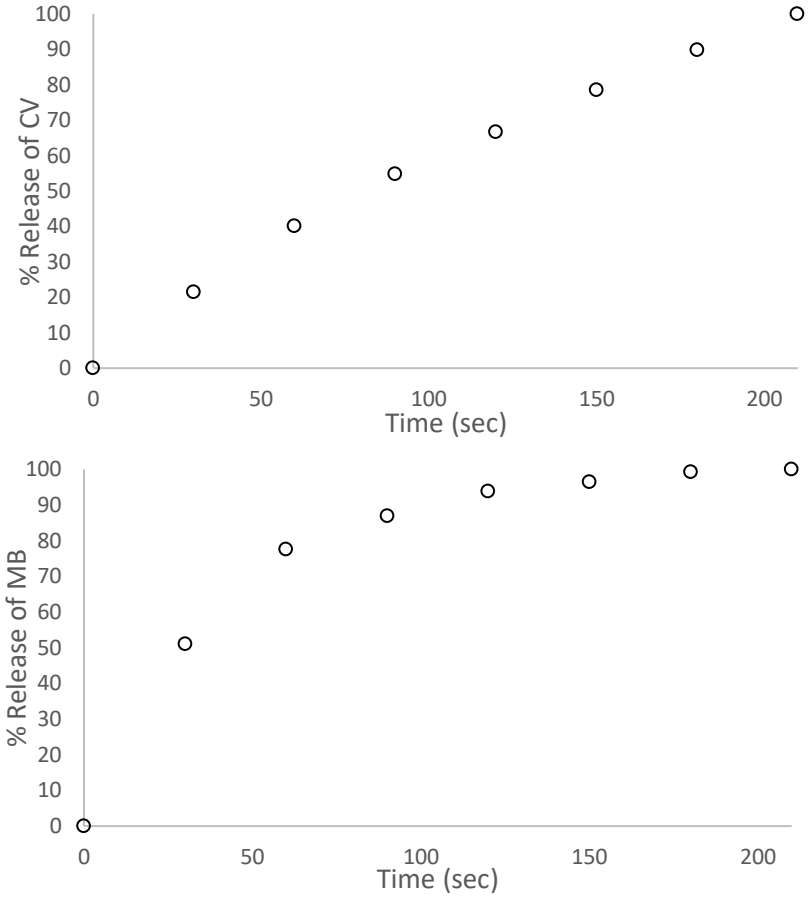

*Figure 4-21 Top: Release of crystal violet and, Bottom: Release of methylene blue from alginate Hydrogel **6**.*

In Figure 4-21, crystal violet shows slower desorption from the hydrogel than methylene blue. This provides further evidence for the greater affinity of crystal violet for the hydrogel than methylene blue. Both dyes show rapid desorption in ethanol, within three and a half minutes.

4.3.4.3 Adsorption by Chitosan Hydrogels

Adsorption of the two basic dyes, crystal violet and methylene blue, by Chitosan Hydrogel **2** was then investigated (Figure 4-22).

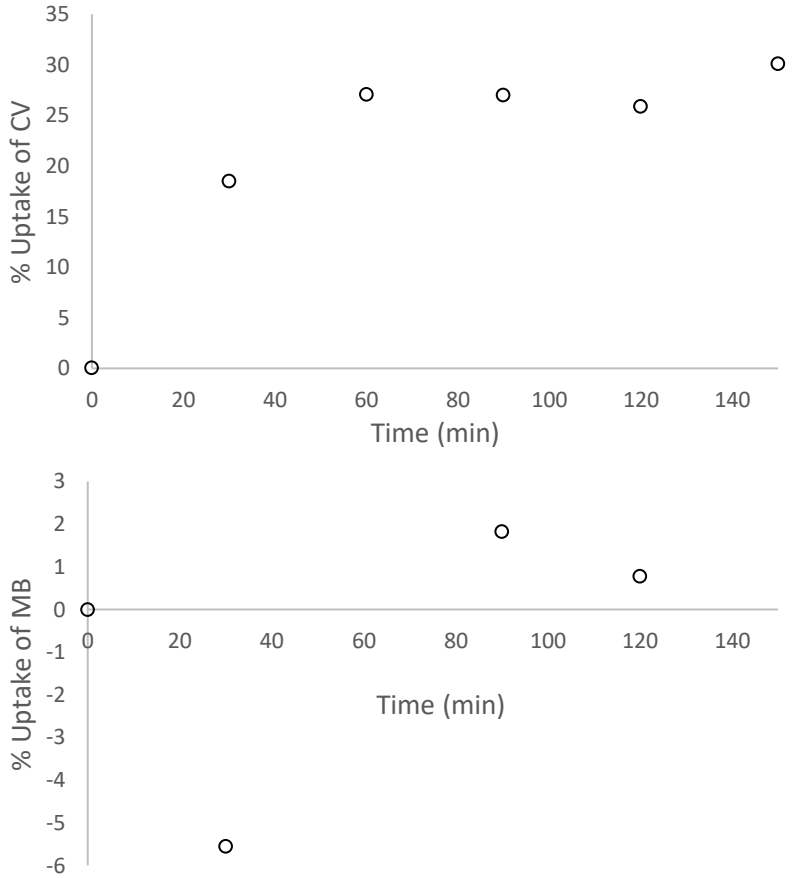

*Figure 4-22 Adsorption by Chitosan Hydrogel **2**, Top: Crystal violet at 590 nm and Bottom: Methylene blue at 670 nm.*

Methylene blue showed no adsorption to the chitosan hydrogel, however, crystal violet showed better adsorption, reaching 30% after 150 minutes in Figure 4-22. This is not as promising as adsorption by the alginate hydrogel (52% after 150 minutes). Therefore, it can be concluded that electrostatic interactions between the dye and polymer chains is key to quick and effective dye adsorption.

4.3.4.4 Adsorption of Basic Dyes by a Cellulose Hydrogel

A cellulose hydrogel was investigated for its ability to adsorb basic dyes. This was observed via UV-Vis spectroscopy (Figure 4-23).

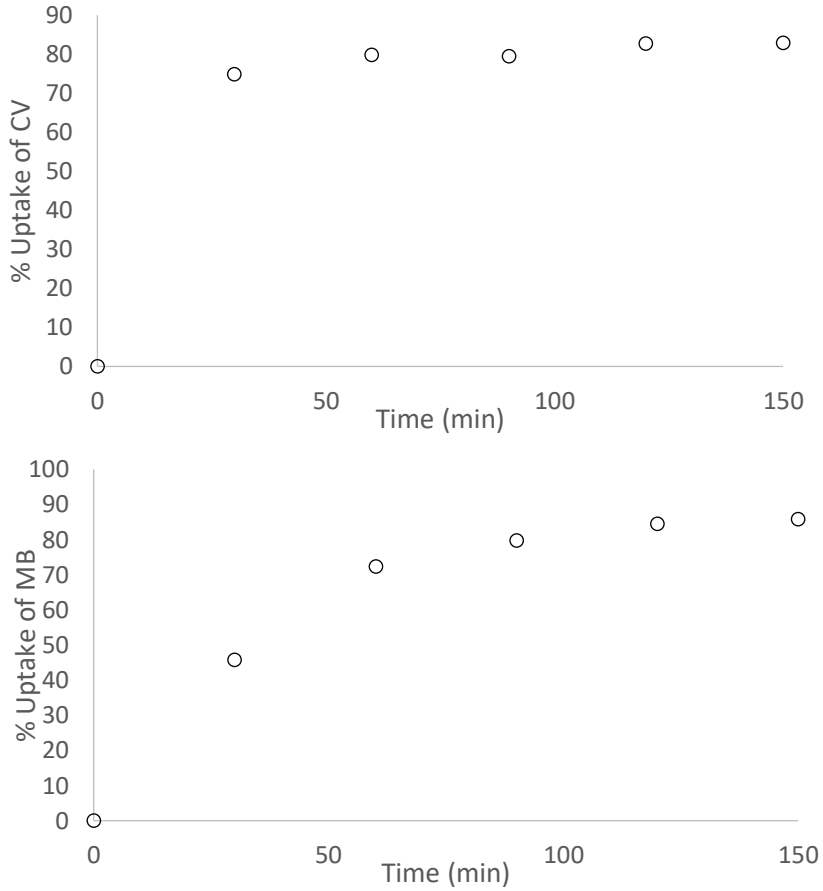

Figure 4-23 Top: Adsorption of crystal violet 590 nm and Bottom: Adsorption of methylene blue 670 nm by a cellulose hydrogel.

From Figure 4-23, it can be observed that crystal violet shows rapid adsorption to cellulose, achieving 75% within 30 minutes. 45% of methylene blue was adsorbed in the same time. This result is a significant improvement from both alginate and chitosan hydrogels. Release of crystal violet and methylene blue by the cellulose hydrogel on incubation with ethanol was not achieved, further confirming the affinity of the hydrogel for the dyes tested.

4.4 Conclusion

Initially chitosan, cellulose and alginate hydrogels were investigated for their adsorptive properties towards various classes of dyes. From the work undertaken, it has become apparent that dye adsorption is considerably aided by attractive electrostatic interactions. This is observable through the research into chitosan hydrogels and their adsorption of RB5 and disperse dyes. Chitosan Hydrogel **2** was able to adsorb 83% of a RB5 solution within 5 hours, whereas it only achieved 36% DO3 and 21% DB3 adsorption in this time. As the two disperse dyes are not charged, and RB5 is anionic it can be inferred this result is related to the charge.

This conclusion is further corroborated by the inability of the hydrogel to release RB5 in pH 3 solution, however, FITC-albumin was able to be released at this pH, owing to it being below the isoelectric point of the protein. As such, the protein is no longer charged, and the electrostatic interactions are removed.

Additionally, two cationic, basic dyes were investigated for their adsorptive properties towards alginate hydrogels, and chitosan hydrogels. 58% of crystal violet and 25% of methylene blue were adsorbed within 180 minutes by an alginate hydrogel, whereas the chitosan hydrogel showed 30% adsorption of crystal violet, and only 1% of methylene blue. The preference of the two dyes for alginate again suggest electrostatic interactions are necessary for dye adsorption.

The chitosan hydrogels showed good adsorptive properties towards indigo and C.I. Sulfur Black 1 wash extract. Indigo wash extract was adsorbed by 15% in 80 minutes, while SB1 was adsorbed by 31% in just 55 minutes. As SB1 possesses an anionically charged nitro group, it may be able to be adsorbed faster than uncharged indigo. This further indicates the requirement for attractive electrostatic interactions in the adsorption of dyes by polymer hydrogels.

4.5 References

[1] Hayashi T. and Thornton P.D. The synthesis and characterisation of thiol-bearing C. I.

Disperse Red 1. *Dyes and Pigments*. 2015 **121** 235–7

[2] Elwakeel K.Z., Abd El-Ghaffar M.A., El-Kousy S.M. and El-Shorbagy H.G. Enhanced Remediation of Reactive Black 5 from Aqueous Media Using New Chitosan Ion Exchangers. *Journal of Dispersion Science and Technology*. 2013 **34** (7) 1008–19

[3] Eren Z. and Acar F.N. Adsorption of Reactive Black 5 from an aqueous solution: equilibrium and kinetic studies. *Desalination*. 2006 **194** (1–3) 1–10

[4] Saha T.K., Bhoumik N.C., Karmaker S., Ahmed M.G., Ichikawa H. and Fukumori Y. Adsorption Characteristics of Reactive Black 5 from Aqueous Solution onto Chitosan. *CLEAN - Soil, Air, Water*. 2011 **39** (10) 984–93

[5] de Luna L.A.V., da Silva T.H.G., Nogueira R.F.P., Kummrow F. and Umbuzeiro G.A. Aquatic toxicity of dyes before and after photo-Fenton treatment. *Journal of Hazardous Materials*. 2014 **276** 332–8

[6] El-Zawahry M.M., Abdelghaffar F., Abdelghaffar R.A. and Hassabo A.G. Equilibrium and kinetic models on the adsorption of Reactive Black 5 from aqueous solution using Eichhornia crassipes /chitosan composite. *Carbohydrate Polymers*. 2016 **136** 507–15

[7] Uchiyama T., Kawauchi A. and DuVal D.L. Quick identification of polymeric dye transfer inhibitors in laundry detergents by pyrolysis-gas chromatography/mass spectrometry. *Journal of Analytical and Applied Pyrolysis*. 1998 **45** (2) 111–9

[8] Murugesan K., Dhamija A., Nam I.-H., Kim Y.-M. and Chang Y.-S. Decolourization of reactive black 5 by laccase: Optimization by response surface methodology. *Dyes and Pigments*. 2007 **75** (1) 176–84

[9] Arslan İ., Balcioğlu I.A. and Bahnemann D.W. Advanced chemical oxidation of reactive dyes in simulated dyehouse effluents by ferrioxalate-Fenton/UV-A and TiO2/UV-A processes. *Dyes and Pigments*. 2000 **47** (3) 207–18

[10] Karcher S., Kornmüller A. and Jekel M. Anion exchange resins for removal of reactive dyes from textile wastewaters. *Water Research*. 2002 **36** (19) 4717–24

[11] Sauer T., Cesconeto Neto G., José H.. and Moreira R.F.P.. Kinetics of photocatalytic degradation of reactive dyes in a TiO2 slurry reactor. *Journal of Photochemistry and Photobiology A: Chemistry*. 2002 **149** (1–3) 147–54

[12] Kim T.-H., Park C. and Kim S. Water recycling from desalination and purification process of reactive dye manufacturing industry by combined membrane filtration. *Journal of Cleaner Production*. 2005 **13** (8) 779–86

[13] Garg V.., Kumar R. and Gupta R. Removal of malachite green dye from aqueous solution by adsorption using agro-industry waste: a case study of Prosopis cineraria. *Dyes and Pigments*. 2004 **62** (1) 1–10

[14] Vakili M., Rafatullah M., Salamatinia B., Abdullah A.Z., Ibrahim M.H., Tan K.B., Gholami Z. and Amouzgar P. Application of chitosan and its derivatives as adsorbents for dye removal from water and wastewater: A review. *Carbohydrate Polymers*. 2014 **113** 115–30

[15] Sun J., Yan X., Lv K., Sun S., Deng K. and Du D. Photocatalytic degradation pathway for azo dye in TiO2/UV/O3 system: Hydroxyl radical versus hole. *Journal of Molecular Catalysis A: Chemical*. 2013 **367** 31–7

[16] Bharathi K.S. and Ramesh S.T. Removal of dyes using agricultural waste as low-cost

adsorbents: a review. *Applied Water Science*. 2013 **3** (4) 773–90

[17] Phan N.H., Rio S., Faur C., Le Coq L., Le Cloirec P. and Nguyen T.H. Production of fibrous activated carbons from natural cellulose (jute, coconut) fibers for water treatment applications. *Carbon*. 2006 **44** (12) 2569–77

[18] Gupta V.K. and Suhas Application of low-cost adsorbents for dye removal – A review. *Journal of Environmental Management*. 2009 **90** (8) 2313–42

[19] Crini G. Non-conventional low-cost adsorbents for dye removal: A review. *Bioresource Technology*. 2006 **97** (9) 1061–85

[20] Yu L., Liu X., Yuan W., Brown L.J. and Wang D. Confined Flocculation of Ionic Pollutants by Poly(l -dopa)-Based Polyelectrolyte Complexes in Hydrogel Beads for Three-Dimensional, Quantitative, Efficient Water Decontamination. *Langmuir*. 2015 **31** (23) 6351–66

[21] Li J., Su Z., Xu H., Ma X., Yin J. and Jiang X. Supramolecular Networks of Hyperbranched Poly(ether amine) (hPEA) Nanogel/Chitosan (CS) for the Selective Adsorption and Separation of Guest Molecules. *Macromolecules*. 2015 **48** (7) 2022–9

[22] Jiang R., Fu Y.-Q., Zhu H.-Y., Yao J. and Xiao L. Removal of methyl orange from aqueous solutions by magnetic maghemite/chitosan nanocomposite films: Adsorption kinetics and equilibrium. *Journal of Applied Polymer Science*. 2012 **125** (S2) E540–9

[23] Rinaudo M. Chitin and chitosan: Properties and applications. *Progress in Polymer Science*. 2006 **31** (7) 603–32

[24] Uzun İ. Kinetics of the adsorption of reactive dyes by chitosan. *Dyes and Pigments*. 2006 **70** (2) 76–83

[25] Guibal E. and Roussy J. Coagulation and flocculation of dye-containing solutions using a biopolymer (Chitosan). *Reactive and Functional Polymers*. 2007 **67** (1) 33–42

[26] Ong S.-T. and Seou C.-K. Removal of reactive black 5 from aqueous solution using chitosan beads: optimization by Plackett–Burman design and response surface analysis. *Desalination and Water Treatment*. 2014 **52** (40–42) 7673–84

[27] Sakkayawong N., Thiravetyan P. and Nakbanpote W. Adsorption mechanism of synthetic reactive dye wastewater by chitosan. *Journal of Colloid and Interface Science*. 2005 **286** (1) 36–42

[28] Burkinshaw S.M. and Paraskevas M. The dyeing of silk: Part 3 the application and wash-off of modified vinyl sulfone dyes. *Dyes and Pigments*. 2011 **88** (2) 212–9

[29] Sadeghi-Kiakhani M., Arami M. and Gharanjig K. Dye removal from colored-textile wastewater using chitosan-PPI dendrimer hybrid as a biopolymer: Optimization, kinetic, and isotherm studies. *Journal of Applied Polymer Science*. 2013 **127** (4) 2607–19

[30] Umpuch C. and Sakaew S. Adsorption characteristics of reactive black 5 onto chitosan-intercalated montmorillonite. *Desalination and Water Treatment*. 2015 **53** (11) 2962–9

[31] Rashid S., Shen C., Chen X., Li S., Chen Y., Wen Y. and Liu J. Enhanced catalytic ability of chitosan–Cu–Fe bimetal complex for the removal of dyes in aqueous solution. *RSC Advances*. 2015 **5** (110) 90731–41

[32] Bayramoglu G., Gursel I., Yilmaz M. and Arica M.Y. Immobilization of laccase on itaconic acid grafted and Cu(II) ion chelated chitosan membrane for bioremediation of hazardous

materials. *Journal of Chemical Technology & Biotechnology*. 2012 **87** (4) 530–9

[33] Boateng J.S., Matthews K.H., Stevens H.N.E. and Eccleston G.M. Wound Healing Dressings and Drug Delivery Systems: A Review. *Journal of Pharmaceutical Sciences*. 2008 **97** (8) 2892–923

[34] Khor E. and Lim L.Y. Implantable applications of chitin and chitosan. *Biomaterials*. 2003 **24** (13) 2339–49

[35] Ahmed E.M. Hydrogel: Preparation, characterization, and applications: A review. *Journal of Advanced Research*. 2015 **6** (2) 105–21

[36] Ladet S., David L. and Domard A. Multi-membrane hydrogels. *Nature*. 2008 **452** (7183) 76–9

[37] Ko H.-F., Sfeir C. and Kumta P.N. Novel synthesis strategies for natural polymer and composite biomaterials as potential scaffolds for tissue engineering. *Philosophical transactions. Series A, Mathematical, physical, and engineering sciences*. 2010 **368** (1917) 1981–97

[38] Ruel-Gariépy E. and Leroux J.-C. In situ-forming hydrogels—review of temperature-sensitive systems. *European Journal of Pharmaceutics and Biopharmaceutics*. 2004 **58** (2) 409–26

[39] Chang C. and Zhang L. Cellulose-based hydrogels: Present status and application prospects. *Carbohydrate Polymers*. 2011 **84** (1) 40–53

[40] Rocher V., Siaugue J.-M., Cabuil V. and Bee A. Removal of organic dyes by magnetic alginate beads. *Water Research*. 2008 **42** (4–5) 1290–8

[41] Lu L., Zhao M. and Wang Y. Immobilization of Laccase by Alginate–Chitosan Microcapsules and its Use in Dye Decolorization. *World Journal of Microbiology and Biotechnology*. 2007 **23** (2) 159–66

[42] Kurade M.B., Waghmode T.R., Xiong J.-Q., Govindwar S.P. and Jeon B.-H. Decolorization of textile industry effluent using immobilized consortium cells in upflow fixed bed reactor. *Journal of Cleaner Production*. 2019 **213** 884–91

[43] Fan J., Shi Z., Lian M., Li H. and Yin J. Mechanically strong graphene oxide/sodium alginate/polyacrylamide nanocomposite hydrogel with improved dye adsorption capacity. *Journal of Materials Chemistry A*. 2013 **1** (25) 7433

[44] He X., Male K.B., Nesterenko P.N., Brabazon D., Paull B. and Luong J.H.T. Adsorption and Desorption of Methylene Blue on Porous Carbon Monoliths and Nanocrystalline Cellulose. *ACS Applied Materials & Interfaces*. 2013 **5** (17) 8796–804

[45] Liu L., Gao Z.Y., Su X.P., Chen X., Jiang L. and Yao J.M. Adsorption Removal of Dyes from Single and Binary Solutions Using a Cellulose-based Bioadsorbent. *ACS Sustainable Chemistry & Engineering*. 2015 **3** (3) 432–42

[46] Luo X. and Zhang L. High effective adsorption of organic dyes on magnetic cellulose beads entrapping activated carbon. *Journal of Hazardous Materials*. 2009 **171** (1–3) 340–7

[47] Morais L.., Freitas O.., Gonçalves E.., Vasconcelos L.. and González Beça C.. Reactive dyes removal from wastewaters by adsorption on eucalyptus bark: variables that define the process. *Water Research*. 1999 **33** (4) 979–88

[48] Ma Z., Kotaki M. and Ramakrishna S. Electrospun cellulose nanofiber as affinity membrane. *Journal of Membrane Science*. 2005 **265** (1–2) 115–23

[49] Annadurai G., Juang R. and Lee D. Use of cellulose-based wastes for adsorption of dyes from aqueous solutions. *Journal of Hazardous Materials*. 2002 **92** (3) 263–74

[50] Saïed N. and Aider M. Zeta Potential and Turbidimetry Analyzes for the Evaluation of Chitosan/Phytic Acid Complex Formation. *Journal of Food Research*. 2014 **3** (2) 71

[51] Yager D.R. and Nwomeh B.C. The proteolytic environment of chronic wounds. *Wound Repair and Regeneration*. 1999 **7** (6) 433–41

[52] Schönfelder U., Abel M., Wiegand C., Klemm D., Elsner P. and Hipler U.-C. Influence of selected wound dressings on PMN elastase in chronic wound fluid and their antioxidative potential in vitro. *Biomaterials*. 2005 **26** (33) 6664–73

[53] Edwards J.V., Yager D.R., Cohen I.K., Diegelmann R.F., Montante S., Bertoniere N. and Bopp A.F. Modified cotton gauze dressings that selectively absorb neutrophil elastase activity in solution. *Wound Repair and Regeneration*. 2001 **9** (1) 50–8

[54] Cohen K. and Mohajer Y. Wound dressings containing complexes of transition metals and alginate for elastase sequestering. US20070009586A1. 2006

[55] Wiegand C., Abel M., Ruth P. and Hipler U.C. Superabsorbent polymer-containing wound dressings have a beneficial effect on wound healing by reducing PMN elastase concentration and inhibiting microbial growth. *Journal of Materials Science: Materials in Medicine*. 2011 **22** (11) 2583–90

Chapter 5. Modified Biopolymers and Biopolymeric Particles for Use as Dye Scavengers

Abstract

In order to produce a dye scavenging polymer or polymeric particle, chitosan and cellulose were modified to give various materials capable of preferentially adsorbing dyes in aqueous solution, thus reducing colour change in the laundry. Cellulose was modified with glycidyl trimethylammonium chloride, an epoxide containing a quaternary amine, to observe the effects of charge on dye transfer inhibition efficacy against indigo dye. In addition, physically and chemically crosslinked chitosan particles were formed and tested for their ability to prevent dye transfer. The particles with a negative zeta potential, and free acid groups, were found to reduce colour change. It was observed that the relationship between the charges of the dyes and the polymeric materials was key to preventing dye transfer.

5.1 Introduction

From the work in the previous chapter, chitosan, alginate and cellulose were found to effectively adsorb dyes in aqueous solution to decolour water. However, the hydrogel form may not be readily applied to the desired application of laundry dye transfer inhibition, as inclusion within a detergent formulation is not readily feasible and a hydrogel residue may remain on the clothes after washing. However, polymers or polymeric particles based on biopolymers such as cellulose, alginate or chitosan, may be able to act as adsorbants to scavenge the dyes in the wash liquor, and therefore prevent the dye depositing onto the fabric, reducing fabric colour change. These biopolymers are non-toxic, abundant in nature, and biodegradable.[1] Additionally, chitosan has antimicrobial properties which may provide a secondary benefit in a laundry application.[2]

5.1.1 Glycidyl Trimethylammonium Chloride-Modified Cellulouse

Glycidyl trimethylammonium chloride (GTAC) is a quaternary amine containing epoxide which can be grafted by ring-opening to hydroxy containing polymers in order to impart amine functionality (Figure 5-1). Cellulose contains hydroxy groups throughout its structure, therefore under basic conditions the hydroxy groups can react *via* nucleophilic substitution by an S_N2 pathway. This allows the ring-opening of the epoxide in GTAC, which introduces the quaternary amine to the cellulose structure through a newly created ether bond.

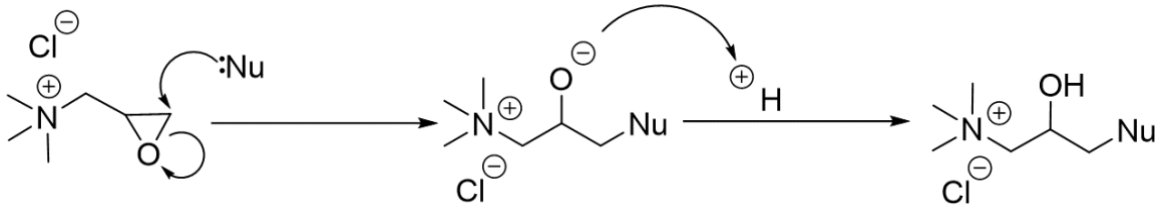

Figure 5-1 Nucleophilic substitution of glycidyl trimethylammonium chloride.

It was proposed that GTAC-modified cellulose would adsorb negatively charged dyes in the laundry wash preferentially, preventing dye transfer in the wash.

5.1.2 Chitosan Particles

The ability of a chitosan-based material to adsorb dyes from aqueous solution was assessed in the previous chapter, however the hydrogel form may not be readily applied to a laundry application as it may break apart from agitation in the laundry cycle, as well as creating an inconvenient waste product for the consumer to dispose of. Therefore, chitosan particles that can be added to a detergent formulation and washed away at the end of the laundry cycle were proposed to create a DTI that is convenient for the consumer, while maintaining the benefits of the hydrogel. Chitosan particles would be able to adsorb the dye from the wash liquor, thus preventing the deposition of the dye onto the fabric.

5.1.2.1 Physically Crosslinked Chitosan Particles

Chitosan particles can be created, whereby the crosslinks are formed through non-covalent bonding, such as electrostatic interactions between the amines of chitosan and a polyanion.

Chitosan-polyethyleneimine microspheres were investigated for their ability to entrap anionic DNA for vaccination against hepatitis B.[3] Polyethyleneimine was used to complex the DNA and condense it into nanoparticles, which was then entrapped in chitosan to form particles. To render the chitosan more hydrophilic, it was chemically modified with mannose to impart water-solubility, and both non-modified and modified chitosan particles were tested for their release of the DNA complex. The microspheres with modified chitosan were found to release 40% of the DNA over 14 days, whereas the non-modified chitosan microspheres released 10% over the same period of time, showing that the controlled *in vitro* release of the DNA can be tuned.

Tripolyphosphate (TPP, Figure 5-2) is a polyanion which has been widely reported for its ability to form electrostatic crosslinks with chitosan.[4–6] Chitosan-TPP particles have been assessed for a variety of applications, including for controlled drug delivery.[7] Shu and Zhu reported the formation of chitosan-TPP particles which, when coated with alginate, form a complex film. The particles provided an improved controlled release profile of the model drug, which achieved 90% loading.[7] The model drug used was a poorly water-soluble dye, brilliant blue, and therefore the efficacy of the chitosan-TPP particles to adsorb the dye provides scope for the application to dye transfer inhibition in laundry detergents.

Chitosan-TPP particles were also assessed for their antimicrobial activity by Pan *et al*.[8] The study found that chitosan-TPP particles had a greater antimicrobial activity against a range of bacteria, such as *Staphylococcus aureus* and *Escherichia coli*, compared to chitosan alone. Chitosan is an effective antimicrobial, and may provide a significant secondary benefit to its inclusion in detergent formulations.[9]

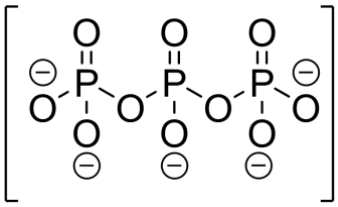

Figure 5-2 Structure of tripolyphosphate.

Polyelectrolyte complexes may be formed between two polymers containing oppositely charged groups, for example the amine groups on chitosan with the acid groups on alginate, and have been explored for their ability to encapsulate drugs for controlled release applications.[10–13] Katuwavila *et al.* compared chitosan-alginate particles to chitosan-TPP particles for their encapsulation efficiency of anti-cancer drug doxorubicin, and found that the polyelectrolyte particles were 95% more efficient at drug loading, and a higher cumulative drug release. As doxorubicin has an aromatic and rigid structure (Figure 5-3) it is comparable to dye molecules, and therefore these results suggest that the chitosan-alginate particles may also be effective dye transfer inhibitors. Consequently, such particles will be analysed and tested for their DTI efficacy, alongside chitosan-TPP particles.

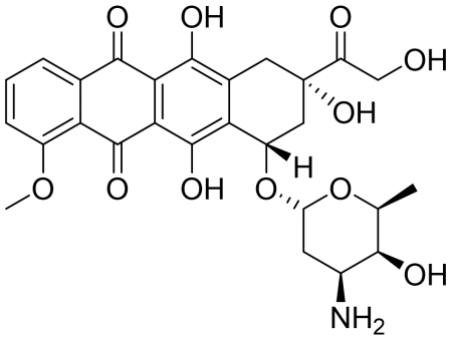

Figure 5-3 Structure of doxorubicin.

5.1.2.2 Chemically Crosslinked Chitosan Particles

Chitosan particles may also be formed by chemical crosslinking, whereby a multivalent molecule reacts to form covalent bonds with two chitosan chains, yielding a crosslinked particle.

Chitosan may be crosslinked by reaction with glutaraldehyde, a small molecule dialdehyde, to form imine crosslinks (Figure 5-4).[14]

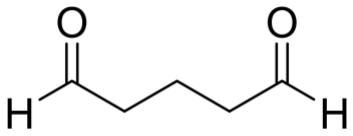

Figure 5-4 Structure of glutaraldehyde.

Crosslinked chitosan has been widely investigated for its ability to immobilise proteins, encapsulate drugs, and for its ability to adsorb dyes and other pollutants, in the form of an aerogel as well as nanoparticles.[15–18] For example, Riegger *et al.* investigated the use of chitosan-glutaraldehyde nanoparticles for their ability to adsorb the painkiller diclofenac (Figure 5-5), achieving a rapid sorption rate of less than two minutes. As with doxorubicin, diclofenac has aromatic groups and is structurally similar to dye molecules; the effective encapsulation of the drug provides scope for encapsulation of dye molecules as well.

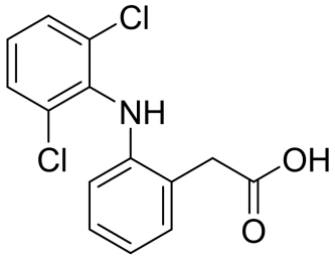

Figure 5-5 Structure of diclofenac.

Additionally, the amine group present in chitosan may form an amide by reaction with carboxylic acids *via* a coupling reaction using *N*-(3-dimethylaminopropyl)-*N*'-ethylcarbodiimide hydrochloride (EDC·HCl, Figure 5-6).

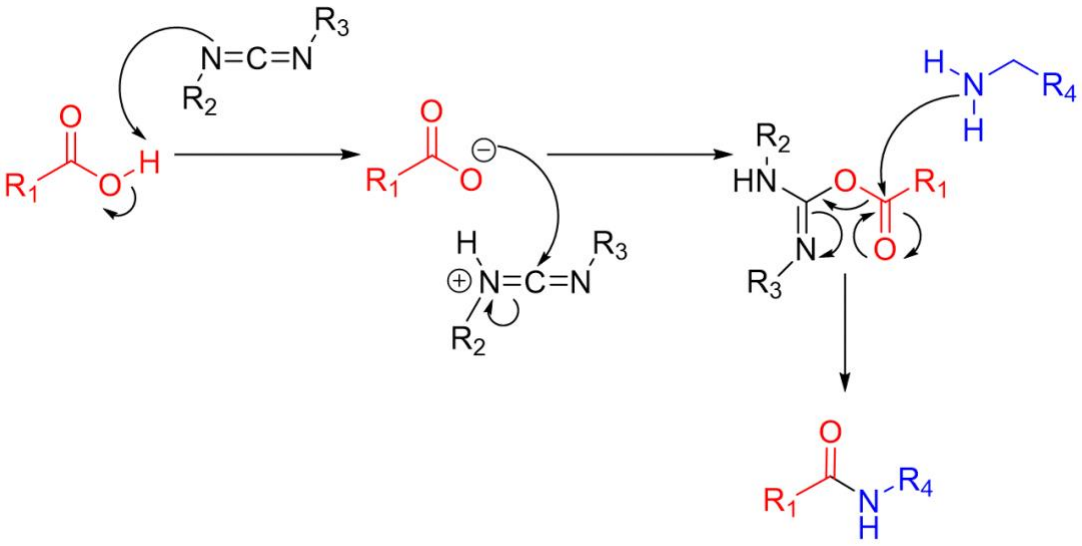

Figure 5-6 EDC coupling to form an amide bond between a primary amine and a carboxylic acid.

Dicarboxylic acids can therefore be used as crosslinkers of chitosan.[19] Bodnar, Hartmann and Borbely reported the formation of chitosan particles using EDC coupling of naturally occurring dicarboxylic acids: citric acid, tartaric acid, succinic acid and malic acid (Figure 5-7).

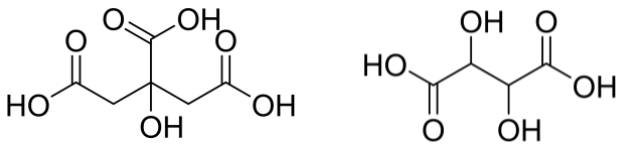

Figure 5-7 Left: Citric acid and Right: Tartaric acid.

Through this route, a variety of charged particles can be achieved. A polycationic material may be produced on the crosslinking of chitosan with a low level of dicarboxylic acid, where the remaining amine groups are not involved in crosslinking. On further crosslinking, the amine groups may become fully reacted to yield a neutral, non-ionic particle. Citric acid contains three carboxylic acid groups and therefore is able to crosslink chitosan and create polyampholytic particles, if there are free amine groups present on the chitosan and free acid groups on the citric acid. On further addition of citric acid, a polyanionic particle will be produced if all the amine groups react, leaving just carboxylate groups from the citric acid. This may provide a route

to creating particles which are capable of scavenging anionic and cationic dyes from the wash liquor in order to prevent dye transfer. Therefore, citric acid crosslinked chitosan particles were made and tested against a variety of dyes for their dye transfer inhibition (DTI) efficacy, as well as chitosan-tartaric acid particles. As the same molar amounts of citric acid or tartaric acid were added, analogous particles were made. Therefore, the tartaric acid particles contain fewer hydroxy groups, and serve as a comparison to the chitosan-citric acid particles.

5.2 Experimental

5.2.1 Fourier Transformed Infrared (FTIR) Spectroscopy

Infrared spectra were obtained on a Bruker Platinum FTIR-ATR spectrometer, using a diamond attenuated total reflectance (ATR) accessory, completing 32 scans in total. Bruker OPUS7.0 software was used to analyse the spectra. TRIOS software was used to plot and analyse the data.

5.2.2 Dynamic Light Scattering (DLS) and Zeta Potential Measurements

A Malvern Instrument ZetaSizer Nano ZSP with a 4mW He-Ne laser at 633 nm, and using an avalanche photodiode detector. The scattered light was collected at an angle of 173°. Measurements were run in triplicate and obtained at 25 °C, using a measurement position of 2.00 mm. Zeta potential values were measured in a folder capillary zeta cell in deionised water.

5.2.3 Centrifugation, Sample Drying and Lyophilisation

Samples were separated by centrifuge with an MSE Mistral 3000i at 25 °C, 1000 rpm. A Buchi R-210 rotary evaporator and a FiStream vacuum oven were used to remove solvent and dry samples. Samples were lyophilised using a VirTis BenchTop Pro freeze dryer (SP Scientific).

5.2.4 GyroWash^2 Studies

Multifibre and dye bleeder washes were performed on a James Heal GyroWash^2 set at 40 °C, for 30 minutes at 40 rpm. The multifibre and dye bleeding fabrics were cut to 4x10 cm swatches

and washed in deionised water (50 mL) or polymer solution (50 mL, 0.1 mg mL^{-1}), with 25 ball bearings. Colour changes were measured using a Spectraflash DataColor unit, which measured the L* a* and b* coordinates, which can be compared to an unwashed sample to give a colour change (ΔE) value. Measurements were made under D65 lighting.

5.2.5 Nanocellulose Modified with Glycidyl Trimethylammonium Chloride

5.2.5.1 Low GTAC Modification of Nanocellulose

An aqueous sodium hydroxide solution (0.140 g in 0.3 mL) was added to nanocellulose gel (4 g, 2.8% nanocellulose in water) and was stirred for one hour. Glycidyl trimethylammonium chloride (GTAC, 0.213 mg, 0.014 mmol) was added dropwise and left to stir for four hours. The resulting suspension was washed *via* centrifugation four times with deionised water (40 mL) and lyophilised. Yield: 0.0825 g

FTIR (cm^{-1}): 3338 (N-H), 3277 (O-H, alcohol), 2902 (C-H, alkyl), 1653 (N-H, bending), 1454 (C-H, alkyl), 1427 (O-H, bending), 1335 (O-H, bending), 1315 (C-N, amine), 1160 (C-O, ether), 1052 (C-N, amine).

5.2.5.2 High GTAC Modification of Nanocellulose

An aqueous sodium hydroxide solution (0.140 g in 0.3 mL) was added to nanocellulose gel (4 g, 2.8% nanocellulose in water) and was stirred for one hour. GTAC (0.47 mg, 0.031 mmol) was added dropwise and left to stir for four hours. The resulting suspension was washed *via* centrifugation four times with deionised water (40 mL) and lyophilised. Yield: 0.095 g

FTIR (cm^{-1}): 3339 (N-H), 3278 (O-H, alcohol), 2902 (C-H, alkyl), 1636 (N-H, bending), 1471 (C-H, alkyl), 1427 (O-H, bending), 1366 (O-H, bending), 1314 (C-N, amine), 1124 (C-O, ether), 1054 (C-N, amine).

5.2.6 Formation of Chitosan Particles Crosslinked with Tripolyphosphate

5.2.6.1 17% TPP to Chitosan by Mass

Chitosan was dispersed in deionised water (100 mL, 1 mg mL^{-1}). The pH was adjusted to 4.5 using concentrated acetic acid and was stirred for one hour to allow the chitosan to dissolve. Separately, sodium tripolyphosphate (TPP) was dissolved in deionised water (20 mL, 1 mg mL^{-1}) and also stirred for one hour. The TPP solution was added dropwise to the chitosan solution with stirring. The combined solution was diluted with deionised water (840 mL) in order to produce a final chitosan concentration of 0.1 mg mL^{-1}. This gave an opalescent solution. Portions of this solution (50 mL) were directly used in the colour change studies.

5.2.6.2 14% TPP to Chitosan by Mass

Chitosan was dispersed in deionised water (24 mL, 1 mg mL^{-1}). The pH was adjusted to 4.5 using concentrated acetic acid and was stirred for one hour to allow the chitosan to dissolve. Separately, TPP was dissolved in deionised water (4 mL, 1 mg mL^{-1}) and also stirred for one hour. The TPP solution was added dropwise to the chitosan solution with stirring. The combined solution was diluted with deionised water (206.4 mL) in order to produce a final chitosan concentration of 0.1 mg mL^{-1}. This gave an opalescent solution. Portions of this solution (50 mL) were directly used in the colour change studies.

5.2.6.3 12% TPP to Chitosan by Mass

Chitosan was dispersed in deionised water (21 mL, 1 mg mL^{-1}). The pH was adjusted to 4.5 using concentrated acetic acid and was stirred for one hour to allow the chitosan to dissolve. Separately, TPP was dissolved in deionised water (3 mL, 1 mg mL^{-1}) and also stirred for one hour. The TPP solution was added dropwise to the chitosan solution with stirring. The combined solution was diluted with deionised water (183.75 mL) in order to produce a final chitosan

concentration of 0.1 mg mL^{-1}. This gave an opalescent solution. Portions of this solution (50 mL) were directly used in the colour change studies.

5.2.7 Formation of Chitosan Particles Crosslinked with Citric Acid

5.2.7.1 10% Citric Acid to Chitosan by Molar Ratio of Reactive Chitosan Groups

Chitosan was dispersed in deionised water (10 mL, 0.25 mg mL^{-1}). The pH of the resultant dispersion was adjusted to 4.5 using concentrated acetic acid and was stirred for one hour to allow the chitosan to dissolve. Separately, citric acid monohydrate was dissolved in deionised water (5 mL, 4.8 mg mL^{-1}) the pH was then adjusted to 6.5 using 1M $NaOH_{(aq)}$. *N*-(3-dimethylaminopropyl)-*N*'-ethylcarbodiimide hydrochloride (EDC·HCl, 89 mg, 0.46 mmol) was then added and the mixture was stirred for 30 minutes at 0 °C. This was then added dropwise to the chitosan solution and stirred at room temperature for 24 hours. This formed an opalescent solution which was then dialysed for 5 days against deionised water with regular changes of the external water. The product was then lyophilised to give a white solid powder. Yield: 0.3652 g

FTIR (cm^{-1}): 3322 (N-H), 3212 (O-H, carboxylic acid), 2873 (C-H, alkyl), 1717 (C=O, carboxylic acid), 1615 (N-H, bending), 1372 (O-H, bending, carboxylic acid), 1056 (C-N, amine).

5.2.7.2 25% Citric Acid to Chitosan by Molar Ratio of Reactive Chitosan Groups

Chitosan was dispersed in deionised water (10 mL, 0.25 mg mL^{-1}). The pH of the resultant dispersion was adjusted to 4.5 using concentrated acetic acid and was stirred for one hour to allow the chitosan to dissolve. Separately, citric acid monohydrate was dissolved in deionised water (5 mL, 12.2 mg mL^{-1}) the pH was then adjusted to 6.5 using 1M $NaOH_{(aq)}$. EDC·HCl (0.22 g, 1.14 mmol) was then added and the mixture was stirred for 30 minutes at 0 °C. This was then added dropwise to the chitosan solution and stirred at room temperature for 24 hours. This formed an opalescent solution which was then dialysed for 5 days against deionised water with

regular changes of the external water. The product was then lyophilised to give a white solid powder. Yield: 0.2885 g

FTIR (cm^{-1}): 3393 (N-H), 3212 (O-H, carboxylic acid), 2873 (C-H, alkyl), 1713 (C=O, carboxylic acid), 1641 (N-H, bending), 1376 (O-H, bending, carboxylic acid), 1046 (C-N, amine).

5.2.7.3 50% Citric Acid to Chitosan by Molar Ratio of Reactive Chitosan Groups

Chitosan was dispersed in deionised water (10 mL, 0.25 mg mL^{-1}). The pH of the resultant dispersion was adjusted to 4.5 using concentrated acetic acid and was stirred for one hour to allow the chitosan to dissolve. Separately, citric acid monohydrate was dissolved in deionised water (5 mL, 24 mg mL^{-1}) the pH was then adjusted to 6.5 using 1M $NaOH_{(aq)}$. EDC·HCl (0.45 g, 2.34 mmol) was then added and the mixture was stirred for 30 minutes at 0 °C. This was then added to the chitosan solution and stirred at room temperature for 24 hours. This formed a white suspension which was then dialysed for 5 days against deionised water with regular changes of the external water. The product was then lyophilised to give a white solid powder. Yield: 0.3121 g

FTIR (cm^{-1}): 3350 (N-H), 3212 (O-H, carboxylic acid), 2891 (C-H, alkyl), 1723 (C=O, carboxylic acid), 1649 (N-H, bending), 1368 (O-H, bending, carboxylic acid), 1066 (C-N, amine).

5.2.8 Formation of Chitosan Particles Crosslinked with Tartaric Acid

5.2.8.1 10% Tartaric Acid to Chitosan by Molar Ratio of Reactive Chitosan Groups

Chitosan was dispersed in deionised water (10 mL, 0.25 mg mL^{-1}). The pH of the resultant dispersion was adjusted to 4.5 using concentrated acetic acid and was stirred for one hour to allow the chitosan to dissolve. Separately, tartaric acid was dissolved in deionised water (5 mL, 3.8 mg mL^{-1}) the pH was then adjusted to 6.5 using 1M $NaOH_{(aq)}$. EDC·HCl (0.096 g, 0.50 mmol) was then added and the mixture was stirred for 30 minutes at 0 °C. This was then added

dropwise to the chitosan solution and stirred at room temperature for 24 hours. This formed a clear solution which was then dialysed for 5 days against deionised water with regular changes of the external water. The product was then lyophilised to give a white solid powder. Yield: 0.2885 g

FTIR (cm^{-1}): 3363 (N-H), 3258 (O-H, carboxylic acid), 2895 (C-H, alkyl), 2869 (C-H, alkyl), 1743 (C=O, carboxylic acid), 1625 (N-H, bending), 1374 (O-H, bending, carboxylic acid), 1062 (C-N, amine).

5.2.8.2 25% Tartaric Acid to Chitosan by Molar Ratio of Reactive Chitosan Groups

Chitosan was dispersed in deionised water (10 mL, 0.25 mg mL^{-1}). The pH of the resultant dispersion was adjusted to 4.5 using concentrated acetic acid and was stirred for one hour to allow the chitosan to dissolve. Separately, tartaric acid was dissolved in deionised water (5 mL, 9.4 mg mL^{-1}) the pH was then adjusted to 6.5 using 1M $NaOH_{(aq)}$. EDC·HCl (0.24 g, 1.25 mmol) was then added and the mixture was stirred for 30 minutes at 0 °C. This was then added dropwise to the chitosan solution and stirred at room temperature for 24 hours. This formed a clear solution which was then dialysed for 5 days against deionised water with regular changes of the external water. The product was then lyophilised to give a white solid powder. Yield: 0.2816 g

FTIR (cm^{-1}): 3369 (N-H), 3263 (O-H, carboxylic acid), 2926 (C-H, alkyl), 2873 (C-H, alkyl), 1733 (C=O, carboxylic acid), 1643 (N-H, bending), 1317 (O-H, bending, carboxylic acid), 1062 (C-N, amine).

5.2.8.3 50% Tartaric Acid to Chitosan by Molar Ratio of Reactive Chitosan Groups

Chitosan was dispersed in deionised water (10 mL, 0.25 mg mL^{-1}). The pH of the resultant dispersion was adjusted to 4.5 using concentrated acetic acid and was stirred for one hour to allow the chitosan to dissolve. Separately, tartaric acid was dissolved in deionised water (5 mL,

18.8 mg mL^{-1}) the pH was then adjusted to 6.5 using 1M $NaOH_{(aq)}$. EDC·HCl (0.48 g, 2.50 mmol) was then added and the mixture was stirred for 30 minutes at 0 °C. This was then added dropwise to the chitosan solution and stirred at room temperature for 24 hours. This formed a clear solution which was then dialysed for 5 days against deionised water with regular changes of the external water. The product was then lyophilised to give a white solid powder. Yield: 0.2483 g

FTIR (cm^{-1}): 3409 (N-H), 3234 (O-H, carboxylic acid), 2928 (C-H, alkyl), 2863 (C-H, alkyl), 1745 (C=O, carboxylic acid), 1635 (N-H, bending), 1313 (O-H, bending, carboxylic acid), 1064 (C-N, amine).

5.2.9 Formation of Chitosan-Alginate Particles

5.2.9.1 1:2 Chitosan to Alginate by Mass

Chitosan was dispersed in deionised water (17 mL, 1 mg mL^{-1}). The pH of the resultant dispersion was adjusted to 4.5 using concentrated acetic acid and stirred for one hour to allow the chitosan to dissolve. Separately, a solution of sodium alginate in deionised water (34 mL, 1 mg mL^{-1}) was stirred for one hour following the addition of calcium chloride (0.06 mg) dissolved in deionised water (1 mL). The chitosan solution was added dropwise to the alginate solution and the resulting, clear, solution was stirred for 24 hours. This solution was then diluted by the further addition of deionised water (448 mL) to give a final concentration of 0.1 mg mL^{-1}. Portions of this solution (50 mL) were then used directly in the washing studies.

5.2.9.2 1:1 Chitosan to Alginate by Mass

Chitosan was dispersed in deionised water (25 mL, 1 mg mL^{-1}). The pH of the resultant dispersion was adjusted to 4.5 using concentrated acetic acid and stirred for one hour to allow the chitosan to dissolve. Separately, a solution of sodium alginate in deionised water (25 mL, 1 mg mL^{-1}) was stirred for one hour following the addition of calcium chloride (0.05 mg) dissolved in deionised

water (1 mL). The chitosan solution was added dropwise to the alginate solution and the resulting, clear, solution was stirred for 24 hours. This solution was then diluted by the further addition of deionised water (449 mL) to give a final concentration of 0.1 mg mL^{-1}. Portions of this solution (50 mL) were then used directly in the washing studies.

5.2.9.3 2:1 Chitosan to Alginate by Mass

Chitosan was dispersed in deionised water (34 mL, 1 mg mL^{-1}). The pH of the resultant dispersion was adjusted to 4.5 using concentrated acetic acid and stirred for one hour to allow the chitosan to dissolve. Separately, a solution of sodium alginate in deionised water (17 mL, 1 mg mL^{-1}) was stirred for one hour following the addition of calcium chloride (0.05 mg) dissolved in deionised water (1 mL). The chitosan solution was added dropwise to the alginate solution and the resulting, clear, solution was stirred for 24 hours. This solution was then diluted by the further addition of deionised water (448 mL) to give a final concentration of 0.1 mg mL^{-1}. Portions of this solution (50 mL) were then used directly in the washing studies.

5.3 Results and Discussion

5.3.1 Modification of Nanocellulose with GTAC

Nanocellulose was successfully modified with GTAC *via* ring-opening of GTAC onto the hydroxy groups of nanocellulose.[20] This reaction was performed with a 'high' level of GTAC modification and a 'low' level to yield two products. Pei *et al.* show the successful grafting of the GTAC moiety through FTIR analysis, by showing the development of a new peak at 1480 cm^{-1} corresponding to the trimethyl group of the GTAC. The peak is shown to increase in intensity with increasing level of GTAC modification. This developed peak is also observable in the FTIR of the two modified nanocelluloses produced, the spectra of which are shown in Figure 5-8.

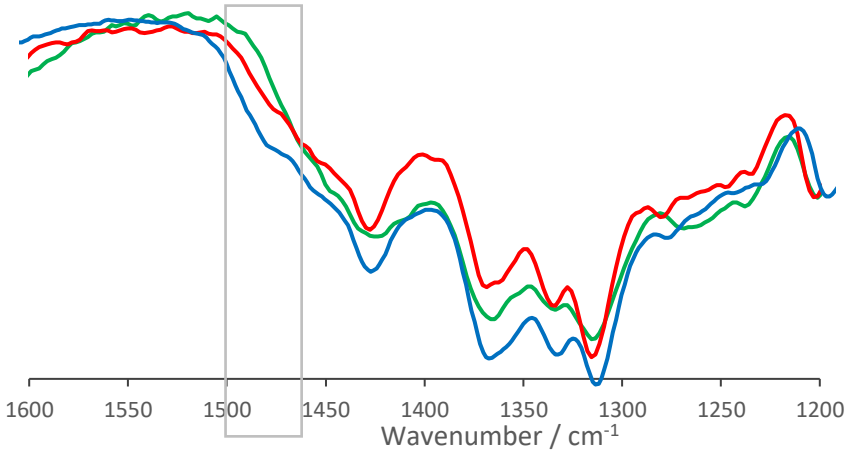

Figure 5-8 FTIR spectrum of nanocellulose (green), GTAC-nanocellulose modified to lower extent (red) and GTAC-nanocellulose modified to a higher extent (blue).

The FTIR spectrum in Figure 5-8 shows the developing trimethyl peak associated with the GTAC, highlighted by a box. The samples were extensively washed with water by centrifugation, whereby the GTAC-cellulose was mixed vigorously with water, centrifuged and the supernatant discarded. This process was repeated four additional times. Therefore, covalent grafting of the GTAC to the cellulose is confirmed. As the product is not soluble in NMR solvents, it is not possible to obtain an NMR spectrum to help confirm the structure.

The zeta potential values of the polymers were measured and are shown in Table 5-1.

Table 5-1 Zeta potentials of nanocellulose and GTAC modified nanocellulose to a low and a high degree.

Sample	Zeta Potential (mV)
Nanocellulose	-19±0.3
GTAC-Nanocellulose (low)	+20±0.2
GTAC-Nanocellulose (high)	+25±0.1

The increasingly positive zeta potential with increasing GTAC content indicates the successful modification of the nanocellulose.

5.3.1.1 GTAC-Nanocellulose for Dye Transfer Inhibition

The two GTAC-modified nanocellulose samples were then dispersed in water and washed with indigo dye bleeding fabric and the colour changes measured. These results were compared to non-modified nanocellulose to observe any effects the GTAC moiety causes (Figure 5-9).

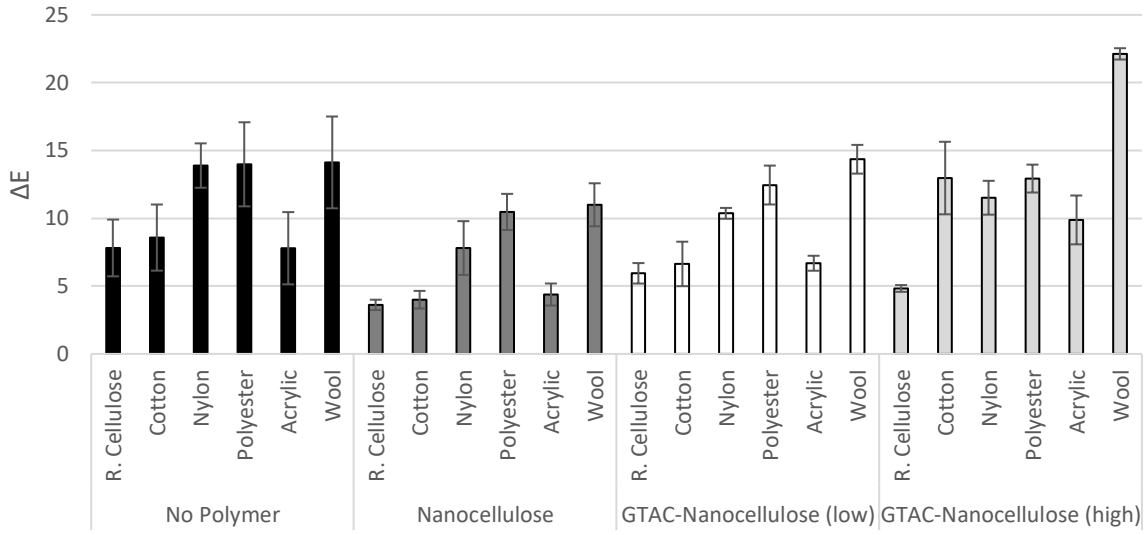

Figure 5-9 A comparison of the colour change caused by indigo in the presence of nanocellulose, and two GTAC-modified nanocellulose samples.

Figure 5-9 indicates that non-modified nanocellulose gives effective dye transfer inhibition for regenerated cellulose, cotton and nylon fibres, a 53.8%, 53.4% and 43.8% reduction in colour change, respectively. This result suggests that the nanocellulose interacts with the cellulosic and nylon fibres and thus prevents dye deposition by blocking adsorption sites. However, for the higher level of GTAC modification of nanocellulose, dye transfer is seen to increase for cotton from 8.58 in the presence of no polymer, to 12.97, a 51.2% increase. Additionally, while the colour change of wool is not significantly altered on addition of unmodified nanocellulose, it increased from a mean ΔE value of 14.1 to 22.1 for the nanocellulose modified to a higher extent, a 36.1% increase. This suggests that cationic GTAC-nanocellulose deposits onto the fabric and attracts the dye molecule to the surface. This is further evidenced by the anionic nanocellulose reducing dye deposition, conceivably due to the electrostatic repulsion of the anionic dye

molecules. These results are highlighted in Figure 5-10 whereby the dye deposition can be visually observed.

Figure 5-10 Photograph of multifibre swatches washed with indigo dye bleeding fabric. From left to right the swatches are washed without polymer, with GTAC-nanocellulose (low) and GTAC-nanocellulose (high).

From Figure 5-10 it can be seen that the GTAC-nanocellulose modified to a higher extent (right) shows a deeper blue colour across the fabric types than that without polymer (left). This shows that dye deposition is worsened in the presence of the modified nanocellulose.

GTAC-nanocellulose modified to a higher extent was also washed with C.I. Sulfur Black 1 (SB1) to observe if the polymer provided benefits for this dye, having worsened indigo deposition (Figure 5-11).

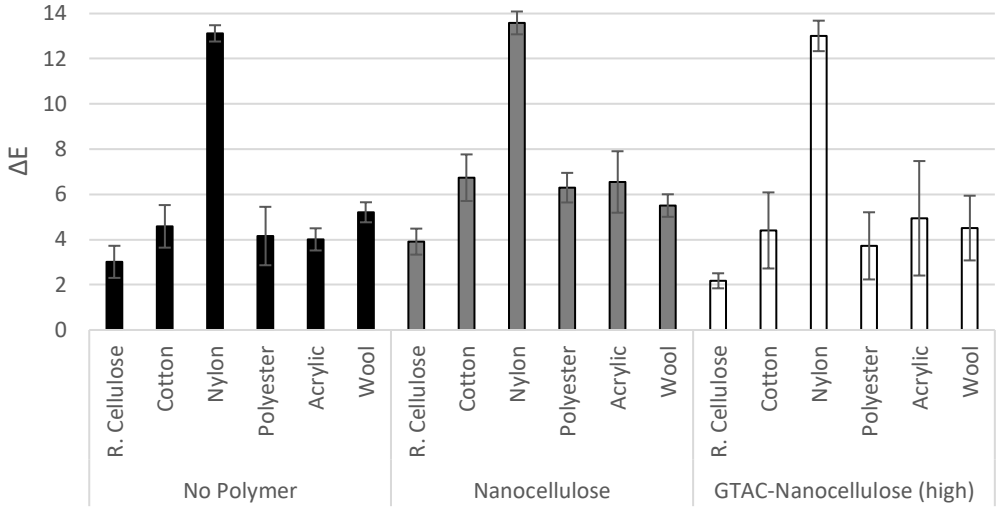

Figure 5-11 A comparison of the colour change caused by SB1 in the presence of nanocellulose, and a GTAC-modified nanocellulose sample.

Neither nanocellulose or the GTAC modified nanocellulose display a reduction in colour change for nylon, and neither show a significant decrease for the other fibre types, suggesting that SB1 is not blocked by the nanocellulose as indigo was. SB1 may have improved penetration of the fabric fibres, resulting in the lack of DTI efficacy observed for the GTAC-nanocellulose samples.

These results suggest the GTAC-nanocellulose deposits onto the fabric attracting the dye to the fabric surface and causing a worsened fabric colour change.

5.3.3 Chitosan-TPP Particle Formation

Chitosan-TPP particles were formed in three percentages by mass of TPP to chitosan: 17%, 14% and 12%.[21] It was proposed that chitosan particles are capable of electrostatically interacting with the dye molecules in the wash liquor to adsorb the dye preferentially and thus reduce colour change.

The samples were diluted with deionised water to give a concentration of 0.1 mg mL^{-1}, and their dimensions measured *via* dynamic light scattering (DLS). The zeta potential values of the

solutions were also collected (Table 5-2). An average of three measurements was taken for each solution.

Table 5-2. Average size and zeta potentials of three chitosan-TPP particle solutions.

TPP % by Mass	Average Hydrodynamic Size (d.nm)	PDI	Zeta Potential (mV)
17	250±16	0.45	+29±2.3
14	363±21	0.44	+29±1.2
12	247±1.2	0.39	+35±1.6

From Table 5-2 it can be observed that particles have formed which are of comparable hydrodynamic sizes in diameter. The largest amount of chitosan in the sample proportionally (12% TPP) gave the highest, most positive zeta potential as expected. However, the zeta potential values of the 17% TPP and 14% TPPP samples are similar.

5.3.3.1 Chitosan-TPP Particles for Dye Transfer Inhibition

The three chitosan-TPP solutions were tested for their efficacy as indigo dye transfer inhibitors. The colour changes were measured and compared for the three particle solutions (Figure 5-12).

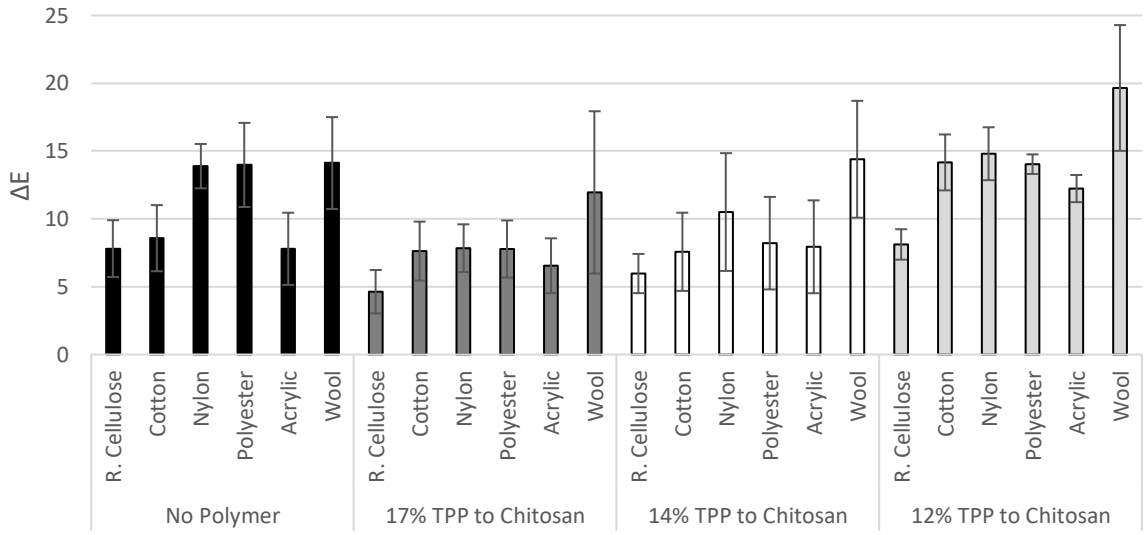

Figure 5-12 A comparison of the colour change caused by indigo in the presence of three chitosan-TPP particle solutions.

Figure 5-12 shows that the 12% TPP-chitosan particle solution has a worsening effect on indigo dye deposition for the hydrophilic fibres. For acrylic fibres, a 57.1% increase in colour change (ΔE) is observed, and cotton gave a 39.4% increase. Additionally, for wool a 28.2% increase in ΔE is observed. Meanwhile, the 17% TPP-chitosan solution shows a 43.6% reduced colour change for nylon and polyester shows a 44.3% decrease. However, the cotton, acrylic and wool values exhibit little change. The small difference in zeta potential (Table 5-2) between 17% and 14% TPP-chitosan particle solutions reflects the similar colour change results. This indicates that the lower, less positive, zeta potential of the solutions results in a more effective DTI. This may be because the chitosan-TPP particles deposit onto the fabric and repel or attract the dye molecules. In particular, the 12% TPP-chitosan particles have fewer crosslinks, resulting in more free amine sites able to interact with dye molecules. The free amines may also hydrogen bond with the fabrics to a greater extent than the 17% TPP-chitosan particles, and therefore will draw the dye molecules to the fabric, similarly to the GTAC-nanocellulose in Section 5.3.1.

The 17% TPP-chitosan solution was then tested for its ability to prevent the transfer of additional dyes. Firstly, C.I. Sulfur Black 1 (SB1) was tested (Figure 5-13).

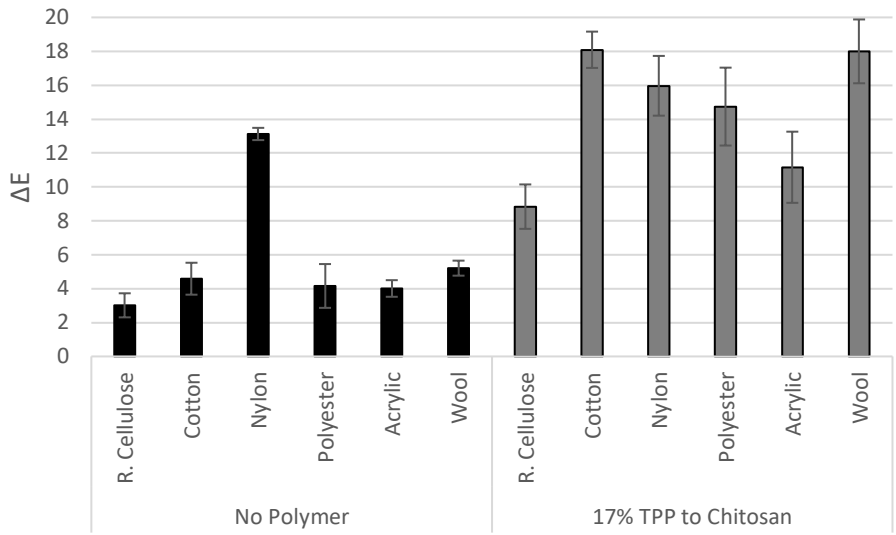

Figure 5-13 A comparison of the colour change caused by SB1 in the presence of no polymer, and the 17% TPP-chitosan particle solution.

From Figure 5-13 it can be observed that the TPP-chitosan particles significantly worsen dye deposition of SB1 on all fabric types. Cotton shows particular discolouration, giving a 74.7% increase in colour change in comparison to the wash without any polymer. Polyester also shows a significant colour change of 71.8%, which is in contrast to the reduced colour change caused by indigo in the presence of the 17% TPP-chitosan particle solution. Where the 17% TPP-chitosan particles are able to block dye deposition of indigo, they may enable the attraction of SB1 to the fabric and to penetrate the fibres, where the indigo is unable to. This suggests that for SB1, the amount of free amine groups in the 17% TPP-chitosan particle solution is sufficient to create an attraction to the particles and thus the fabric, but is insufficient for the less charged indigo.

Secondly, the solution was tested for its efficacy against the redeposition of C.I. Direct Orange 39 (DO39, Figure 5-14).

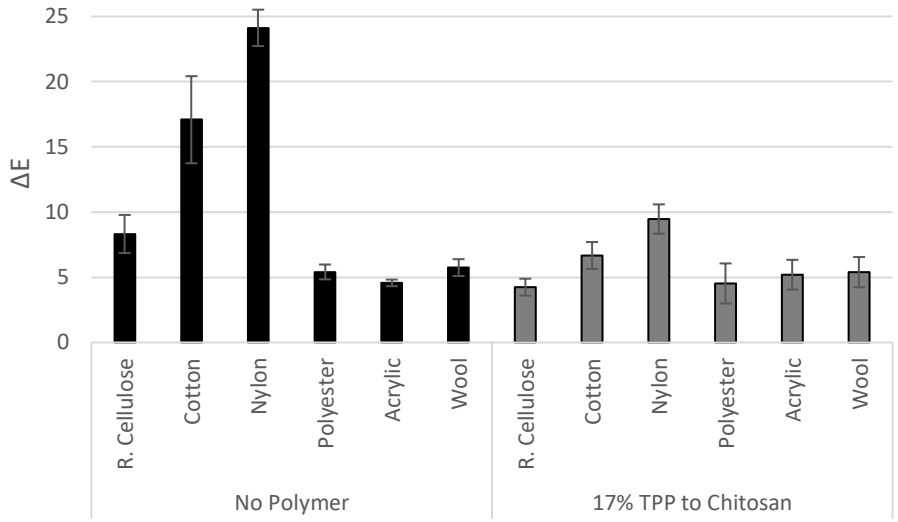

Figure 5-14 A comparison of the colour change caused by DO39 in the presence of the 17% TPP-chitosan particle solution.

Figure 5-14 shows that the chitosan-TPP particle solution reduces colour change on cellulose, cotton and nylon fibres. Nylon shows a particularly significant reduction in colour change, from 24.1 to 9.6, a 60.1% reduction in colour change. This is particularly encouraging as DO39 causes a high level of discolouration onto nylon in comparison to other fabric types. It is therefore likely that the chitosan-TPP particles are able to repel the dye molecules from the fabric surface. Alternatively, the DO39 and indigo molecules are small and therefore the chitosan-TPP particles may be capable of encapsulating them in the wash liquor. This may not be possible for larger dye species which may explain the differing effects between indigo, SB1 and DO39.

The 17% TPP-chitosan solution was then tested against C.I. Reactive Red 141 (RR141, Figure 5-15).

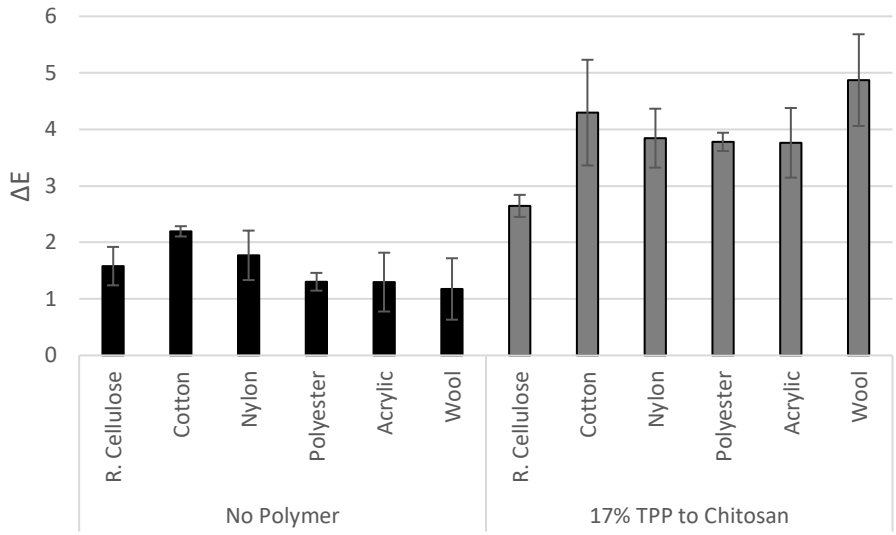

Figure 5-15 A comparison of the colour change caused by RR141 in the presence of the 17% TPP-chitosan particle solution.

Similarly to SB1, Figure 5-15 shows that RR141 causes an increased colour change in the presence of the chitosan particles on all fabric types, in particular cotton, showing a 48.8% increase in colour change from 2.2 to 4.3. This suggests that RR141 interacts in a similar manner to SB1, whereby the chitosan-TPP particles increase attraction between the dye to the fabric surface. RR141 is a larger dye molecule than DO39 and indigo, and therefore the particles may not be able to encapsulate the dye, but instead cause it to deposit onto the fabric surface due to its higher molecular weight.

Finally, the 17% TPP-chitosan solution was tested against C.I. Reactive Black 5 (RB5, Figure 5-16).

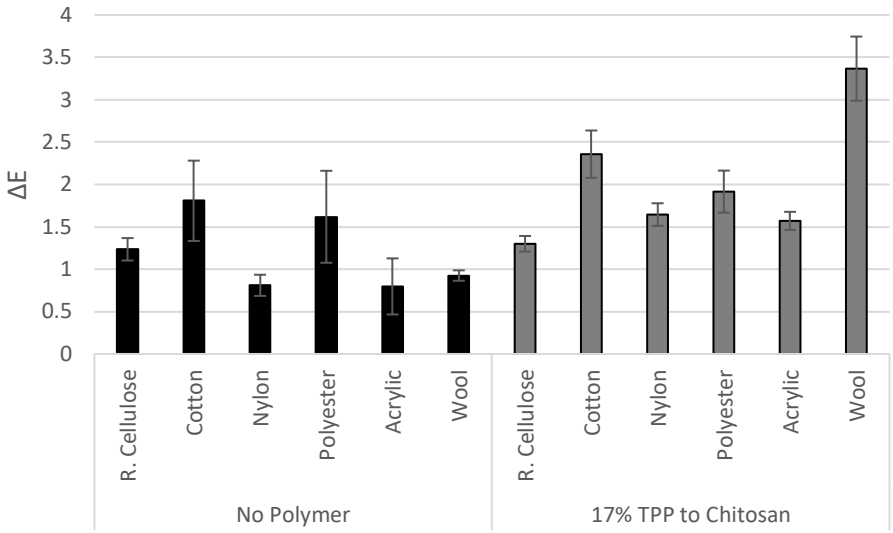

Figure 5-16 A comparison of the colour change caused by RB5 in the presence of the 17% TPP-chitosan particle solution.

In the absence of polymer, RB5 does not cause a high level of discolouration in comparison to indigo, however the colour change is seen to worsen for nylon, acrylic and wool in the presence of chitosan-TPP particles. Nylon gives an 83% increase in colour change, acrylic a 49.0% increase, and wool give the largest increase at 72.7%. RB5 is a larger dye molecule than DO39 and indigo, so it is less likely to be encapsulated, and is highly water-soluble and anionic. This suggests, similarly to RR141 and SB1, that the chitosan particles facilitate interaction between highly charged, highly soluble dyes, and the fabric surface.

In summary, for the larger and more anionic dyes, the dye deposition is worsened on inclusion of the chitosan-TPP particle solution. However, for the smaller, less anionic dye molecules like DO39 and indigo, the 17% TPP-chitosan particle solution exhibits a clear DTI benefit. This may be due to the smaller size enabling encapsulation of the dyes, or may be due to reduced electrostatic interactions between the dye and the particles when deposited onto the fabric.

5.3.3.2 Chitosan-TPP Particles as Dye Scavengers and Dye Fixatives

It was proposed that a sacrificial swatch may be made, doped with the 12% TPP-chitosan particle solution in order to preferentially attract the fugitive dye molecules, to prevent colour change in the wash onto the garment. To investigate whether the chitosan-TPP particles could be used to create a dye scavenging swatch to act as a 'colour catcher' in the laundry, a swatch of white cotton was pre-treated by soaking in the 12% TPP-chitosan particle solution and then air dried. This was then washed in plain deionised water with a dye bleeding indigo swatch and a multifibre swatch. The colour change caused by indigo onto the multifibre swatch was measured. This was compared to a wash that included a plain cotton swatch that was not pre-treated in the chitosan-TPP solution (Figure 5-17).

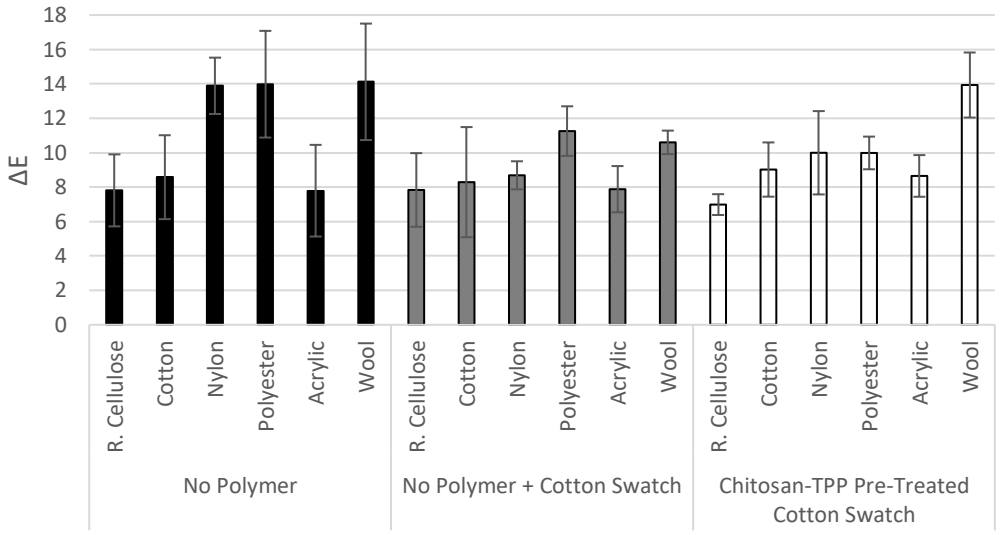

Figure 5-17 A comparison of the colour change caused by indigo in the presence of a cotton swatch which was previously treated by a 12% TPP-chitosan particle solution, and that with a cotton swatch that was not pre-treated.

Figure 5-17 shows there is little effect caused by including a doped cotton swatch to act as a sacrificial dye scavenger, in comparison to a non-doped swatch, as none of the fabric types show any significant increase or decrease in colour change in the presence of the doped swatch. This shows that the swatch does not preferentially adsorb indigo dye from the wash solution, despite the affinity indigo has for the particles.

Secondly, the particle solutions were tested for their ability to act as a potential dye fixative, to prevent the dye from bleeding from the fabric in the first place. An indigo dye bleeding swatch was pre-treated in a 12% TPP-chitosan solution and dried, and then washed in deionised water with a multifibre. This was compared to a wash where the denim was pre-soaked in deionised water only, in order to ensure any benefits observed were not due simply to dye being removed in the soaking process (Figure 5-18).

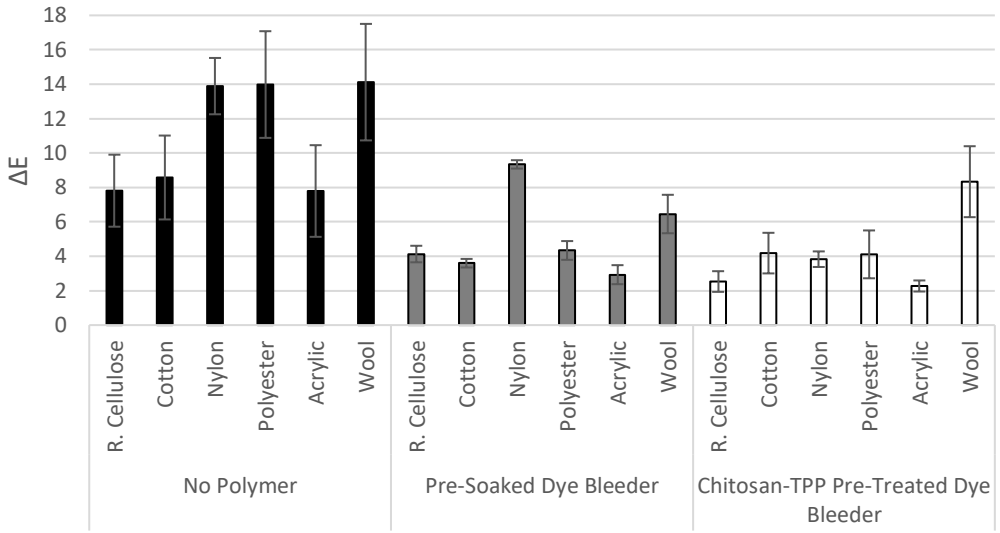

Figure 5-18 A comparison of the colour change caused by indigo dye bleeding fabric which was previously treated by a 12% TPP-chitosan particle solution, and that with a dye bleeding swatch that was pre-soaked in plain, deionised water.

By pre-treating the dye bleeding fabric with the particle solution, a reduced colour change is observed for nylon fabric, reducing in colour change caused by a dye bleeding fabric pre-soaked in deionised water. The colour change for nylon is reduced from 9.34 to 3.83, a 59.0% decrease. This benefit does not extend across all fibre types and therefore does not imply that the particles are acting as a dye fixative, but does suggest that the particles are deposited on the dye bleeding fabric and are preventing dye transfer in the subsequent wash. This provides further evidence to support the worsened colour change observed in Section 5.3.3, that may be caused by the particles interacting with the dye and drawing the molecules to the fabric surface.

5.3.4 Chemically Crosslinked Chitosan Particle Formation

Chitosan was chemically modified with citric acid and tartaric acid in varying ratios *via* EDC coupling.[19] As crosslinked chitosan is insoluble in NMR solvents, modification was confirmed by FTIR analysis and through measurement of the zeta potential values of each sample, when compared to unmodified chitosan. The FTIR spectra of the citric acid and tartaric acid modified chitosan samples are shown in Figure 5-19 and Figure 5-20.

Figure 5-19 A comparison of the FTIR spectra of chitosan to the chitosan modified with citric acid by 10%, 25% and 50%.

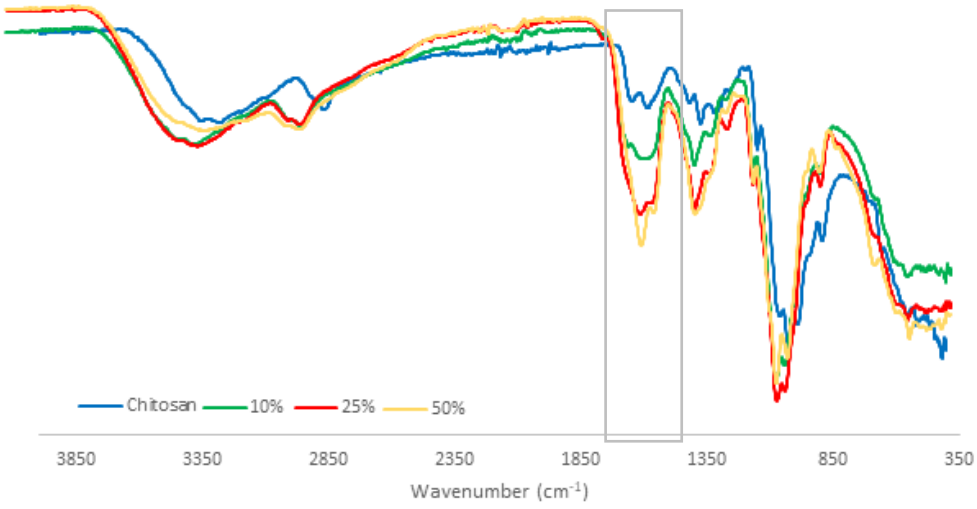

Figure 5-20 A comparison of the FTIR spectra of chitosan to the chitosan modified with tartaric acid by 10%, 25% and 50%.

Each modified chitosan showed a larger relative intensity in the region of 1690 cm^{-1} relating to the C=O of the newly formed amide bond from the reaction of the carboxylic acid with the amine groups in chitosan. This is in comparison to the peak at 1029 cm^{-1} which is assigned to the amine peak in the chitosan, for the C-N bond which is not affected by the introduction of the crosslinker.

Successful chitosan crosslinking is further confirmed by the zeta potential values of the six products. As citric acid has three acid groups, the varying levels of citric acid were expected to produce ampholytic particle solutions, whereby the free amine groups of the chitosan and the acid groups were evident. If all the amine groups reacted, this would produce an anionic particle solution. The zeta potential values were measured, and the size of the particles measured *via* DLS (Table 5-3).

Table 5-3 Average size and zeta potential of chitosan-citric acid and chitosan-tartaric acid particle solutions.

Acid % by Mass	Average Hydrodynamic Size (d.nm)	PDI	Zeta Potential (mV)
10% Citric Acid	549±51	0.48	+11±0.2
25% Citric Acid	233±42	0.82	+5.0±0.9
50% Citric Acid	405±165	0.54	+2.7±1.2
10% Tartaric Acid	578±95	0.50	+18±0.6
25% Tartaric Acid	493±74	0.65	+8.3±2.5
50% Tartaric Acid	726±98	0.55	+4.6±1.0

From Table 5-3 it can be seen that the zeta potential of the particles becomes less positive as the acid content increases. This is due to a reduced number of amine sites in the chitosan, as they have successfully reacted with the citric acid and tartaric acid crosslinker molecules.

5.3.4.1 Chemically Crosslinked Chitosan Particles for Dye Transfer Inhibition

The chitosan-citric acid particles were then tested for their ability to prevent indigo dye transfer (Figure 5-21).

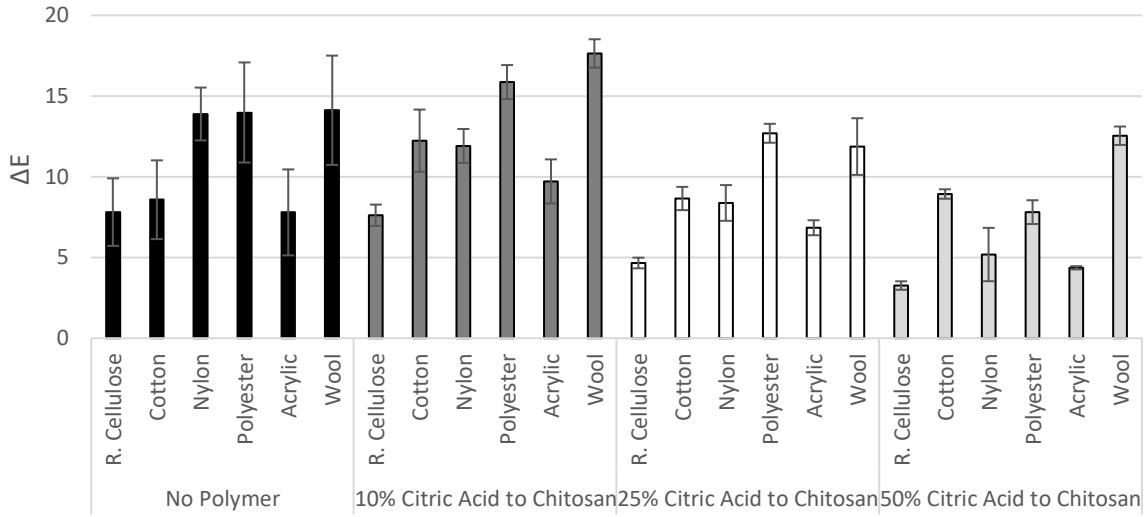

Figure 5-21 A comparison of the colour change caused by indigo in the presence of three chitosan-citric acid particle solution.

Figure 5-21 shows that on increasing citric acid modification of the chitosan, the colour change caused by indigo reduces. This is also proportional to the zeta potential reducing, as outlined in Table 5-3. The least modified chitosan does not have a significant effect on colour change overall. However, the 25% and 50% citric acid-chitosan particles show a reduction in colour change, particularly onto nylon a 39.7% and 62.7% reduction in colour change. This suggests that the particles are depositing onto the fabric and repelling the dye, whereas the 10% citric acid-chitosan particles do not have sufficient free acid groups to repel the dye molecules from the surface of the fabric. This is similar to the chitosan-TPP particle solutions, whereby the 12% TPP-chitosan particles were found to worsen dye deposition of indigo, when the more crosslinked 17% TPP-chitosan particles reduced colour change.

The chitosan-tartaric acid particles were also tested for their ability to prevent indigo dye transfer (Figure 5-22).

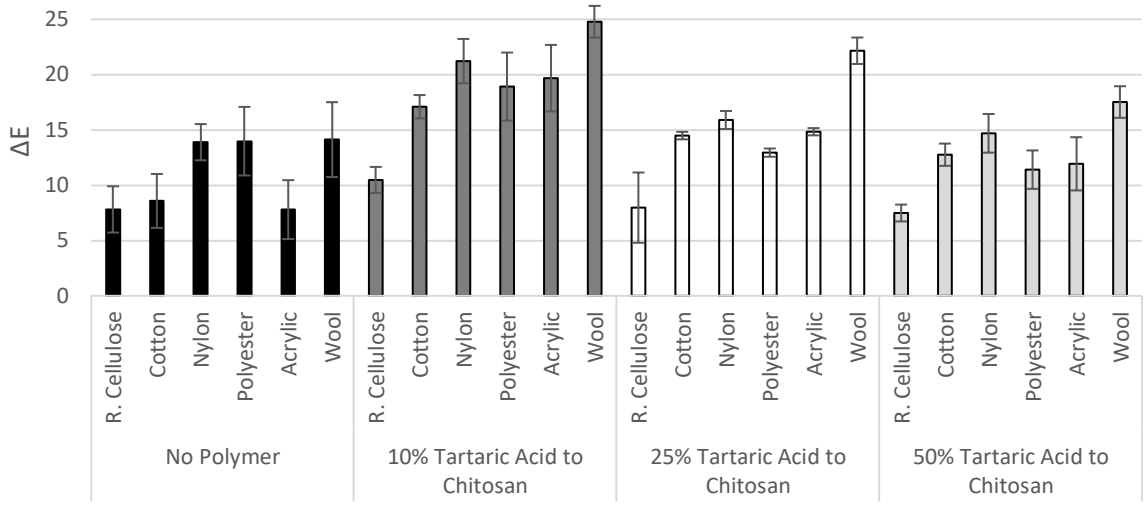

Figure 5-22 A comparison of the colour change caused by indigo in the presence of three chitosan-tartaric acid particle solution.

Unlike the citric acid containing particles, the 10% tartaric acid-chitosan particles show a worsening effect for the colour change caused by indigo onto all fabric types. Onto nylon, the colour change is increased by 34.5%, and onto wool by 43.0%. The 50% tartaric acid-chitosan particles do not increase or decrease colour change significantly over all the fabric types. As tartaric acid only contains two carboxylic acid groups, both may be reacted with the free amine groups of chitosan to reduce the overall zeta, without introducing free acid groups. This is indicated by the overall more positive zeta potential values for the tartaric acid containing particles, than the citric acid containing particles shown in Table 5-3. For example, the 10% tartaric acid containing particles have a zeta potential value of +18 mV, whereas the 10% citric acid containing particles have a value of +11 mV. This may mean that the dye is not being repelled by free acid groups from the fabric surface.

In order to assess the efficacy of the particles for other dyes, one particle solution of either chitosan-citric acid and chitosan-tartaric acid were washed with C.I. Sulfur Black 1 (SB1), C.I. Direct Orange 39 (DO39) and C.I. Reactive Red 141 (RR141).

Firstly, SB1 was investigated (Figure 5-23).

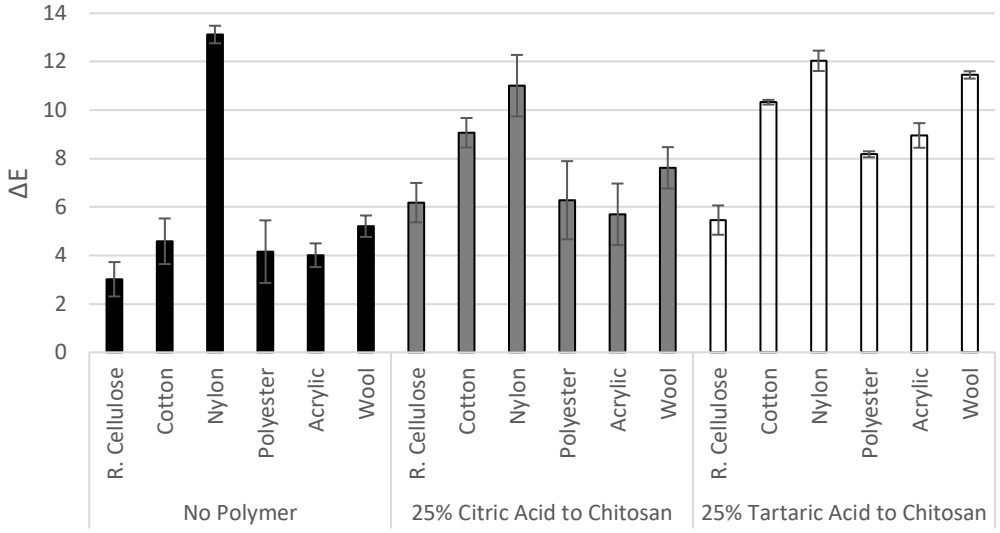

Figure 5-23 A comparison of the colour change caused by SB1 in the presence of a chitosan-citric acid and a chitosan-tartaric acid particle solution.

Figure 5-23 shows that the citric acid particles are capable of reducing deposition of the SB1 dye onto nylon by 16.1% but worsens colour change onto cotton by 49.5%. The tartaric acid particles worsen dye deposition onto all fibre types except nylon. The worsened colour change may be explained as citric acid and tartaric acid are reducing agents, which may produce the *leuco* form of SB1. This therefore would increase dye deposition of the SB1, particularly onto cotton fibres, as the dye is able to penetrate the fibres and bring about a colour change.

Secondly, DO39 was washed with the chitosan-citric acid and chitosan-tartaric acid particles (Figure 5-24).

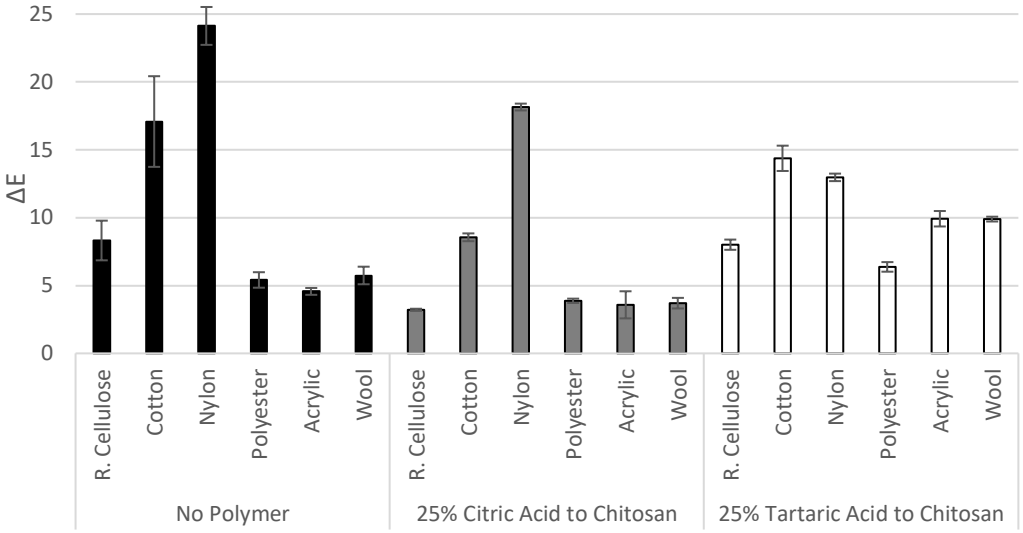

Figure 5-24 A comparison of the colour change caused by DO39 in the presence of a chitosan-citric acid and a chitosan-tartaric acid particle solution.

As for SB1, the chitosan-citric acid and chitosan-tartaric acid particles are seen to reduce colour change caused by DO39 onto nylon. The citric acid particles reduce the colour change by 24.6% on nylon, and the tartaric acid particles give a 46.2% reduction. The improved efficacy of the tartaric acid particles may suggest they are able to adsorb the dye and remain in solution, similarly to PVP which is found to be effective at preventing DO39 deposition, as observed in Chapter 3. As DO39 has a small structure and a negative zeta potential, it can be expected that the particles would repel the dye from depositing onto the fabric. As the tartaric acid particles are have fewer anionic groups than the citric acid particles, the repulsive forces between the dye and particle are weaker, and as such the DTI effect is less overall across the fibre types, despite a larger reduction onto nylon.

Finally, the particles were tested for their ability to prevent the dye deposition of RR141 (Figure 5-25).

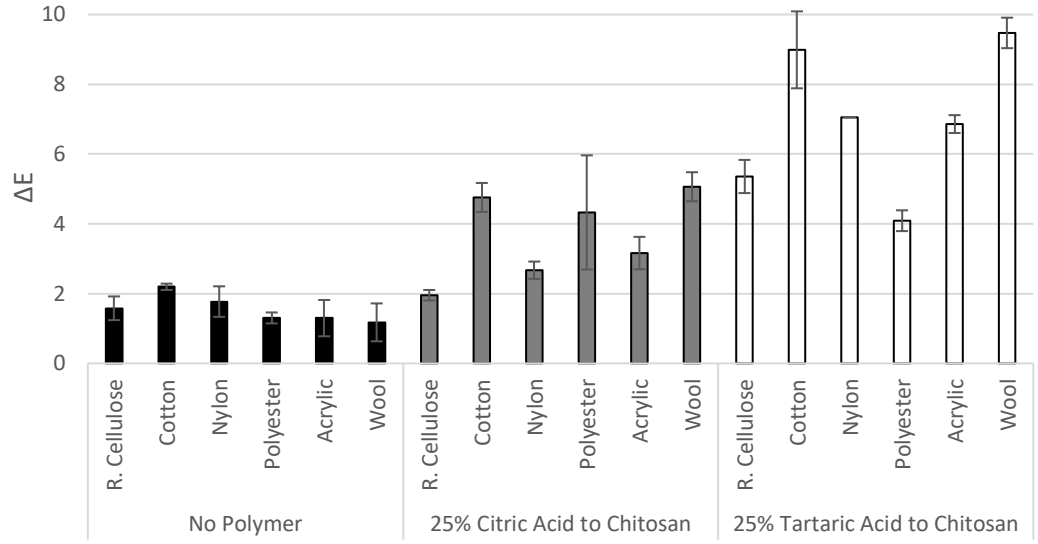

Figure 5-25 A comparison of the colour change caused by RR141 in the presence of a chitosan-citric acid and a chitosan-tartaric acid particle solution.

Colour change by RR141 is found to increase in the presence of the tartaric acid-containing particles onto all fibre types, as shown in Figure 5-25. In particular, dye deposition is worsened onto cotton and wool, by 75.7% and 81.4% respectively. Colour change is increased in the presence of the citric acid particles, but to a lesser extent than the tartaric acid particles. The particle may not have a sufficient number of anionic groups to repel the dyes from the fabric surface, but the free amines in chitosan may attract the dye to the fabric, worsening deposition.

5.3.5 Chitosan-Alginate Particle Formation

As chitosan possesses primary amine groups and alginate has free carboxylic acid groups, physically crosslinked particles may form between the two biopolymers.[10] Particles containing three ratios of chitosan to alginate were produced and their zeta potential values collected and their particle sizes were measured *via* DLS (Table 5-4).

Table 5-4 Average size and zeta potential of three chitosan-alginate particle solutions.

Chitosan to Alginate Ratio	Average Hydrodynamic Size (d.nm)	PDI	Zeta Potential (mV)
1:2	482±24	0.58	-39±0.1
1:1	580±79	0.94	-22±0.0
2:1	2436±170	0.36	+28±0.2

Table 5-4 shows that on increasing the chitosan amount, the more positive the zeta potential value of the nanoparticle dispersion becomes, indicating more free amine groups present in the particle solution. Additionally, the particle size diameter is shown to increase with increasing chitosan content.

5.3.5.1 Chitosan-Alginate Particles for Dye Transfer Inhibition

Firstly, chitosan and alginate were dispersed in water and washed with indigo dye bleeding fabric for comparison with the particle solutions (Figure 5-26).

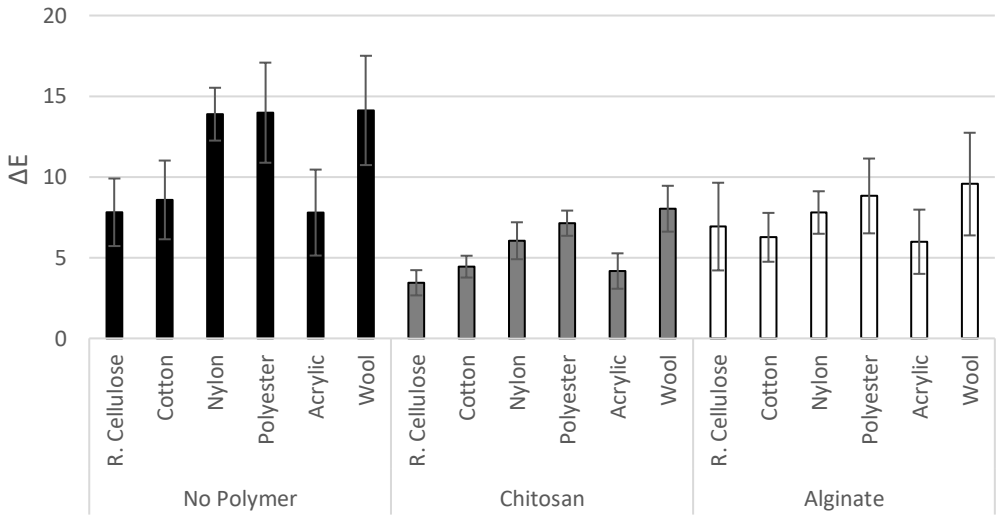

Figure 5-26 A comparison of the colour change caused by indigo in the presence of chitosan and alginate.

Figure 5-26 shows that chitosan and alginate alone are effective at preventing the dye deposition of indigo. Chitosan is not soluble in water, and therefore a dispersion was used to

carry out the washes. The dispersion was found to have a zeta potential of +13 mV. The low zeta potential value indicates that the chitosan is not soluble in water and indicates an unstable dispersion, which has a cationic surface charge. While chitosan shows a reduced colour change for all dyes, on visual inspection of the fabric chitosan aggregates are observed on the fabric which have adsorbed the dye and are therefore blue in colour. In contrast, alginate is water-soluble, and the zeta potential value of –44 mV reflects the stability and solubility of alginate in water. Therefore, it was expected that chitosan-alginate particles would enable the solubilisation and thus stability of the chitosan, and bring about effective dye transfer inhibition of both anionic and cationic dyes.

The chitosan-alginate particles were then washed with indigo dye bleeding fabric and the colour change was measured (Figure 5-27).

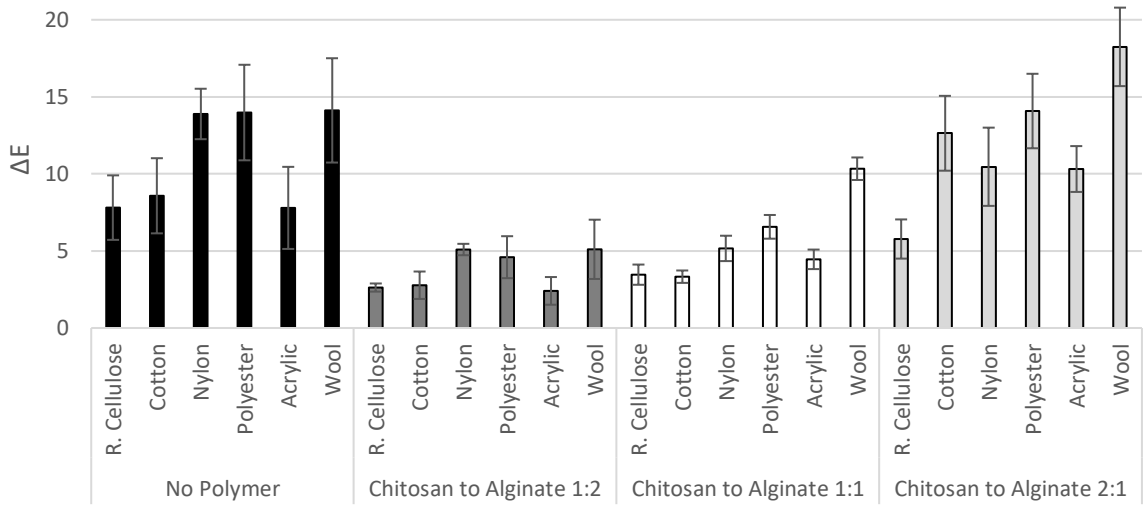

Figure 5-27 A comparison of the colour change caused by indigo in the presence of three chitosan-alginate particle solutions.

From Figure 5-27 it can be observed that the chitosan to alginate particles have an effect on dye deposition onto all fabric types. For example, the 1:2 ratio, with a high alginate content, shows a 67.7% reduction in colour change onto cotton, and 67.2% decrease onto polyester. This suggests that the particles deposit onto the fabric and repel the dye, owing to the overall negative zeta potential of the high alginate content particles. This result is in contrast to the

overall lack of effect caused by the 2:1 ratio, with high chitosan content, which shows a mean increase in colour change caused by indigo onto cotton, acrylic and wool of 32.1%, 24.5% and 22.6%, respectively. This further provides evidence that the particles deposit onto the fabric, and in this case attract the dye to the fabric surface, due to the overall positive charge of the 2:1 chitosan-alginate particles.

The three chitosan-alginate particle solutions were then tested against C.I. Sulfur Black 1 (SB1, Figure 5-28).

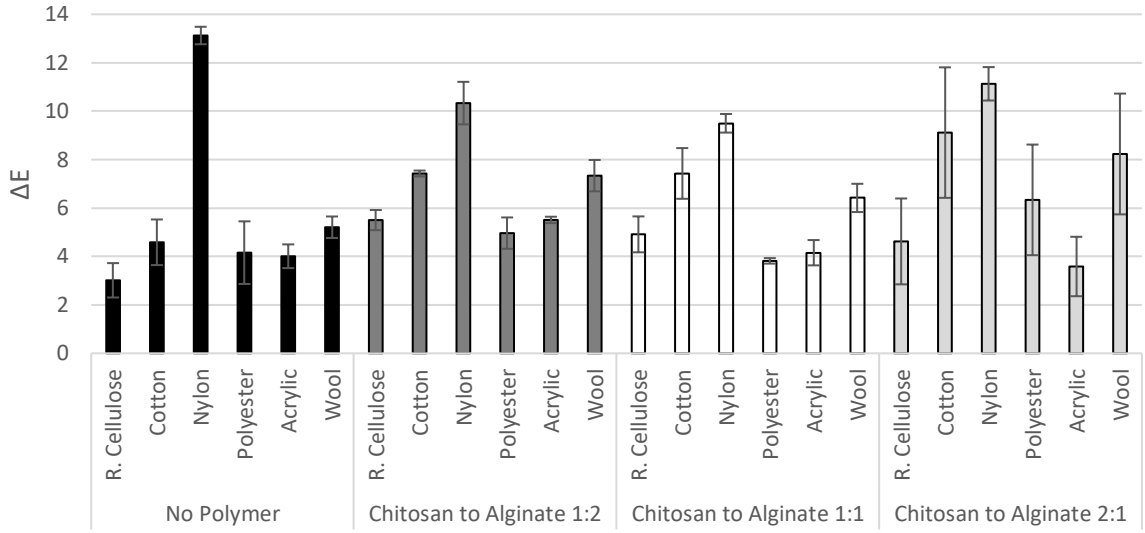

Figure 5-28 A comparison of the colour change caused by SB1 in the presence of three chitosan-alginate particle solutions.

Figure 5-28 shows that the chitosan-alginate particles reduce the colour change caused by SB1 onto nylon, the fibre type most discoloured by SB1. For the chitosan to alginate 1:1 ratio, nylon shows a 27.6% decrease in colour change. This benefit is not observed across all the fibre types, however. Cotton shows a worsened discolouration for the 1:1 ratio, the colour change increasing from 4.58 to 7.43, a 38.4% increase. As SB1 is a cotton dye, this result may suggest that the particle solution is aiding the dyeing of the receiver fabric with the fugitive SB1 molecule. SB1 is applied to cotton when reduced, therefore the conditions created by the particle solution may be sufficiently acidic to cause the dye the penetrate the cotton fibres and thus worsen colour change.

The chitosan-alginate particles were also tested against C.I. Direct Orange 39 (DO39, Figure 5-29).

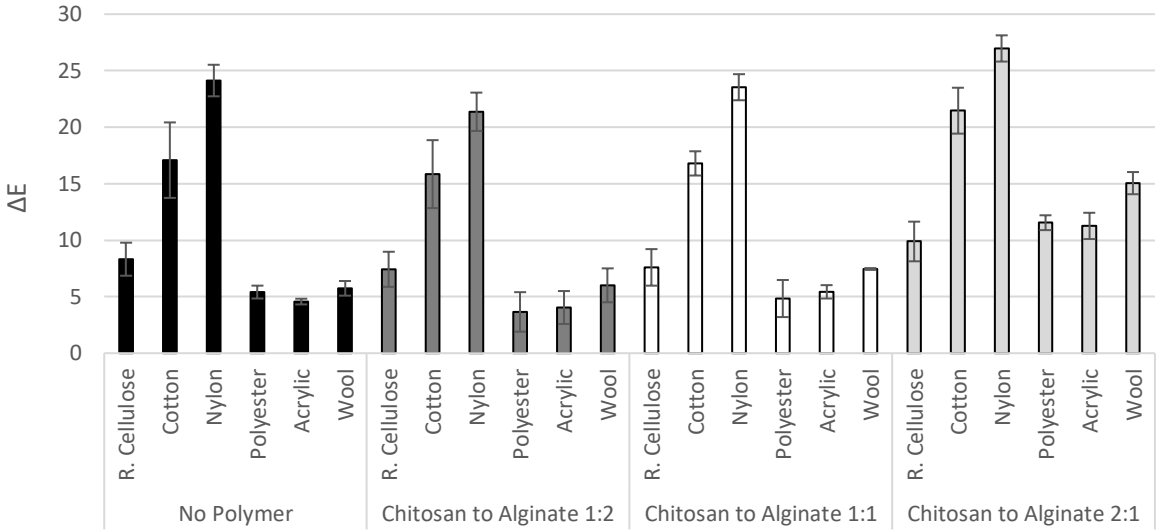

Figure 5-29 A comparison of the colour change caused by DO39 in the presence of three chitosan-alginate particle solutions.

For DO39, the 1:2 and 1:1 chitosan-alginate particles do not have a significant effect on colour change. Unlike for indigo, this shows that the particles do not repel the dye from depositing onto the fabric. Additionally, the worsened effect observed for the 2:1 particle solution suggests that the particles are again depositing onto the fabric and drawing the dye to the fibre, causing discolouration. For example, the colour change onto polyester is increased from 5.40 to 11.55, a 53.2% increase. As the 2:1 particle solution had a positive zeta potential, this suggests the particles interact with the fibres and draw the dye molecules to it.

5.4 Conclusion

The GTAC-nanocelluloses do not reduce colour change caused by indigo on various fibre types. In particular, the nanocellulose modified to a high extent with GTAC, and therefore the most positively charged, was found to worsen indigo dye deposition onto cotton and wool with a 33.8% and 36.1% increase in colour change, respectively. This indicates that the GTAC-nanocellulose deposited onto the fabric surface and attracted the dye to the fabric, increasing discolouration.

Chitosan particles were investigated for their ability to preferentially adsorb dyes in the wash to prevent dye deposition. Initially, physically crosslinked particles were formed using TPP, a polyanion, to crosslink with the amine groups on chitosan. Particles containing three ratios of chitosan to TPP were formed and tested for their ability to prevent dye transfer. The particles with the lowest ratio of chitosan to TPP were found to reduce dye deposition of indigo, whereas those with fewer crosslinks at a higher chitosan to TPP ratio were found to worsen dye deposition. This suggests that the interactions between the dye and the polymer, as well as the polymer and the fabric, are important to consider. The increased extent of the attraction between the dye and the polymer may also increase the affinity of the dye to the fabric, thus causing a worsened dye deposition overall.

Following these results, polymeric particles with an overall negative zeta potential were explored, in order to repel the dyes from the fabric rather than scavenging the dye in the wash liquor. Chitosan was physically crosslinked with citric acid, which contains three acid groups, and tartaric acid, which contains two acid groups. This was in order to create particles with varying levels of primary amine groups provided by the chitosan, and carboxylic acid groups provided by the crosslinker. The citric acid particles containing the highest amount of free acid groups were found to be more effective dye transfer inhibitors against indigo and DO39 dyes.

Finally, chitosan-alginate physically crosslinked particles were formed and tested. Analogous to the citric acid crosslinked particles, the particles with the higher alginate content and therefore the greater amount of acid groups, were successful DTIs against indigo. This again supports the rationale that the particles deposit onto the fabric and repel the dye from depositing.

5.5 References

[1] Rescignano N., Fortunati E., Armentano I., Hernandez R., Mijangos C., Pasquino R. and Kenny J.M. Use of alginate, chitosan and cellulose nanocrystals as emulsion stabilizers in the synthesis of biodegradable polymeric nanoparticles. *Journal of Colloid and Interface Science*. 2015 **445** 31–9

[2] Ma Z., Garrido-Maestu A. and Jeong K.C. Application, mode of action, and in vivo activity of chitosan and its micro- and nanoparticles as antimicrobial agents: A review. *Carbohydrate Polymers*. 2017 **176**

[3] Zhou X., Liu B., Yu X., Zha X., Zhang X., Chen Y., Wang X., Jin Y., Wu Y., Chen Y., Shan Y., Chen Y., Liu J., Kong W. and Shen J. Controlled release of PEI/DNA complexes from mannose-bearing chitosan microspheres as a potent delivery system to enhance immune response to HBV DNA vaccine. *Journal of Controlled Release*. 2007 **121** (3) 200–7

[4] Xu Y. and Du Y. Effect of molecular structure of chitosan on protein delivery properties of chitosan nanoparticles. *International Journal of Pharmaceutics*. 2003 **250** (1) 215–26

[5] Oh J.K., Lee D.I. and Park J.M. Biopolymer-based microgels/nanogels for drug delivery applications. *Progress in Polymer Science*. 2009 **34** (12) 1261–82

[6] Ko J.., Park H.., Hwang S.., Park J.. and Lee J.. Preparation and characterization of chitosan microparticles intended for controlled drug delivery. *International Journal of Pharmaceutics*. 2002 **249** (1–2) 165–74

[7] Shu X.Z. and Zhu K.J. A novel approach to prepare tripolyphosphate/chitosan complex beads for controlled release drug delivery. *International Journal of Pharmaceutics*. 2000 **201** (1) 51–8

[8] Pan C., Qian J., Fan J., Guo H., Gou L., Yang H. and Liang C. Preparation nanoparticle by ionic cross-linked emulsified chitosan and its antibacterial activity. *Colloids and Surfaces A: Physicochemical and Engineering Aspects*. 2019 **568** 362–70

[9] Liu H. and Gao C. Preparation and properties of ionically cross-linked chitosan nanoparticles. *Polymers for Advanced Technologies*. 2009 **20** (7) 613–9

[10] Katuwavila N.P., Perera A.D.L.C., Samarakoon S.R., Soysa P., Karunaratne V., Amaratunga G.A.J. and Karunaratne D.N. Chitosan-Alginate Nanoparticle System Efficiently Delivers Doxorubicin to MCF-7 Cells. *Journal of Nanomaterials*. 2016 **2016** 1–12

[11] Körpe D.A., Malekghasemi S., Aydın U. and Duman M. Fabrication of monodispersive nanoscale alginate–chitosan core–shell particulate systems for controlled release studies. *Journal of Nanoparticle Research*. 2014 **16** (12) 2754

[12] Wang F., Yang S., Yuan J., Gao Q. and Huang C. Effective method of chitosan-coated alginate nanoparticles for target drug delivery applications. *Journal of Biomaterials Applications*. 2016 **31** (1) 3–12

[13] Mincheva R., Bougard F., Paneva D., Vachaudez M., Fustin C.-A., Gohy J.-F., Manolova N., Rashkov I. and Dubois P. Polyelectrolyte complex nanoparticles from *N* -carboxyethylchitosan and polycationic double hydrophilic diblock copolymers. *Journal of Polymer Science Part A: Polymer Chemistry*. 2009 **47** (8) 2105–17

[14] Monteiro O.A.. and Airoldi C. Some studies of crosslinking chitosan–glutaraldehyde interaction in a homogeneous system. *International Journal of Biological Macromolecules*. 1999 **26** (2–3) 119–28

[15] Salzano de Luna M., Ascione C., Santillo C., Verdolotti L., Lavorgna M., Buonocore G.G., Castaldo R., Filippone G., Xia H. and Ambrosio L. Optimization of dye adsorption capacity and mechanical strength of chitosan aerogels through crosslinking strategy and graphene oxide addition. *Carbohydrate Polymers*. 2019 **211** 195–203

[16] Ibanescu A., Alexandrica M.C., Hritcu D., Chiscan O. and Popa M.I. Magnetite/chitosan

composite particles as adsorbents for Reactive Blue 19 dye. *Green Materials*. 2018 **6** (4) 149–56

[17] Riegger B.R., Kowalski R., Hilfert L., Tovar G.E.M. and Bach M. Chitosan nanoparticles via high-pressure homogenization-assisted miniemulsion crosslinking for mixed-matrix membrane adsorbers. *Carbohydrate Polymers*. 2018 **201** 172–81

[18] Zeraatkar Moghaddam A., Ghiamati E., Pourashuri A. and Allahresani A. Modified nickel ferrite nanocomposite/functionalized chitosan as a novel adsorbent for the removal of acidic dyes. *International Journal of Biological Macromolecules*. 2018 **120** 1714–25

[19] Bodnar M., Hartmann J.F. and Borbely J. Preparation and Characterization of Chitosan-Based Nanoparticles. 2005

[20] Pei A., Butchosa N., Berglund L.A. and Zhou Q. Surface quaternized cellulose nanofibrils with high water absorbency and adsorption capacity for anionic dyes. *Soft Matter*. 2013 **9** (6) 2047

[21] Rampino A., Borgogna M., Blasi P., Bellich B. and Cesàro A. Chitosan nanoparticles: Preparation, size evolution and stability. *International Journal of Pharmaceutics*. 2013 **455** (1–2) 219–28

Chapter 6. mPEG Terminated Polyesters for Use as Dye Transfer Inhibitors

This chapter is based on work which has been filed provisionally for a patent by P&G as:

WO patent application *Cleaning Compositions*, submitted June 2019

Abstract

Polymeric dye transfer inhibitors may interact with a fabric surface in the laundry and block the deposition of fugitive dyes. Therefore, a range of dye transfer inhibitors were produced by polycondensation reactions that are effective in preventing the transfer of unbound indigo dye to a variety of fibre types. Amphiphilic block copolymers are reported that contain sections designed to promote polymer-fabric interactions, and hydrophilic poly(ethylene glycol) sections that inhibit indigo-fabric interaction. Such polymers were found to hold great promise for inclusion within laundry detergent formulations as dye transfer inhibitors.

6.1 Introduction

Previous results reported in this thesis have shown that biopolymeric particles are capable of reducing dye transfer when they deposit onto fabric, and can repel or block the deposition of the dye onto the fabric. However, the particles were expected to encapsulate the dye in solution, rather than depositing onto the fabric. Due to this, some dye deposition was worsened by the presence of the biopolymeric particles that deposit onto the fabric and attract the dye to the fabric surface. Therefore, polymers which interact with the fabric to block or repel dye deposition will be investigated, in particular, methoxy-poly(ethylene glycol)-*co*-polyesters, due to their amphiphilic nature and ability to interact with common fabrics.

6.1.1 Block Copolymer Polyesters for Antifouling Applications

Block copolymers containing polyesters have been explored as anti-fouling coatings of ship hulls to prevent the attachment of marine organisms, as well as in biomedical applications for protein and cell-adhesion resistance.[1–4]

Zheng *et al.* investigated the mechanism of action of anti-fouling coatings by molecular simulations of the interactive forces between the protein and water molecules bound by the coating.[5] The coating forms a self-assembled monolayer, which attracts a hydration layer of tightly bound water molecules at the surface. They found that it was the water molecules that repel the protein, not the polymer, but that a polymer capable of extensively hydrogen bonding to water molecules exhibits repulsion of the protein. A more flexible polymer chain was found to exert greater repulsive forces on proteins. This is because the disordered monolayer allows a greater number of water molecules to penetrate the surface.[5] Therefore in order to achieve a successful anti-fouling coating the hydration layer, and thus the hydrophilic block, is key.[6]

Li *et al.* reported the synthesis of hydrophilic polyesters bearing oligo(ethylene glycol)methyl-ether functionality. The polyesters were synthesised *via* ring opening polymerisation of δ-valerolactones for use in preventing non-specific protein adsorption in biomedical applications.[1] The authors selected aliphatic polyesters for their biodegradability as the ester bond is susceptible to hydrolysis, and their biocompatibility. A polyester was tested for its anti-fouling ability by forming a self-assembled monolayer onto a gold surface. They found that the polyester was capable of preventing the adsorption of bovine serum albumin to a similar extent as a surface coated with methoxy-poly(ethylene glycol) (mPEG), a commonly used anti-fouling polymer.[1] The two coated surfaces were both hydrophilic, as confirmed by their contact angles of 48.7^{o} for the polyester and 31.8^{o} for the mPEG surface. This study shows the ability of polyesters in anti-fouling coatings, and reiterates the importance of an hydrophilic component in order to be successful in this application.

Water-soluble polyesters may therefore be applied to dye transfer inhibition as they may prevent deposition of dyes onto fabrics in an analogous manner.

6.1.2 Block Copolymer Polyesters for Drug Delivery

Amphiphilic block-copolymer polyesters have been widely investigated for their ability to form micelles to enable drug delivery of pharmaceuticals that otherwise have low solubility, and thus low bioavailability, once delivered to the body.[7–10] Micelle formation occurs when an amphiphilic diblock copolymer self-assembles in solution. The hydrophilic block forms a shell in which the hydrophobic section, or 'core', is protected from the aqueous environment, creating a core-shell particle.[11,12] The interior of the micelle is an hydrophobic environment which can be exploited to deliver drugs that are insoluble in aqueous media to the body, which is an aqueous system.[13] The ester bond in polyesters is prone to hydrolysis and therefore is ideal for controlled release applications in drug delivery.[10,14]

Poly-3-hydroxybutyrate is a polyester that degrades *via* hydrolysis of the ester bond into *D*-3-hydroxybutyrate, which occurs naturally in human blood. It was selected by Luo *et al.* for use as the hydrophobic block, when modified to poly[(*R*)-3-hydroxybutyrate-(*R*)-3-hydroxyhexanoate], in a copolymer with PEG and poly(propylene glycol) (PPG) in order to create thermosensitive micelles.[15] PEG was selected to impart hydrophilicity to the polymer, and to allow polymer self-assembly into micelles, the formation of which was confirmed by transmission electron microscopy (TEM). The blood compatibility of the selected anticancer drug docetaxel was found to improve when encapsulated by the novel polyester copolymer, in comparison to commercial formulations using surfactants such as Tween 80. The drug-loaded polymeric micelles were found to inhibit melanoma growth in *in vivo* studies.[15]

Siafaka *et al.* investigated the formation of nanoparticles by PEG-poly(propylene succinate) (PPS) copolymers functionalised with folic acid, in order to encapsulate ixabepilone, an anticancer drug.[16] PPS is a biocompatible polyester with a higher biodegradation rate than that of

commonly used poly(lactic acid), poly(glycolic acid) and poly(ε-caprolactone), due to its low degree of crystallinity.[14] Folic acid was conjugated to the PEG-PPS copolymers in order to provide targeting capability of the self-assembled nanoparticles for cancer cells. The nanoparticles were found to enter HeLA cancer cells, which exhibit a folic acid receptor. Additionally, the encapsulated drug was found to show a greater release of the drug by 55%, in comparison to the free drug, indicating the improved solubility.[16] This demonstrates the polyester polymers are capable of encapsulating the drug molecule, as well as then delivering it *via* targeted delivery using the folic acid receptor on HeLa cells.

Owing to the structural similarity of drug molecules to dye molecules, amphiphilic block copolymers may therefore be used to encapsulate dye molecules, in order to act as dye transfer inhibitors (DTIs).

6.1.3 Block Copolymer Polyesters in Laundry Detergent Formulations

Methoxy-poly(ethylene glycol)-*co*-poly(ester)s were produced using dimethyl terephthalate and a diol as the monomers for the polyester block, by Koch *et al.* as reported in a patent, which indicates a commercially viable class of polymers that have shown a dye transfer inhibition effect against indigo dye onto nylon thread.[17]

This polymer was designed to prevent the redeposition of indigo in the stonewashing process of denim treatment, but a similar polymer concept may be adapted for use as a DTI in laundry detergents. Due to its high hydrophobicity, traditional PVP-type DTIs are not effective against the redeposition of indigo. The polyester block is able to interact with hydrophobic fibres such as polyamides, while the PEG block creates a physical barrier, preventing dye redeposition by blocking dye adsorption sites.

The patent however does not provide colour change results, and specifies the polymers were designed to prevent indigo dye transfer onto polyamide fabrics specifically.[17] It is therefore necessary to test the polymers with alternative dyes onto different fabric types, and optimise the polymer through structural modification. From this, the mode of action of the polymer can be confirmed in order to assess the efficacy of the mechanism, and therefore the type of DTI polymer.

In addition, amphiphilic polyesters have been used as soil release polymers in detergent formulations.[18,19] Soil release polymers are added to detergent formulations in order to improve the cleaning qualities of the detergent, since the advent of synthetic fabrics such as polyester and quick, cold water wash cycles, traditional detergents have lost efficacy.[20] Because of the hydrophobic nature of polyester fabric, it interacts favourably with oily substances which create soils on the garment that are difficult to disperse into the laundry liquor.[21,22] This is different to hydrophilic fibres such as cotton which readily adsorb water, and expel oily soils. Polyester fabrics are therefore surface modified to increase the hydrophilicity and thus improve the removal of oily stains and soils in the laundering process. However, through subsequent washes, the surface treatment can be removed and therefore results in increased soiling.[23] Soil release polymers are used to improve the cleaning quality of detergents for hydrophobic fabric, by increasing the surface hydrophilicity of the hydrophobic fibres again.[24] The polymers are designed to interact with, and deposit onto, the fibres in the laundry wash. This prevents soil deposition by creating a hydration layer, analogous to anti-biofouling polymers, which repels soils from redepositing onto the fibres in the wash, as well as protecting the fabric from future soiling.[25] Cationic polyester soil release polymers were also found to act as effective fabric softening agents and antistatic agents, when added to a rinse-added fabric conditioning formulation.[26,27] However, the late addition in the laundering process would prevent the efficacy of the polymer as a dye transfer inhibitor, but indicates the potential secondary benefits provided by the soil release type polymers.

The polyester block of the copolymer is formed by the polycondensation reaction between a diol, *e.g.* ethylene glycol, and dimethyl terephthalate (Figure 6-1). This may then be reacted with methoxy-poly(ethylene glycol) (mPEG) at each chain terminus to produce an mPEG capped polyester.

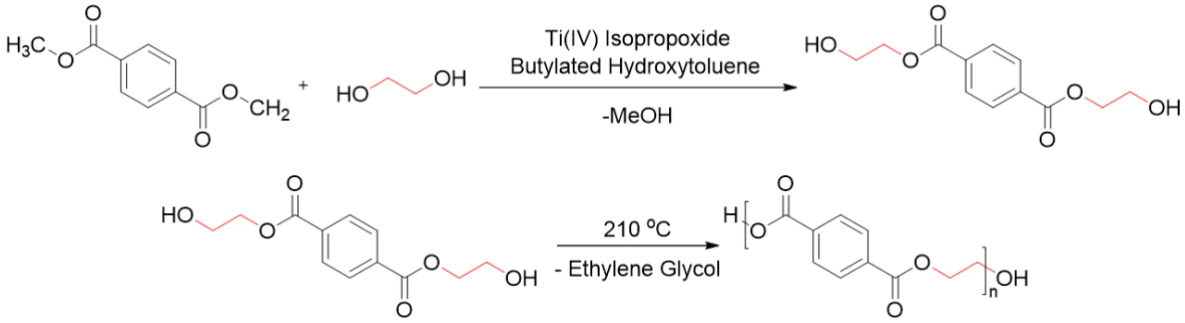

Figure 6-1 Two-step polycondensation reaction to form poly(ethylene terephthalate) from dimethyl terephthalate and ethylene glycol.

The diol, highlighted in red in Figure 6-1, may be substituted for alternative diols which also contain different functional groups, in order to optimise the polymer properties and improve the efficacy of the DTI polymer. This eliminates the need for post-modification of the polymer by including the additional functionality in the one-pot synthesis.

This chapter will focus on testing three polymers based of those reported in the patent outlined by Koch *et al*. with various dyes, and onto multiple fabric types. This was done by synthesising the polymers and testing their DTI efficacy by washing a strip of a dye bleeding fabric and a multifibre together in a solution of the polymer in water. This simulates the laundry conditions, rather than a stonewashing scenario, and determine if such polymers are suitable for incorporation within laundry detergent formulations.

Experiments will then focus on determining the mode of action of the polymers by altering the hydrophilicity and hydrophobicity of the DTI to observe the effect on the DTI efficacy. A worsened DTI efficacy on increasing the hydrophilicity will show that the polymer favours residence in the aqueous phase of the laundry liquor, and therefore does not interact with the

fabric. This would suggest that the original polymer interacts with the fabric, and thus works *via* a dye blocking mechanism of action.

Finally, a series of polymers will be synthesised incorporating various functionality into the polymer by selecting different diols and triols as monomers for the polyester synthesis. This will allow for an examination of the interactions and properties the polymer requires in order to be a successful DTI.

6.2 Experimental

6.2.1 Nuclear Magnetic Resonance (NMR) Spectroscopy

All ^{1}H NMR spectra obtained were recorded using a Bruker AVANCE 500 spectrometer at 500 MHz, for 128 scans. NMR spectra were obtained using 500 MHz Norell® NMR tubes. MestreNova® Research Lab software was used to analyse and integrate the spectra, and the chemical shifts were reference to trimethylsilane at 0 ppm.

6.2.2 Fourier Transformed Infrared (FTIR) Spectroscopy

Infrared spectra were obtained on a Bruker Platinum FTIR-ATR spectrometer, using a diamond attenuated total reflectance (ATR) accessory, completing 32 scans in total. Bruker OPUS7.0 software was used to analyse the spectra. TRIOS software was used to plot and analyse the data.

6.2.3 Centrifugation, Sample Drying and Lyophilisation

Samples were separated by centrifuge with an MSE Mistral 3000i at 25 °C, 1000 rpm. A Buchi R-210 rotary evaporator and a FiStream vacuum oven were used to remove solvent and dry samples. Samples were lyophilised using a VirTis BenchTop Pro freeze dryer (SP Scientific).

6.2.4 Scanning Electron Microscopy (SEM)

SEM analyses were carried out with a JEOL JSM-6610LV microscope (Oxford Instruments), using a field emission electron gun as an electron source. The fabric samples were mounted onto a

stub and a Quorum Q150RS sputter coater was used to give a 30 µm gold coat over the sample to provide surface conductivity.

6.2.5 Advanced Polymer Chromatography (APC)

Waters ACQUITY Advanced Polymer Chromatography was used to determine the molecular weight of the polymers. The polymers were dissolved in THF (1 mg mL^{-1}) and passed through a 0.22 µm PTFE filter. The values are calibrated to poly(methyl methacrylate) standards. An ACQUITY APC AQ column was used which is packed with bridged poly(ethylene) hybrid particles. An ACQUITY refractive index detector was used. The column was heated to 40 °C and the flow rate set to 0.5 mL min^{-1}. THF was run through the column for 2 minutes prior to each run. Empower 3 software was used to calculate the molecular weight.

6.2.6 GyroWash^2 Studies

Multifibre and dye bleeder washes were performed on a James Heal GyroWash^2 set at 40 °C, for 30 minutes at 40 rpm. The multifibre and dye bleeding fabrics were cut to 4x10 cm swatches, and washed in deionised water (50 mL) or polymer solution (50 mL, 0.1 mg mL^{-1}), with 25 ball bearings. Colour changes were measured using a Spectraflash DataColor unit, which measured the L* a* and b* coordinates, which can be compared to an unwashed sample to give a colour change (ΔE) value. Measurements were made under D65 lighting.

6.2.7 Overall synthetic procedure of mPEG-polyesters

For all polymers, all reagents were weighed into a three necked round bottom flask, fitted with a distillation head, bridge and flask, with an internal thermometer and placed under a constant flow of N_2(g). The reaction mixture was heated to 150 °C and over 48 hours was slowly raised to 210 °C. This temperature was maintained for a further 72 hours. The reaction product was then allowed to cool and was dissolved in deionised water (100 mL) before being dialysed for 5 days and then dried *in vacuo*. The individual conditions and reagents are outlined for each polymer.

6.2.7.1 $mPEG_{500}$-polyester containing 1,2-propanediol (DTI1) synthesis

$mPEG_{500}$ (11.06 g, 22.12 mmol), dimethyl terephthalate (2.29 g, 11.79 mol), 1,2-propanediol (1.79 g, 23.52 mol), butylated hydroxytoluene (0.013 g, 0.059 mmol) and Ti(IV) isopropoxide (0.013 mL, 0.042 mmol) were weighed and placed in a three-neck round bottom flask. The reaction procedure outline in Section 6.2.1 was then followed. Yield: 15.16 g, light brown oil. Mw: 3046 Da, PDI: 1.02

^{1}H NMR (500 MHz, DMSO) δ 8.23 – 7.89 (m, 10H, ArH), 4.68 – 4.52 (m, 2H, CH), 4.43 (dd, *J* = 16.4, 11.9 Hz, 9H, CH_3), 3.84 – 3.35 (m, 178H, CH_2), 3.24 (t, *J* = 5.7 Hz, 15H, CH_3), 1.53 – 0.92 (m, 3H, CH_2).

FTIR (cm^{-1}): 3550 (-O-H, alcohol), 2863 (-C-H, alkyl), 1719 (-C=O, ester), 1270 (-C-O, aromatic ester), 1095 (-C-O, alcohol), 942 (-C=C-, alkene) 732 (-C-H, aromatic).

6.2.7.2 $mPEG_{500}$-polyester containing glycerol and ethylene glycol (DTI2) synthesis

$mPEG_{500}$ (8.83 g, 17.66 mmol), dimethyl terephthalate (5.34 g, 27.50 mol), glycerol (2.28 g, 24.76 mmol), ethylene glycol (0.69 g, 11.12 mmol), butylated hydroxytoluene (0.01 g, 0.059 mmol) and Ti(IV) isopropoxide (0.01 mL, 0.042 mmol) were weighed and placed in a three-neck round bottom flask. The reaction procedure outline in Section 6.2.1 was then followed. Yield: 8.76 g, brown viscous liquid. Mw: 3729 Da, PDI: 1.06

^{1}H NMR (500 MHz, $CDCl_3$) δ 8.34 – 7.77 (m, 4H, ArH), 4.96 – 4.61 (m, 1H, CH), 4.59 – 4.23 (m, 3H, CH_2), 3.99 – 3.48 (m, 16H. CH_2), 3.40 (d, *J* = 29.5 Hz, 1H, CH_3), 2.50 (s, 3H, OH).

FTIR (cm^{-1}): 3489 (O-H, alcohol), 2871 (C-H, alkyl), 1719 (C=O, ester), 1250 (C-O, aromatic ester), 1095 (C-O, alcohol), 942 (C=C, alkene) 730 (C-H, aromatic).

6.2.7.3 $mPEG_{500}$-polyester containing glycerol and 2,2'-dimethyl-1,3-propanediol (DTI3) synthesis

$mPEG_{500}$ (12.80 g, 25.60 mmol), dimethyl terephthalate (7.76 g, 39.96 mmol), glycerol (2.21 g, 24.00 mmol), 2,2'-dimethyl-1,3-propanediol (2.90 g, 27.84 mmol), butylated hydroxytoluene (0.02 g, 0.12 mmol) and Ti(IV) isopropoxide (0.02 mL, 0.084 mmol) were weighed and placed in a three-neck round bottom flask. The reaction procedure outline in Section 6.2.1 was then followed. Yield: 15.73 g, brown viscous liquid. Mw: 4451 Da, PDI: 1.11

^{1}H NMR (500 MHz, $CDCl_3$) δ 8.09 (dd, *J* = 7.2, 2.4 Hz, 7H, ArH), 4.70 (s, 1H, CH), 4.59 – 4.37 (m, 4H, CH_2), 4.32 – 4.14 (m, 3H, CH_2), 3.87 – 3.48 (m, 40H, CH_2), 3.37 (d, *J* = 1.1 Hz, 3H, CH_3), 2.69 – 2.13 (m, 2H, OH), 1.31 – 0.92 (m, 5H, CH_3).

FTIR (cm^{-1}): 3497 (O-H, alcohol), 3285 (O-H, alcohol), 2869 (C-H, alkyl), 1717 (C=O, ester), 1246 (C-O, aromatic ester), 1091 (C-O, alcohol), 1015 (OC=O, anhydride), 944 (C=C, alkene) 728 (C-H, aromatic).

6.2.7.4 $mPEG_{750}$-polyester containing glycerol and 2,2'-dimethyl-1,3-propanediol (DTI4) synthesis

$mPEG_{750}$ (12.67 g, 0.0169 mol), dimethyl terephthalate (5.13 g, 0.0264 mol), glycerol (1.46 g, 0.0159 mol), 2,2'-dimethyl-1,3-propanediol (1.92 g, 0.0184 mol), butylated hydroxytoluene (0.013 g, 0.059 mmol) and Ti(IV) isopropoxide (0.013 mL, 0.042 mmol) were weighed and placed in a three-neck round bottom flask. The reaction procedure outline in Section 6.2.1 was then followed. Yield: 16.57 g brown oil. Mw: 4907 Da, PDI: 1.56

^{1}H NMR (501 MHz, $CDCl_3$) δ 8.18 – 7.93 (m, 40H, ArH), 4.65 (d, *J* = 33.2 Hz, 3H, CH), 4.48 (d, *J* = 4.6 Hz, 21H, CH_2), 4.34 – 4.02 (m, 21H, CH_2), 3.86 – 3.45 (m, 393H, CH_2), 3.37 (d, *J* = 9.0 Hz, 18H, CH_3), 2.46 (s, 17H, OH), 1.30 – 0.84 (m, 26H, CH_3).

FTIR (cm^{-1}): 3495 (O-H, alcohol), 2866 (C-H, alkyl), 1718 (C=O, ester), 1268 (C-O, aromatic ester), 1095 (C-O, alcohol), 947 (C=C, alkene) 730 (C-H, aromatic).

6.2.7.5 $mPEG_{5000}$-polyester containing glycerol and 2,2'-dimethyl-1,3-propanediol (DTI5) synthesis

$mPEG_{5000}$ (12.80 g, 2.56 mmol), dimethyl terephthalate (0.776 g, 4.00 mmol), glycerol (0.221 g, 2.40 mmol), 2,2'-dimethyl-1,3-propanediol (0.290 g, 2.78 mmol), butylated hydroxytoluene (0.002 g, 0.00908 mmol) and Ti(IV) isopropoxide (0.01 mL, 0.0338 mmol) were weighed and placed in a three-neck round bottom flask. The reaction procedure outline in Section 6.2.1 was then followed. Yield: 12.27 g brown solid. Mw: 1675 Da, PDI: 1.05

^1H NMR (501 MHz, $CDCl_3$) δ 8.14 – 7.91 (m, 11H, ArH), 4.66 (t, *J* = 11.0 Hz, 1H, CH), 4.48 – 4.37 (m, 5H, CH_2), 4.28 – 4.06 (m, 13H, CH_2), 4.03 – 3.33 (m, 558H, CH_2), 3.30 (s, 5H, CH_3), 2.91 (s, 10H, OH), 1.38 – 0.54 (m, 6H, CH_3).

FTIR (cm^{-1}): 3481 (O-H, alcohol), 2877 (C-H, alkyl), 1721 (C=O, ester), 1466 (C-H, alkane), 1341 (O-H, alcohol), 1280 (C-O, aromatic ester), 1101 (C-O, alcohol), 958 (C=C, alkene), 842 (C-H, aromatic).

6.2.7.6 $mPEG_{500}$-polyester containing glycerol and 2,2'-dimethyl-1,3-propanediol at 1.5 times the molar ratio (DTI6) synthesis

$mPEG_{500}$ (6.40 g, 0.0128 mol), dimethyl terephthalate (5.83 g, 0.0302 mol), glycerol (1.66 g, 0.0180 mol), 2,2'-dimethyl-1,3-propanediol (2.17 g, 0.0208 mol), butylated hydroxytoluene (0.02 g, 0.0908 mmol) and Ti(IV) isopropoxide (0.02 mL, 0.0676 mmol) were weighed and placed in a three-neck round bottom flask. The reaction procedure outline in Section 6.2.1 was then followed. Yield: 12.03 g brown oil. Mw: 3117 Da, PDI: 1.02

^{1}H NMR (501 MHz, $CDCl_3$) δ 8.25 – 7.96 (m, 9H, ArH), 4.74 (d, *J* = 38.6 Hz, 1H, CH), 4.59 – 4.32 (m, 4H, CH_2), 4.32 – 4.16 (m, 4H, CH_2), 3.91 – 3.47 (m, 28H, CH_2), 3.37 (d, *J* = 1.9 Hz, 2H, CH_3), 1.34 – 0.92 (m, 8H, CH_3).

FTIR (cm^{-1}): 3491 (-O-H, alcohol), 2867 (-C-H, alkyl), 1715 (-C=O, ester), 1605 (-C=C-, conjugated alkene), 1456 (-C-H, alkane), 1370 (-O-H, alcohol), 1264 (-C-O, aromatic ester), 1095 (-C-O, alcohol), 1015 (-C=C-, alkene), 728 (-C-H, aromatic).

6.2.7.7 $mPEG_{500}$-polyester containing pentaerythritol and 2,2'-dimethyl-1,3-propanediol (DTI7) synthesis

$mPEG_{500}$ (12.81 g, 0.02562 mol), dimethyl terephthalate (7.77 g, 0.0400 mol), pentaerythritol (3.27 g, 0.0240 mol), 2,2'-dimethyl-1,3-propanediol (2.91 g, 0.0279 mol), butylated hydroxytoluene (0.02 g, 0.0908 mmol) and Ti(IV) isopropoxide (0.02 mL, 0.0676 mmol) were weighed and placed in a three-neck round bottom flask. The reaction procedure outline in Section 6.2.1 was then followed. Yield: 22.80 g light brown oil. Mw: 4316 Da, PDI: 1.12

^{1}H NMR (501 MHz, $CDCl_3$) δ 8.17 – 7.91 (m, 9H, ArH), 4.64 – 4.34 (m, 6H, CH_2), 4.30 – 4.04 (m, 4H, CH_2), 3.87 – 3.42 (m, 89H, CH_2), 3.34 (s, 7H, CH_3), 2.80 (s, 5H, OH), 1.24 – 0.78 (m, 7H, CH_3).

FTIR (cm^{-1}): 3470 (O-H, alcohol), 2866 (C-H, alkyl), 1718 (C=O, ester), 1452 (C-H, alkane), 1349 (O-H, alcohol), 1264 (C-O, aromatic ester), 1091 (C-O, alcohol), 1016 (C=C, alkene), 941 (C=C, alkene), 849 (C-H, aromatic), 730 (C-H, aromatic).

6.2.7.8 $mPEG_{750}$-polyester containing pentaerythritol and 2,2'-dimethyl-1,3-propanediol (DTI8) synthesis

$mPEG_{750}$ (9.61 g, 0.0128 mol), dimethyl terephthalate (3.89 g, 0.0200 mol), pentaerythritol (1.64 g, 0.0120 mol), 2,2'-dimethyl-1,3-propanediol (1.46 g, 0.014 mol), butylated hydroxytoluene (0.01 g, 0.0454 mmol) and Ti(IV) isopropoxide (0.01 mL, 0.0338 mmol) were

weighed and placed in a three-neck round bottom flask. The reaction procedure outline in Section 6.2.1 was then followed. Yield: 11.43 g brown oil. Mw: 2206 Da, PDI: 1.13

^{1}H NMR (500 MHz, $CDCl_3$) δ 8.28 – 7.75 (m, 25H, ArH), 4.66 – 4.35 (m, 18H, CH_2), 4.20 (dd, *J* = 24.3, 14.2 Hz, 4H, CH_2), 3.99 – 3.41 (m, 319H, CH_2), 3.35 (s, 14H, CH_3), 2.42 (s, 30H, OH), 1.50 – 0.69 (m, 9H, CH_3).

FTIR (cm^{-1}): 3478 (O-H, alcohol), 2871 (C-H, alkyl), 1721 (C=O, ester), 1455 (C-H, alkane), 1349 (O-H, alcohol), 1268 (C-O, aromatic ester), 1090 (C-O, alcohol), 1017 (C=C, alkene), 948 (C=C, alkene), 844 (C-H, aromatic), 730 (C-H, aromatic).

6.2.7.9 $mPEG_{500}$-polyester containing ethylene glycol and 2-amino-2-methyl-1,3-propanediol (DTI9) synthesis

$mPEG_{500}$ (12.78 g, 0.0256 mol), dimethyl terephthalate (7.77 g, 0.0400 mol), ethylene glycol (1.48 g, 0.0238 mol), 2-amino-2-methyl-1,3-propanediol (2.92 g, 0.0278 mol), butylated hydroxytoluene (0.02 g, 0.0908 mmol) and Ti(IV) isopropoxide (0.02 mL, 0.0676 mmol) were weighed and placed in a three-neck round bottom flask. The reaction procedure outline in Section 6.2.1 was then followed. Yield: 10.51 g, amber oil. Mw: 3377 Da, PDI: 1.03

^{1}H NMR (500 MHz, DMSO) δ 8.20 – 7.81 (m, 17H, Ar), 4.68 – 4.07 (m, 16H, CH_2), 3.76 (dt, *J* = 45.8, 22.7 Hz, 7H, CH_2), 3.70 – 3.29 (m, 133H, CH_2), 3.28 – 3.17 (m, 11H, CH_3), 1.50 – 1.38 (m, 5H, CH_3), 1.27 – 1.20 (m, 3H, NH).

FTIR (cm^{-1}): 3481 (O-H, alcohol), 3303 (N-H, stretching), 2863 (C-H, alkyl), 1717 (C=O, ester), 1645 (N-H bending), 1409 (C-H, alkane), 1270 (C-O, aromatic ester), 1095 (C-O, alcohol), 1017 (C=C, alkene), 713 (C-H, aromatic).

6.2.7.10 $mPEG_{500}$-polyester containing ethylene glycol and diethanolamine (DTI10) synthesis

$mPEG_{500}$ (12.81 g, 0.02562 mol), dimethyl terephthalate (7.77 g, 0.0400 mol), ethylene glycol (1.51 g, 0.0243 mol), diethanolamine (2.91 g, 0.0280 mol), butylated hydroxytoluene (0.02 g, 0.0908 mmol) and Ti(IV) isopropoxide (0.02 mL, 0.0676 mmol) were weighed and placed in a three-neck round bottom flask. The reaction procedure outline in Section 6.2.1 was then followed. Yield: 15.08 g, brown oil. Mw: 5841 Da, PDI: 1.27

^{1}H NMR (501 MHz, $CDCl_3$) δ 8.15 – 7.89 (m, 30H, ArH), 7.48 – 7.31 (m, 3H, NH), 4.72 – 4.56 (m, 14H, CH_2), 4.44 (dd, *J* = 5.4, 4.1 Hz, 15H, CH_2), 4.06 – 3.37 (m, 219H, CH_2), 3.31 (s, 18H, CH_3).

FTIR (cm^{-1}): 3495 (O-H, alcohol), 3320 (N-H, stretching), 2867 (C-H, alkyl), 1715 (C=O, ester), 1635 (N-H bending), 1409 (C-H, alkane), 1250 (C-O, aromatic ester), 1095 (C-O, alcohol), 1017 (C=C, alkene), 730 (C-H, aromatic).

6.2.7.11 $mPEG_{500}$-polyester containing ethylene glycol and pentanediol (DTI11) synthesis

$mPEG_{500}$ (12.81 g, 0.0256 mol), dimethyl terephthalate (7.77 g, 0.0400 mol), ethylene glycol (1.51 g, 0.0243 mol), pentanediol (2.91 g, 0.280 mol), butylated hydroxytoluene (0.02 g, 0.0908 mmol) and Ti(IV) isopropoxide (0.02 mL, 0.0676 mmol) were weighed and placed in a three-neck round bottom flask. The reaction procedure outline in Section 6.2.1 was then followed. Yield: 19.46 g brown oil. Mw: 4409 Da, PDI: 1.11

^{1}H NMR (501 MHz, $CDCl_3$) δ 8.23 – 7.93 (m, 15H, ArH), 4.70 (d, *J* = 16.1 Hz, 2H, CH_2), 4.56 – 4.25 (m, 13H, CH_2), 3.98 – 3.89 (m, 2H, CH_2), 3.86 – 3.47 (m, 88H, CH_2), 3.35 (s, 7H, CH_3), 1.96 – 1.39 (m, 14H, CH_2).

FTIR (cm^{-1}): 3501 (O-H, alcohol), 2867 (C-H, alkyl), 1713 (C=O, ester), 1409 (C-H, alkane), 1270 (C-O, aromatic ester), 1099 (C-O, alcohol), 1019 (C=C, alkene), 726 (C-H, aromatic).

6.2.7.12 $mPEG_{500}$-polyester containing glycerol and 2-amino-2-methyl-1,3-propanediol (DTI12) synthesis

$mPEG_{500}$ (12.78 g, 0.0256 mol), dimethyl terephthalate (7.77 g, 0.0400 mol), glycerol (2.21 g, 0.0240 mol), 2-amino-2-methyl-1,3-propanediol (2.92 g, 0.277 mol), butylated hydroxytoluene (0.02 g, 0.0908 mmol) and Ti(IV) isopropoxide (0.02 mL, 0.0676 mmol) were weighed and placed in a three-neck round bottom flask. The reaction procedure outline in Section 6.2.1 was then followed. Yield: 19.75 g amber-brown oil. Mw: 2117, PDI: 1.11

^{1}H NMR (501 MHz, $CDCl_3$) δ 8.17 – 7.80 (m, 58H, ArH), 4.78 – 4.61 (m, 4H, CH), 4.57 – 4.31 (m, 45H, CH_2), 4.12 (ddd, *J* = 16.8, 11.5, 8.6 Hz, 11H, CH_2), 3.90 – 3.44 (m, 326H, CH_2), 3.36 (d, *J* = 1.2 Hz, 22H, CH_3), 2.11 (d, *J* = 79.3 Hz, 11H, OH), 1.69 – 1.39 (m, 19H, CH_3), 1.30 (dd, *J* = 25.5, 22.6 Hz, 8H, NH).

FTIR (cm^{-1}): 3468 (-O-H, alcohol), 3278 (-N-H) 2867 (-C-H, alkyl), 1718 (-C=O, ester), 1645 (-N-H, bending), 1409 (-O-H, alcohol), 1264 (-C-O, aromatic ester), 1099 (-C-O, alcohol), 1017 (-C=C-, alkene), 844 (-C-H, aromatic), 732 (-C-H, aromatic).

6.2.7.13 $mPEG_{500}$-polyester containing glycerol and diethanolamine (DTI13) synthesis

$mPEG_{500}$ (12.81 g, 0.02562 mol), dimethyl terephthalate (7.77 g, 0.0400 mol), glycerol (2.24 g, 0.0243 mol), diethanolamine (2.98 g, 0.0283 mol), butylated hydroxytoluene (0.02 g, 0.0908 mmol) and Ti(IV) isopropoxide (0.02 mL, 0.0676 mmol) were weighed and placed in a three-neck round bottom flask. The reaction procedure outline in Section 6.2.1 was then followed. Yield: 17.48 g brown oil. Mw: 4943 Da, PDI: 1.16

^{1}H NMR (501 MHz, $CDCl_3$) δ 8.07 (s, 140H, ArH), 7.42 (s, 4H, NH), 4.72 (d, *J* = 29.0 Hz, 11H, CH), 4.66 (s, 24H, CH_2), 4.46 (s, 80H, CH_2), 4.36 (s, 14H, CH_2), 3.95 – 3.43 (m, 917H, CH_2), 3.33 (s, 79H, CH_3), 3.17 (s, 74H, OH).

FTIR (cm^{-1}): 3480 (O-H, alcohol), 2867 (C-H, alkyl), 1717 (C=O, ester), 1639 (N-H, bending), 1454 (C-H, alkane), 1350 (O-H, alcohol), 1250 (C-O, aromatic ester), 1095 (C-O, alcohol), 1015 (C=C, alkene), 730 (C-H, aromatic).

6.2.7.14 $mPEG_{500}$-polyester containing tris(hydroxymethyl)aminomethane and 2,2'-dimethyl-1,3-propanediol (DTI14) synthesis

$mPEG_{500}$ (12.81 g, 0.02562 mol), dimethyl terephthalate (7.77 g, 0.0400 mol), 2,2'-dimethyl-1,3-propanediol (2.91 g, 0.0279 mol), tris(hydroxymethyl)aminomethane (2.91 g, 0.0240 mol), butylated hydroxytoluene (0.02 g, 0.0908 mmol) and Ti(IV) isopropoxide (0.02 mL, 0.0676 mmol) were weighed and placed in a three-neck round bottom flask. The reaction procedure outline in Section 6.2.1 was then followed. Yield: 17.72 g brown oil. M_w: 6799 Da, PDI: 1.30

^{1}H NMR (501 MHz, $CDCl_3$) δ 8.19 – 7.81 (m, 18H, ArH), 4.58 (t, *J* = 34.6 Hz, 5H, CH_2), 4.53 – 4.39 (m, 10H, CH_2), 4.32 – 4.15 (m, 3H, CH_2), 3.98 – 3.45 (m, 91H, CH_2), 3.37 (d, *J* = 1.5 Hz, 7H, CH_3), 1.81 (s, 4H, OH), 1.26 – 0.92 (m, 5H, CH_3).

FTIR (cm^{-1}): 3448 (O-H, alcohol), 2869 (C-H, alkyl), 1718 (C=O, ester), 1650 (N-H, bending), 1456 (C-H, alkane), 1408 (O-H, bending), 1265 (C-O, aromatic ester), 1098 (C-O, alcohol), 1016 (C=C, alkene), 949 (C=C, alkene), 853 (C-H, aromatic), 730 (C-H, aromatic).

6.2.7.15 $mPEG_{500}$-polyester containing tris(hydroxymethyl)aminomethane and ethylene glycol (DTI15) synthesis

$mPEG_{500}$ (8.83 g, 0.0177 mol), dimethyl terephthalate (5.34 g, 0.0275 mol), ethylene glycol (1.00 g, 0.0161 mol), tris(hydroxymethyl)aminomethane (3.00 g, 0.0248 mol), butylated hydroxytoluene (0.01 g, 0.0454 mmol) and Ti(IV) isopropoxide (0.01 mL, 0.0338 mmol) were weighed and placed in a three-neck round bottom flask. The reaction procedure outline in Section 6.2.1 was then followed. Yield: 9.90 g brown oil. M_W: 3458 Da, PDI: 1.32

^{1}H NMR (500 MHz, $CDCl_3$) δ 8.10 – 7.43 (m, 4H, ArH), 4.90 – 4.50 (m, 5H, CH_2), 4.41 (dd, *J* = 22.1, 18.6 Hz, 3H, CH_2), 3.94 – 3.34 (m, 25H, CH_2), 3.30 (s, 2H, CH_3).

FTIR (cm^{-1}): 3448 (O-H, alcohol), 2867 (C-H, alkyl), 1719 (C=O, ester), 1643 (N-H, bending), 1458 (C-H, alkane), 1409 (O-H, bending), 1264 (C-O, aromatic ester), 1091 (C-O, alcohol), 1015 (C=C, alkene), 952 (C=C, alkene), 864 (C-H, aromatic), 711 (C-H, aromatic).

6.2.8 Consumer Load Testing

Miele W3922 washing machines set to a short cotton cycle (1 hour 25 mins) were used to perform the wash tests. Ariel Compact HDL liquid laundry detergent (35 mL) was added to each wash load, alongside DTI polymer solution (0.1 mg mL^{-1}, 100 ppm) per wash. For the Ariel only washes, the same protocol was followed, however no polymer solution was added. In each wash a tracer fabric with 20 types of white fabrics were added in order to assess the level of discolouration. Following the completion of the wash, the colour change values were measured by spectrophotometry.

6.3 Results and Discussion

6.3.1 mPEG-*co*-Polyesters for Blocking Dye Deposition

Initially, three water-soluble polyesters (DTI**1**, **2** and **3**) were synthesised, each containing a range of different monomers to be incorporated into the backbone. Each polymer contained $mPEG_{500}$ to impart water solubility. The polyester was formed by reacting dimethyl terephthalate (DMT) with different diols or glycerol, a triol, in order to impart different properties. The diols used included 2,2'-dimethyl-1,3-propanediol, ethylene glycol and 1,2-propanediol (Figure 6-2). Glycerol was used to create a branched polymer network, owing to its tri-functionality. It was anticipated that the hydoxyl groups may improve interaction with the

fibres through hydrogen bonding. The polymers and the monomers included in them are set out in Appendix 1.

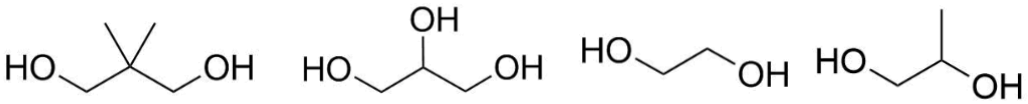

Figure 6-2. Left to right: 2,2'-dimethyl-1,3-propanediol, glycerol, ethylene glycol and 1,2-propanediol.

The polyester backbone of DTI**1** was based on 1,2-propanediol, with dimethyl terephthalate and $mPEG_{500}$. A proton NMR was obtained to confirm the structure (Figure 6-3).

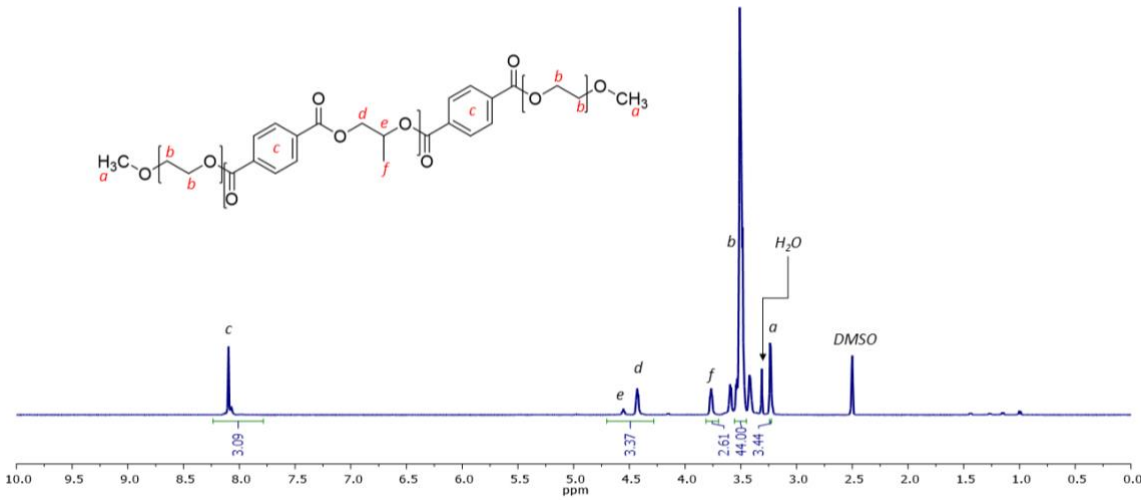

*Figure 6-3 ^{1}H NMR spectrum of 1,2-propanediol containing polymer (DTI**1**) in DMSO-d_6.*

Figure 6-3 shows the inclusion of the 1,2-propandiol into the structure of the polymer indicated by the presence of the peaks *d*, *e* and *f* which correspond the protons in the 1,2-propanediol monomer. The aromatic to PEG ratio was calculated as 1:18. The FTIR also confirmed the structure (Appendix 2).

DTI**2** was synthesised with glycerol and ethylene glycol. A proton NMR confirmed the structure (Figure 6-4).

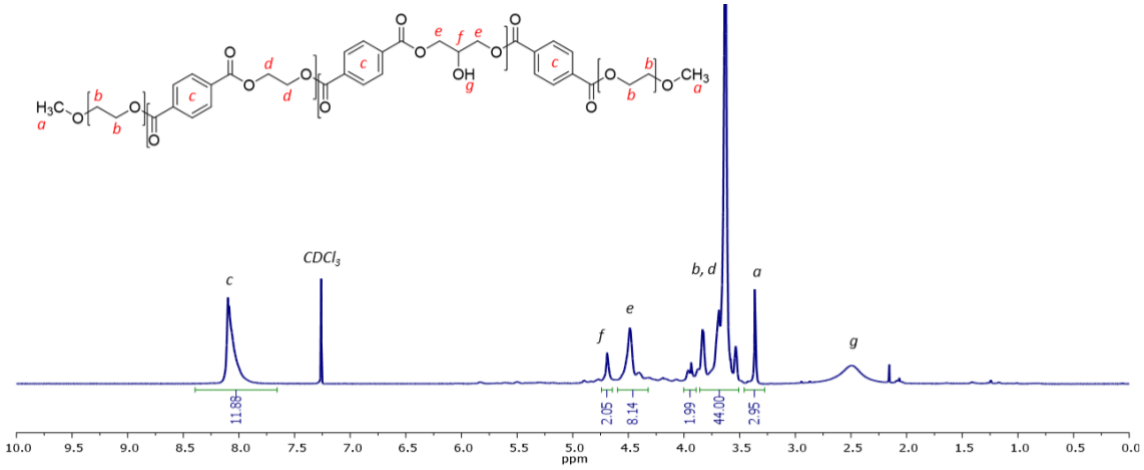

*Figure 6-4 ^{1}H NMR spectrum of glycerol and ethylene glycol containing polymer (DTI**2**) in $CDCl_3$.*

From Figure 6-4 it can be seen that the hydroxy group relating to the glycerol is not entirely reacted. The expectation was that the polymer would branch at the hydroxy site, however, the presence of the -OH peak labelled *g* shows that this has not occurred. An hydroxy peak in the FTIR spectrum of DTI**2** also indicates that extensive branching has not occurred (Appendix 3). The aromatic to PEG ratio was calculated and found to be 1:4.

DTI**3** was synthesised with 2,2'-dimethyl-1,3-propanediol and glycerol. This was also analysed by ^{1}H NMR (Figure 6-5).

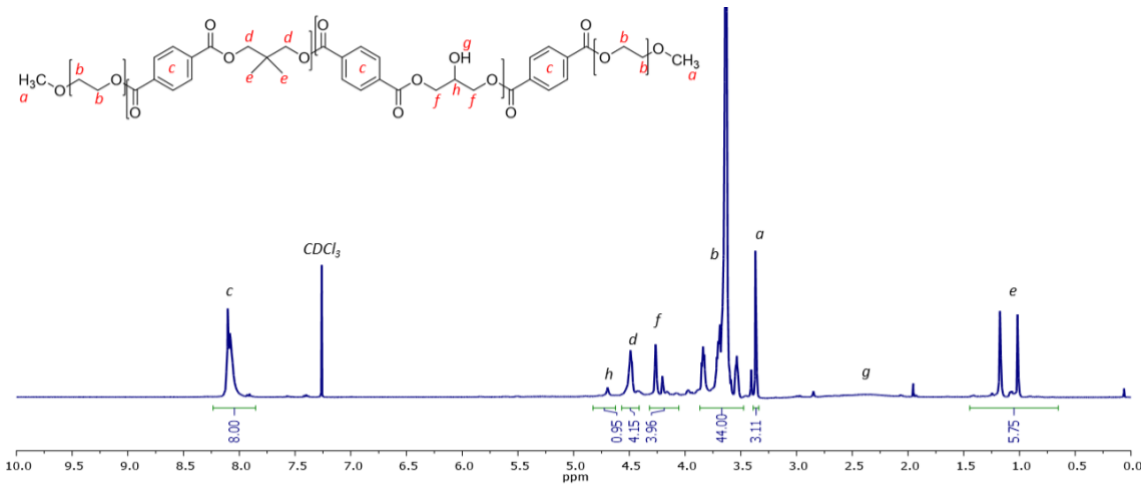

*Figure 6-5 ^{1}H NMR spectrum of 2,2'-dimethyl-1,3-propanediol and glycerol containing polymer (DTI**3**) in $CDCl_3$.*

Figure 6-5 shows both the 2,2'-dimethyl-1,3-propanediol and the glycerol were successfully incorporated into the polymer structure. However, as with DTI**2** the spectrum shows an hydroxy peak, labelled *g*, which indicates the glycerol has not branched. Therefore, the effect of the presence of the free hydroxy group will be observed, alongside the added steric bulk of the 2,2'-dimethyl-1,3-propanediol monomer in comparison to the ethylene glycol analogue in DTI**2**. The aromatic to PEG ratio was calculated as 1:6. The FTIR also confirmed the structure of DTI**3**, showing an hydroxy peak (Appendix 4).

The three polymers were then investigated for their ability to prevent dye deposition, in particular against indigo and C.I. Sulfur Black 1 (SB1) dye bleeding fabrics.

6.3.1.1 Indigo Dye Transfer Inhibition by DTI1, 2 and 3

The three polymers were washed with an indigo dye bleeding fabric and a multifibre. The colour change caused by indigo onto the multifibre swatch was measured and compared, in order to ascertain the extent of any benefits given by the polymers (Figure 6-6).

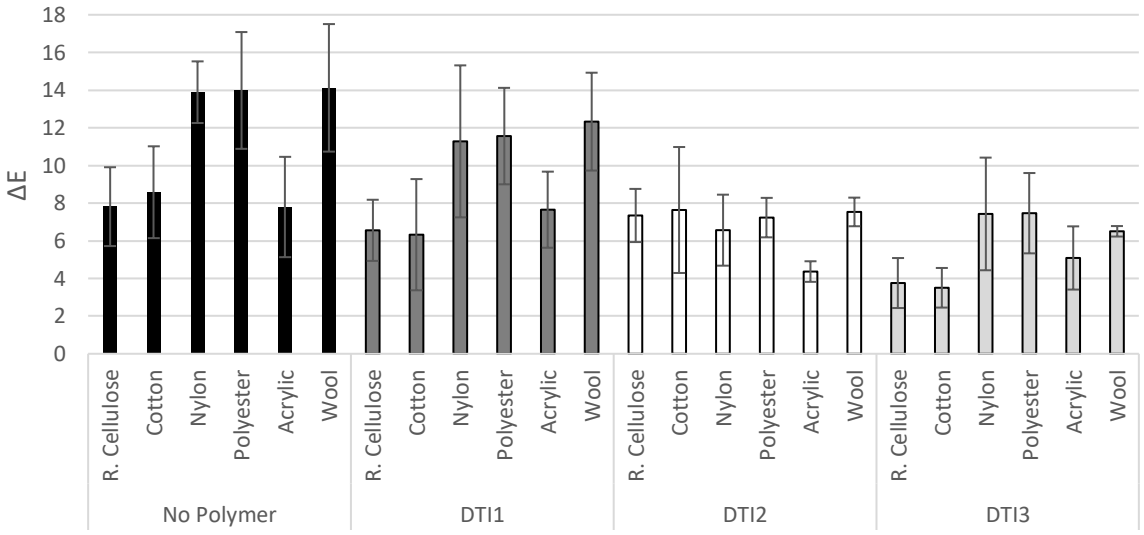

*Figure 6-6 A comparison of colour change caused by indigo in the presence of DTI**1**, **2** and **3**.*

Figure 6-6 shows that DTI**2** and **3** out-perform DTI**1**, with DTI**3** showing the overall best efficacy, including a reduction in colour change of over 50% on cotton and wool. This is a surprising result as the polymers are expected to interact with the hydrophobic fibres through hydrophobic

interactions of the polyester segment and the receiver fabric, blocking dye adsorption sites. The added benefit of efficacy for the hydrophilic fibres such as cotton and wool suggest hydrogen bonding should be to considered in the design of DTI polymers of this class. Additionally, the increasing level of steric bulk and branching is an important consideration, indicating the bulkier the polymer, the more effective it is as blocking dye deposition.

6.3.1.2 SB1 Dye Transfer Inhibition by DTI1, 2 and 3

In addition to indigo, SB1 was also investigated for its dye transfer properties in the presence of the three polymers (DTI**1**, **2** and **3**) (Figure 6-7).

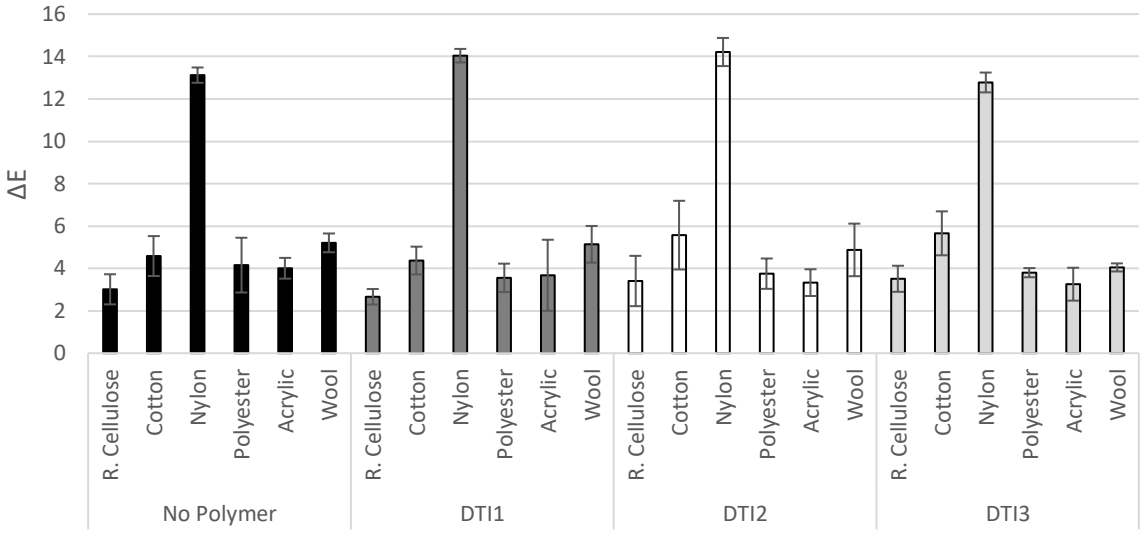

*Figure 6-7 A comparison of colour change caused by SB1 in the presence of DTI**1**, **2** and **3**.*

From Figure 6-7 it can be seen that none of the polymers reduced colour change caused by SB1. This indicates therefore that the properties of the dye are an important consideration, as well as considering the fibre properties. It is therefore clear that while a blocking mechanism of action may work for some dyes such as Indigo, it will be necessary to employ other DTI polymers in order to prevent deposition of other dyes, such as SB1.

6.3.1.3 Dye Transfer Inhibition by DTI3 for Further Dyes

From the colour change study with indigo, DTI**3** was selected as the most promising DTI candidate. This was therefore tested for its efficacy and C.I. Direct Orange 39 (DO39), C.I. Reactive Red 141 (RR141) and C.I. Reactive Black 5 (RB5).

DTI**3** was tested for its DTI efficacy against DO39 (Figure 6-8).

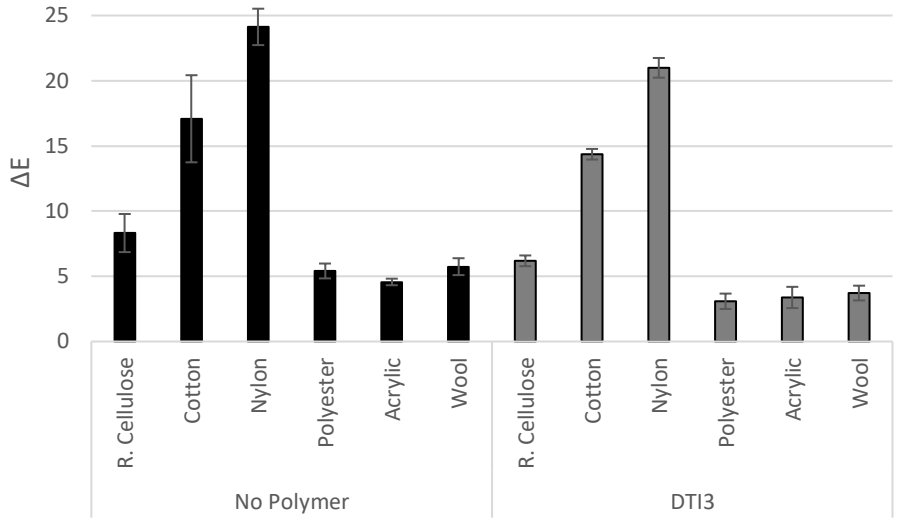

*Figure 6-8 A comparison of colour change caused by DO39 in the absence of polymer and in the presence DTI**3**.*

Figure 6-8 shows that DTI**3** has limited efficacy against DO39, but shows a reduced mean colour change for nylon, polyester and wool. Nylon shows a reduction in colour change from 24.13 to 21.00, a 17.1% reduction. It is encouraging that DTI**3** is able to reduce dye deposition for DO39 unlike for SB1, and again indicates the complex nature of dye transfer inhibition and the many considerations in polymer design.

RR141 was also tested with DTI3 (Figure 6-9).

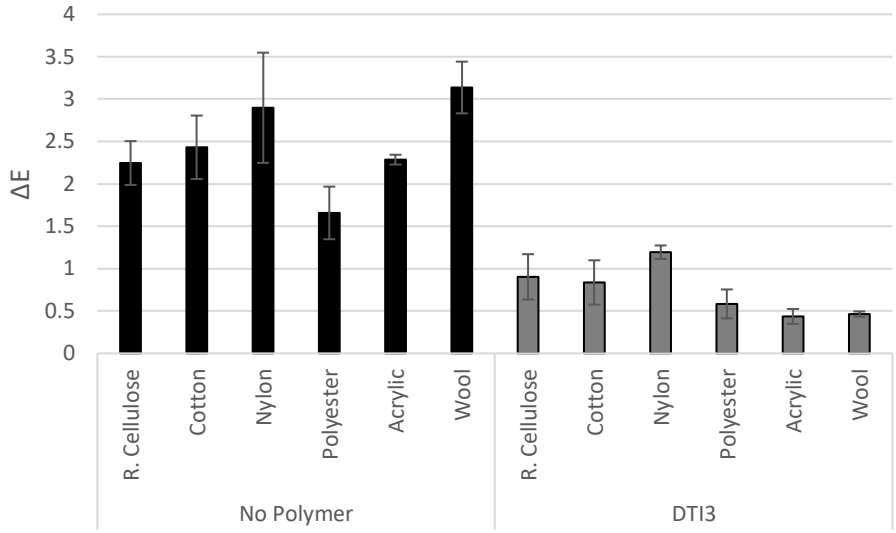

*Figure 6-9 A comparison of colour change caused by RR141 in the absence of polymer and in the presence DTI**3**.*

Without any polymer, RR141 does not cause as much colour change as DO39, SB1 or indigo, reaching a ΔE of 3.00 for nylon and 3.13 for wool. DTI**3** reduces the colour change onto all fibres as shown in Figure 6-9, with a 60% reduction onto nylon and 85% onto wool. This is highly promising result as it shows the colour change can be brought below a value of one with DTI**3**, and is effective across the whole range of fibre types, particularly cotton, showing a 65.8% reduction, which the reactive dye is designed to dye.

RB5 also shows a lower but significant level of colour change (Figure 6-10).

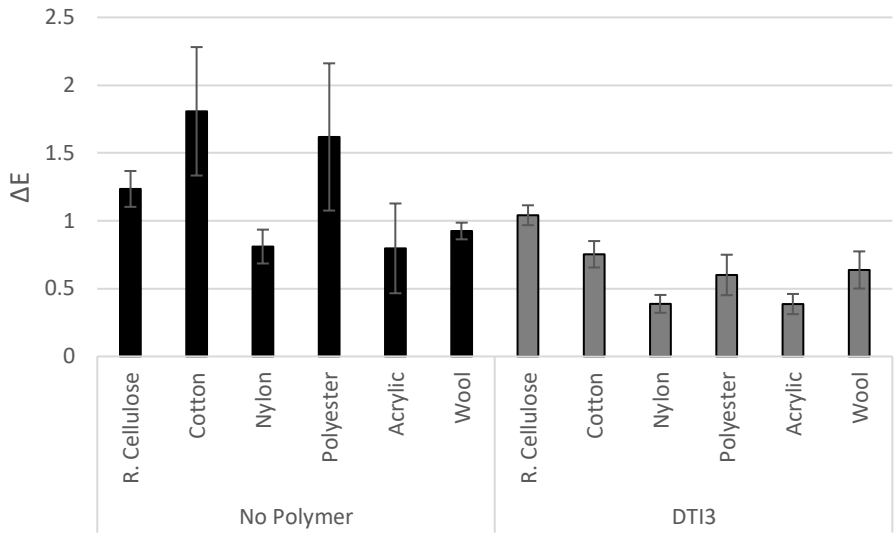

*Figure 6-10 A comparison of colour change caused by RB5 in the absence of polymer and in the presence DTI**3**.*

As with RR141, the colour change caused by RB5 is reduced to below one with DTI**3**, for all but one fibre type, regenerated cellulose, as seen in Figure 6-10. The reduction in colour change for cotton and polyester are particularly significant, giving a 57.1% reduction, and 62.5% respectively.

The results for the five dyes analysed indicate that nylon is the fibre that is subject to the greatest overall colour change in the absence of polymer. Therefore, future polymer designs may be focused on targeting the reduction in dye deposition onto nylon. This may be done by designing DTI polymers that are capable of hydrogen bonding with the nylon fibre, such as polyamides or amine containing polymers, like the nylon itself.

6.3.2 Mode of Action of DTI3

DTI**3** has been found to be a successful DTI polymer, particularly against indigo. However, it is unclear whether the polymer works *via* a blocking mechanism, whereby it interacts with the fabric, or by complexation or encapsulation of the dye in the wash solution.

In order to investigate the mode of action of DTI**3**, a variety of methods were implemented. Firstly, pre-treatments of the polymer onto the fabric were carried out, and secondly, alternative

polymers based on DTI**3** were synthesised with varying length of hydrophilic and hydrophobic blocks.

6.3.2.1 DTI3 Pre-Treatment Studies

In order to assess if DTI**3** interacts with the fibre in the wash, and if it remains on the fabric after washing, multifibre swatches were washed with the polymer either once or twice before being washed with a dye bleeding fabric in plain, deionised water, in the absence of additional polymer. It was proposed that if the DTI efficacy is maintained in the final wash, polymer-fabric interaction has occurred in the previous washes in the presence of DTI**3**. This will be observable by comparable ΔE values for all washes, including the final wash cycle in which DTI**3** is not added. The wash conditions of the pre-treatment washes are outlined in Table 6-1.

*Table 6-1 The wash conditions of the DTI**3** pre-treatment study showing whether the dye bleeding swatch or the polymer were present in the wash.*

Sample Name	Wash 1		Wash 2		Wash 3	
	Dye Bleeding Swatch	DTI3	Dye Bleeding Swatch	DTI3	Dye Bleeding Swatch	DTI3
1 Pre-treatment	No	Yes	Yes	No	N/A	N/A
2 Pre-treatments	No	Yes	No	Yes	Yes	No

The colour change results of these tests were compared to that of a wash without polymer, and a standard DTI**3** wash with no pre-treatment (Figure 6-11).

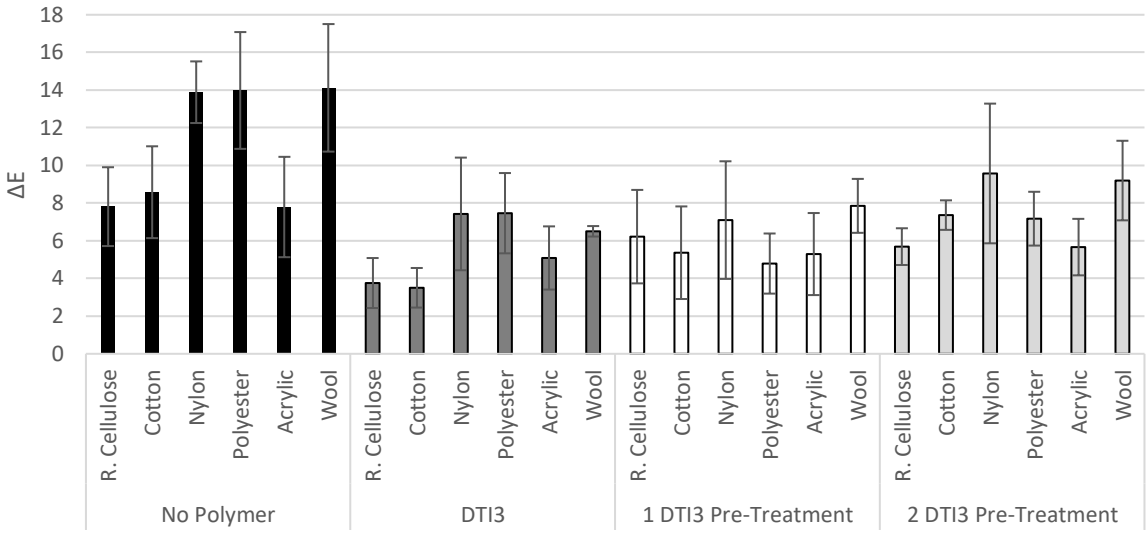

*Figure 6-11 A comparison of the colour change caused by indigo dye bleeder onto a multifibre swatch, without polymer, with DTI**3**, after one pre-treatment of DTI**3** and after two pre-treatment cycles of DTI**3**.*

From Figure 6-11 it can be seen that the two pre-treatment studies show a reduced colour change to that without polymer. This indicates the mode of action of DTI**3** to be one of a blocking mechanism, whereby the polymer deposits on the fabric in the wash and prevents deposition by blocking the adsorption sites on the fabric. These results prove the polymer is deposited onto the fabric and is maintaining some DTI efficacy in the second and third washes.

The cellulosic fibres, however, show a reduced efficacy in the pre-treatment studies. This is shown by the colour change onto cotton going from 3.50 for a regular wash with DTI**3**, to 5.37 for the first pre-treatment wash, and 7.36 for the second pre-treatment wash. This suggests that the polymer washes off the hydrophilic fibres to a greater extent than the hydrophobic fibres, as expected owing to their similarity to soil release polymers.

To observe if the polymer is significantly deposited onto the fabric to the point where it might cause an effect on the feel of the fabric, SEM images were obtained of cotton, nylon, polyester and wool after washing with DTI3, and having been washed with plain water (Figure 6-12).

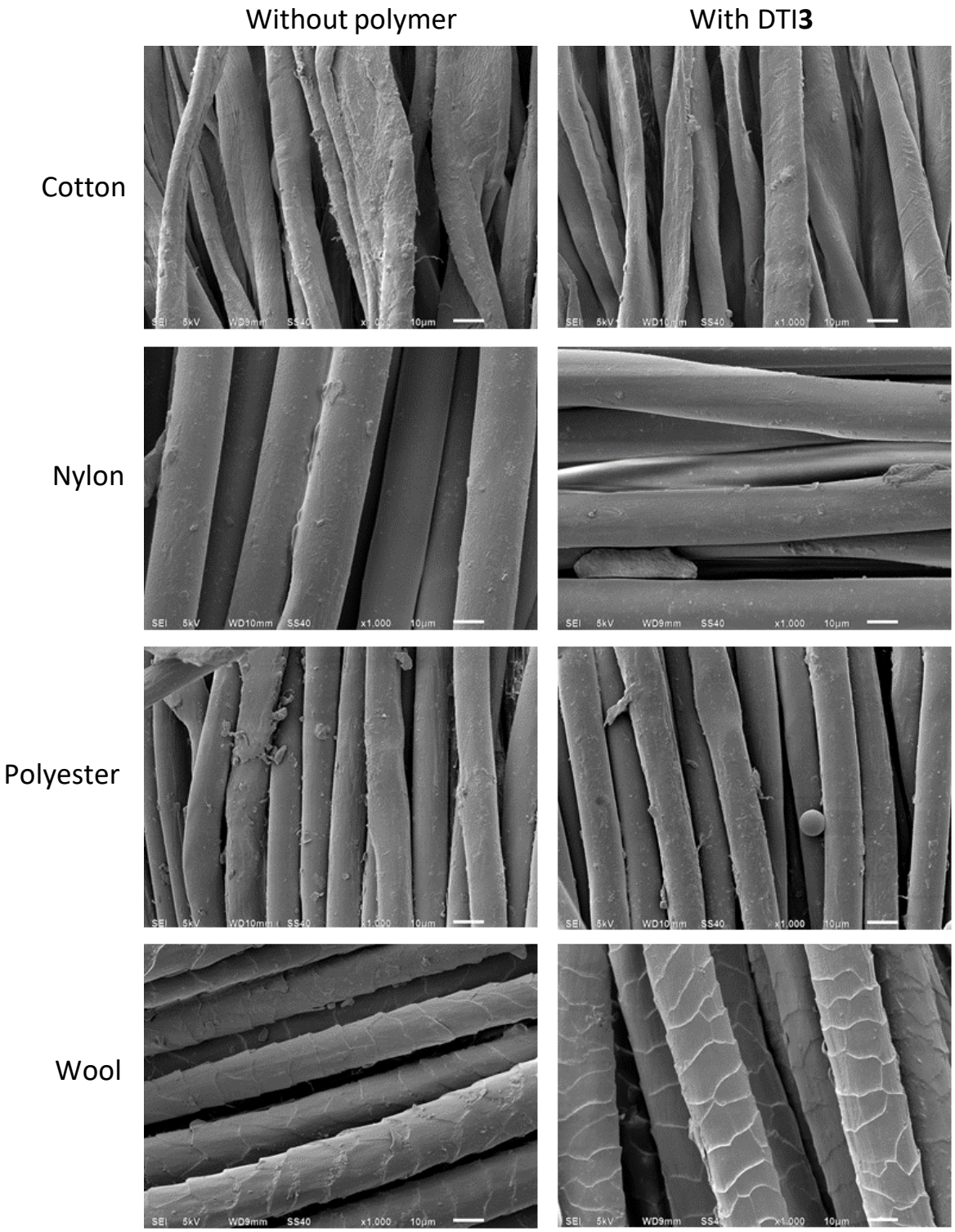

*Figure 6-12 SEM images of cotton, nylon, polyester and wool treated either with plain water, or DTI**3** aqueous solution.*

It may have been expected to see a sticky residue of the polymer on the fabrics, however Figure 6-12 shows that there are no observable deposits of the polymer onto them.

6.3.2.3 Effect of varying mPEG chain length in DTI3

Two polymers were synthesised whereby the molar ratio of the mPEG block to the polyester block was kept consistent, but the molecular weight of the mPEG was changed from 500 g mol^{-1} to either 750 g mol^{-1} (DTI**4**) or 5000 g mol^{-1} (DTI**5**). This was in order to observe what effect modifying the hydrophilicity of the polymer would have on the performance of the polymer as a DTI agent. Successful synthesis of the polymers was confirmed by ^{1}H NMR (Figure 6-13 and Figure 6-14).

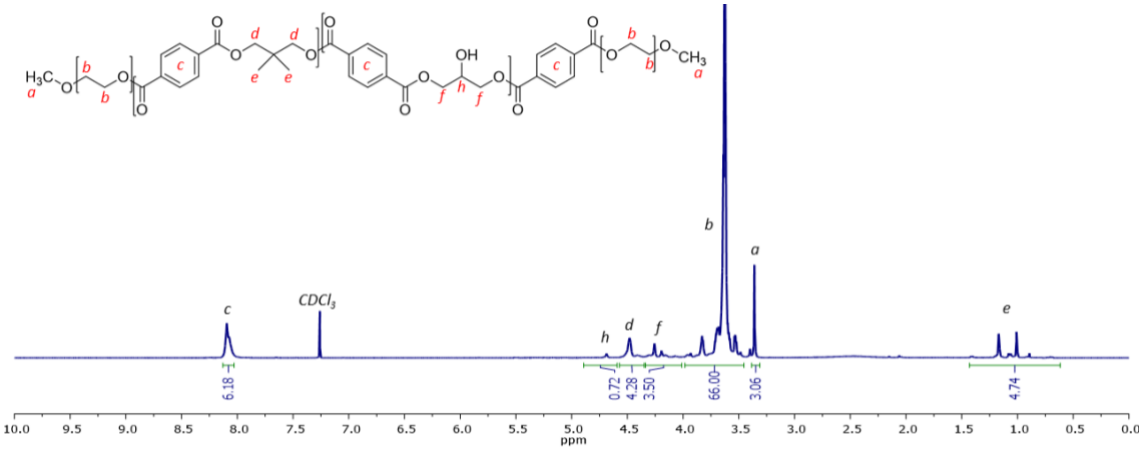

*Figure 6-13 ^{1}H NMR of DTI3 with mPEG$_{750}$ in place of mPEG$_{500}$ (DTI**4**) in CDCl$_3$.*

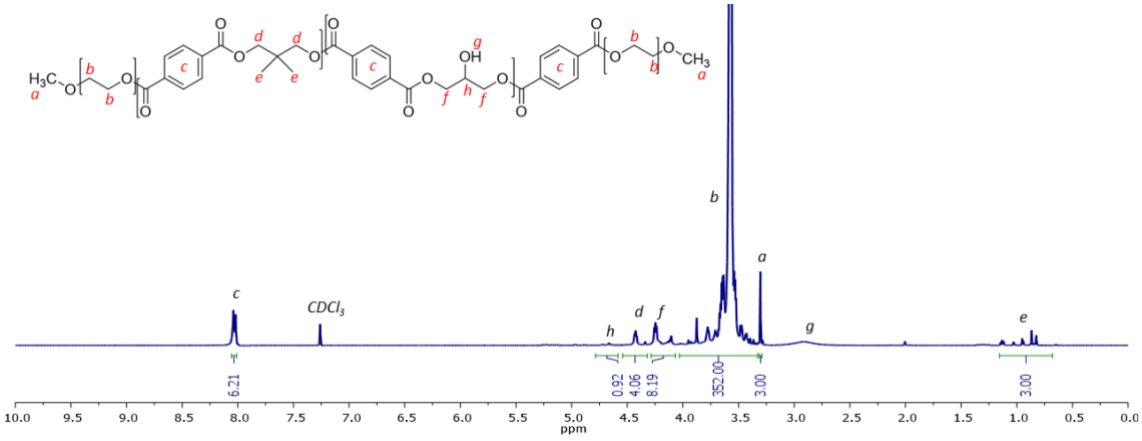

*Figure 6-14^{1}H NMR of DTI**3** with mPEG$_{5000}$ in place of mPEG$_{500}$ (DTI**5**) in CDCl$_3$.*

Both spectra in Figure 6-13 and Figure 6-14 are integrated relative to the PEG block, whereby the peak at 3.5-3.75 ppm has a set integration for the number of known protons in the PEG block. For mPEG$_{500}$ this is 44, for mPEG$_{750}$ it is 66 and mPEG$_{5000}$ it is 352. From the NMR spectra it can be observed that the two polymers are of similar chemical composition, both possessing

the same peaks in similar integration ratios, except peak *b* which relates to the PEG block. For example, the peak relating to the methyl groups (peak *e*) at 1 ppm both have an integration of *approx.* 4, showing that a similar amount of 2,2'-dimethyl-1,3-propanediol has been incorporated into each polymer. The FTIR spectra showed hydroxy, aromatic, methyl and ethylene group peaks (Appendix 5 and Appendix 6).

The ratio of aromatic groups to the PEG block for each polymer was calculated in order to observe the ratio of hydrophobicity to hydrophilicity. For DTI**4**, peak *c* is integrated at 6.55 to the PEG block at 44. Therefore, the ratio is 1:7 for DTI**4**. This is in contrast to DTI**5**, where the ratio is calculated as 1:51. This therefore shows the vast difference in hydrophilicity of the two polymers and allows for the determination of the effect of hydrophilicity on polymer DTI performance.

The two polymers were washed with indigo dye bleeding fabric to assess their DTI efficacy (Figure 6-15).

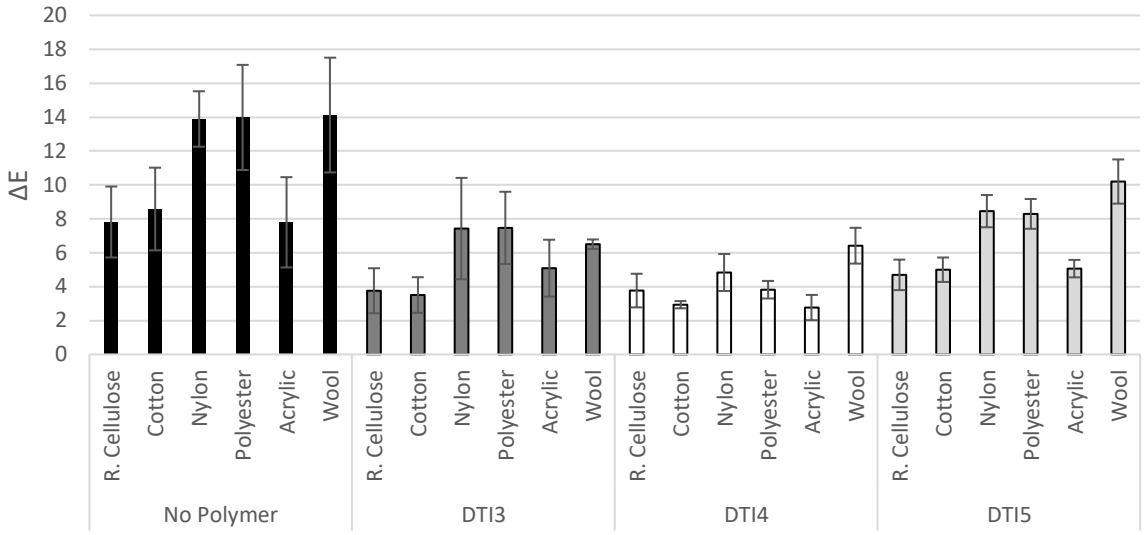

*Figure 6-15 A comparison of the colour change caused by indigo in the presence of DTI**3**, and DTI**4** or DTI**5**.*

From Figure 6-15 it can be observed that the hydrophilicity of the polymer has a moderate effect on the efficacy of the polymer as a DTI. By increasing the molecular weight of the mPEG block to 750 g mol^{-1} (DTI**4**) there is a mild improvement in the mean colour change value, particularly on nylon and polyester in comparison to that of the original polymer. For nylon, a 35.0% decrease from the original polymer to DTI**4** is observed, and a 48.8% decrease for polyester. However, the values for regenerated cellulose and cotton are consistent with each other for the two polymers.

In contrast, there is a moderate worsening effect in mean colour change for all fibre types when the hydrophilicity is significantly increased to 5000 g mol^{-1} (DTI**5**), particularly for nylon and polyester. Polyester shows a 10.1% increase from DTI**3** to DTI**5** for the colour change caused by indigo, and nylon gives a 12.1% increase. The increased hydrophilic character of the polymer suggests polymer-water interactions are favoured over polymer-fabric interactions. As the DTI efficacy reduces when $mPEG_{5000}$ is included in the formulation (DTI**5**), it may be hypothesised that the polymer does not complex the dye in the wash water, but blocks the deposition of the dye onto the fabric in the case of DTI**3** and DTI**4**.

These results highlight that the hydrophilic-hydrophobic balance of the polymer is an important consideration of this type of DTI agent, as well as giving evidence for a mode of action whereby the polymer interacts with the fibre and blocks dye deposition, rather than encapsulating or complexing the dye in the wash solution.

6.3.2.4 Effect of Increasing the Polyester Chain Length

A further polymer was synthesised based on DTI**3**, containing $mPEG_{500}$ but with the molar ratio of the polyester block increased by 50% relative to the PEG content, in order to further assess the effect of the hydrophobic-hydrophilic balance (DTI**6**). The polymer was found to be insoluble in water. This polymer was analysed by ^1H NMR (Figure 6-16).

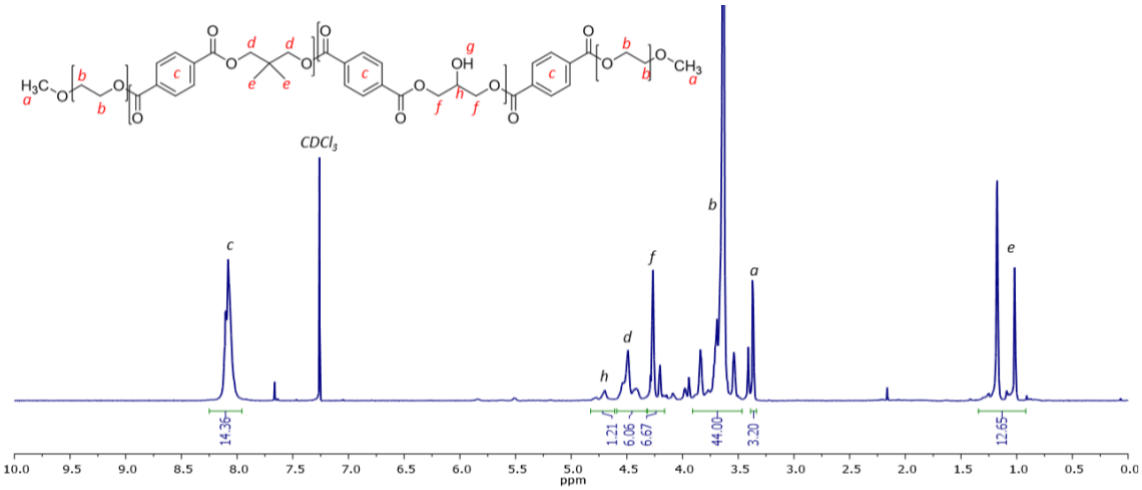

Figure 6-16 ^1H NMR of DTI3 with 50% increase in polyester starting materials (DTI**6**) in $CDCl_3$.

The ^1H NMR in Figure 6-16 shows the successful synthesis of the polymer, as the integrations of the peaks associated with the polyester block are approximately. twice the integration of those in DTI**3**. For example, the peak labelled *c* in both the spectra goes from an integration value of 8 for DTI**3** to 14.36 ppm for DTI**6**, showing that DTI**6** has increased polyester content. The aromatic to hydrophilic ratio was also calculated for DTI**6** and was found to be 1:3 and therefore shows an increased hydrophobic content in comparison to that of DTI**3** (1:6). The FTIR spectrum further confirmed the structure of DTI**6** (Appendix 7).

This polymer was dispersed in water and washed with indigo dye bleeding fabric and compared to DTI**3** (Figure 6-17).

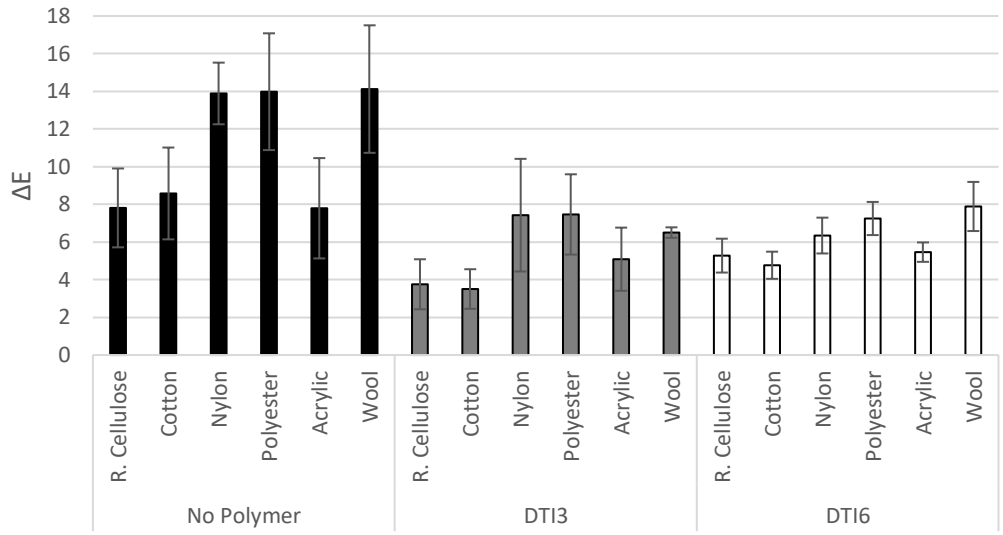

*Figure 6-17 A comparison of the colour change caused by indigo in the presence of DTI**3**, and that with 50% increased polyester content (DTI**6**).*

From Figure 6-17 it can be observed that increasing the hydrophobic content of the polymer, moderately increases the mean colour change for the hydrophilic fibres in comparison to DTI**3**. For example, the colour change onto cotton is increased by 26.6% from DTI**3** to DTI**6**. This therefore provides further evidence that the polymer interacts with the fibres in order to reduce colour change. This is not counter balanced by an improvement in colour change for the hydrophobic fibre types in comparison to DTI**3**, which have similar ΔE values for DTI**6**.

6.3.3 Effect of Polyester Block Modification on Indigo Dye Transfer

Attempts to produce more effective DTIs, by including monomers that add branching and/or amine groups to the polymer where then made. Due to the success of DTI**3**, it was hypothesised that the inclusion of glycerol in the polymer backbone provided a branched polymer with greater steric bulk, which was a more effective DTI compared to the linear analogue. Therefore, alcohol containing monomers pentaerythritol, 2-amino-2-methyl-1,3-propanediol, diethanolamine and

tris(hydroxymethyl) aminomethane were incorporated into the polymer structures (Figure 6-18).

Figure 6-18 Left to right: Pentaerythritol, 2-amino-2-methyl-1,3-propanediol, diethanolamine and tris(hydroxymethyl)aminomethane.

6.3.3.1 Pentaerythritol Containing Polymers

Pentaerythritol replaced glycerol in the DTI**3** formulation to observe the effect of increasing the branching further (DTI**7**). The inclusion of the pentaerythritol was confirmed by ^{1}H NMR (Figure 6-19).

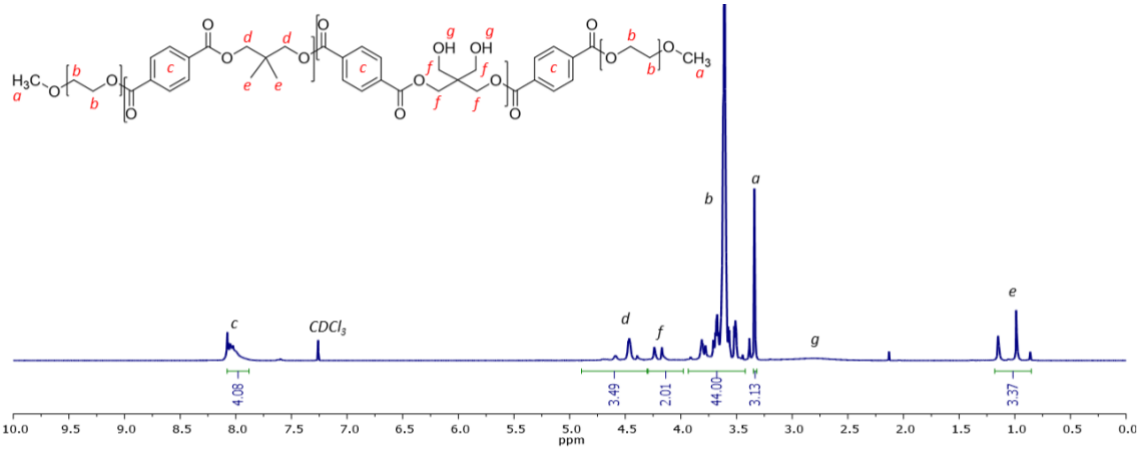

*Figure 6-19 ^{1}H NMR of pentaerythritol containing polymer DTI**7** in $CDCl_3$.*

The ^{1}H NMR spectrum shows a small hydroxy peak at 2.75 ppm (Figure 6-19), which indicates that not all the hydroxy groups of the pentaerythritol have reacted. The incorporation of hydroxy groups provides further hydrogen bonding capability to the polymer, and may therefore be exploited for polymer-fibre interaction, as well as enhanced polymer solubility in aqueous solution. Consequently, it may be predicted that anionic dyes will be repelled from DTI**7** treated fibres. The aromatic group to PEG block ratio was calculated to be 1:10. The FTIR spectrum of DTI**7** also showed an hydroxy peak, alongside aromatic, ethylene, aromatic and methyl group peaks (Appendix 8).

A second polymer (DTI**8**) was synthesised with $mPEG_{750}$ and pentaerythritol that possessed enhanced water-solubility compared to DTI**7** and the ^{1}H NMR spectrum obtained (Figure 6-20).

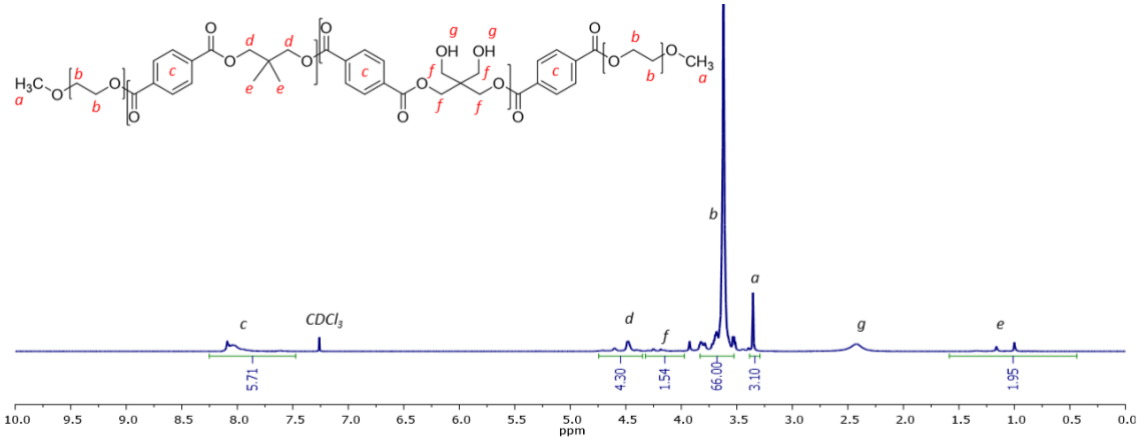

*Figure 6-20 ^{1}H NMR spectrum of mPEG$_{750}$ and pentaerythritol containing polymer (DTI**8**) in $CDCl_3$.*

The ^{1}H NMR spectrum of DTI**8** shows an hydroxy peak labelled *g* at 2.5 ppm, which again shows the presence of free hydroxy groups in the polymer backbone. This is confirmed by the presence of an hydroxy peak in the FTIR spectrum of the polymer. The aromatic groups to PEG block content were found to be in the ratio of 1:13, which shows a moderate increase in hydrophilicity to DTI**7**. The FTIR spectrum further confirmed the structure of DTI**8** (Appendix 9).

The two polymers were then investigated for their ability to prevent the dye transfer of indigo (Figure 6-21).

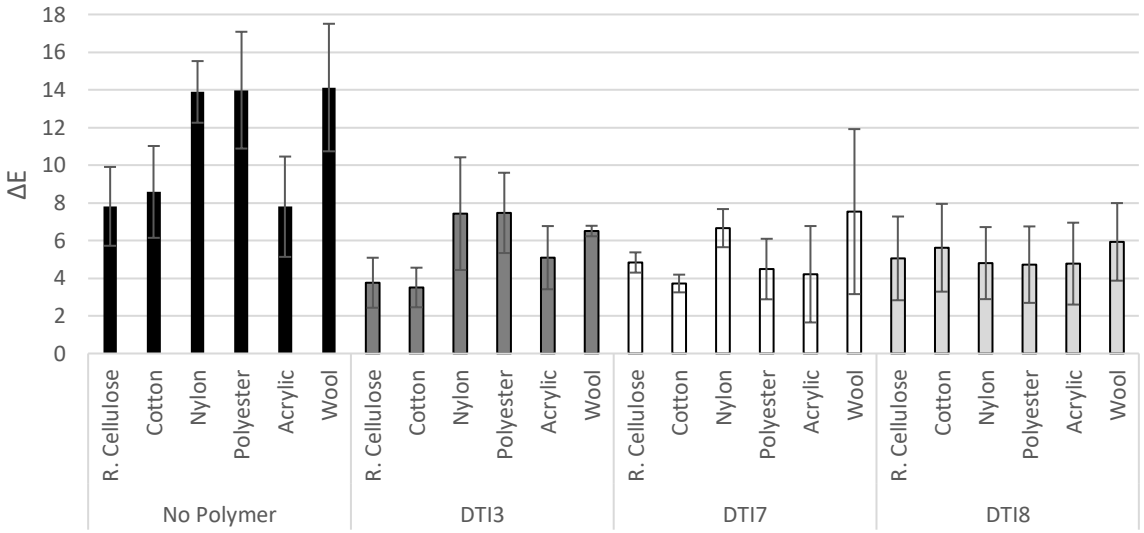

*Figure 6-21 A comparison of the colour change caused by indigo in the presence of the pentaerythritol containing polymer with mPEG$_{500}$ (DTI**7**) and mPEG$_{750}$ (DTI**8**).*

It can be observed from Figure 6-21 that both polymers are effective DTI agents against indigo, particularly for hydrophobic fibres, nylon and polyester. Colour change onto nylon reduces from a mean value of 13.98 in the absence of polymer to 4.80 in the presence of DTI**8**, and from 13.98 to 4.72 for polyester. This result is also an improvement on the mean colour change caused by indigo in the presence of DTI**3** (7.42 and 7.46 respectively).

6.3.3.2 Primary and Secondary Amine Containing Polymers

Further polymers were produced in order to generate ever-more effective DTIs. The primary amine containing 2-amino-2-methyl-1,3-propanediol, and secondary amine diethanolamine were incorporated into the formulation of DTI**2** (DTI**9** and DTI**10**, respectively), and the polymer structures confirmed by ^{1}H NMR (Figure 6-22 and Figure 6-23).

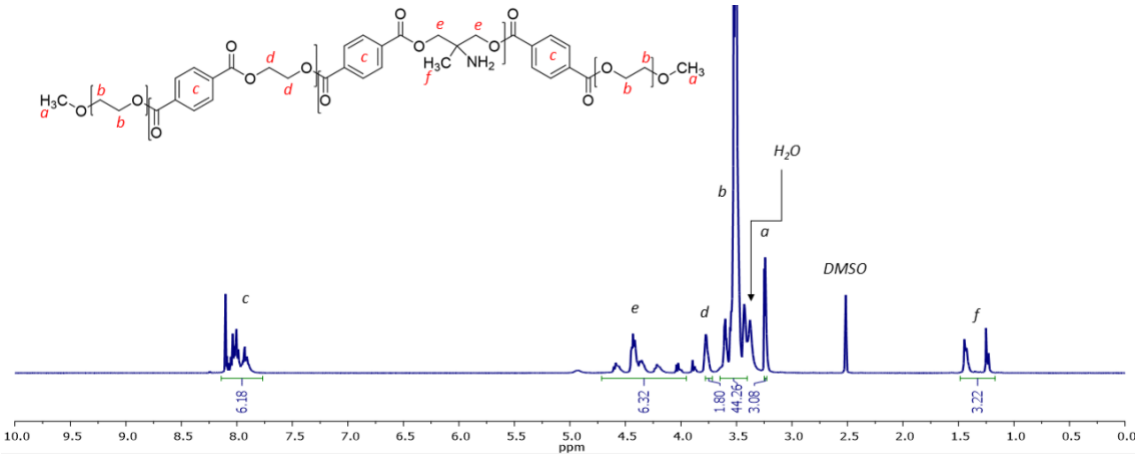

*Figure 6-22 ^{1}H NMR spectrum of the 2-amino-2-methyl-1,3-propanediol containing polymer (DTI**9**) in DMSO-d_6.*

The ^{1}H NMR spectrum in Figure 6-22 shows the incorporation of the amine monomer into the polymer structure by the presence of the peak labelled *f*. The amine peak is observable in the polymer FTIR spectrum (Appendix 10). The aromatic to PEG ratio was calculated as 1:8.

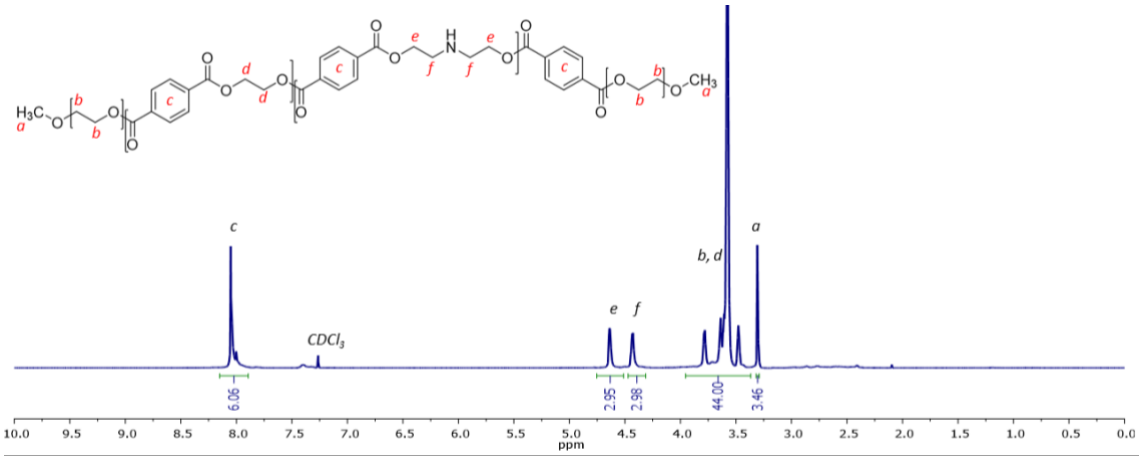

*Figure 6-23 ^{1}H NMR spectrum of the diethanolamine containing polymer (DTI**10**) in $CDCl_3$.*

Figure 6-23 shows the successful incorporation of the diethanolamine into the polymer structure, due to the presence of the ethylene peaks relating to the diethanolamine monomer labelled *e* and *f*. The inclusion of the amine is confirmed in the FTIR spectrum of the polymer (Appendix 11). The aromatic to PEG block ratio was found to be 1:7, showing therefore a similar hydrophilicity to DTI**9**.

The polymers were tested for their DTI efficacy against indigo (Figure 6-24).

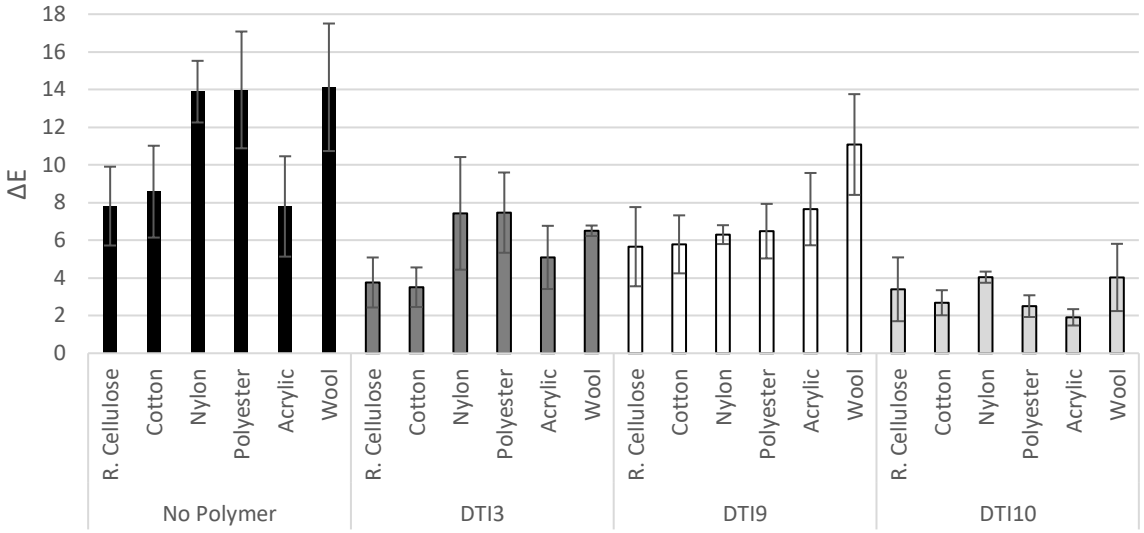

*Figure 6-24 A comparison of the colour change caused by indigo in the presence of DTI3, the 2-amino-2-methyl-1,3-propanediol containing polymer (DTI**9**) and the diethanolamine containing polymer (DTI**10**).*

From Figure 6-24 it can be observed that DTI**10** has improved DTI efficacy compared to DTI**3** against indigo. In particular, a reduction in colour change by 45.6% for nylon is observed, between DTI**3** and DTI**10**. Additionally, a 66.5% reduction in colour change for polyester is seen for DTI**10** in comparison to DTI**3**. DTI**9** is also an effective DTI, however, it is not as effective as DTI**3** or DTI**10** in general.

The polymer containing diethanolamine (DTI**10**) was found to be more effective at preventing dye transfer caused by indigo dye bleeding fabric than DTI**3**. In order to assess whether this improvement was due to the hydrogen bonding capability of the amine, or the increased monomer length of diethanolamine in comparison to glycerol, pentanediol was substituted into the structure (DTI**11**). Pentanediol is a diol of a comparative molar mass to diethanolamine. The structure of the polymer was confirmed by ^{1}H NMR (Figure 6-25).

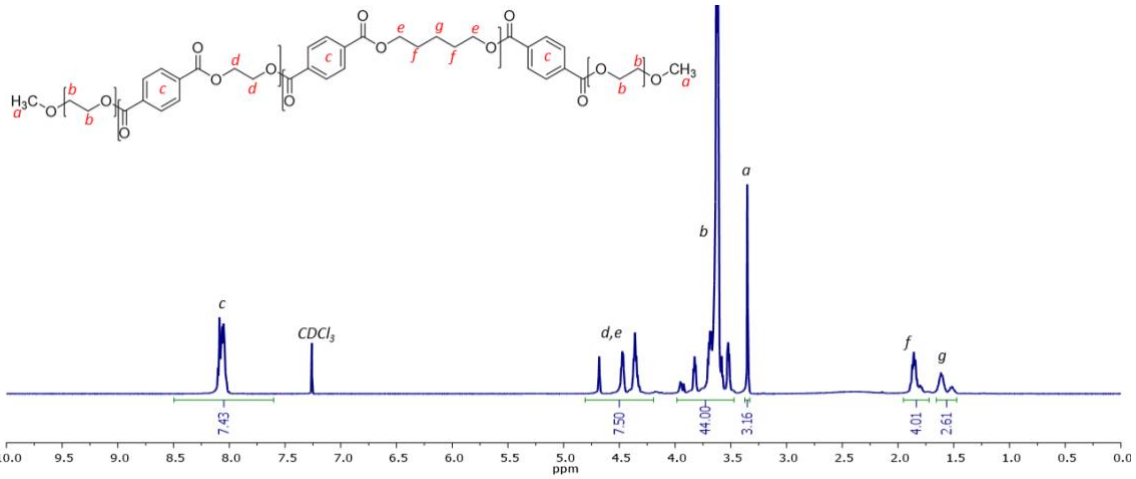

*Figure 6-25 ^{1}H NMR spectrum of the pentanediol containing polymer (DTI**11**) in $CDCl_3$.*

Figure 6-25 shows the pentanediol is included in the polymer structure by the presence of the peaks at *e*, *f*, and *g*. The aromatic to PEG ratio was calculated as 1:6. The FTIR spectrum also confirmed the inclusion of the pentanediol (Appendix 12).

The pentanediol containing polymer was then tested for its ability to prevent the dye transfer of indigo, and compared to the diethanolamine containing polymer (Figure 6-26).

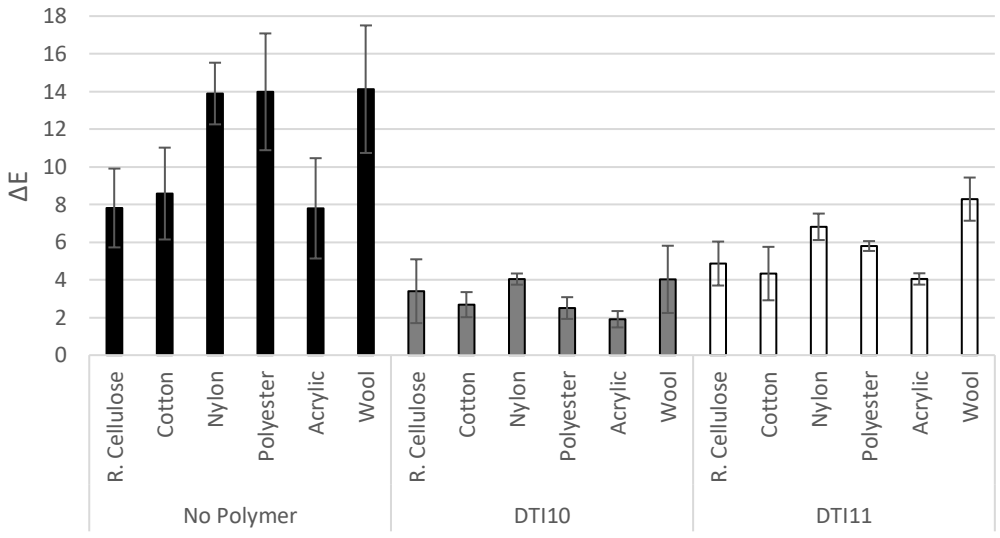

*Figure 6-26 A comparison of the colour change caused by indigo in the presence of the diethanolamine containing polymer (DTI**10**) and the pentanediol containing polymer (DTI**11**).*

Figure 6-26 shows that whilst DTI**11** remains an effective DTI against indigo, it is not as effective as the diethanolamine-containing polymer (DTI**10**). For example, DTI**10** has a ΔE for nylon of 4.0, whereas this increases to 6.8 for DTI**11**. DTI**11** shows a lower colour change across all fibre types

compared to DTI**10**, showing that the additional hydrogen bonding site the diethanolamine provides may improve the efficacy further, particularly for nylon, polyester and wool.

In order to assess if the inclusion of free hydroxy groups would improve the efficacy of DTI**9** and DTI**10**, the ethylene glycol was replaced by glycerol to synthesise DTI**12** and DTI**13.** The successful synthesis was confirmed by ^{1}H NMR (Figure 6-27 and Figure 6-28).

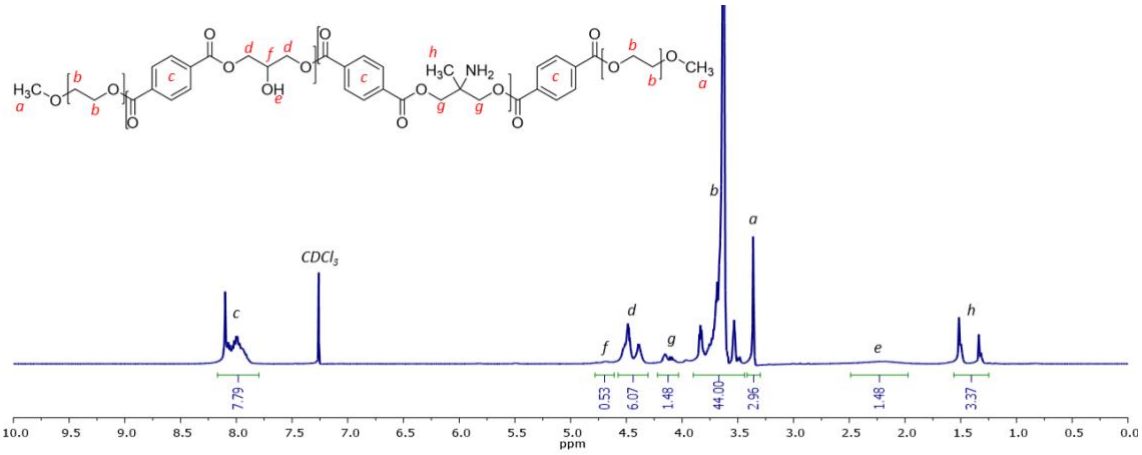

*Figure 6-27 ^{1}H NMR spectrum of the 2-amino-2-methyl-1,3-propanediol and glycerol containing polymer (DTI**12**) in $CDCl_3$.*

From Figure 6-27 the inclusion of glycerol and the amine into the structure is confirmed. The hydroxy peak labelled *e* shows the glycerol is not completely reacted or branched. The amine and hydroxy group can be observed *via* the FTIR spectrum (Appendix 13). The aromatic to PEG ratio was calculated as 1:6.

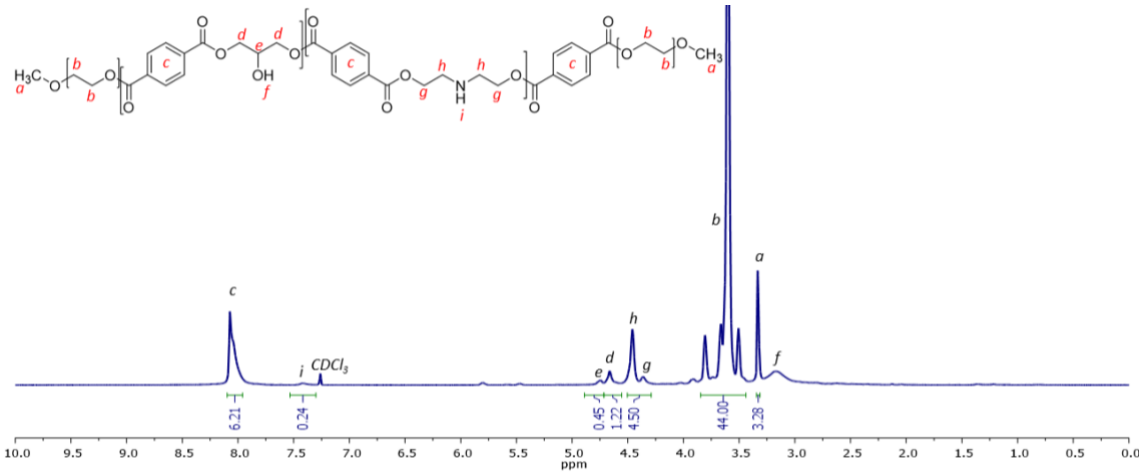

*Figure 6-28 ^{1}H NMR spectrum of the diethanolamine and glycerol containing polymer (DTI**13**) in $CDCl_3$.*

The ^{1}H NMR spectrum of DTI**13** in Figure 6-28 shows the inclusion of the glycerol and diethanolamine into the polymer structure. The hydroxy peak labelled *f* shows the glycerol is again not fully reacted and therefore not fully branched. The peaks labelled *g*, *h* and *i* show the inclusion of the amine containing monomer into the polymer. The aromatic to PEG ratio was calculated and found to be 1:7. The FTIR spectrum further confirmed the structure (Appendix 14).

DTI**12** and DTI**13** were tested for their DTI efficacy against indigo in order to assess the effect of branching and amine inclusion on the ability of the polymer to prevent dye transfer (Figure 6-29).

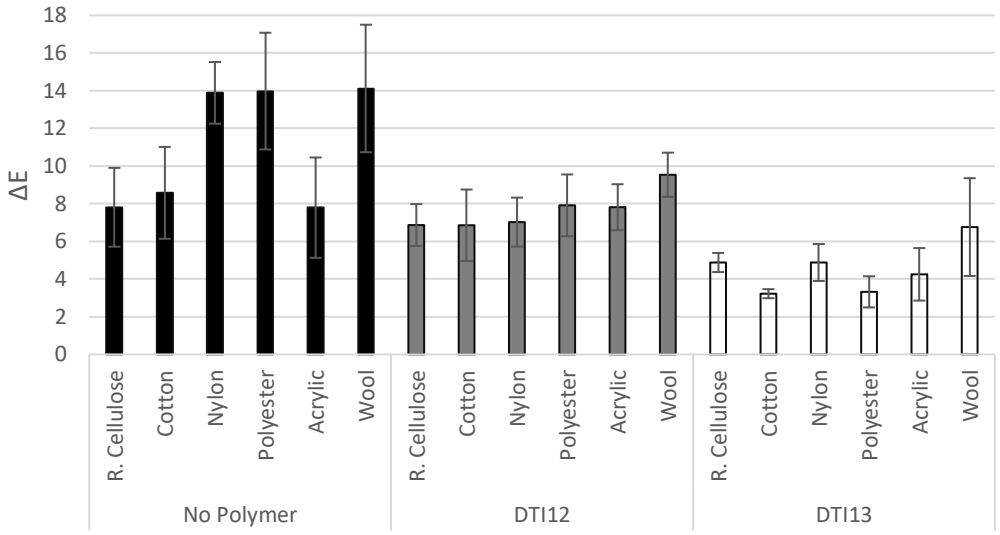

*Figure 6-29 A comparison of the colour change caused by indigo in the presence of the 2-amino-2-methyl-1,3-propanediol and glycerol containing polymer (DTI**12**) and the diethanolamine and glycerol containing polymer (DTI**13**).*

Figure 6-29 shows that DTI**13** is an effective DTI agent, particularly for polyester, whereby the colour change reduces to 3.32, from 14.0 in the absence of polymer, a 76.3% reduction. This result is, however, less effective than that of DTI**10**, which shows an 82.1% overall reduction in colour change caused by indigo onto polyester (Figure 6-24). These results are in agreement with the results from the pentaerythritol-containing polymers, whereby the polymers did not improve on DTI efficacy against indigo in comparison to those with glycerol. However, the presence of free hydroxy groups is important for DTI efficacy, as evidenced by the superior efficacy of DTI**3** in comparison to DTI**1**, which does not contain hydroxy groups.

Following the results of DTI**13** it was proposed that tris(hydroxymethyl)aminomethane be incorporated into the polymer structure to provide branching and hydrogen bonding sites. Tris(hydroxymethyl)aminomethane contains a primary amine and three hydroxy groups. The polymer is able to branch, and presents an amine group which may interact with the fibres of the receiver fabric. The monomer was incorporated into the structure of DTI**2** and DTI**3** in place of glycerol (producing DTI**14** and DTI**15**), and the successful synthesis was confirmed by ^{1}H NMR (Figure 6-30 and Figure 6-31).

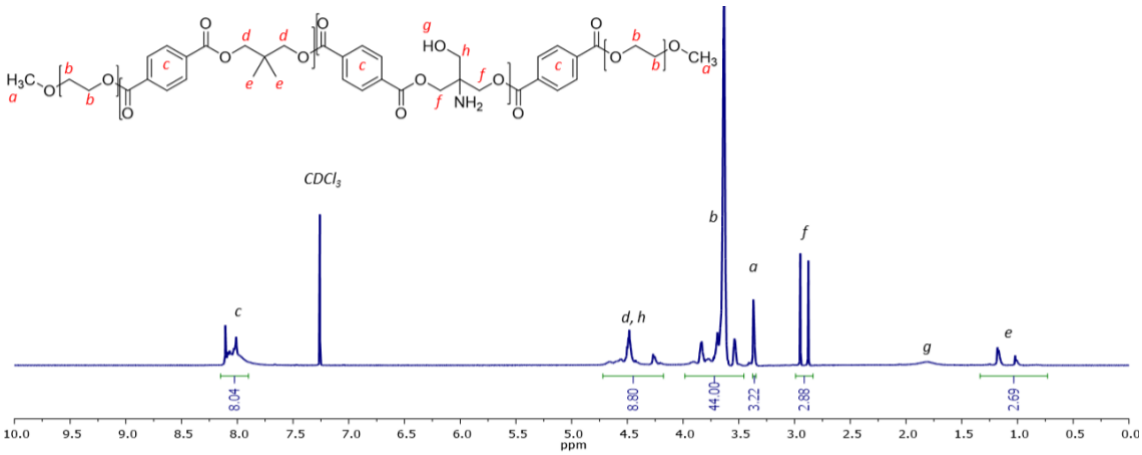

*Figure 6-30 ^{1}H NMR spectrum of the tris(hydroxymethyl)aminomethane and 2,2'-dimethyl-1,3-propanediol containing polymer (DTI**14**) in $CDCl_3$.*

The inclusion of tris(hydroxymethyl)aminomethane into the polymer structure is indicated by the presence of the hydroxy peak labelled *g* and the methylene peaks labelled *f* and *h*. This was also confirmed by FTIR of the polymer (Appendix 15). The ratio of aromatic groups to PEG was calculated as 1:5.

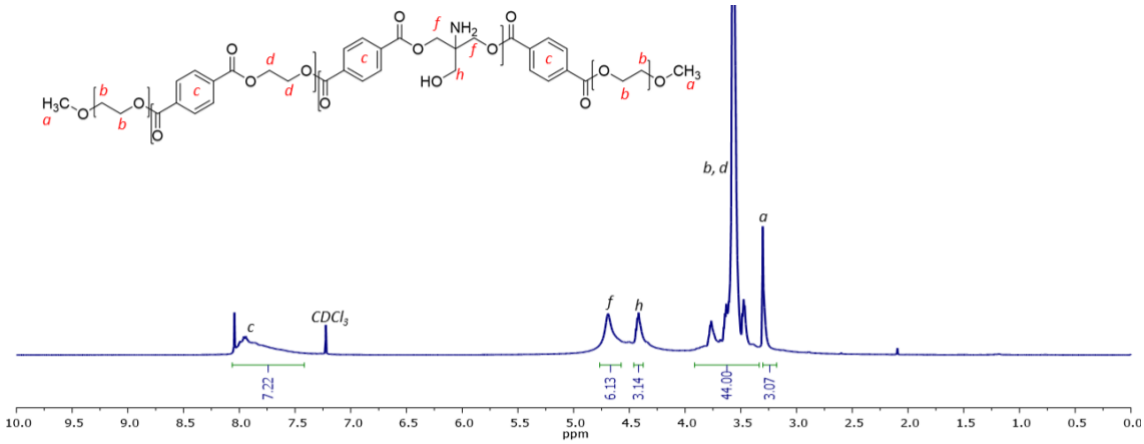

*Figure 6-31 ^{1}H NMR spectrum of the tris(hydroxymethyl)aminomethane and ethylene glycol containing polymer (DTI**15**) in $CDCl_3$.*

The ^{1}H NMR spectrum in Figure 6-31 shows the presence of the methylene groups *f* and *h* in the polymer, indicating the inclusion of the amine containing monomer. The hydroxy and amine peak is observable in the FTIR of the polymer (Appendix 16). The aromatic group to PEG block ratio was found to be 1:6.

The two polymers were tested for their DTI efficacy against indigo (Figure 6-32).

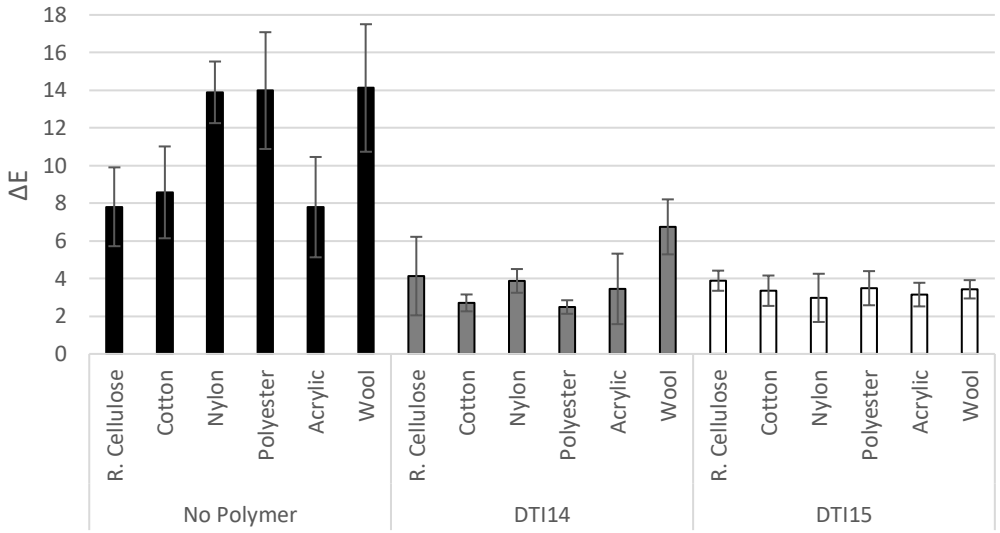

Figure 6-32 A comparison of the colour change caused by indigo in the presence of two tris(hydroxymethyl)aminomethane containing polymers.

Figure 6-32 indicates that the tris(hydroxymethyl)aminomethane containing polymers are both highly successful DTI agents, as both show a reduction in colour change caused by indigo for all fibre types. DTI**15** gives a mean colour change reduction of 78.5% and 75.0% onto nylon and

polyester respectively. Additionally, cotton is reduced by 60.8% and wool by 75.7%. This broad range of efficacy against indigo suggests that the inclusion of both amine and hydroxy groups into the polymer, in one monomeric unit, provides significant advantage.

6.3.3.3 Effect of Polyester Block Modification on Dye Transfer Inhibition of Further Dyes

Due to the efficacy of DTI**8**, **9**, **10**, **12**, **13**, **14** and **15** against indigo, they were tested for their ability to prevent the colour change caused by C.I. Sulfur Black 1, C.I. Direct Orange 39, C.I. Reactive Red141 and C.I. Reactive Black 5.

6.3.3.4 Dye Transfer Inhibition of DTI8

Firstly, DTI**8** was then tested for its ability to prevent dye transfer of C.I. Sulfur Black 1 (SB1, Figure 6-33).

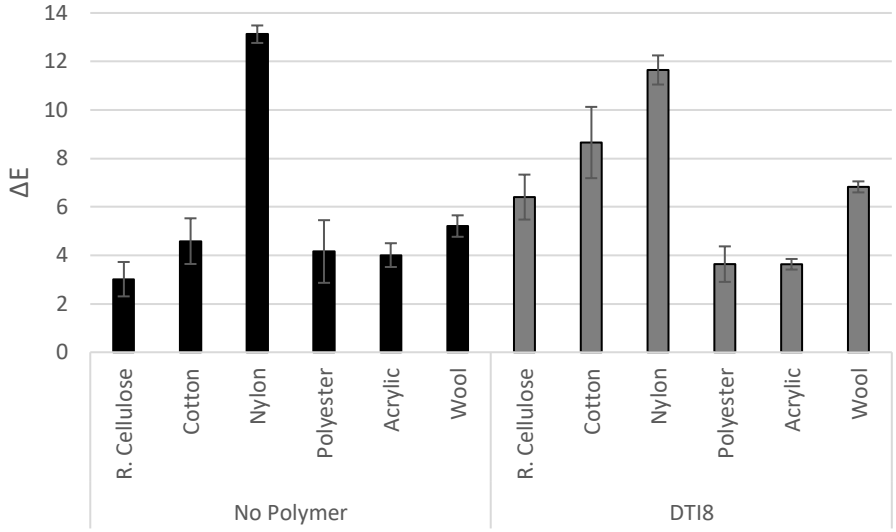

*Figure 6-33 A comparison of the colour change caused by SB1 in the presence of the pentaerythritol and mPEG$_{750}$ polymer (DTI**8**).*

In Figure 6-33, it can be observed that DTI**8** increases colour change of SB1 onto cotton by 47.1% and 23.8% for wool, but decreases the mean colour change onto nylon by 11.2%. The reduction in colour change onto nylon and polyester show that the polymer is interacting with those fabrics and preventing dye deposition.

DTI**8** was also tested against C.I. Direct Orange 39 (DO39, Figure 6-34).

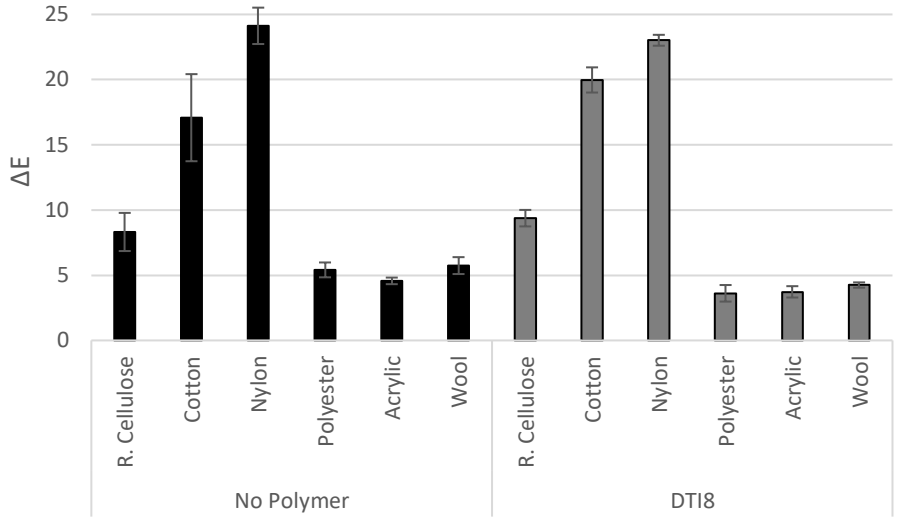

*Figure 6-34 A comparison of the colour change caused by DO39 in the presence of the pentaerythritol and mPEG$_{750}$ polymer (DTI**8**).*

Figure 6-34 shows that the colour change caused by DO39 reduces in the presence of DTI**8** for polyester, which shows a 33.1% decrease in colour change, and for wool which gives a 26.0% decrease. Acrylic also shows a 21.0% decrease in colour change. While it does not significantly reduce the colour change onto nylon, which shows the highest level of discolouration, this result is encouraging as it has efficacy for hydrophobic and hydrophilic fibre types.

DTI**8** was then tested against C.I. Reactive Red 141 (RR141, Figure 6-35).

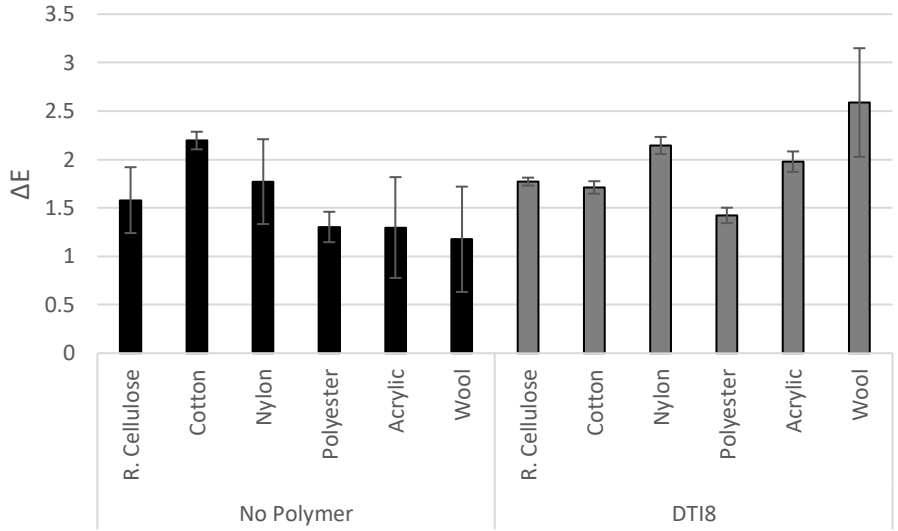

*Figure 6-35 A comparison of the colour change caused by RR141 in the presence of the pentaerythritol and mPEG$_{750}$ polymer (DTI**8**).*

From Figure 6-35 it can be seen that DTI**8** does not reduce colour change caused by RR141, except onto cotton, which shows a 22.3% decrease in colour change. However, this is counterbalanced by a worsened colour change onto nylon, acrylic and wool by 17.2%, 35.0% and 31.3% respectively.

The reduced efficacy of DTI**8** against the additional dyes in comparison to indigo indicate the variety of interactions that prevent dye transfer. The presence of hydroxy groups in the pentaerythritol may not significantly improve the interaction between the polymer and the fabric surface, therefore.

6.3.3.5 DTI Efficacy of DTI9 and DTI10

DTI**9** and DTI**10** were then tested against SB1 (Figure 6-36).

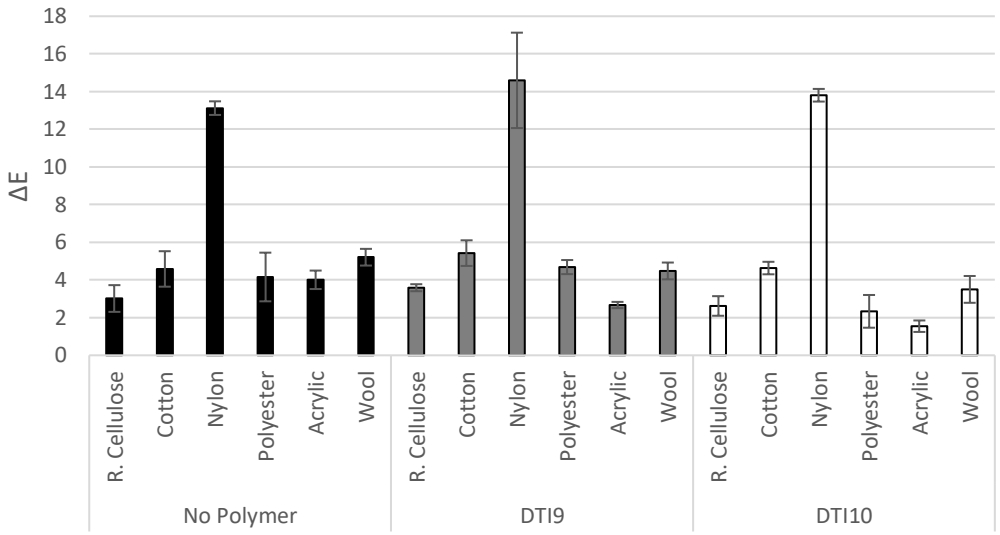

*Figure 6-36 A comparison of the colour change caused by SB1 in the presence of the 2-amino-2-methyl-1,3-propanediol containing polymer (DTI**9**) and the diethanolamine containing polymer (DTI**10**).*

Figure 6-36 shows that neither DTI**9** nor DTI**10** have significant efficacy at preventing the dye transfer of SB1. This is shown by the similar ΔE values for the fibres for both polymers and in the absence of polymer.

DTI**9** and DTI**10** were then tested against DO39 (Figure 6-37).

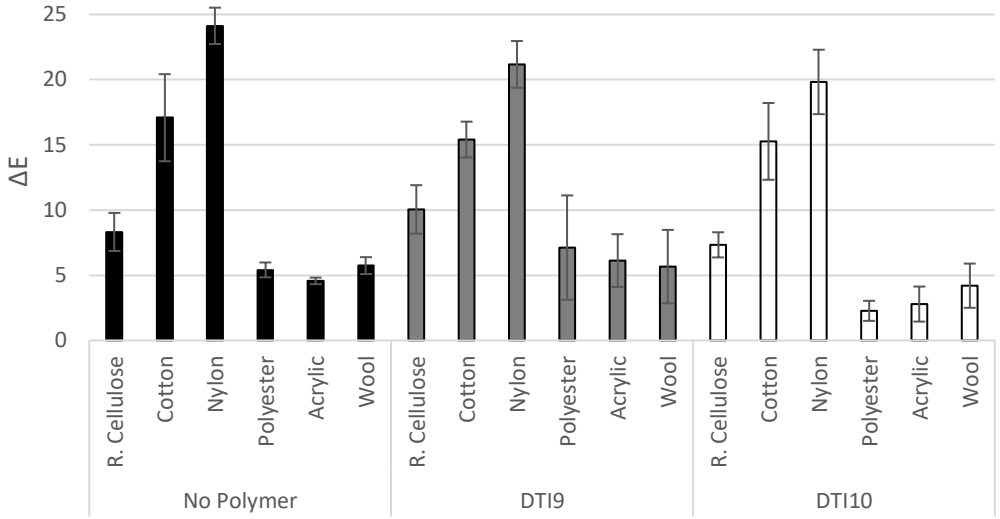

*Figure 6-37 A comparison of the colour change caused by DO39 in the presence of DTI**3**, the 2-amino-2-methyl-1,3-propanediol containing polymer (DTI**9**) and the diethanolamine containing polymer (DTI**10**).*

Figure 6-37 shows that for the cellulosic fibres, which direct dyes are very effective at dyeing, there is not a significant reduction in colour change. However, DTI**10** provides an improvement in colour change for the nylon and polyester fibres, showing a reduction in colour change by 17.7% and 58.0% respectively. This is encouraging as DO39 shows a high level of discolouration onto nylon.

DTI**10** was then tested against RR141 (Figure 6-38).

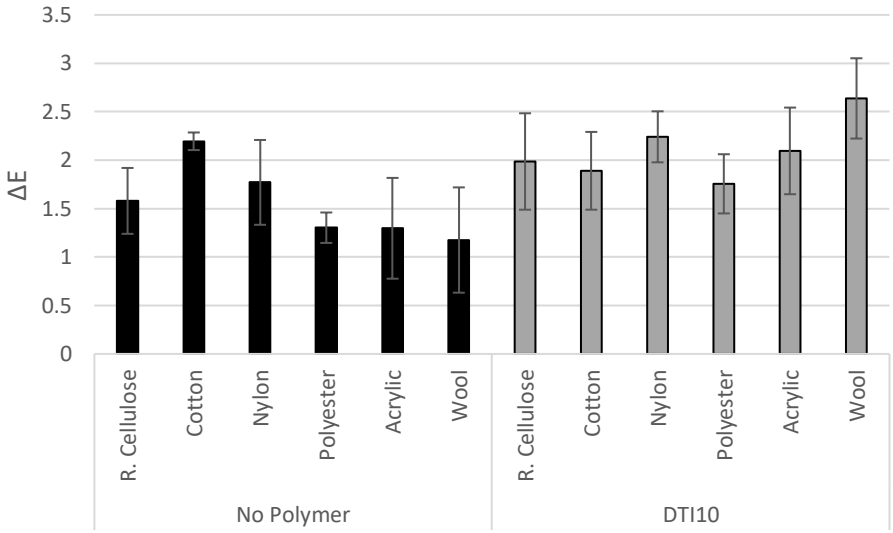

*Figure 6-38 A comparison of the colour change caused by RR141 in the presence of the diethanolamine containing polymer (DTI**10**).*

It can be seen from Figure 6-38 that DTI**10** does not provide DTI efficacy against RR141. The mean values for DTI**10** are higher for all fabric types except cotton, however, the error bars overlap for all fibre types except wool. The colour change is increased onto wool by 56.0%. This therefore suggests that the polymer is interacting with the wool fibres and drawing the dye to the fabric.

DTI**10** was also tested against C.I. Reactive Black 5 (RB5, Figure 6-39).

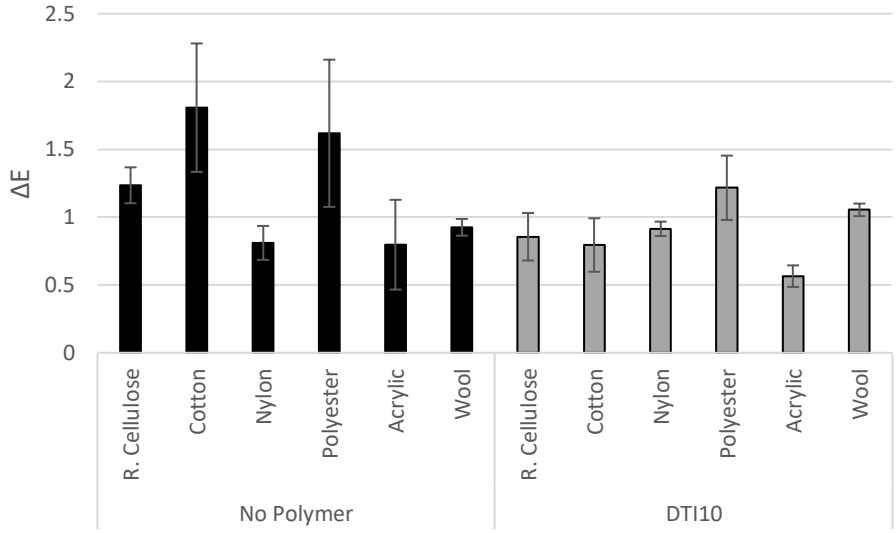

*Figure 6-39 A comparison of the colour change caused by RB5 in the presence of the diethanolamine containing polymer (DTI**10**).*

Figure 6-39 shows that DTI**10** reduces colour change caused by RB5 onto cellulosic fibres and polyester. Cotton shows a decrease in mean colour change by 56.4%, and polyester by 24.7%. RB5 is particularly effective at dyeing and discolouring cotton so the reduction in colour change to below a ΔE of one is a significant improvement and shows that the mPEG-*co*-polyester DTI polymers are interacting with the hydrophilic, as well as hydrophobic, fibres.

The diethanolamine containing polymers show an improved efficacy against the additional dyes to the pentaerythritol polymers in the previous section, indicated particularly by the DO39 and RB5 results. This therefore suggests that the inclusion of the amine group is improving interaction between the fabric and the polymer, and more effectively blocking dye deposition.

However, the mean increase in the deposition of RR141 may suggest that the amine groups in the polymer are attracting the negatively charged dye molecule to the fabric surface.

6.3.3.6 DTI Efficacy of DTI12 and DTI13

DTI**12** and DTI**13** were tested for DTI efficacy against SB1 (Figure 6-40).

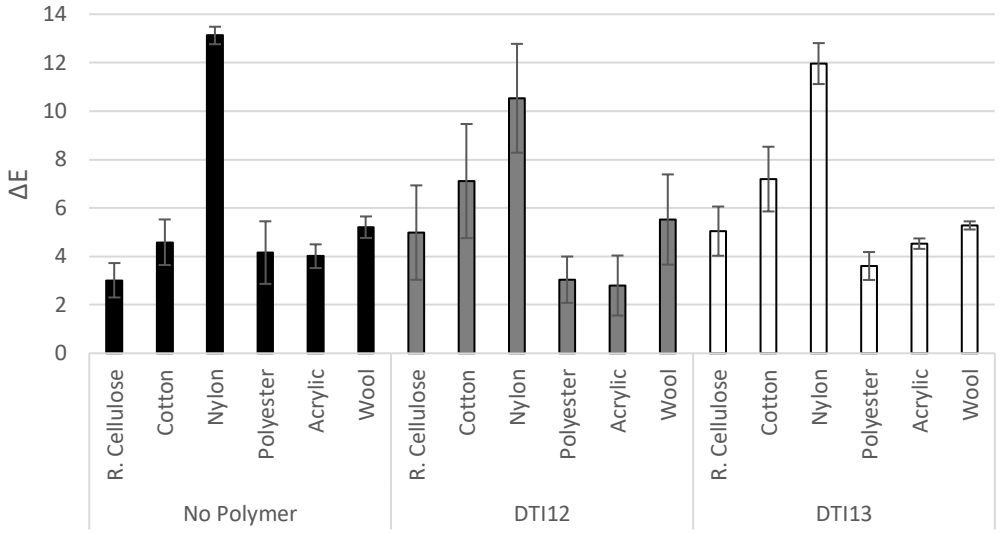

*Figure 6-40 A comparison of the colour change caused by SB1 in the presence of the 2-amino-2-methyl-1,3-propanediol and glycerol containing polymer (DTI**12**) and the diethanolamine and glycerol containing polymer (DTI**13**).*

Figure 6-40 shows that both DTI**12** and DTI**13** have limited DTI efficacy against SB1. A mean reduction in colour change is observed for nylon, giving a 19.7% and 8.84% reduction, respectively, for the two polymers. This is a good result, due to the significant discolouration SB1 produces on nylon fabrics. However, the mean colour change is worsened onto the cotton fabrics.

DTI**12** and DTI**13** were tested against DO39 (Figure 6-41).

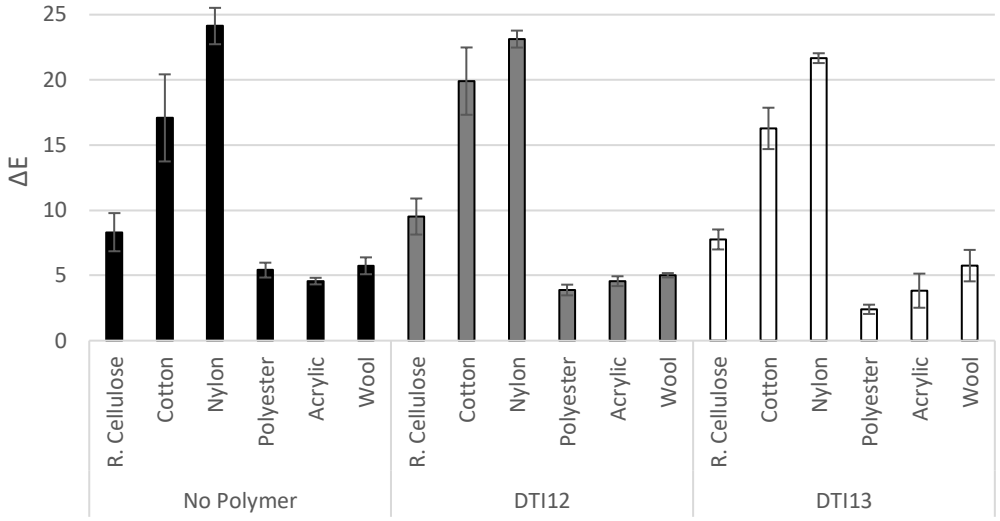

*Figure 6-41 A comparison of the colour change caused by DO39 in the presence of the 2-amino-2-methyl-1,3-propanediol and glycerol containing polymer (DTI**12**) and the diethanolamine and glycerol containing polymer (DTI**13**).*

DTI**13** is seen to reduce colour change caused by DO39 in Figure 6-41, particularly onto nylon and polyester, whereby it shows a 10.2% and 55.6% reduction respectively. Again, since DO39 causes a significant degree of discolouration onto nylon, this improvement is encouraging. The improvement onto nylon and polyester indicates that the DTI polymer is interaction with the hydrophobic fibres, to block dye deposition more effectively than for the hydrophilic fibres.

DTI**12** and DTI**13** were washed with RR141 to observe any DTI efficacy (Figure 6-42).

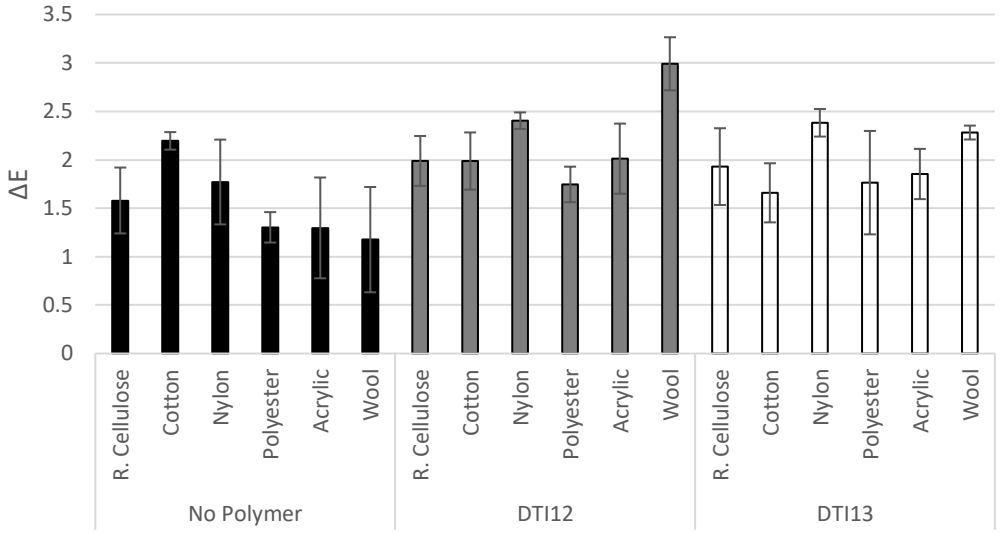

*Figure 6-42 A comparison of the colour change caused by RR141 in the presence of the 2-amino-2-methyl-1,3-propanediol and glycerol containing polymer (DTI**12**) and the diethanolamine and glycerol containing polymer (DTI**13**).*

From Figure 6-42 it can be seen that the overall dye deposition of RR141 is not reduced in the presence of DTI**12** or DTI**13**. For both DTI polymers, a moderate decrease in mean colour change is observed onto cotton, DTI**12** gives a 9.55% reduction and DTI**13** gives a 24.5% reduction. However, this is outweighed by a significant increase in colour change onto wool for both DTI**12** and DTI**13**, giving a 61.2% and 49.1% increase respectively.

The results for DTI**12** and DTI**13** show that the inclusion of the glycerol monomer into the polymer structure does not overall reduce dye deposition of the additional dyes studied.

6.3.3.7 DTI Efficacy of DTI14 and DTI15

DTI**14** and DTI**15** were then washed with SB1 dye bleeding fabric to test the DTI efficacy of the polymers (Figure 6-43).

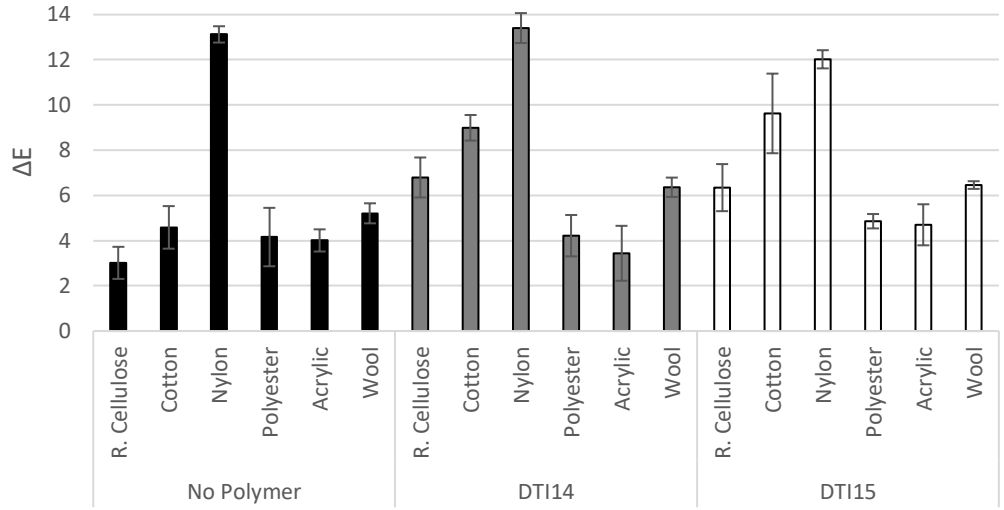

Figure 6-43 A comparison of the colour change caused by SB1 in the presence of two tris(hydroxymethyl)aminomethane containing polymers.

Figure 6-43 shows that the polymers are not effective at preventing the deposition of SB1 dye. In fact, the dye deposition of SB1 onto cotton fibres is seen to increase by 49.1% for DTI**14** and 52.4% for DTI**15**.

DTI**14** and DTI**15** were then investigated for their DTI efficacy against DO39 (Figure 6-44).

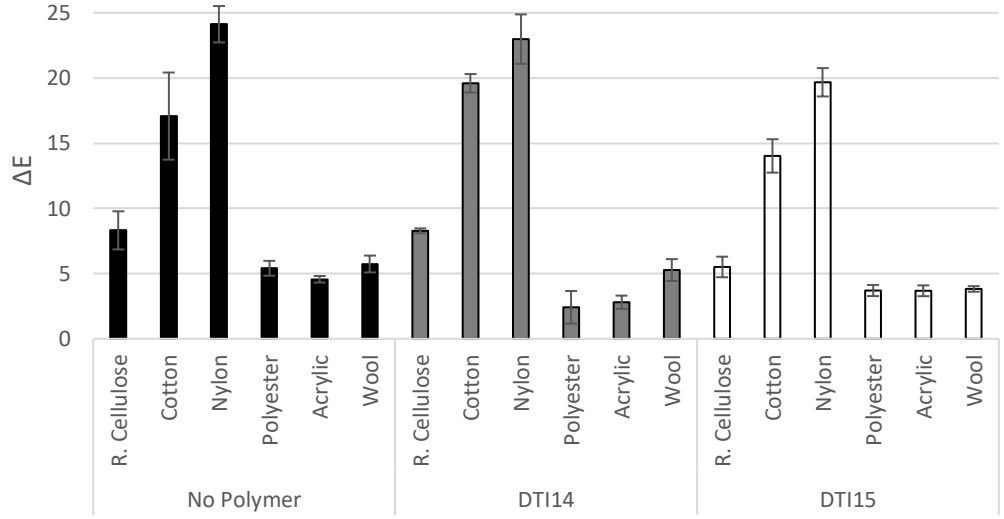

Figure 6-44 A comparison of the colour change caused by DO39 in the presence of two tris(hydroxymethyl)aminomethane containing polymers.

DTI**15** is effective at reducing colour change of DO39 onto the cellulosic fibres and nylon. The mean colour change onto nylon is reduced by 4.8% for DTI**14** and 18.4% for DTI**15**. Additionally, DTI**15** shows a reduction in colour change onto polyester and wool by 31.6% and 33.3% respectively. The range of fibres that the polymer is effective for shows the polymer is versatile in its DTI action.

The two polymers were also tested against RR141 (Figure 6-45).

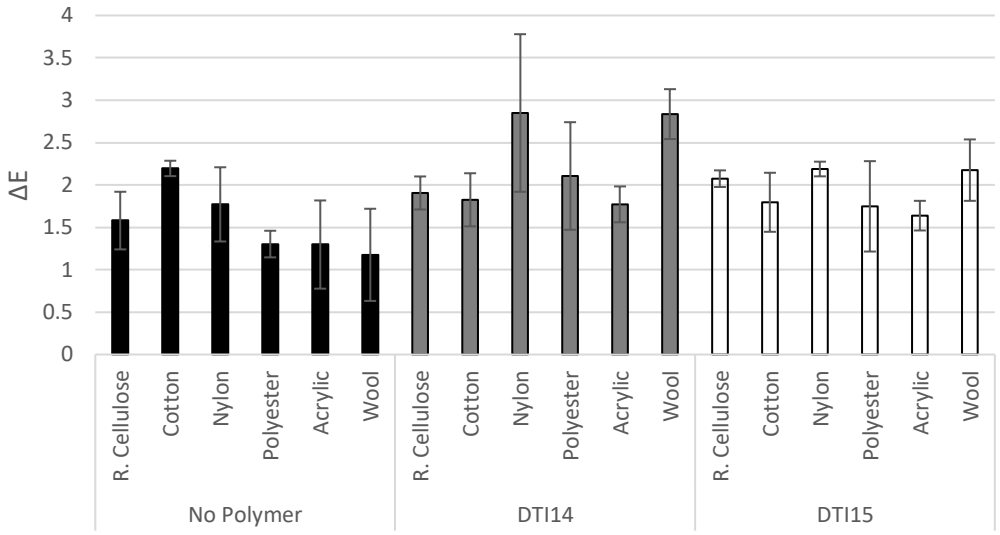

Figure 6-45 A comparison of the colour change caused by RR141 in the presence of two tris(hydroxymethyl)aminomethane containing polymers.

Finally, Figure 6-45 shows the colour change caused by RR141 in the presence of DTI**14** and DTI**15**. The dye deposition is found to worsen on average for each fibre type except cotton, for both polymers. DTI**15** shows a reduction in mean colour change onto cotton of 18%. However, wool is seen to be discoloured by a 45.9% increase in colour change for DTI**15**.

These results show that the amine and hydroxy containing polymer does not improve dye deposition to a great extent for any dye types. Therefore, the results in this section suggest that the inclusion of a secondary amine containing monomer improves colour change caused by DO39 and RB5. However, when also polymerised with glycerol, this efficacy is lost. This therefore suggests that the polymers may be binding the DO39 in the wash solution, analogously to PVP to prevent dye transfer, and the inclusion of hydroxy groups reduces the complexation.

However, the inclusion of the amine appears to worsen the dye deposition of RR141, whereas the pentaerythritol containing polymer improves colour change onto cotton fibres but worsens deposition onto wool. This therefore indicates that the polymer is not encapsulating the dye, as it would reduce colour change across all fabric types. Colour change caused by SB1 is not found to significantly reduce in the presence of any polymers, but a small improvement for nylon is observed for the pentaerythritol containing polymer. Again, this suggests that the dye is being repelled from the fabric surface.

A trend is observed for SB1 and RR141, whereby an improvement in colour change on one fabric type for a dye is counterbalanced by a worsened effect of the dye deposition onto another fabric. For example, DTI**8** improves deposition of SB1 onto nylon, but worsens onto cotton. Additionally, RR141 deposition is reduced onto cotton for DTI**13** but worsened onto wool. This may be due to an excess of dye in the wash liquor that was preventing from depositing onto one fabric, and thus deposits onto another.

The various polymers may therefore interact with the different dyes by various modes of action. By improving interaction of a polymer to a specific fabric type, this may reduce the interactions of the polymer with another fabric type. Additionally, the polymers may work by differing methods, this is seen by the efficacy of some polymers for DO39, which is effectively encapsulated by PVP, and the lack of DTI efficacy of for other dyes.

6.3.4 Consumer Trial Testing

In order to obtain a more realistic value for colour change whereby the complexity of the various fabric and dyes is taken into account, consumer testing of real laundry loads was performed.

DTI**3**, DTI**10** and DTI**15** were tested on consumer loads at the Procter and Gamble Newcastle Innovation Centre. Each polymer was added to 20 consumer wash loads alongside regular Ariel detergent, and a 'tracer'. The tracer was a swatch of fabric with 20 white fabrics of varying compositions attached. This was dried on completion of the wash cycle and the colour change values were measured, compiling the results of the various fabric types. The results of the consumer wash loads are shown in Figure 6-46.

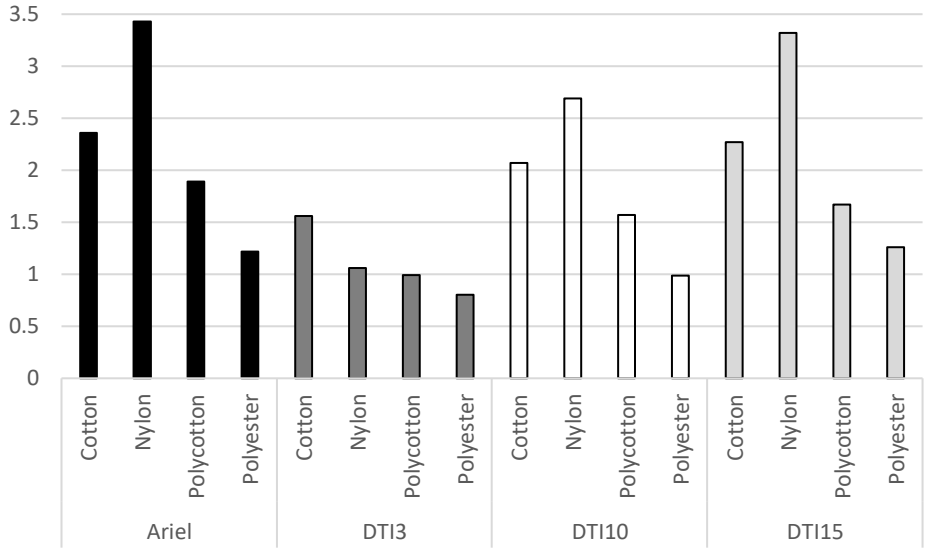

Figure 6-46 A comparison of the efficacy of DTI3, DTI10 and DTI15 on consumer wash loads.

From Figure 6-46 it can be seen that DTI**3** is the overall most effective DTI polymer. According to P&G, a ΔE greater than 1.7 is an observable difference, therefore the DTI**3** values all reduce colour change to below this value. The results of the consumer trials and the results for the additional dyes except indigo indicate that a compromise must be made for overall efficacy of the DTI polymer. This therefore indicates that the polymers that are most effective at reducing colour change for indigo overall, may not be the most effective polymer all round.

6.4 Conclusion

Several novel polymers were successfully synthesised that have potential for use as DTIs against indigo dye. All the polymers created were designed to present a central polyester region intended for fibre interaction, and terminal hydrophilic regions that were intended to form a

hydration layer that prevents fibre-dye interaction. In all instances it was imperative that the polymer presented excellent dispersibility in aqueous solution. Initially, the glycerol containing polymer, DTI**3**, was found to be a highly effective DTI against indigo, showing a mean reduction of 50% in colour change for cotton. It was proposed that the presence of unreacted hydroxy groups from the inclusion of glycerol into the polymer provided the polymer with increased hydrogen bonding capability that improved fibre-polymer interactions. Further testing revealed that the polymer deposits onto multifibre swatches, as DTI efficacy was maintained in further washes in which polymer was not added. This provides evidence that the DTI is effective due to the DTI adsorption onto the fabric, preventing dye deposition. Further polymers were synthesised that are also excellent candidates for use as DTIs. DTI**10** incorporated diethanolamine into the polymer structure, and revealed a significant reduction in dye transfer caused by indigo; providing an 82% reduction in colour change onto polyester. Additionally, DTI**15**, which incorporated tris(hydroxymethyl)aminomethane into the polymer structure, showed an 80% reduction for the colour change caused by indigo onto nylon fabric. Three polymers were then taken forward to consumer trials, and DTI**3** was found the perform best, despite DTI**15** providing superior efficacy against indigo. The positive results presented demonstrate the significant potential that relatively small concentrations of amphiphilic copolymers have as DTIs, and their potential for inclusion in commercial laundry detergent formulations.

6.5 References

[1] Li X., Li H., Zhao Y., Tang X., Ma S., Gong B. and Li M. Facile synthesis of well-defined hydrophilic polyesters as degradable poly(ethylene glycol)-like biomaterials. *Polymer Chemistry*. 2015 **6** (36) 6452–6

[2] Ma C., Xu W., Pan J., Xie Q. and Zhang G. Degradable Polymers for Marine Antibiofouling: Optimizing Structure To Improve Performance. *Industrial & Engineering Chemistry Research*. 2016 **55** (44) 11495–501

[3] Li P., Cai X., Wang D., Chen S., Yuan J., Li L. and Shen J. Hemocompatibility and anti-biofouling property improvement of poly(ethylene terephthalate) via self-polymerization of dopamine and covalent graft of zwitterionic cysteine. *Colloids and Surfaces B:*

Biointerfaces. 2013 **110** 327–32

[4] Tah T. and Bernards M.T. Nonfouling polyampholyte polymer brushes with protein conjugation capacity. *Colloids and Surfaces B: Biointerfaces*. 2012 **93** 195–201

[5] Zheng J., Li L., Tsao H.-K., Sheng Y.-J., Chen S. and Jiang S. Strong Repulsive Forces between Protein and Oligo (Ethylene Glycol) Self-Assembled Monolayers: A Molecular Simulation Study. *Biophysical Journal*. 2005 **89** (1) 158–66

[6] Yandi W., Mieszkin S., Martin-Tanchereau P., Callow M.E., Callow J.A., Tyson L., Liedberg B. and Ederth T. Hydration and Chain Entanglement Determines the Optimum Thickness of Poly(HEMA- *co* -PEG $_{10}$ MA) Brushes for Effective Resistance to Settlement and Adhesion of Marine Fouling Organisms. *ACS Applied Materials & Interfaces*. 2014 **6** (14) 11448–58

[7] Kataoka K., Harada A. and Nagasaki Y. Block copolymer micelles for drug delivery: design, characterization and biological significance. *Advanced Drug Delivery Reviews*. 2001 **47** (1) 113–31

[8] Miyata K., Christie R.J. and Kataoka K. Polymeric micelles for nano-scale drug delivery. *Reactive and Functional Polymers*. 2011 **71** (3) 227–34

[9] Zhou Z., Murdoch W.J. and Shen Y. Synthesis of an esterase-sensitive degradable polyester as facile drug carrier for cancer therapy. *Journal of Polymer Science Part A: Polymer Chemistry*. 2016 **54** (4) 507–15

[10] Palmiero U.C., Maraldi M., Manfredini N. and Moscatelli D. Zwitterionic Polyester-Based Nanoparticles with Tunable Size, Polymer Molecular Weight, and Degradation Time. 2018

[11] Mochida Y., Cabral H., Miura Y., Albertini F., Fukushima S., Osada K., Nishiyama N. and Kataoka K. Bundled Assembly of Helical Nanostructures in Polymeric Micelles Loaded with Platinum Drugs Enhancing Therapeutic Efficiency against Pancreatic Tumor. *ACS Nano*. 2014 **8** (7) 6724–38

[12] Venditti I. Morphologies and functionalities of polymeric nanocarriers as chemical tools for drug delivery: A review. *Journal of King Saud University - Science*. 2017

[13] Liu Z., Wang Y. and Zhang N. Micelle-like nanoassemblies based on polymer–drug conjugates as an emerging platform for drug delivery. *Expert Opinion on Drug Delivery*. 2012 **9** (7) 805–22

[14] Vassiliou A.A., Papadimitriou S.A., Bikiaris D.N., Mattheolabakis G. and Avgoustakis K. Facile synthesis of polyester-PEG triblock copolymers and preparation of amphiphilic nanoparticles as drug carriers. *Journal of Controlled Release*. 2010 **148** (3) 388–95

[15] Luo Z., Jiang L., Ding C., Hu B., Loh X.J., Li Z. and Wu Y.-L. Surfactant Free Delivery of Docetaxel by Poly[(R)-3-hydroxybutyrate-(R)-3-hydroxyhexanoate]-Based Polymeric Micelles for Effective Melanoma Treatments. *Advanced Healthcare Materials*. 2018 **7** (23) 1801221

[16] Siafaka P., Betsiou M., Tsolou A., Angelou E., Agianian B., Koffa M., Chaitidou S., Karavas E., Avgoustakis K. and Bikiaris D. Synthesis of folate- pegylated polyester nanoparticles encapsulating ixabepilone for targeting folate receptor overexpressing breast cancer cells. *Journal of Materials Science: Materials in Medicine*. 2015 **26** (12) 275

[17] Koch H. Method of Preventing or Minimizing Dye Redeposition by Use of Polyesters.

US20080028539A1. 2004

[18] Koch H. Amphiphile polymers based on polyester with condensed acetal groups which are liquid at room temperature and are used in detergents and cleaning agents. US6537961B1. 1998

[19] Lang F.P., Laborda S., Borchers G. and Morschhaeuser R. Anionic Soil Release Polymers. US20090036641A1. 2006

[20] Loughnan B.J., Hulskotter F., Scialla S., Brooker A.T., Ure C., Ebert S., Ludolph B., Wigbers C., Maas S., Boeckh D. and Eidamshaus C. Cleaning compositions containing a polyetheramine, a soil release polymer, and a carboxymethylcellulose. WO2014160821A1. 2014

[21] O'Lenick Jr A.J. Soil Release Polymers. *Journal of Surfactants and Detergents*. 1999 **2** (4) 553–7

[22] Watson R.A., Gosselink E.P. and Price K.N. Cotton soil release polymers. US6291415B1. 2000

[23] Cohrs C., Fischer D., Peerlings H. and Mutch K. Laundry detergents containing soil release polymers. WO2016075178A1. 2015

[24] Basadur M.S. Compositions for imparting renewable soil release finish to polyester-containing fabrics. US3893929A. 1973

[25] Kumar V.N.G. and Moulee A. Soil release polymers and laundry detergent compositions containing them. US6764992B2. 2001

[26] Trinh T., Gosselink E.P. and Hardy F.E. Rinse-added fabric conditioning compositions containing fabric softening agents and cationic polyester soil release polymers and preferred cationic soil release polymers therefor. US5405542A. 1990

[27] Gosselink E.P., Hardy F.E. and Trinh T. Rinse-added fabric conditioning compositions containing fabric sofening agents and cationic polyester soil release polymers and preferred cationic soil release polymers therefor. US4956447A. 1989

Chapter 7. mPEG-Poly(Amino Acid)s Synthesised *via N*-Carboxyanhydride Ring Opening Polymerisation for Dye Transfer Inhibition

This chapter is based on work published as:

Mohamed H. A., Khuphe M., Boardman S. J., Shepherd S., Phillips R. M., Thornton P. D. and Willans C. E., Polymer encapsulation of anticancer silver-*N*-heterocyclic carbene complexes, *RSC Advances*, 2018, **8**, 10474 - 10477

Abstract

N-Carboxyanhydride ring opening polymerisation is a controlled method of synthesising poly(amino acid)s. A series of diblock copolymers polymerised from methoxy-poly(ethylene glycol)-amine macroinitiators were synthesised, containing repeat units of L-phenylalanine, γ-benzyl-L-glutamate and N-ε-carboxybenzyl-L-lysine as the poly(amino acid) block. These polymers were investigated for their efficacy as dye transfer inhibitors for indigo dye in the laundry process. Polymers containing poly(γ-benzyl-L-glutamate) were found to be the most effective against indigo, however, in contrast the polymers containing poly(L-phenylalanine) were found to be overall the most effective against other dyes. This shows that poly(amino acid)s may be expanded upon to produce DTIs that can protect against a range of dyes for a range of fabrics in detergent formulations.

7.1 Introduction

Amino acids can be polymerised to form random or coded copolymers such as polypeptides, or chains of a single amino acid repeat unit, such as poly(amino acid)s, which may form a block in

a larger block copolymer.[1,2] Amino acids each have a unique R group which imparts varying functionality to the monomer, such as an acid, amine or aromatic group. The various functionalities available when using amino acids as monomers allows for a large range of polymers with a variety of properties and functionalities to be produced, including amphiphilic polymers. As poly(amino acid)s are derived from amino acids, they are biocompatible, biodegradable and renewable.[3] Due to these desirable properties, such polymers have attracted interest in a variety of applications including drug delivery, biomimetics, biosensors and tissue scaffolds.[4–8] Poly(amino acid)s provide a route to producing polymers that can be included in detergent formulations, and to observe the effects of varying functionality on dye transfer inhibition (DTI) efficacy, through the use of particular amino acids as monomers, namely glutamic acid, lysine and phenylalanine. Each repeat unit of the polymer contains a peptide bond capable of hydrogen bonding with the fabric, as well as any additional functionality provided by the R group of the amino acid, which may allow for interaction between the fabric and the polymer, in order to block dye deposition.

7.1.1 *N*-Carboxyanhydride Ring Opening Polymerisation

N-Carboxyanhydride (NCA) ring opening polymerisation (ROP) is a relatively facile robust method to producing poly(amino acid)s, negating the need for the laborious Merrifield solid phase synthesis used for poly(peptide) synthesis.[1,9] The desired amino acid is converted into a cyclic monomer, an NCA, *via* the Fuchs-Farthing method whereby triphosgene reacts with the amino acid to cyclise it in good yields, while limonene or α-pinene act as a scavenger for hydrochloric acid produced in the reaction.[10,11] The reaction proceeds *via* an intermediate *N*-chloroformyl amino acid, which upon the loss of an HCl moiety, produces the cyclised amino acid monomer (Figure 7-1).

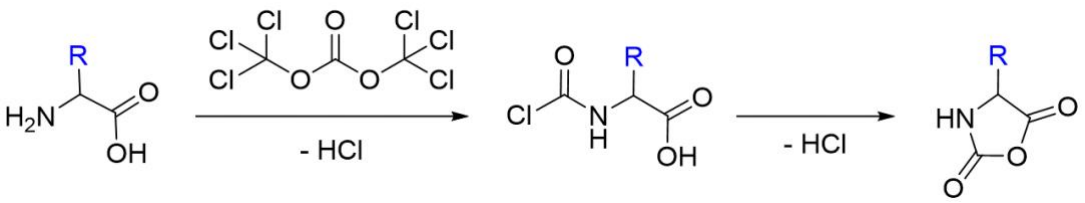

Figure 7-1 Reaction scheme of the synthesis of an NCA monomer via the Fuchs-Farthing method, the R group of the amino acid is highlighted in blue.

Upon isolation and purification, the NCA monomer may be polymerised *via* ROP to produce the desired poly(amino acid). NCA ROP proceeds *via* living anionic polymerisation, meaning the NCA monomer polymerises until it is depleted, generating an active chain end on the elimination of CO_2.[12] Living polymerisations provide a controlled route to well-defined polymer synthesis.[13,14] This is because the rate of initiation is greater than the rate of propagation. This results in instantaneous initiation of the polymer chain, and the propagation of each chain occurs at the same rate, resulting with a narrow polydispersity index (PDI).[15,16] NCA ROP therefore gives a reliable, highly defined product.[17]

NCA ROP is initiated by a nucleophile amine, often a primary amine group, which may be on the terminus of an existing polymer chain, an initiator, or may be a pendant group on a surface. This allows for the grafting of the poly(amino acid) onto existing surfaces[18] or with amine terminated polymers (Figure 7-2).[16,19] It also enables the formation of copolymers with biologically relevant structures, such as carbohydrates, to produce glycopolypeptides.[20] This allows for a wide range of potential products such as amphiphilic polymers. These can be produced by a number of ways such as: grafting an hydrophilic poly(amino acid) to an hydrophobic one, or; using an hydrophilic block such as methoxy-poly(ethylene glycol)-amine (mPEG-NH_2) as a macroinitiator for the polymerisation of an hydrophobic NCA monomer. NCA ROP may also be used simply to introduce blocks of varying functionality into the polymer structure.[21]

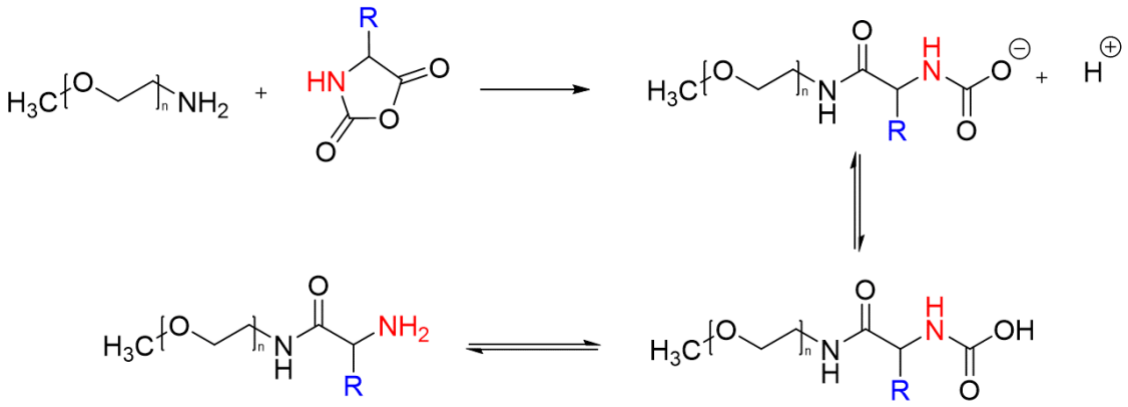

Figure 7-2 Reaction scheme of N-carboxyanhydride ring opening polymerisation initiated from methoxy-PEG-NH_2 showing the generation of the free amine terminus associated with the amino acid residue (red) to allow for propagation of the polymerisation.

The poly(amino acid)s synthesised are degradable into non-toxic amino acids.[2,16,22,23] This therefore provides a more environmentally-friendly route to producing polymers for laundry detergent, where the effluent generated is released into the environment.

7.1.2 Use of Poly(Amino Acid)s in Laundry Applications

Poly(amino acids) are used in detergent formulations, particularly in order to preserve the integrity and therefore the appearance of the fibres of a garment, and to reduce physical damage to the garment fibres on the laundering process.[24] It is also claimed that some poly(amino acid)s such as polylysine can reduce colour fading, caused by dye molecules becoming dislodged when damage to the garment fibres occurs.[24] The free amine in the lysine residue can also be used to react with 'benefit' agents such as a perfume, antibacterial agents, or brighteners.[25,26] While polylysine is used in detergent formulations, there is no indication of the use of it as a dye transfer inhibitor. This gives a potential secondary advantage to the use of polylysine, while still protecting the fibres. Poly(amino acid)s containing aspartic acid, glutamic acid, lysine or ornithine repeat units, have been found to enhance cleaning of soils and clays from garments when included in detergent formulations, showing that they also possess cleansing properties that may act synergistically with surfactants in the laundry process.[27–29]

Diblock copolymers synthesised *via* NCA ROP of lysine and phenylalanine have been found to possess antimicrobial properties.[30] Additionally, polylysine, polyarginine and polyhistidine, as well as random copolymers thereof, are used in detergent formulations as anti-microbial agents.[31,32] Therefore the application of poly(amino acid)s as DTIs could provide a route to secondary benefits of their use.

It is therefore of interest to investigate water-soluble poly(amino acid)s for their ability to prevent dye transfer in the wash, as this may provide an additional benefit to their use in laundry detergents, alongside those already outlined. Therefore, a series of mPEG-*b*-poly(amino acid)s was synthesised based on lysine, phenylalanine and glutamic acid. These three amino acids were selected owing to their varying functionalities, in order to observe the effect, if any of these functional groups on the DTI efficacy of the polymers. The polymers were synthesised *via* NCA ROP using an mPEG-NH_2 macroinitiator in order to impart functionality, and to mimic the successful mPEG-poly(ester) DTI polymers outlined previously.

7.2 Experimental

7.2.1 Nuclear Magnetic Resonance (NMR) Spectroscopy

All ^{1}H NMR spectra obtained were recorded using a Bruker AVANCE 500 spectrometer at 500 MHz, for 128 scans. NMR spectra were obtained using 500 MHz Norell® NMR tubes. MestreNova® Research Lab software was used to analyse and integrate the spectra, and the chemical shifts were reference to trimethylsilane at 0 ppm.

7.2.2 Fourier Transformed Infrared (FTIR) Spectroscopy

Infrared spectra were obtained on a Bruker Platinum FTIR-ATR spectrometer, using a diamond attenuated total reflectance (ATR) accessory, completing 32 scans in total. Bruker OPUS7.0 software was used to analyse the spectra. TRIOS software was used to plot and analyse the data.

7.2.3 Centrifugation, Sample Drying and Lyophilisation

Samples were separated by centrifuge with an MSE Mistral 3000i at 25 °C, 1000 rpm. A Buchi R-210 rotary evaporator and a FiStream vacuum oven were used to remove solvent and dry samples. Samples were lyophilised using a VirTis BenchTop Pro freeze dryer (SP Scientific).

7.2.4 Dynamic Light Scattering (DLS)

A Malvern Instrument ZetaSizer Nano ZSP with a 4mW He-Ne laser at 633 nm, and using an avalanche photodiode detector. The scattered light was collected at an angle of 173°. Measurements were run in triplicate and obtained at 25 °C, using a measurement position of 2.00 mm.

7.2.5 GyroWash^2 Studies

Multifibre and dye bleeder washes were performed on a James Heal GyroWash^2 set at 40 °C, for 30 minutes at 40 rpm. The multifibre and dye bleeding fabrics were cut to 4x10 cm swatches, and washed in deionised water (50 mL) or polymer solution (50 mL, 0.1 mg mL^{-1}), with 25 ball bearings. Colour changes were measured using a Spectraflash DataColor unit, which measured the L* a* and b* coordinates, which can be compared to an unwashed sample to give a colour change (ΔE) value. Measurements were made under D65 lighting.

7.2.6 Synthesis of *N*-carboxyanhydride monomers

7.2.6.1 Synthesis of L-phenylalanine *N*-carboxyanhydride

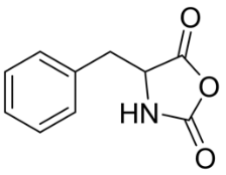

A round bottom flask with a magnetic stirrer was fitted with a reflux condenser and dropping funnel. Under an inert atmosphere, triphosgene (3.81 g, 12.8 mmol) in anhydrous THF (20 mL) was added dropwise to α-pinene (4.02 g, 30.7 mmol) and L-phenylalanine (5 g, 30.3 mmol) in anhydrous THF (80 mL) and stirred under reflux for 2 hours. Approximately one third of solvent was removed *in vacuo*. The solution was then added to cold hexane (150 mL) and a white crystalline solid was precipitated

out. The precipitate was collected by gravity filtration and dried *in vacuo*. A white crystalline material was yielded. IR and NMR spectra were obtained. Yield: 4.33 g, 22.6 mmol, 74.9%

^{1}H NMR (500 MHz, DMSO) δ 9.20 (s, 1H, NH), 7.45-7.30 (m, 5H, ArH), 4.76 (s, 1H, αCH), 3.2 (s, 2H, CH_2).

FTIR (cm^{-1}): 3277 (N-H, amine), 2922 (C-H, alkyl), 1847 (-C=O, anhydride), 1766 (-C=O, anhydride), 1454 (C=C, Ar), 1295 (C-O, anhydride), 1117 (C-O, anhydride), 917 (C=C, Ar), 752(C-H, Ar), 699 (C-H, Ar).

7.2.6.2 Synthesis of γ-benzyl-L-glutamate *N*-carboxyanhydride

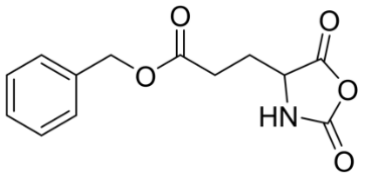

A round bottom flask with a magnetic stirrer was fitted with a reflux condenser and dropping funnel. Under an inert atmosphere, triphosgene (2.08 g, 7.02 mmol) in anhydrous ethyl acetate (20 mL) was added dropwise to α-pinene (1.91 g, 14.05 mmol) and γ-benzyl-L-glutamate (5 g, 21.07 mmol) in anhydrous ethyl acetate (80 mL) and stirred under reflux for 2 hours. Approximately one third of solvent was removed *in vacuo*. The solution was then added to cold hexane (150 mL) and a white crystalline solid was precipitated out. The precipitate was collected by gravity filtration and dried *in vacuo*. A white crystalline material was yielded. IR and NMR spectra were obtained. Yield: 4.89 g, 18.8 mmol, 88%

^{1}H NMR (500 MHz, DMSO) δ 7.45 – 7.12 (m, 5H, ArH), 5.19 – 4.88 (m, 2H, CH_2), 4.04 (dd, *J* = 56.5, 49.4 Hz, 1H, αCH), 2.20 (s, 2H, CH_2), 2.09 – 1.65 (m, 2H, CH_2).

FTIR (cm^{-1}): 3320 (N-H), 3032 (C-H, alkyl), 2936 (C-H, alkyl), 2865 (C-H, alkyl), 1847 (C=O, anhydride), 1774 (C=O, anhydride), 1529 (C=C, Ar), 1255 (C-O, anhydride), 925 (C=C, Ar), 740 (C-H, Ar).

7.2.6.3 Synthesis of *N*-ε-carboxybenzyl-L-lysine *N*-carboxyanhydride

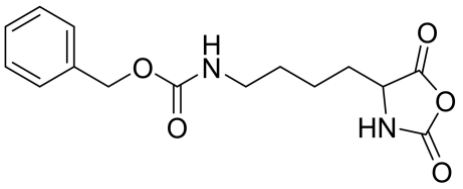

A round bottom flask with a magnetic stirrer was fitted with a reflux condenser and dropping funnel. Under an inert atmosphere, triphosgene (1.76 g, 5.95 mmol) in anhydrous ethyl acetate (20 mL) was added dropwise to α-pinene (1.61 g, 11.89 mmol) and *N*-ε-carboxybenzyl-L-lysine (5 g, 17.84 mmol) in anhydrous ethyl acetate (80 mL) and stirred under reflux for 2 hours. Approximately one third of solvent was removed *in vacuo*. The solution was then added to cold hexane (150 mL) and a white crystalline solid was precipitated out. The precipitate was collected by gravity filtration and dried *in vacuo*. A white crystalline material was yielded. IR and NMR spectra were obtained. Yield: 4.83 g, 15.77 mmol, 88%

^{1}H NMR (500 MHz, DMSO) δ 9.10 (s, 1H, NH), 7.53 – 7.16 (m, 6H, ArH), 5.00 (s, 2H, CH_2), 4.57 – 4.32 (m, 1H, α), 2.99 (dd, *J* = 12.1, 6.1 Hz, 2H, CH_2), 1.88 – 1.56 (m, 2H, CH_2), 1.49 – 1.20 (m, 4H, CH_2).

FTIR (cm^{-1}): 3338 (N-H), 3032 (C-H, alkyl), 2942 (C-H, alkyl), 2869 (C-H, alkyl), 1853 (-C=O, anhydride), 1770 (-C=O, anhydride), 1546 (C=C, Ar), 1137 (C-O, anhydride), 938 (C=C, Ar), 748 (C-H, Ar).

7.2.7 NCA ROP of Phe NCA with $mPEG_{22}$-NH_2 Macroinitiator

7.2.7.1 Synthesis of $mPEG_{22}$-*b*-poly(L-phenylalanine)$_3$ (SJB105)

A Schlenk tube was degassed and backfilled with $N_{2(g)}$ and loaded with $mPEG_{22}$-NH_2 (0.1 g, 0.1 mmol) and L-phenylalanine NCA (0.096 g, 0.5 mmol). Anhydrous DMF (20 mL) was added and the reaction was stirred under a constant stream of $N_{2(g)}$ for seven days at room temperature. The reaction mix was precipitated into ice cold diethyl ether (150 mL) and incubated at -5 °C for 24 hours. The mixture was then centrifuged and the supernatant

decanted. The product was washed three time with ice cold ethyl acetate and centrifuged. The resulting off-white solid was dried *in vacuo* at 50 °C for 48 hours. Yield: 0.1733 g.

^{1}H NMR (500 MHz, DMSO) δ 7.31 – 7.07 (m, 15H, ArH), 4.54 (s, 3H, CH), 3.98 – 3.41 (m, 88H, CH_2), 3.24 (s, 3H, CH_3), 2.92 (dd, *J* = 34.2, 12.3 Hz, 6H, CH_2).

FTIR (cm^{-1}): 3328 (N-H), 3287 (N-H), 3026 (C-H, alkyl), 2865 (C-H, alkyl), 1664 (C=O, amide), 1631 (C=C, Ar), 1519 (C=C, Ar), 1243 (C-N, amide), 1097 (C-O, aliphatic ether), 946 (C=C, Ar), 695 (C-H, Ar).

7.2.7.2 Synthesis of $mPEG_{22}$-*b*-poly(L-phenylalanine)$_4$ (SJB104)

A Schlenk tube was degassed and backfilled with $N_{2(g)}$ and loaded with $mPEG_{22}$-NH_2 (0.1 g, 0.1 mmol) and L-phenylalanine NCA (0.287 g, 1.5 mmol). Anhydrous DMF (20 mL) was added and the reaction was stirred under a constant stream of $N_{2(g)}$ for seven days at room temperature. The reaction mix was precipitated into ice cold diethyl ether (150 mL) and incubated at -5 °C for 24 hours. The mixture was then centrifuged and the supernatant decanted. The product was washed three time with ice cold ethyl acetate and centrifuged. The resulting off-white solid was dried *in vacuo* at 50 °C for 48 hours. Yield: 0.3454 g.

^{1}H NMR (500 MHz, DMSO) δ 7.20 (d, *J* = 17.1 Hz, 20H, ArH), 4.52 (s, 4H, CH), 3.45 (d, *J* = 46.5 Hz, 88H, CH_2), 3.24 (s, 3H, CH_3), 2.94 (s, 9H, CH_2).

FTIR (cm^{-1}): 3320 (N-H), 3283 (N-H), 3030 (C-H, alkyl), 2863 (C-H, alkyl), 1662 (C=O, amide), 1631 (C=C, Ar), 1515 (C=C, Ar), 1239 (C-N, amide), 1105 (C-O, aliphatic ether), 697 (C-H, Ar).

7.2.7.3 Synthesis of $mPEG_{22}$-*b*-poly(L-phenylalanine)$_5$ (SJB95)

A Schlenk tube was degassed and backfilled with $N_{2(g)}$ and loaded with $mPEG_{22}$-NH_2 (0.1 g, 0.1 mmol) and L-phenylalanine NCA (0.191 g, 1.0 mmol). Anhydrous DMF (20 mL) was added and the reaction was stirred under a constant stream of $N_{2(g)}$ for seven days at room temperature. The reaction mix was precipitated into ice cold diethyl ether (150 mL) and

incubated at -5 °C for 24 hours. The mixture was then centrifuged and the supernatant decanted. The product was washed three time with ice cold ethyl acetate and centrifuged. The resulting off-white solid was dried *in vacuo* at 50 °C for 48 hours. Yield: 0.2602 g.

^{1}H NMR (500 MHz, DMSO) δ 7.39 – 6.97 (m, 25H, ArH), 4.53 (s, 5H, CH), 3.47 (d, *J* = 31.2 Hz, 88H, CH_2), 3.24 (s, 3H, CH_3), 2.92 (d, *J* = 20.7 Hz, 10H, CH_2).

FTIR (cm^{-1}): 3324 (N-H), 3285 (N-H), 3028 (C-H, alkyl), 2865 (C-H, alkyl), 1662 (C=O, amide), 1629 (C=C, Ar), 1519 (C=C, Ar), 1241 (C-N, amide), 1103 (C-O, aliphatic ether), 695 (C-H, Ar).

7.2.8 NCA ROP of BLG NCA with $mPEG_{22}$-NH_2 Macroinitiator

7.2.8.1 Synthesis of $mPEG_{22}$-*b*-poly(γ-benzyl-L-glutamate)$_3$ (SJB101p)

A Schlenk tube was degassed and backfilled with $N_{2(g)}$ and loaded with $mPEG_{22}$-NH_2 (0.1 g, 0.1 mmol) and γ-benzyl-L-glutamate NCA (0.263 g, 1.0 mmol). Anhydrous DMF (20 mL) was added and the reaction was stirred under a constant stream of $N_{2(g)}$ for seven days at room temperature. The reaction mix was precipitated into ice cold diethyl ether (150 mL) and incubated at -5 °C for 24 hours. The mixture was then centrifuged and the supernatant decanted. The product was washed three time with ice cold ethyl acetate and centrifuged. The resulting off-white solid was dried in vacuo at 50 °C for 48 hours. Yield: 0.1306 g.

^{1}H NMR (500 MHz, DMSO) δ 7.33 (t, J = 19.3 Hz, 20H, ArH), 5.05 (t, J = 18.0 Hz, 8H, CH_2), 4.26 (d, J = 12.7 Hz, 3H, CH), 3.73 – 3.39 (m, 88H, CH_2), 3.24 (s, 3H, CH_3), 2.00 – 1.63 (m, 10H, CH_2).

FTIR (cm^{-1}): 3287 (N-H), 3034 (C-H, alkyl), 2873 (C-H, alkyl), 1729 (C=O, benzyl), 1649 (C=O, amide), 1543 (C=C, Ar), 1454 (C-H, alkyl), 1343 (C-N, amide), 1239 (C-N, amide), 1142 (C-O, aliphatic ether), 1101 (C-O, aliphatic ether), 950 (C=C, Ar), 697 (C-H, Ar).

7.2.8.2 Synthesis of $mPEG_{22}$-*b*-poly(γ-benzyl-L-glutamate)$_7$ (SJB100p)

A Schlenk tube was degassed and backfilled with $N_{2(g)}$ and loaded with $mPEG_{22}$-NH_2 (0.1 g, 0.1 mmol) and γ-benzyl-L-glutamate NCA (0.132 g, 0.5 mmol). Anhydrous DMF (20 mL) was added and the reaction was stirred under a constant stream of $N_{2(g)}$ for seven days at room temperature. The reaction mix was precipitated into ice cold diethyl ether (150 mL) and incubated at -5 °C for 24 hours. The mixture was then centrifuged and the supernatant decanted. The product was washed three time with ice cold ethyl acetate and centrifuged. The resulting off-white solid was dried *in vacuo* at 50 °C for 48 hours. Yield: 0.1398 g.

^{1}H NMR (500 MHz, DMSO) δ 7.30 (d, *J* = 30.5 Hz, 34H, ArH), 5.07 (s, 13H, CH_2), 4.20 (d, *J* = 56.4 Hz, 2H, CH), 3.75 – 3.41 (m, 88H, CH_2), 3.24 (s, 3H, CH_3), 1.88 (d, *J* = 48.4 Hz, 12H, CH_2).

FTIR (cm^{-1}): 3287 (N-H), 3030 (C-H, alkyl), 2867 (C-H, alkyl), 1731 (C=O, benzyl), 1649 (C=O, amide), 1625 (C=C, Ar), 1545 (C=C, Ar), 1452 (C-H, alkyl), 1248 (C-N, amide), 1160 (C-O, aliphatic ether), 1095 (C-O, aliphatic ether), 697 (C-H, Ar).

7.2.8.3 Synthesis of $mPEG_{22}$-*b*-poly(γ-benzyl-L-glutamate)$_{23}$ (SJB102p)

A Schlenk tube was degassed and backfilled with $N_{2(g)}$ and loaded with $mPEG_{22}$-NH_2 (0.1 g, 0.1 mmol) and γ-benzyl-L-glutamate NCA (0.395 g, 1.5 mmol). Anhydrous DMF (20 mL) was added and the reaction was stirred under a constant stream of $N_{2(g)}$ for seven days at room temperature. The reaction mix was precipitated into ice cold diethyl ether (150 mL) and incubated at -5 °C for 24 hours. The mixture was then centrifuged and the supernatant decanted. The product was washed three time with ice cold ethyl acetate and centrifuged. The resulting off-white solid was dried *in vacuo* at 50 °C for 48 hours. Yield: 0.4653 g.

^{1}H NMR (500 MHz, DMSO) δ 7.31 (dd, *J* = 18.6, 12.1 Hz, 115H, ArH), 5.25 – 4.84 (m, 45H, CH_2), 4.13 – 3.73 (m, 15H, CH), 3.48 (d, *J* = 20.1 Hz, 88H, CH_2), 3.24 (s, 3H, CH_3), 2.30 – 1.73 (m, 60H, CH_2).

FTIR (cm^{-1}): 3287 (N-H), 3034 (C-H, alkyl), 2873 (C-H, alkyl), 2865(N-H), 1729 (C=O, benzyl), 1651 (C=O, amide), 1547 (C=C, Ar), 1454 (C-H, alkyl), 1388 (C-N, amide), 1244 (C-N, amide), 1156 (C-O, aliphatic ether), 1117 (C-O, aliphatic ether), 952 (C=C, Ar), 744 (C-H, Ar), 693 (C-H, Ar).

7.2.8.4 Deprotection of $mPEG_{22}$-*b*-poly(γ-benzyl-L-glutamate)$_{23}$

$mPEG_{22}$-*b*-$PBLG_{23}$ (0.5 g, 0.077 mmol) was added to a mixture of trifluoroacetic acid (7 mL) and hydrogen bromide in acetic acid (33%, 3 mL) and stirred for 48 hours. The resulting mixture was precipitated into ice cold diethyl ether (20 mL) and stored at -5 °C for a further 24 hours. The mixture was then centrifuged and the supernatant decanted. The product was washed three time with ice cold diethyl ether and centrifuged. The product was washed three time with ice cold ethyl acetate and centrifuged. The resulting creamy orange solid was dried *in vacuo* at 50 ^{O}C for 48 hours.

^{1}H NMR (500 MHz, DMSO) δ 4.31 – 3.89 (m, 30H, CH), 3.51 (s, 88H, CH_2), 3.21 (d, *J* = 26.0 Hz, 3H, CH_3), 2.26 (t, *J* = 29.0 Hz, 53H, OH), 2.07 – 1.59 (m, 40H, CH_2).

FTIR (cm^{-1}): 3065 (broad, O-H, carboxylic acid),3285 (N-H), 3065 (C-H, alkyl), 2910 (C-H, alkyl), 2865(N-H), 1706 (C=O, carboxylic acid), 1649 (C=O, amide), 1545 (C=C, Ar), 1407 (C-H, alkyl), 1248 (C-N, amide), 1168 (C-O, aliphatic ether), 1080 (C-O, aliphatic ether), 946 (C=C, Ar), 789 (C-H, Ar), 609 (C-H, Ar).

7.2.8.5 Synthesis of $mPEG_{22}$-*b*-poly(γ-benzyl-L-glutamate)$_{43}$ (SJB116p)

A Schlenk tube was degassed and backfilled with $N_{2(g)}$ and loaded with $mPEG_{22}$-NH_2 (0.1 g, 0.1 mmol) and γ-benzyl-L-glutamate NCA (0.789 g, 3.0 mmol). Anhydrous DMF (20 mL) was added and the reaction was stirred under a constant stream of $N_{2(g)}$ for seven days at room temperature. The reaction mix was precipitated into ice cold diethyl ether (150 mL) and incubated at -5 °C for 24 hours. The mixture was then centrifuged and the supernatant

decanted. The product was washed three time with ice cold ethyl acetate and centrifuged. The resulting off-white solid was dried *in vacuo* at 50 °C for 48 hours. Yield: 0.4481 g.

^{1}H NMR (500 MHz, DMSO) δ 7.31 (dd, *J* = 16.9, 11.7 Hz, 214H, ArH), 5.03 (d, *J* = 26.9 Hz, 81H, CH_2), 3.93 (dd, *J* = 85.2, 46.5 Hz, 34H, CH), 3.62 – 3.40 (m, 88H, CH_2), 3.24 (s, 3H, CH_3), 2.04 (dd, *J* = 91.5, 63.9 Hz, 114H, CH_2).

FTIR (cm^{-1}): 3283 (N-H), 3030 (C-H, alkyl), 2869 (C-H, alkyl), 2865(), 1731 (C=O, benzyl), 1647 (C=O, amide), 1541 (C=C, Ar), 1452 (C-H, alkyl), 1384 (C-N, amide), 1244 (C-N, amide), 1164(C-O, aliphatic ether), 958 (C=C, Ar), 738 (C-H, Ar), 693 (C-H, Ar).

7.2.9 NCA ROP of BLG NCA with $mPEG_{113}$-NH_2 Macroinitiator

7.2.9.1 Synthesis of $mPEG_{113}$-*b*-poly(γ-benzyl-L-glutamate)$_{12}$ (SJB118p)

A Schlenk tube was degassed and backfilled with $N_{2(g)}$ and loaded with $mPEG_{113}$-NH_2 (0.1 g, 0.02 mmol) and γ-benzyl-L-glutamate NCA (0.0789 g, 0.3 mmol). Anhydrous DMF (20 mL) was added and the reaction was stirred under a constant stream of $N_{2(g)}$ for seven days at room temperature. The reaction mix was precipitated into ice cold diethyl ether (150 mL) and incubated at -5 °C for 24 hours. The mixture was then centrifuged and the supernatant decanted. The product was washed three time with ice cold ethyl acetate and centrifuged. The resulting off-white solid was dried *in vacuo* at 50 °C for 48 hours. Yield: 0.3568 g.

^{1}H NMR (500 MHz, DMSO) δ 7.30 (d, *J* = 23.6 Hz, 60H, ArH), 5.06 (s, 284H, CH_2), 3.92 (s, 7H, CH), 3.51 (s, 440H, CH_2), 3.24 (s, 3H, CH_3), 2.01 (d, *J* = 7.5 Hz, 22H, CH_2).

FTIR (cm^{-1}): 3283 (N-H), 2877 (C-H, alkyl), 1731 (C=O, benzyl), 1651 (C=O, amide), 1547 (C=C, Ar), 1466 (C-H, alkyl), 1341 (C-N, amide), 1278 (C-N, amide), 1239 (C-O, aliphatic ether), 1099 (C-O, aliphatic ether), 958 (C=C, Ar), 842 (C-H, Ar), 697 (C-H, Ar).

7.2.10 NCA ROP of BLG NCA with $mPEG_{295}$-NH_2 Macroinitiator

7.2.10.1 Synthesis of $mPEG_{295}$-*b*-poly(γ-benzyl-L-glutamate)$_{25}$ (SJB117p)

A Schlenk tube was degassed and backfilled with $N_{2(g)}$ and loaded with $mPEG_{295}$-NH_2 (0.1 g, 0.00769 mmol) and γ-benzyl-L-glutamate NCA (0.0304 g, 0.12 mmol). Anhydrous DMF (20 mL) was added and the reaction was stirred under a constant stream of $N_{2(g)}$ for seven days at room temperature. The reaction mix was precipitated into ice cold diethyl ether (150 mL) and incubated at -5 °C for 24 hours. The mixture was then centrifuged and the supernatant decanted. The product was washed three time with ice cold ethyl acetate and centrifuged. The resulting off-white solid was dried *in vacuo* at 50 °C for 48 hours. Yield: 0.3130 g.

^{1}H NMR (500 MHz, DMSO) δ 7.26 (s, 123H, ArH), 5.04 (s, 47H, CH_2), 4.42 – 4.09 (m, 11H, CH), 3.47 (d, *J* = 32.8 Hz, 1144H, CH_2), 3.25 – 3.24 (m, 3H, CH_3), 2.13 – 1.78 (m, 123H, CH_2).

FTIR (cm^{-1}): 3285 (N-H), 2887 (C-H, alkyl), 1729 (C=O, benzyl), 1655 (C=O, amide), 1464 (C-H, alkyl), 1341 (C-N, amide), 1276 (C-N, amide), 1237 (C-O, aliphatic ether), 1091 (C-O, aliphatic ether), 956 (C=C, Ar), 842 (C-H, Ar).

7.2.11 NCA ROP of Z-Lys NCA with $mPEG_{22}$-NH_2 Macroinitiator

7.2.11.1 Synthesis of $mPEG_{22}$-*b*-poly(*N*-ε-carboxybenzyl-L-lysine)$_2$ (SJB122p)

A Schlenk tube was degassed and backfilled with $N_{2(g)}$ and loaded with $mPEG_{22}$-NH_2 (0.05 g, 0.05 mmol) and *N*-ε-carboxybenzyl-L-lysine NCA (0.46 g, 1.5 mmol). Anhydrous DMF (20 mL) was added and the reaction was stirred under a constant stream of $N_{2(g)}$ for seven days at room temperature. The reaction mix was precipitated into ice cold diethyl ether (150 mL) and incubated at -5 °C for 24 hours. The mixture was then centrifuged and the supernatant decanted. The product was washed three time with ice cold ethyl acetate and centrifuged. The resulting off-white solid was dried *in vacuo* at 50 °C for 48 hours. Yield: 0.1495 g.

^{1}H NMR (500 MHz, DMSO) δ 7.96 (s, 2H, NH), 7.58 – 7.11 (m, 10H, ArH), 5.01 (s, 4H, CH_2), 3.91 – 3.47 (m, 88H, CH_2), 3.24 (d, *J* = 1.8 Hz, 3H, CH_3), 2.93 (dd, *J* = 44.8, 9.9 Hz, 10H, CH_2), 1.84 – 1.16 (m, 15H, CH_2).

FTIR (cm^{-1}): 3338 (N-H), 3032 (C-H, alkyl), 2867 (C-H, alkyl), 1686 (C=O, amide), 1454 (C-H, alkyl), 1343 (C-N, amide), 1239 (C-N, amide), 1103 (C-O, aliphatic ether), 946 (C=C, Ar), 842 (C-H, Ar).

7.2.11.2 Synthesis of mPEG$_{22}$-*b*-poly(*N*-ε-carboxybenzyl-L-lysine)$_3$ (SJB120p)

A Schlenk tube was degassed and backfilled with $N_{2(g)}$ and loaded with mPEG$_{22}$-NH_2 (0.05 g, 0.05 mmol) and *N*-ε-carboxybenzyl-L-lysine NCA (0.153 g, 0.5 mmol). Anhydrous DMF (20 mL) was added and the reaction was stirred under a constant stream of $N_{2(g)}$ for seven days at room temperature. The reaction mix was precipitated into ice cold diethyl ether (150 mL) and incubated at -5 °C for 24 hours. The mixture was then centrifuged and the supernatant decanted. The product was washed three time with ice cold ethyl acetate and centrifuged. The resulting off-white solid was dried *in vacuo* at 50 °C for 48 hours. Yield: 0.1687 g.

^{1}H NMR (500 MHz, DMSO) δ 8.14 (s, 3H, NH), 7.52 – 7.06 (m, 14H, ArH), 5.01 (s, 5H, CH_2), 3.54 (d, *J* = 23.3 Hz, 88H, CH_2), 3.25 (s, 3H, CH_3), 2.99 (s, 5H, CH_2), 1.80 – 1.20 (m, 16H, CH_2).

FTIR (cm^{-1}): 3509 (N-H), 3311 (N-H), 3034 (C-H, alkyl), 2867 (C-H, alkyl), 1704 (C=O, amide), 1688 (N-H, bending, amine), 1535 (C=C, Ar), 1454 (C-H, alkyl), 1341 (C-N, amide), 1244 (C-N, amide), 1095 (C-O, aliphatic ether), 950 (C=C, Ar), 844 (C-H, Ar), 699 (C-H, Ar).

7.2.11.3 Synthesis of mPEG$_{22}$-*b*-poly(*N*-ε-carboxybenzyl-L-lysine)$_6$ (SJB121p)

A Schlenk tube was degassed and backfilled with $N_{2(g)}$ and loaded with mPEG$_{22}$-NH_2 (0.1 g, 0.1 mmol) and *N*-ε-carboxybenzyl-L-lysine NCA (0.153 g, 0.5 mmol). Anhydrous DMF (20 mL) was added and the reaction was stirred under a constant stream of $N_{2(g)}$ for seven days at room temperature. The reaction mix was precipitated into ice cold diethyl ether (150 mL) and incubated at -5 °C for 24 hours. The mixture was then centrifuged and the supernatant

decanted. The product was washed three time with ice cold ethyl acetate and centrifuged. The resulting off-white solid was dried *in vacuo* at 50 °C for 48 hours. Yield: 0.2376 g.

^{1}H NMR (500 MHz, DMSO) δ 8.27 – 7.94 (m, 5H, NH), 7.27 (d, *J* = 50.5 Hz, 30H, ArH), 5.00 (s, 10H, CH_2), 3.51 (s, 88H, CH_2), 3.24 (s, 3H, CH_3), 3.07 – 2.86 (m, 10H, CH_2), 1.76 – 1.04 (m, 32H, CH_2).

FTIR (cm^{-1}): 3491 (N-H), 3295 (N-H), 3067 (C-H, alkyl), 2867 (C-H, alkyl), 1686 (C=O, amide), 1627 (N-H, bending, amine), 1539 (C=C, Ar), 1454 (C-H, alkyl), 1343 (C-N, amide), 1252 (C-N, amide), 1103 (C-O, aliphatic ether), 946 (C=C, Ar), 842 (C-H, Ar), 695 (C-H, Ar).

7.3 Results and Discussion

A variety of diblock copolymers were synthesised *via* NCA ROP, using methoxy-PEG-amine (mPEG-NH_2) as the macroinitiator. To do this, three amino acids were converted into NCAs in order to create the poly(amino acid) block. The three amino acids selected were γ-benzyl-L-glutamate, *N*-ε-carboxybenzyl-L-lysine and L-phenylalanine. These were chosen owing to their differing functionality of acid, amine and aromatic groups, in order to assess the key interactions required to improve dye transfer inhibition (DTI).

The poly(amino acid) block was expected to interact with the fibres by intermolecular forces such as hydrogen bonds, while the PEG block creates an hydration layer between the fabric and the aqueous wash solution to prevent dye deposition *via* a blocking mechanism, analogous to PEG-based anti-fouling surface coatings.[33,34] The amide groups in the poly(amino acid) chain were expected to hydrogen bond with the fibres. It was also expected that the aromatic groups of the phenylalanine would provide additional intermolecular interactions through hydrophobic interactions and π-π stacking to the fibres containing aromatic groups, such as polyester and wool. Whereas the acid groups in glutamate and the amine groups in lysine would provide additional hydrogen bonding capability, beyond the peptide bonds already present in the poly(amino acid) backbone.

7.3.1 mPEG$_{22}$-*b*-poly(L-phenylalanine)$_n$ Polymers

Firstly, the phenylalanine NCA monomer was successfully synthesised, as confirmed by ^{1}H NMR and FTIR analysis (Appendix 17 and Appendix 18). Then three mPEG$_{22}$-*b*-poly(L-phenylalanine)$_n$ polymers were synthesised, in order to observe the effect of the inclusion of aromatic groups on DTI efficacy, as well as the amphiphilic nature of the polymers. Phenylalanine (Phe) NCA was reacted with mPEG$_{22}$-NH$_2$ to produce three polymers with differing lengths of the poly(Phe) chain, creating an amphiphilic diblock copolymer. The successful synthesis was confirmed by ^{1}H NMR and FTIR shown in Figure 7-3 and Figure 7-4 respectively.

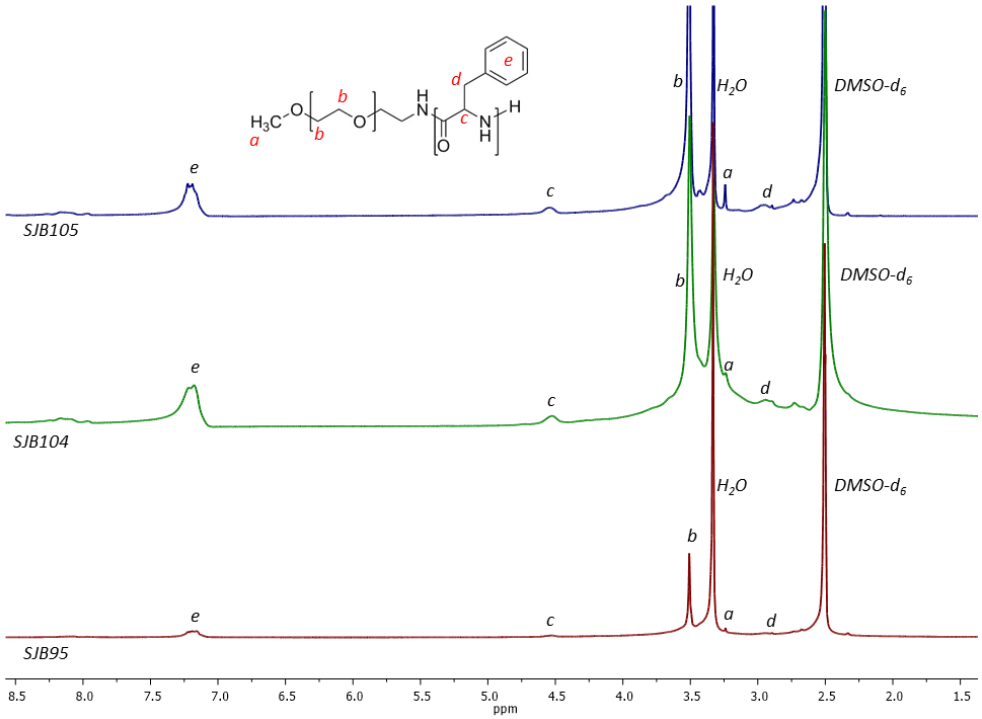

Figure 7-3 ^{1}H NMR spectra of three mPEG$_{22}$-b-poly(L-phenylalanine)$_n$ polymers in DMSO-d$_6$.

The ^{1}H NMR spectra in Figure 7-3 show the PEG block and the aromatic groups of the Phe block, confirming the successful synthesis of the polymers.

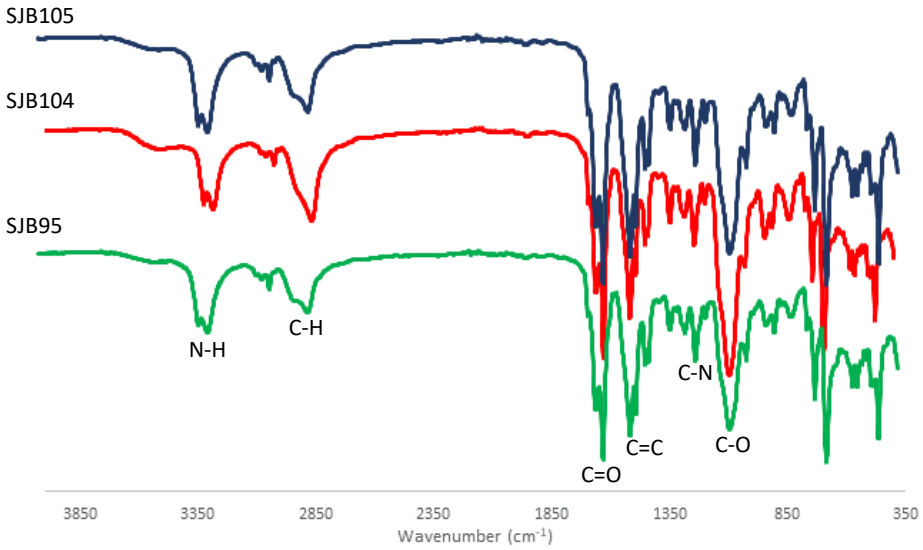

Figure 7-4 FTIR spectra of three mPEG$_{22}$-b-poly(L-phenylalanine)$_n$ polymers.

The FTIR spectrum shows the presence of the amide alongside the ether group of PEG, further confirming the grafting of the poly(Phe) block to the PEG. The number of Phe repeat units was determined by comparing the ^{1}H NMR integration value of the aromatic peak of the phenylalanine unit, representing five protons, to the peak for the PEG protons at 3.5 ppm, representing 88 protons. The calculated poly(Phe) block lengths of the three polymers are outlined in Table 7-1 alongside the zeta potential values of the polymers in water.

Table 7-1 The calculated Phe chain lengths of three mPEG$_{22}$-b-poly(Phe) polymers synthesised.

Polymer	PEG peak Integration	Phe peak Integration	Number of Phe Units	PEG:Phe Ratio
SJB105	88	15.17	3	7.3:1
SJB104	88	20.34	4	5.5:1
SJB95	88	24.52	5	4.4:1

As the polymerisation reaction proceeds, the polymer is precipitated from solution due to its increasing insolubility, and therefore the length of the Phe chain becomes limited.

These polymers were then tested for their DTI efficacy against indigo, by washing with an indigo dye bleeding fabric swatch, a multifibre strip (which is the receiving fabric for dye deposition), and a polymer aqueous solution (50 mL, 0.1 mg mL^{-1}), along with 25 ball bearings, at 40 °C for 30 minutes at 40 rpm. The colour change (ΔE) caused by indigo on the variety of fabrics on the multifibre swatch was measured and compared for each polymer DTI solution (Figure 7-5).

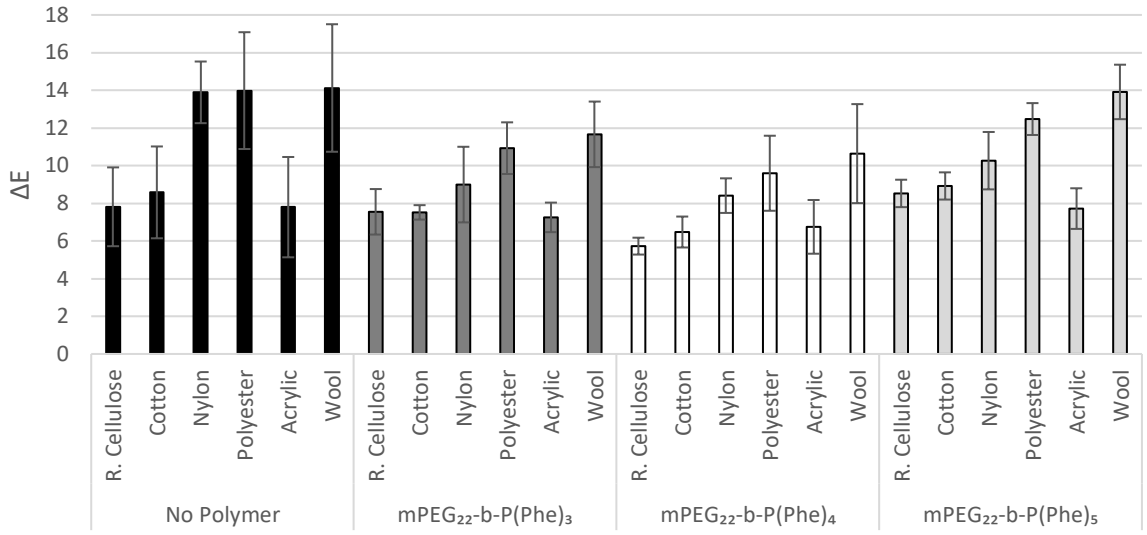

Figure 7-5 A comparison of the colour change caused by indigo in the presence of three $mPEG_{22}$-b-poly(Phe)$_n$ polymers.

Figure 7-5 shows the $mPEG_{22}$-*b*-poly(L-phenylalanine)$_n$ polymers possess some DTI efficacy, particularly for nylon and polyester fibre types. This is shown by a 39.5% reduction in ΔE for nylon, from 13.89 without a DTI polymer, to a mean value of 8.41 with $mPEG_{22}$-*b*-poly(Phe)$_4$. This efficacy is also evident for polyester for $mPEG_{22}$-*b*-poly(Phe)$_3$ and $mPEG_{22}$-*b*-poly(Phe)$_4$, showing a reduction in ΔE from 13.98 to 10.92 and 9.59 respectively (21.9% and 31.4% reduction). The reduced efficacy for the hydrophilic fibres shows that the polymer may interact with the fibre by hydrophobic interactions, or π-π stacking with the polyester fibres, in order to block dye deposition and prevent colour change.

7.3.2 mPEG$_{22}$-*b*-poly(γ-benzyl-L-glutamate)$_n$ Polymers

Due to the reduced solubility of poly(Phe) in various polymerisation solvents such as DMF and chloroform as the reaction proceeds, and due to the limited DTI efficacy of the mPEG-*b*-poly(Phe) polymers, poly(amino acid)s with greater solubility in polar solvents were created. This allows for the synthesis of longer poly(amino acid) chains, as well as the introduction of various R groups on the amino acid. Therefore, γ-benzyl-L-glutamate was converted into an NCA monomer, rather than the unprotected L-glutamic acid (Glu). The successful synthesis of the BLG NCA was confirmed by ^{1}H NMR and FTIR (Appendix 19 and Appendix 20). This was then polymerised *via* NCA ROP using mPEG$_{22}$-NH$_2$ as a macroinitiator, yielding three polymers with blocks of poly(γ-benzyl-L-glutamate) (PBLG) of varying chain lengths. The successful synthesis of the polymers was confirmed by ^{1}H NMR (

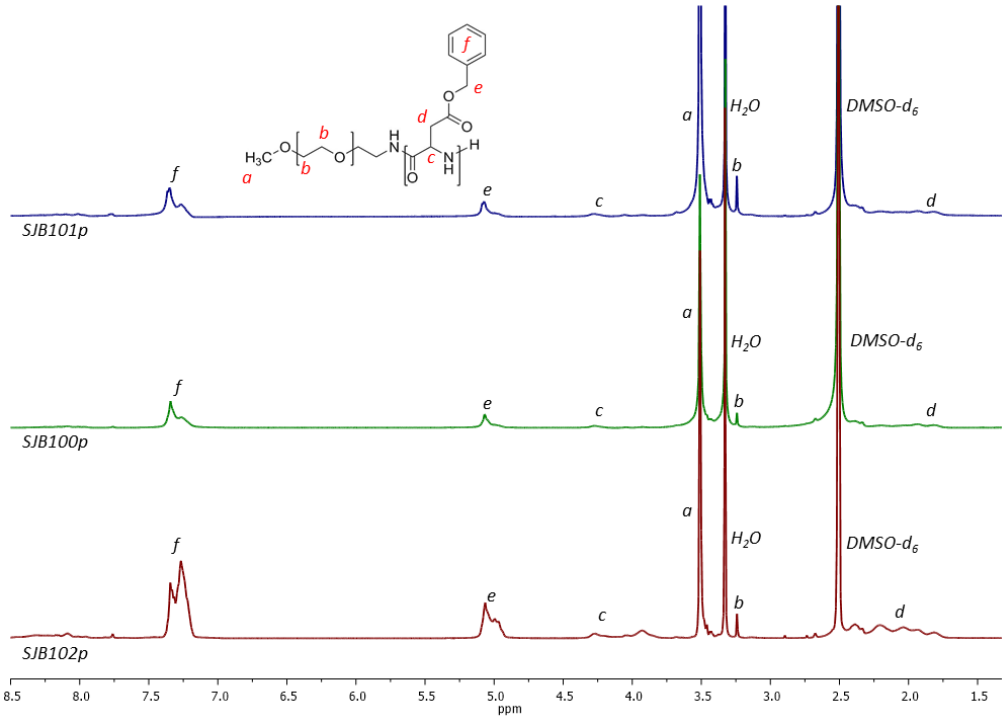

Figure 7-6) and FTIR (Figure 7-7).

Figure 7-6 ^{1}H NMR spectra of three mPEG$_{22}$-b-poly(γ-benzyl-L-glutamate)$_n$ polymers in DMSO-d$_6$.

The ^{1}H NMR spectra show the PEG block, alongside the aromatic groups and methyl groups associated with the BLG block.

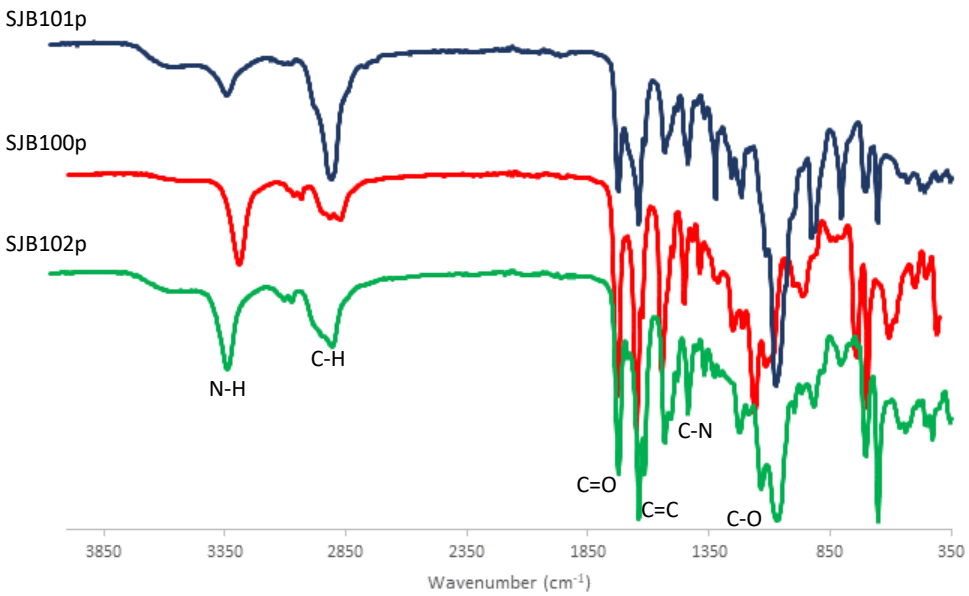

Figure 7-7 FTIR spectra of three mPEG$_{22}$-b-poly(γ-benzyl-L-glutamate)$_n$ polymers.

The FTIR spectrum shows the presence of the amide alongside the ether group of PEG, further confirming the grafting of the poly(BLG) block to the PEG. The number of PBLG repeat units was determined by comparing the ^{1}H NMR integration value of the aromatic peak of the benzyl group representing five protons, to the PEG peak at 3.5 ppm representing 88 protons. The block length of the PBLG chains of the three mPEG$_{22}$-b-PBLG$_n$ polymers are outlined in

Table 7-2.

Table 7-2 The calculated PBLG chain lengths of three mPEG$_{22}$-b-PBLG$_n$ polymers synthesised.

Polymer	PEG peak Integration	PBLG peak Integration	Number of PBLG Units	PEG:PBLG Ratio
SJB101p	88	15.68	3	7.3:1
SJB100p	88	34.09	7	3.1:1
SJB102p	88	114.88	23	1:1

Polymer	PEG peak Integration	PBLG peak Integration	Number of PBLG Units	PEG:PBLG Ratio
SJB101p	88	15.68	3	7.3:1
SJB100p	88	34.09	7	3.1:1
SJB102p	88	114.88	23	1:1

The three polymers were washed with an indigo dye bleeding swatch in order to assess their DTI efficacy (Figure 7-8). The polymers were not deprotected before the washes and as such were amphiphilic, due to the hydrophobic nature of the PBLG block.

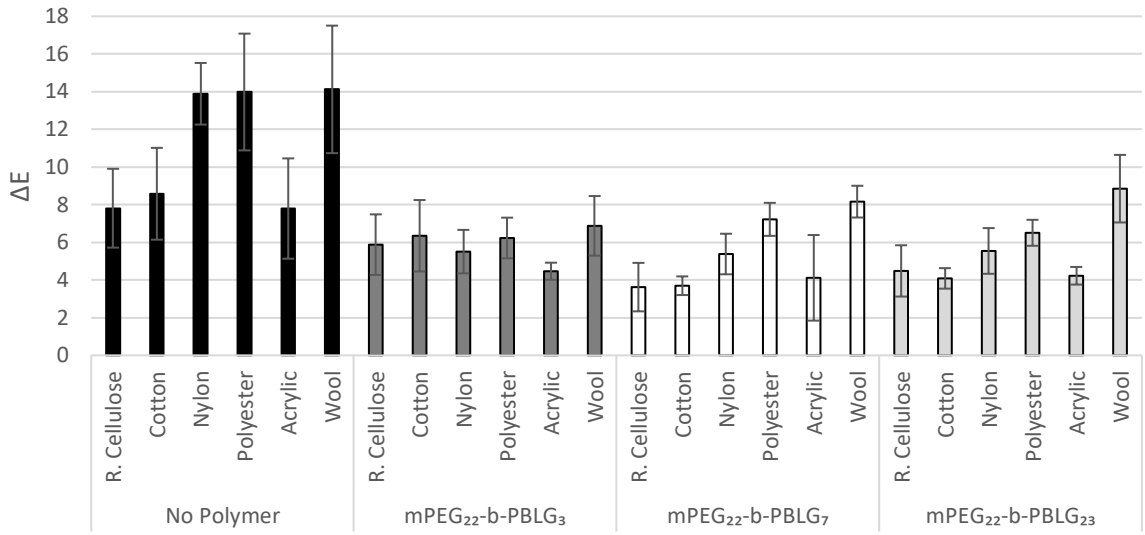

Figure 7-8 A comparison of the colour change caused by indigo in the presence of three mPEG$_{22}$-b-PBLG$_n$ polymers.

From Figure 7-8 it can be observed that the mPEG$_{22}$-*b*-PBLG$_n$ polymers provide a significant DTI effect against indigo, in particular for the nylon and polyester fabric types. mPEG$_{22}$-*b*-PBLG$_{23}$ shows a reduction in colour change for nylon from 13.89 to 5.54, a 60.1% reduction, while for polyester there is a 53.4% reduction. This shows an even greater efficacy than the mPEG$_{22}$-*b*-poly(Phe)$_n$ polymers outlined in Section 7.3.1, which indicates the additional capability of the PBLG unit to hydrogen bond, as well as π-π stacking provided by the protecting group, offers increased opportunity for the polymer to interact with the fabric and thus block dye deposition. This again highlights the importance of hydrogen bonding capability in the polymers used for DTI agents.

In order to increase the number of groups available for hydrogen bonding and π-π stacking, a further polymer was synthesised further increasing the size of the PBLG block. The resulting polymer was characterised using ^{1}H NMR and FTIR (Appendix 21 and Appendix 22). This was found to have been successfully synthesised with a chain length of 43 units (Table 7-3).

Table 7-3 The calculated PBLG chain length of the $mPEG_{22}$-b-PBLG polymer synthesised with a larger BLG block.

Polymer	PEG peak Integration	PBLG peak Integration	Number of PBLG Units	PEG:PBLG Ratio
SJB116p	88	212.97	43	1:2

This polymer was then tested for its DTI efficacy against indigo and compared to $mPEG_{22}$-*b*-$PBLG_{23}$ (Figure 7-9).

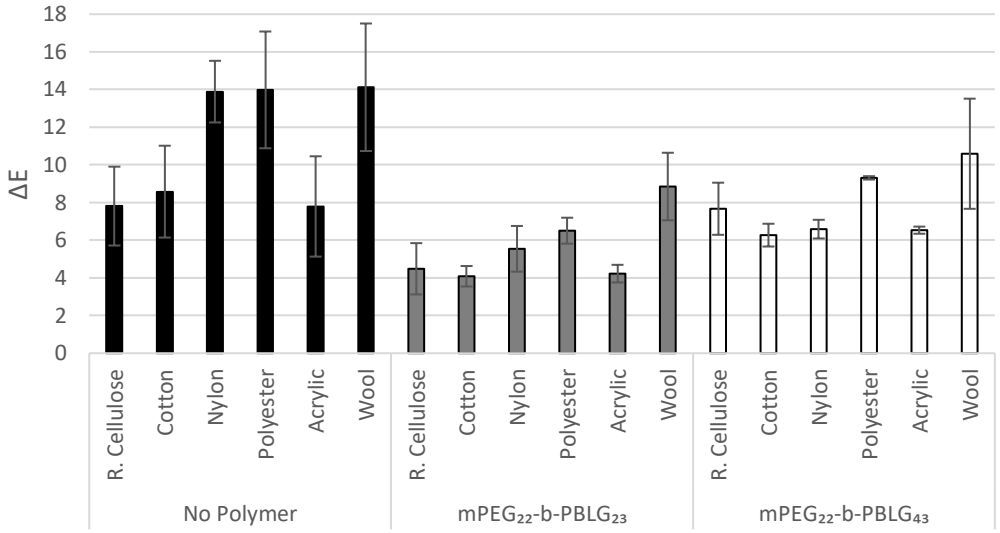

Figure 7-9 A plot to show the colour change caused by indigo in the presence of an $mPEG_{22}$-b-PBLG polymer with an increased PBLG content.

It can be observed from Figure 7-9 that increasing the BLG chain length does not further improve DTI efficacy from $mPEG_{22}$-*b*-$PBLG_{23}$, however it still offers an effective DTI for nylon and polyester fabric types (52.6% and 33.4% reduction respectively).

In order to assess the effect of an anionic polymer, with increased water solubility, $mPEG_{22}$-*b*-$PBLG_{23}$ was deprotected to give $mPEG_{22}$-*b*-poly(glutamic acid) (Glu), which was confirmed by ^1H NMR (Appendix 27). The ability of the polymer to prevent dye transfer of indigo was assessed and compared with its protected analogue (Figure 7-10).

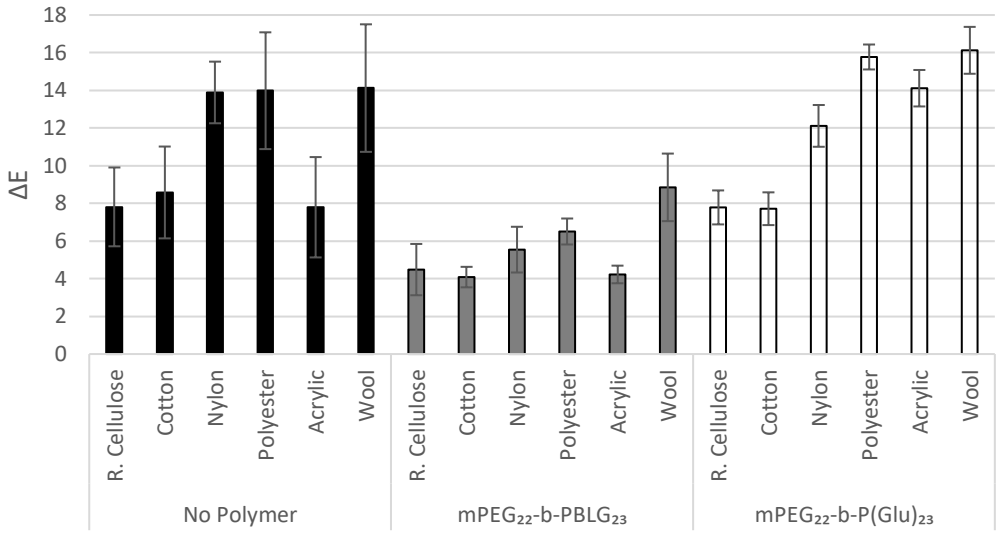

Figure 7-10 A comparison of the colour change caused by indigo in the presence of $mPEG_{22}$-b-$PBLG_{23}$ and $mPEG_{22}$-b-poly(Glu)$_{23}$.

On deprotection of the PBLG block, the DTI efficacy is reduced, shown in Figure 7-10 by the increased colour change from the protected polymer. For example, where nylon shows a 60.1% reduction in colour change for $mPEG_{22}$-*b*-$PBLG_{23}$, $mPEG_{22}$-*b*-poly$(Glu)_{23}$ only shows a decrease of 12.9%. On average across the fibre types there is little improvement, or there is a worsening of the dye deposition caused in the presence of $mPEG_{22}$-*b*-poly$(Glu)_{23}$ from the absence of polymer. This indicates that the free acid groups of the poly(Glu) block does not provide any benefit to the DTI effect of the polymer, as well as removing the π-π stacking capability provided by the benzyl protecting group. This may also be due to the increased water-solubility of the polymer on deprotection, and as such a reduced tendency to interact with the fabric to block dye deposition, but rather to remain in the aqueous phase.

7.3.3 mPEG-*b*-poly(γ-benzyl-L-glutamate)$_n$ Polymers with Varying mPEG Chain Length

Due to the success of the mPEG$_{22}$-*b*-PBLG$_n$ polymers outlined in Section 7.3.2, and their ability to prevent indigo dye transfer, two additional polymers were synthesised and characterised with ^{1}H NMR and FTIR (Appendix 23 to Appendix 26). mPEG$_{113}$-NH$_2$ and mPEG$_{295}$-NH$_2$ were used as macroinitators for γ-benzyl-L-glutamate NCA, the block lengths of which are calculated in Table 7-4.

Table 7-4 The calculated BLG chain lengths of the mPEG$_{113}$-b-PBLG and mPEG$_{295}$-b-PBLG polymers synthesised.

Polymer	PEG peak Integration	PBLG peak Integration	Number of PBLG Units	PEG:PBLG Ratio
SJB118p	440	60.49	12	9.4:1
SJB117p	1144	123.78	25	11.8:1

Polymer	PEG peak Integration	PBLG peak Integration	Number of PBLG Units	PEG:PBLG Ratio
SJB118p	440	60.49	12	9.4:1
SJB117p	1144	123.78	25	11.8:1

These polymers were then investigated for their ability to prevent dye transfer of indigo (Figure 7-11).

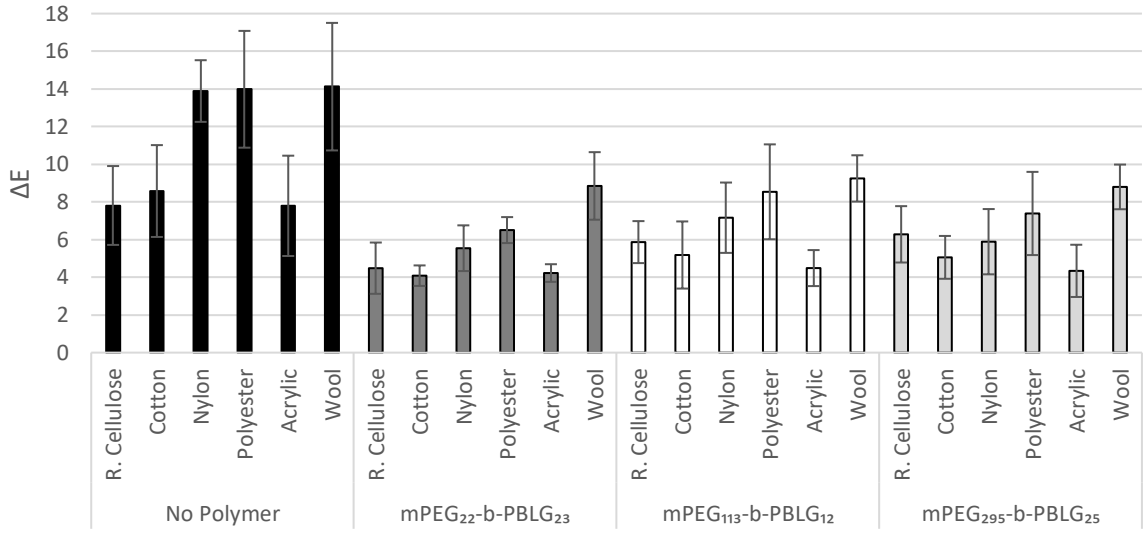

Figure 7-11 A comparison of the colour change caused by indigo in the presence of mPEG$_{22}$-b-PBLG$_{23}$, mPEG$_{113}$-b-PBLG$_{12}$ and mPEG$_{295}$-b-PBLG$_{25}$.

From Figure 7-11 it can be observed that increasing the polymer molecular weight overall, in these cases, does not significantly improve or reduce the DTI efficacy. However, the polymers are still effective as DTI agents, particularly for nylon and polyester. For example, $mPEG_{295}$-*b*-$PBLG_{25}$ exhibits a mean colour change of 5.89 for nylon, which is a reduction of 57.6%, in comparison to $mPEG_{22}$-*b*-$PBLG_{23}$ which gave a 60.1% decrease. This shows the polymer still interacts with the fabric on increasing PEG content, which increases water-solubility of the polymer. A lower molecular weight PEG block is therefore found to be sufficient to prevent dye transfer. This result, alongside that of the polymer with an increased PBLG chain length ($mPEG_{22}$-*b*-$PBLG_{43}$), show that hydrophilicity is a key parameter to consider in the design of DTI polymers.

7.3.4 $mPEG_{22}$-*b*-poly(*N*-ε-carboxybenzyl-L-lysine)$_n$ Polymers

To investigate the effect of additional amine groups in the poly(amino acid) chain, three $mPEG_{22}$-*b*-poly(*N*-ε-carboxybenzyl-L-lysine)$_n$ polymers were synthesised. The NCA was successfully synthesised as confirmed by ^{1}H NMR and FTIR (Appendix 28 and Appendix 29). The pendant amine group of the lysine (Lys) was protected with a carboxybenzyl (Z) protecting group in order to ensure the Z-Lys NCA monomer only reacted at the amine in the amino acid backbone, and not at the pendant amine site. The successful synthesis of the polymers was confirmed by ^{1}H NMR (Figure 7-12) and FTIR (Figure 7-13).

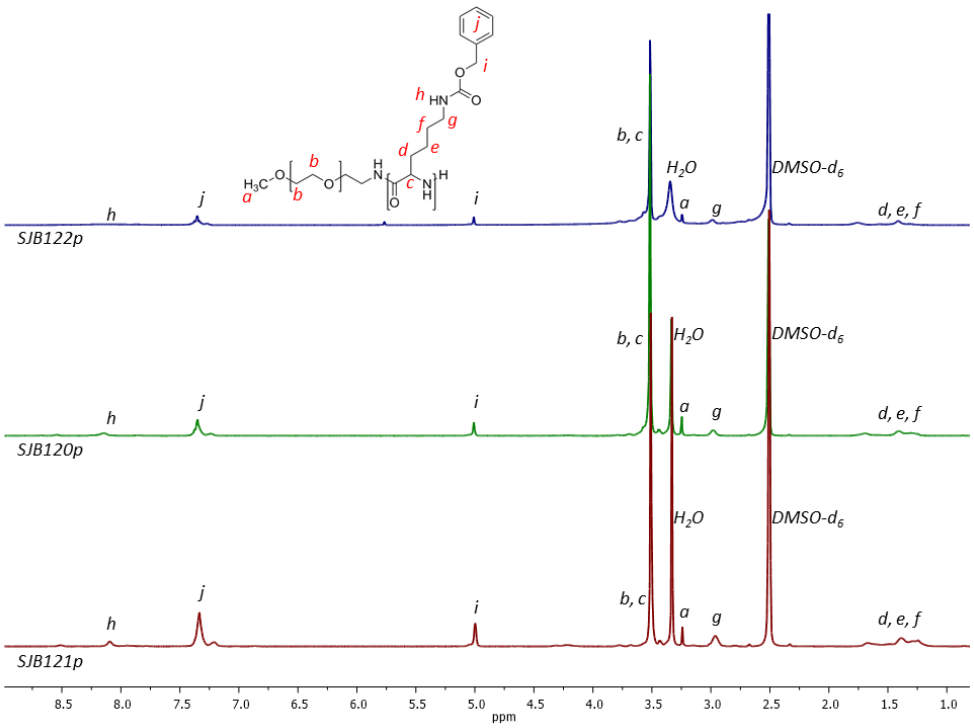

Figure 7-12 ^{1}H NMR spectra of three $mPEG_{22}$-b-poly(N-ε-carboxybenzyl-L-lysine)$_n$ polymers in DMSO-d_6.

The ^{1}H NMR spectra show the presence of the PEG group, alongside the aromatic and amide groups present in the Z-Lys chain.

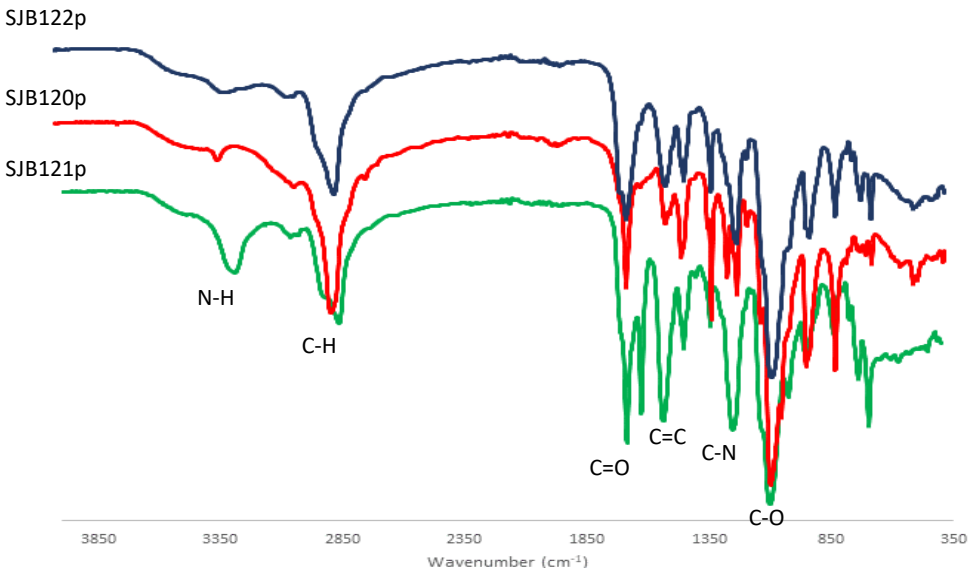

Figure 7-13 FTIR spectra of three $mPEG_{22}$-b-poly(N-ε-carboxybenzyl-L-lysine)$_n$ polymers.

The FTIR spectrum shows the presence of the amide alongside the ether group of PEG, further confirming the grafting of the poly(Z-Lys) block to the PEG. The number of Z-Lys units was determined by comparing the ^{1}H NMR integration of the Z peak representing five protons, to the PEG peak representing 88 protons at 3.2 ppm (Table 7-5).

Table 7-5 The calculated Z-Lys chain lengths of three mPEG-b-poly(Z-Lys)$_n$ polymers synthesised.

Polymer	PEG peak Integration	Z-Lys peak Integration	Number of Z-Lys Units	PEG:Z-Lys Ratio
SJB122p	88	10.02	2	11:1
SJB120p	88	13.64	3	7.3:1
SJB121p	88	29.34	6	3.7:1

The short length of the lysine chains is due to increased steric hindrance of the polymer as the polymerisation proceeds, preventing further polymerisation.

The three polymers were then tested for their DTI efficacy against indigo dye (Figure 7-14).

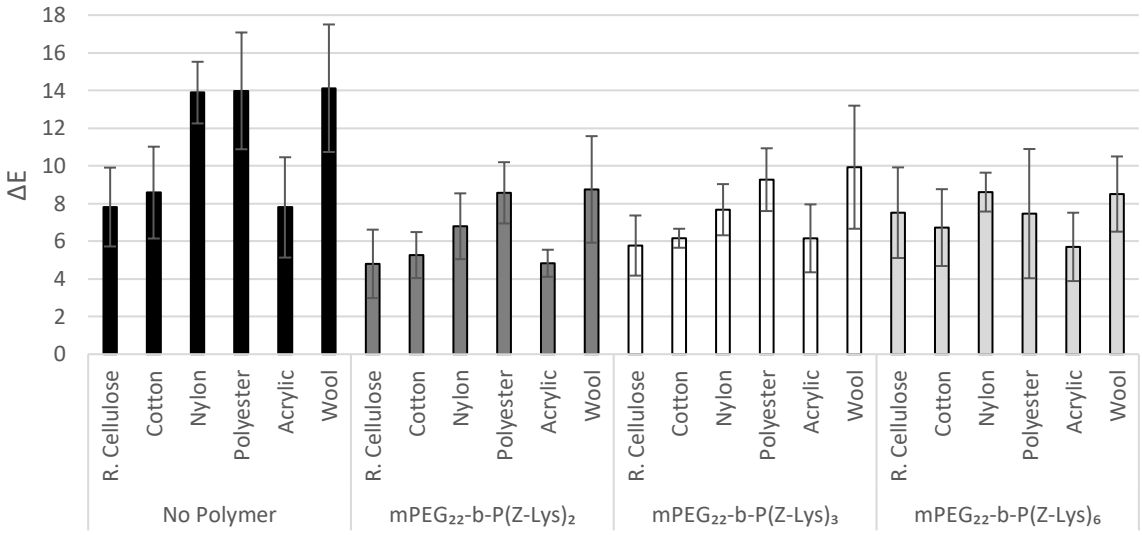

Figure 7-14 A comparison of the colour change caused by indigo in the presence of four mPEG$_{22}$-b-poly(Z-Lys) polymers.

From Figure 7-14 it can be seen that the mPEG$_{22}$-*b*-poly(Z-Lys) polymers are effective DTI polymers against indigo, in particular mPEG$_{22}$-*b*-poly(Z-Lys)$_2$, which shows a reduction in colour

change from 13.89 to 6.79 for nylon fabric, a reduction of 51.1%, and also shows a 38.7% reduction for polyester. This is more effective than the $mPEG_{22}$-*b*-poly(Phe)$_n$ polymers, but less effective than the $mPEG_{22}$-*b*-$PBLG_n$ polymers.

This shows that the additional hydrogen bonding capability provided by the PBLG and the Z-Lys polymer backbones, in comparison to the Phe containing polymers, is necessary to provide significant DTI efficacy. A key difference between the BLG and the Z-Lys polymers is the increased molecular weight and steric bulk of the Z-Lys repeat unit. This therefore means in a 0.1 mg mL^{-1} solution, there are fewer polymer chains because the effective concentration is reduced, and therefore fewer hydrogen bonding groups in the polymer available to bring about a DTI effect.

7.3.5 Further Colour Change Testing of mPEG-*b*-poly(amino acid)s

To further examine the efficacy of the mPEG-*b*-poly(amino acid)s outlined in this chapter, one polymer from each class previously outline was investigated for its DTI efficacy against C.I. Direct Orange 39 (DO39), C.I. Sulfur Black 1 (SB1) and C.I. Reactive Red 141 (RR141). The polymers were then compared against each other for each dye.

Firstly, SB1 was investigated, for $mPEG_{22}$-*b*-poly(Phe)$_4$, $mPEG_{22}$-*b*-$PBLG_{23}$ and $mPEG_{22}$-*b*-poly(Z-Lys)$_6$ (Figure 7-15).

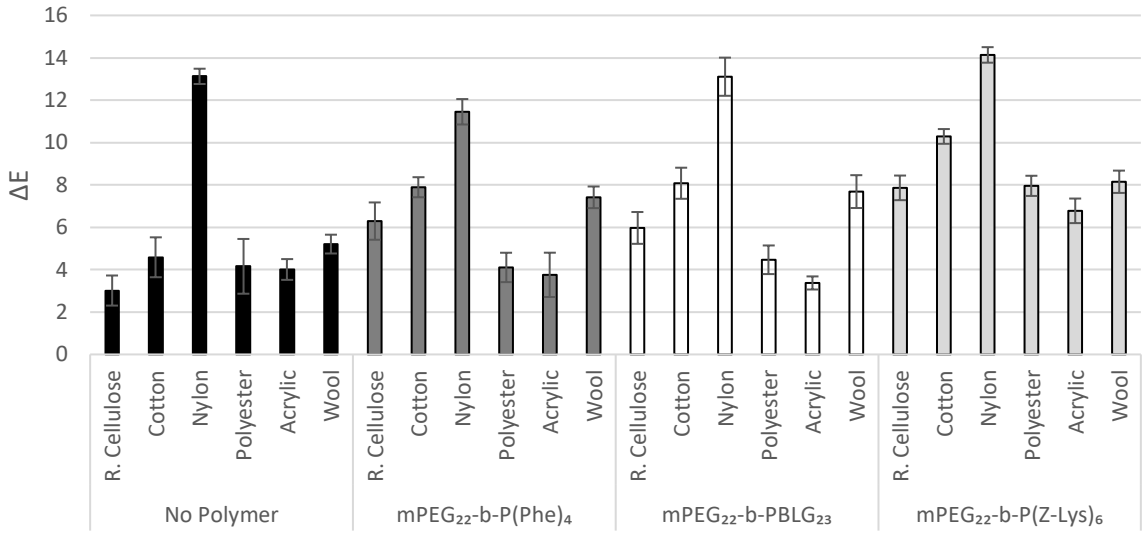

Figure 7-15 A comparison of the colour change caused by SB1 in the presence of $mPEG_{22}$-b-poly(Phe)$_4$, $mPEG_{22}$-b-$PBLG_{23}$ and $mPEG_{22}$-b-poly(Z-Lys)$_6$ polymers.

Figure 7-15 shows the $mPEG_{22}$-*b*-poly(Phe)$_4$ has an improved DTI efficacy against SB1 for nylon fabric, which is particularly discoloured by SB1 in the absence of polymer, reducing from 13.1 to 11.5, a 12.7% reduction. However, deposition is worsened onto cotton and wool by 41.9% and 29.7% respectively. The PBLG and Z-Lys based polymers, however, do not show an improvement in discolouration caused by SB1. In particular, a worsening effect on colour change is observed for the Z-Lys polymer for all the fabric types. The polymer may interact with the fibres in order to block indigo dye deposition of indigo, but this interaction may enable the deposition of the SB1 dye, through ionic interactions. This may explain the worsening effect observed for SB1, where there is an improvement for indigo.

The polymers were then tested against DO39 (Figure 7-16).

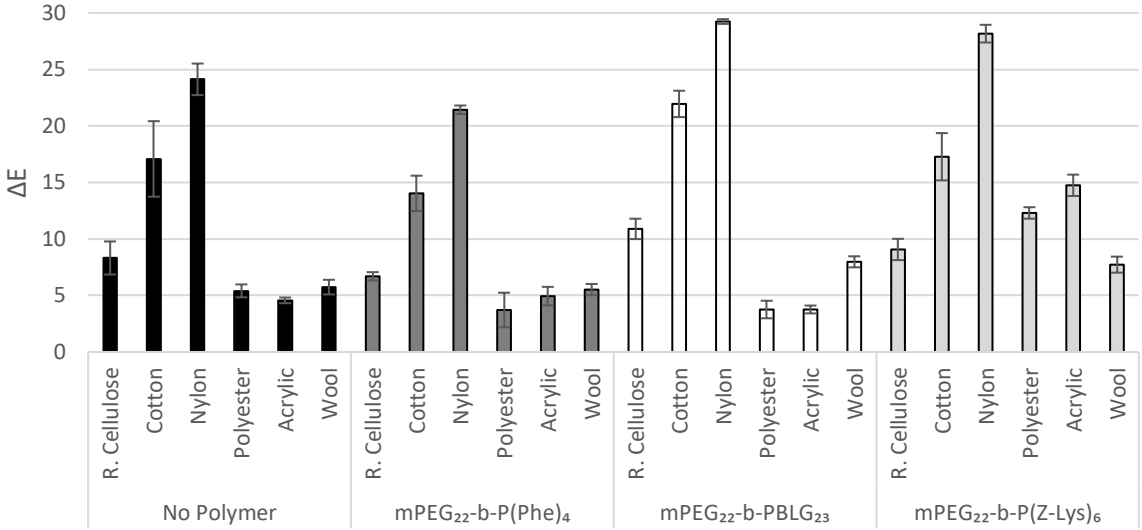

Figure 7-16 A comparison of the colour change caused by DO39 in the presence of $mPEG_{22}$-b-$poly(Phe)_5$, $mPEG_{22}$-b-$PBLG_{23}$ and $mPEG_{22}$-b-$poly(Z\text{-}Lys)_6$ polymers.

Similarly to SB1, $mPEG_{22}$-*b*-$poly(Phe)_4$ shows a reduction in colour change caused by DO39, onto nylon in particular. The colour change is reduced from 24.13 to 21.43, an 11.2% reduction This is in contrast to the PBLG polymer which shows no improvement, and even worsens the colour change onto nylon by 17.5%, and to the Z-Lys polymer which worsens the deposition onto nylon, polyester and acrylic. As DO39 is a highly water-soluble dye, this shows that the polymers which were effective against indigo, are less effective against a more water-soluble dye.

Finally, the polymers were tested for the DTI efficacy against RR141 (Figure 7-17).

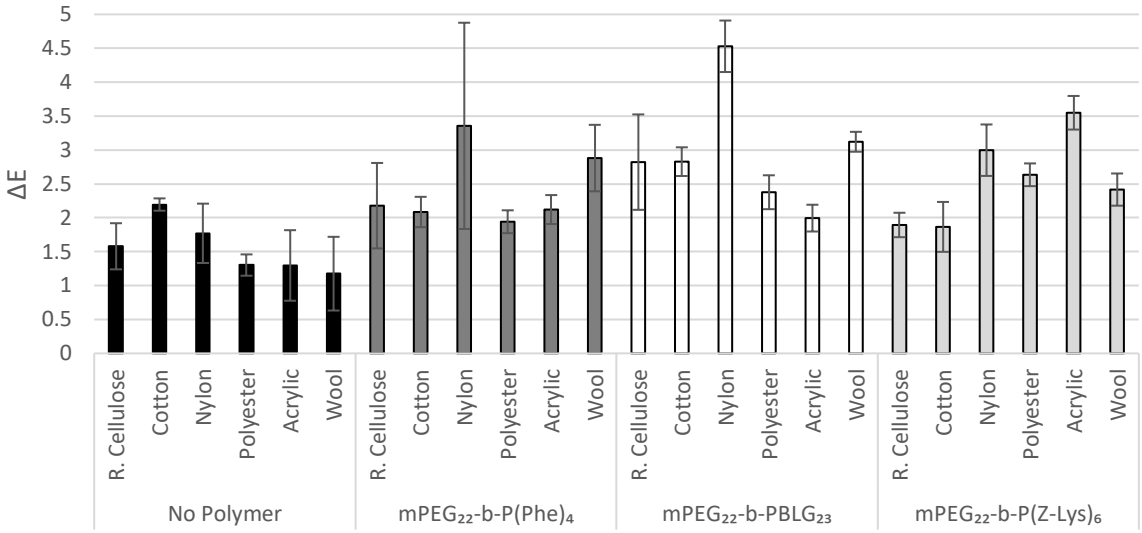

Figure 7-17 A comparison of the colour change caused by RR141 in the presence of $mPEG_{22}$-b-poly(Phe)$_4$, $mPEG_{22}$-b-$PBLG_{23}$ and $mPEG_{22}$-b-poly(Z-Lys)$_6$ polymers.

From Figure 7-17 it can be observed that the presence of all three of the polymers has an overall worsening effect on the discolouration caused by RR141. This is particularly evident on nylon fibres, for example $mPEG_{22}$-*b*-$PBLG_{23}$ shows a 60.9% increase in colour change. The polymers may facilitate the deposition of the highly anionic, water-soluble dye by reducing the charge barrier between the anionic fabric and the dye.

However, RR141 does not show the same degree of discolouration as the previously mentioned dyes, and therefore the discolouration caused in the presence of the polymer is only a marginally significant colour change to the naked eye, with a 'just noticeable difference' being a ΔE of 1.

7.4 Conclusion

A variety of block copolymers were synthesised successfully *via* NCA ROP of three amino acids: L-phenylalanine, γ-benzyl-L-glutamate and *N*-ε-carboxybenzyl-L-lysine. Firstly, the $mPEG_{22}$-*b*-poly(Phe) polymers were investigated for their ability to prevent dye transfer of indigo dye. They were found to be moderately effective, particularly for nylon and polyester fabric types, with a

reduction in a colour change of 40% and 31% respectively, in the presence of $mPEG_{22}$-*b*-poly(Phe)$_4$.

Secondly, $mPEG_{22}$-*b*-$PBLG_n$ polymers were tested for their DTI efficacy against indigo. Overall, the PBLG polymers were more effective DTIs against indigo than the Phe polymers, showing a 60% reduction in colour change for nylon, and 54% reduction for polyester. $mPEG_{22}$-*b*-poly(γ-benzyl-L-glutamate)$_{43}$ was synthesised, however it was not found to improve on the efficacy of the shorter PBLG polymers, this shows that increased molecular weight, and hydrophobicity, does not encumber efficacy. A further two polymers were synthesised, from $mPEG_{113}$-NH_2 and $mPEG_{295}$-NH_2 macroinitiators, in order to investigate the effects of the PEG to PBLG ratio. These polymers were not found to be overall more or less effective than the shorter mPEG chain polymers, and therefore shows that while the water-solubility of the polymer is important, the molecular weight of the polymer does not have a large impact on the efficacy. $mPEG_{22}$-*b*-poly(Glu)$_{23}$ gave similar results to tests performed without polymer, revealing that the deprotected polymer lacked efficacy. This may be due to the free acid groups of the glutamic acid preferring to interact with the aqueous phase of the wash liquor, and therefore meaning it does not interact with the fabric to prevent deposition of the dye. This therefore shows that the amphiphilic nature of the protected polymer is important. This is also beneficial for the final product as a reduced number of synthetic steps, by negating the need for the deprotection step, is more cost-effective.

Three $mPEG_{22}$-*b*-poly(Z-Lys) polymers were synthesised and tested against indigo. These were found to be more effective than the Phe based polymers, but less effective than the BLG based polymers. The most effective Z-Lys polymer ($mPEG_{22}$-*b*-poly(Z-Lys)$_2$) showed a reduction in colour change onto nylon of 51% and a reduction onto polyester of 39%. This suggests that the increased steric bulk and molecular weight of the Z-Lys monomer in comparison to the γ-benzyl-L-glutamate monomer may cause a moderate hindrance to the DTI efficacy.

Finally, one polymer from each class was tested against SB1, DO39 and RR141. For SB1 and DO39, the Phe based polymer was found to be most effective, bringing about a reduction in colour change onto nylon of 15% and 11% respectively. However, no polymer was found to be effective against RR141. This serves to highlight the complexity of the nature of the polymer-fibre-dye interaction and how best to combat it.

7.5 References

[1] Deng C., Wu J., Cheng R., Meng F., Klok H.-A. and Zhong Z. Functional polypeptide and hybrid materials: Precision synthesis via α-amino acid N-carboxyanhydride polymerization and emerging biomedical applications. *Progress in Polymer Science*. 2014 **39** (2) 330–64

[2] Rodriguez-Galan A., Pelfort M., Aceituno J.E. and Puiggali J. Comparative studies on the degradability of poly(ester amide)s derived fromL- andL,D-alanine. *Journal of Applied Polymer Science*. 1999 **74** (9) 2312–20

[3] Wibowo S.H., Sulistio A., Wong E.H.H., Blencowe A. and Qiao G.G. Polypeptide films via N-carboxyanhydride ring-opening polymerization (NCA-ROP): past, present and future. *Chemical Communications*. 2014 **50** (39) 4971

[4] Khuphe M., Mahon C.S. and Thornton P.D. Glucose-bearing biodegradable poly(amino acid) and poly(amino acid)-poly(ester) conjugates for controlled payload release. *Biomaterials Science*. 2016 **4** (12) 1792–801

[5] Khuphe M., Kazlauciunas A., Huscroft M. and Thornton P.D. The formation of biodegradable micelles from a therapeutic initiator for enzyme-mediated drug delivery. *Chemical Communications*. 2015 **51** (8) 1520–3

[6] Mohamed H.A., Khuphe M., Boardman S.J., Shepherd S., Phillips R.M., Thornton P.D. and Willans C.E. Polymer encapsulation of anticancer silver-N-heterocyclic carbene complexes †. *RSC A*. 2018 **8** (19) 10474–7

[7] Fan J. and Wooley K.L. Stimuli-Triggered Sol-Gel Transitions of Polypeptides Derived from a-Amino Acid N-Carboxyanhydride (NCA) Polymerizations. *Chem. Asian J*. 2016 **11** 437–47

[8] Fan J., Li R., He X., Seetho K., Zhang F., Zou J. and Wooley K.L. Construction of a versatile and functional nanoparticle platform derived from a helical diblock copolypeptide-based biomimetic polymer. *Polym. Chem.* 2014 **5** (13) 3977–81

[9] Huang J. and Heise A. Stimuli responsive synthetic polypeptides derived from N-carboxyanhydride (NCA) polymerisation. *Chemical Society Reviews*. 2013 **42** (17) 7373

[10] Lu H., Wang J., Song Z., Yin L., Zhang Y., Tang H., Tu C., Lin Y. and Cheng J. Recent advances in amino acid N-carboxyanhydrides and synthetic polypeptides: chemistry, self-assembly and biological applications. *Chem. Commun.* 2014 **50** (2) 139–55

[11] Dmitrovic V., Habraken G.J.M., Hendrix M.M.R.M., Habraken W.J.E.M., Heise A., de With G., Sommerdijk N.A.J.., Dmitrovic V., Habraken G.J.M., Hendrix M.M.R.M., Habraken

W.J.E.M., Heise A., De With G. and Sommerdijk N.A.J.. Random Poly(Amino Acid)s Synthesized by Ring Opening Polymerization as Additives in the Biomimetic Mineralization of CaCO3. *Polymers*. 2012 **4** (2) 1195–210

[12] Peggion E., Terbojevich M., Cosani A. and Colombini C. Mechanism of N-Carboxyanhydride (NCA) Polymerization in Dioxane. Initiation by Carbon-14-Labeled Amines [1]. *Journal of the American Chemical Society*. 1966 **88** (15) 3630–2

[13] Hadjichristidis N., Iatrou H., Pitsikalis M. and Mays J. Macromolecular architectures by living and controlled/living polymerizations. *Progress in Polymer Science*. 2006 **31** (12) 1068–132

[14] Lavilla C., Byrne M. and Heise A. Block-Sequence-Specific Polypeptides from α-Amino Acid N-Carboxyanhydrides: Synthesis and Influence on Polypeptide Properties. *Macromolecules*. 2016 **49** (8) 2942–7

[15] Yagci Y. and Atilla Tasdelen M. Mechanistic transformations involving living and controlled/living polymerization methods. *Progress in Polymer Science*. 2006 **31** (12) 1133–70

[16] Habraken G.J.M., Heise A. and Thornton P.D. Block Copolypeptides Prepared by N-Carboxyanhydride Ring-Opening Polymerization. *Macromolecular Rapid Communications*. 2012 **33** (4) 272–86

[17] Quadir M.A., Morton S.W., Deng Z.J., Shopsowitz K.E., Murphy R.P., Epps T.H. and Hammond P.T. PEG–Polypeptide Block Copolymers as pH-Responsive Endosome-Solubilizing Drug Nanocarriers. *Molecular Pharmaceutics*. 2014 **11** (7) 2420–30

[18] Deng C., Tian H., Zhang P., Sun J., Chen X. and Jing X. Synthesis and Characterization of RGD Peptide Grafted Poly(ethylene glycol)-b-Poly(L-lactide)-b-Poly(L-glutamic acid) Triblock Copolymer. 2006

[19] Kwon G., Naito M., Yokoyama § M, Okano T., Sakurai Y. and Kataoka^ K. *Micelles Based on AB Block Copolymers of Poly(ethylene oxide) and Poly(beta-benzyl L-aspartate)* vol 9

[20] Kramer J.R. and Deming T.J. Glycopolypeptides via Living Polymerization of Glycosylated-l -lysine *N* -Carboxyanhydrides. *Journal of the American Chemical Society*. 2010 **132** (42) 15068–71

[21] Peng H., Xiao Y., Mao X., Chen L., Crawford R. and Whittaker A.K. Amphiphilic Triblock Copolymers of Methoxy-poly(ethylene glycol)- *b* -poly(l -lactide)- *b* -poly(l -lysine) for Enhancement of Osteoblast Attachment and Growth. *Biomacromolecules*. 2009 **10** (1) 95–104

[22] Adams M.L., Lavasanifar A. and Kwon G.S. Amphiphilic block copolymers for drug delivery. *Journal of Pharmaceutical Sciences*. 2003 **92** (7) 1343–55

[23] Okada M. Chemical syntheses of biodegradable polymers. *Progress in Polymer Science*. 2002 **27** (1) 87–133

[24] Randall S.L., Panandiker R.K., Gosselink E.P., Mohr B. and Boeckh D. Laundry detergent compositions with amino acid based polymers to provide appearance and integrity benefits to fabrics laundered therewith. US6407053B1. 1998

[25] Smets J., Wevers J., Saini G. and Trujillo Rosaldo R. Laundry and cleaning and/or fabric care composition. US7601681B2. 1999

[26] Bettiol J.L., Busch A., Denutte H., Laudamiel C. and Smets J. Laundry and cleaning

compositions. US20040147426A1. 1998

[27] Thomaides J.S., Rodrigues K.A. and Petersen P.M. Amino acid copolymers having pendent polysaccharide moieties and uses thereof. US6160110A. 1999

[28] Price K.N., Gosselink E.P. and Deinhammer R.S. Laundry detergent compositions comprising polyamines and mid-chain branched surfactants. US6677289B1. 2000

[29] Price K., Gosselink E. and Deinhammer R. Laundry detergent compositions comprising polyamines and mid-chain branched surfactants. US20040077514A1. 2003

[30] Su X., Zhou X., Tan Z. and Zhou C. Highly efficient antibacterial diblock copolypeptides based on lysine and phenylalanine. *Biopolymers*. 2017 **107** (11) e23041

[31] Bettiol J.L.P., Smets J. and Lane Boyer S. Laundry detergent and/or fabric care composition comprising a modified antimicrobial protein. US645410B1. 1999

[32] Bhakoo M. Antibacterial compositions. US5629282A. 1994

[33] Ding X., Yang C., Lim T.P., Hsu L.Y., Engler A.C., Hedrick J.L. and Yang Y.-Y. Antibacterial and antifouling catheter coatings using surface grafted PEG-b-cationic polycarbonate diblock copolymers. *Biomaterials*. 2012 **33** (28) 6593–603

[34] Chang Y., Ko C.-Y., Shih Y.-J., Quémener D., Deratani A., Wei T.-C., Wang D.-M. and Lai J.-Y. Surface grafting control of PEGylated poly(vinylidene fluoride) antifouling membrane via surface-initiated radical graft copolymerization. *Journal of Membrane Science*. 2009 **345** (1–2) 160–9

Conclusion

A variety of mechanisms to prevent dye transfer in laundry washes have been explored in this thesis. This was in order to produce a polymeric additive which may be included in a detergent formulation or otherwise incorporated into a laundry wash load.

Initially, research focused on adsorbants for dye sequestration in order to remove the dye from the laundry liquor. Hydrogels formed from the biopolymers chitosan, cellulose and alginate were formed and examined for their ability to adsorb dyes, as determined by UV-Visible spectroscopy. Biopolymers were selected for their natural abundance, low cost and renewable origins. Chitosan was found to adsorb anionic dye C.I. Reactive Black 5 rapidly, as well as FITC-albumin, indicating the wide-ranging applications that the hydrogels may be applied to. The hydrogel was able to release the FITC-albumin, but not the dye. Alginate hydrogels were able to adsorb and release the cationic dyes methylene blue and crystal violet, two dyes that chitosan hydrogels demonstrated little affinity towards. This showed the scope of biopolymers to sequester dyes, and so biopolymeric particles were explored for their ability to be added to detergent formulations, for ease of use. Biopolymeric particles formed of chitosan and alginate were found to worsen indigo dye deposition where the charge of the particles formed was net positive, but reduced dye deposition when net negative. Therefore, this result indicated that the particles were not sequestering the dye and maintaining it in solution, but rather were depositing onto the fabric surface and attracting or repelling the dye.

Therefore, polymers that were designed to interact with the fabric and block dye deposition were investigated. A series of methoxy-poly(ethylene glycol)-*co*-polyesters were synthesised and varying functional groups incorporated into the polymer backbone, in order to tune the interaction between the fabric and the polymer. It was found that the inclusion of amine and hydroxy groups that are

capable of potentially hydrogen bonding with the fabric effectively, prevented the dye transfer of indigo in particular. Following this work, methoxy-poly(ethylene glycol)-*b*-poly(amino acid)s were synthesised *via* *N*-carboxyanhydride ring-opening polymerisation of the amino acids L-phenylalanine, γ-benzyl-L-glutamate and *N*-ε-carboxybenzyl-L-lysine. The polymers that contained γ-benzyl-L-glutamate blocks were found to be most effective at preventing the dye transfer of indigo, but those with phenylalanine chains were found to be the most effective against a range of dyes tested.

This research therefore shows the wide scope of polymeric additives to prevent dye transfer in the laundry. Future work may focus further on developing neutrally charged polymers that may interact with fabrics but have no net charge and thus prevent interaction with the dyes by either electrostatic repulsion or attraction. This is because dyes have a variety of charges and therefore the most effective method to reduce colour change across the dye classes may be to prevent interaction between the dye and DTI polymer. Such a system may be at the expense of the most effective polymer against indigo, the dye which causes the highest level of discolouration, however, to obtain a broad span of efficacy, a compromise may be necessary. Many of the polymers developed may be included in a specific 'denim care' detergent formulation. Alternatively, a detergent may be developed which contains two classes of dye transfer inhibitor which act by different mechanism of action. This may allow the two to act synergistically to prevent dye deposition by blocking dye deposition and by complexation or encapsulation.

List of Publications

Boardman S. J., Lad R., Green D. C. and Thornton P. D. Chitosan hydrogels for targeted dye and protein adsorption. *Journal of Applied Polymer Science*. 2017 **134** (21)

Mohamed H. A., Khuphe M., Boardman S. J., Shepherd S., Phillips R. M., Thornton P. D. and Willans C. E., Polymer encapsulation of anticancer silver-*N*-heterocyclic carbene complexes, *RSC Advances*, 2018, **8**, 10474 – 10477

WO patent application *Cleaning Compositions*, submitted June 2019

Appendices

Appendix 1 Table of DTI polymers and their constituent monomers

	DTI**1**	DTI**2**	DTI**3**	DTI**4**	DTI**5**	DTI**6**	DTI**7**	DTI**8**	DTI**9**	DTI**10**	DTI**11**	DTI**12**	DTI**13**	DTI**14**	DTI**15**
Ethylene Glycol	✓	✓							✓	✓	✓				✓
1,2-Propanediol	✓														
2,2'-Dimethyl-1,3-propanediol			✓	✓	✓	✓	✓	✓						✓	
Glycerol		✓	✓	✓	✓	✓						✓	✓		
Pentaerythritol							✓	✓							
2-Amino-2-methyl-1,3-propanediol									✓			✓			
Diethanolamine										✓			✓		
Pentanediol											✓				
Tris(hydroxymethyl) aminomethane														✓	✓

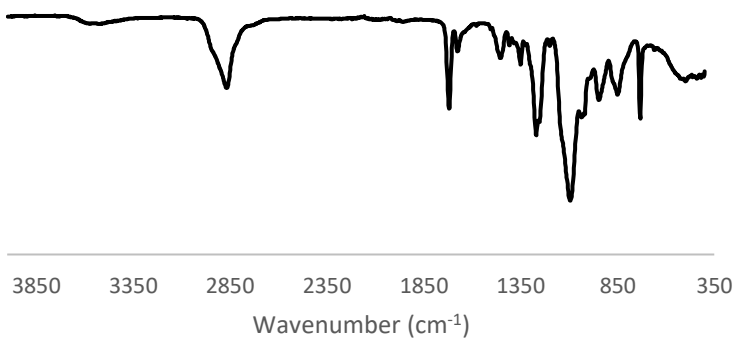

*Appendix 2. FTIR spectrum of DTI**1**.*

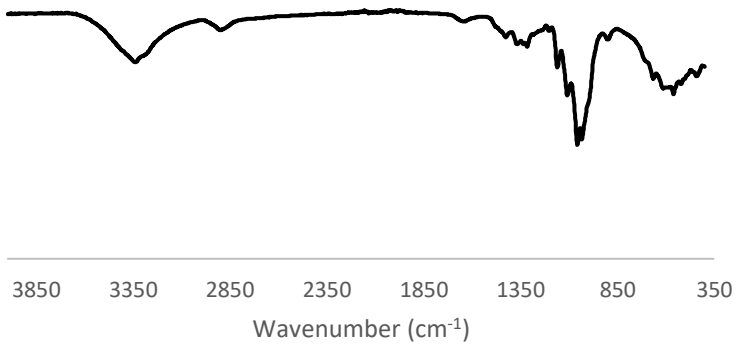

*Appendix 3. FTIR spectrum of DTI**2**.*

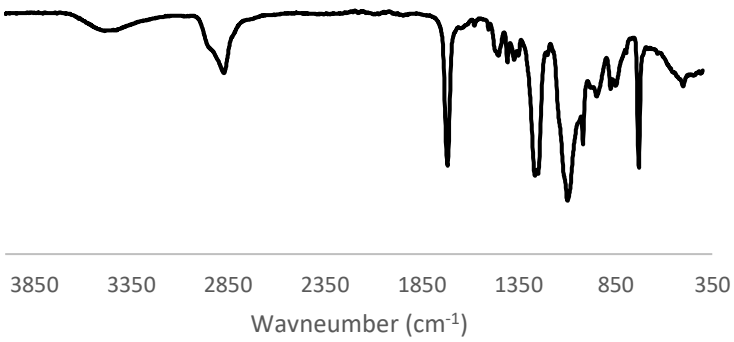

*Appendix 4. FTIR spectrum of DTI**3**.*

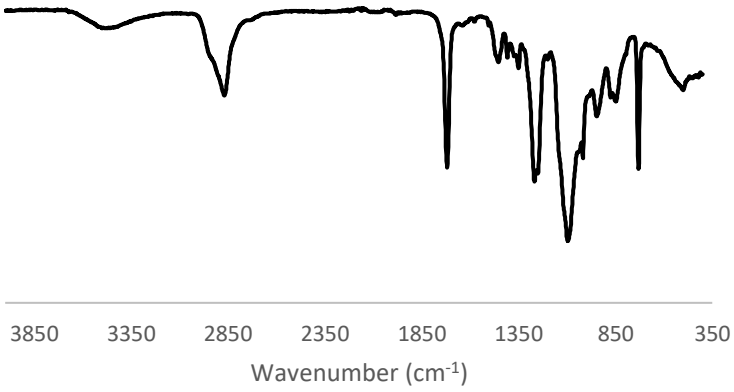

*Appendix 5. FTIR spectrum of DTI**4**.*

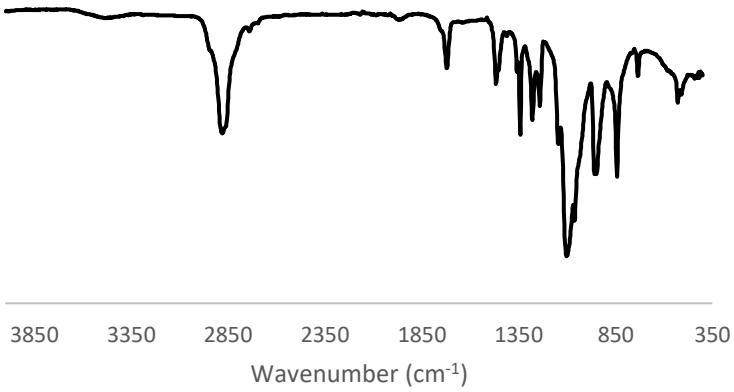

*Appendix 6. FTIR spectrum of DTI**5**.*

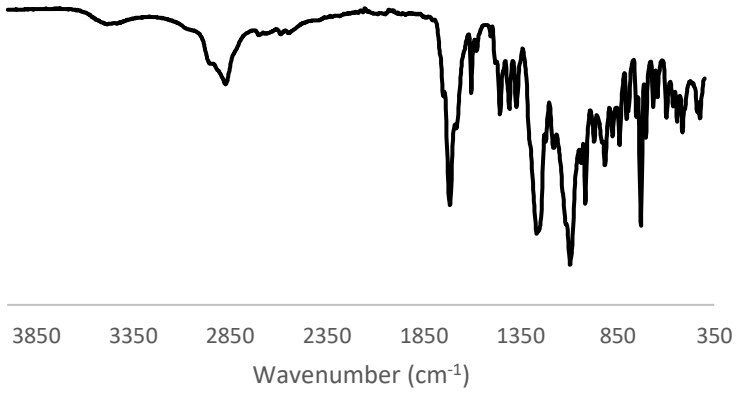

*Appendix 7. FTIR spectrum of DTI**6**.*

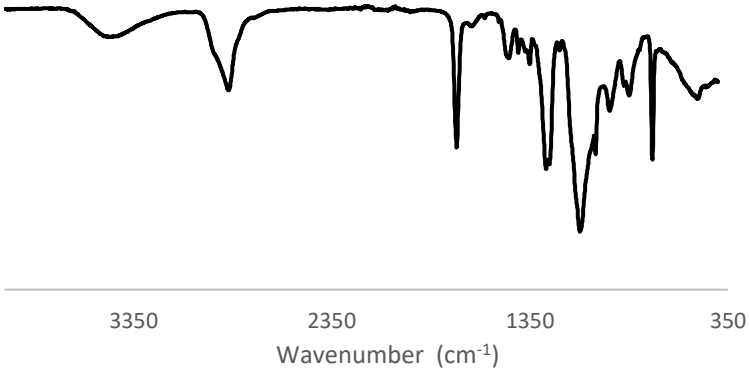

*Appendix 8. FTIR spectrum of DTI**7**.*

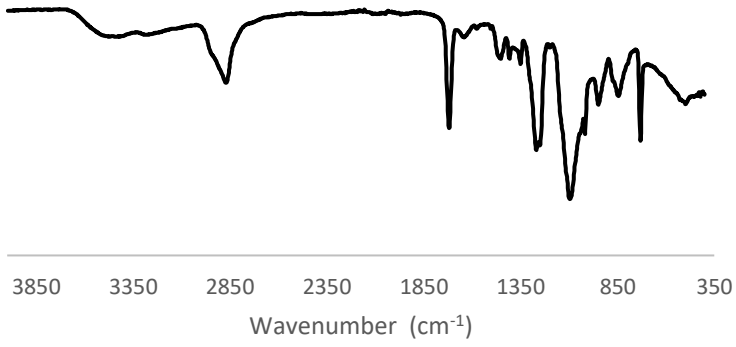

*Appendix 9. FTIR spectrum of DTI**8**.*

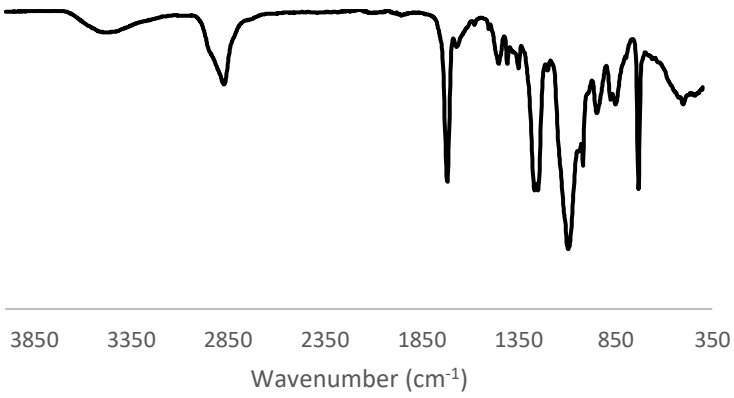

*Appendix 10. FTIR spectrum of DTI**9**.*

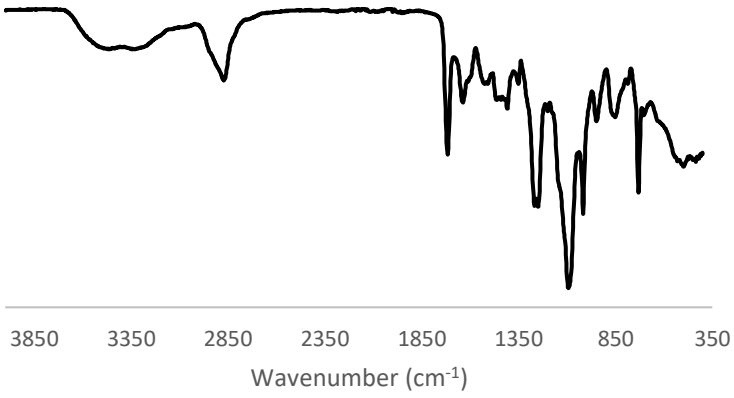

*Appendix 11. FTIR spectrum of DTI**10**.*

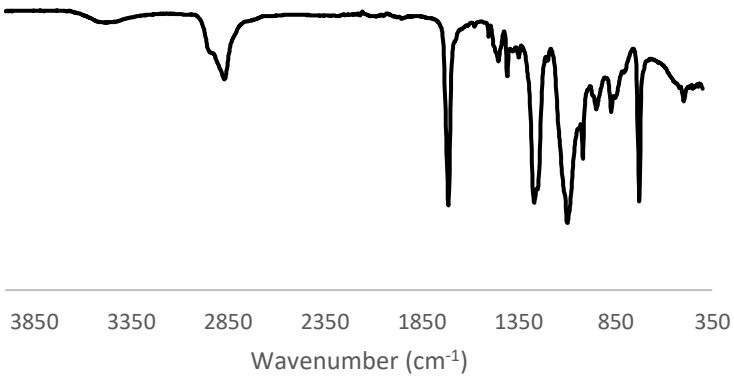

*Appendix 12. FTIR spectrum of DTI**11**.*

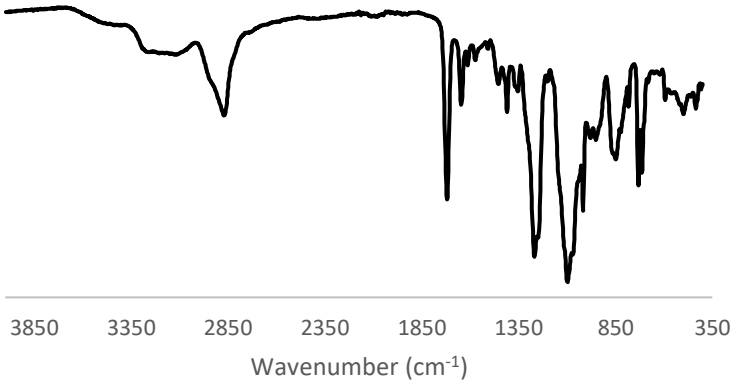

*Appendix 13. FTIR spectrum of DTI**12**.*

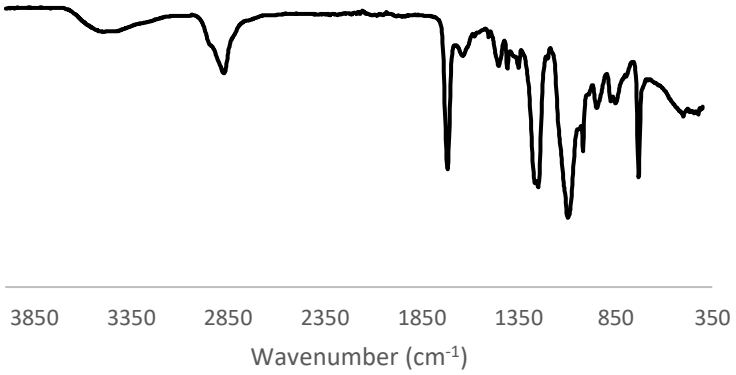

*Appendix 14. FTIR spectrum of DTI**13**.*

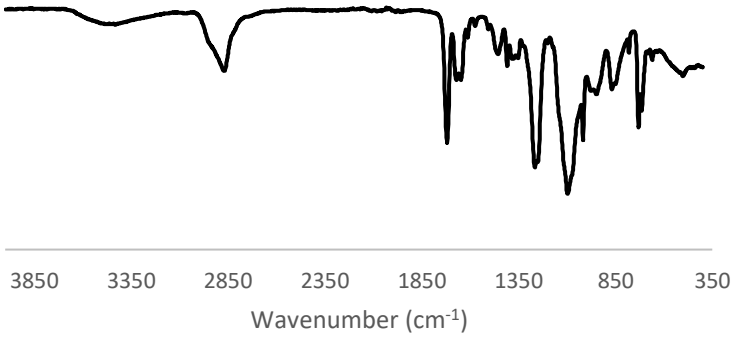

*Appendix 15. FTIR spectrum of DTI**14**.*

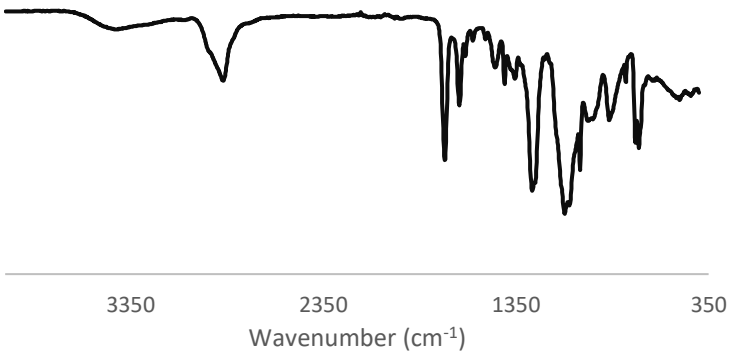

*Appendix 16. FTIR spectrum of DTI**15**.*

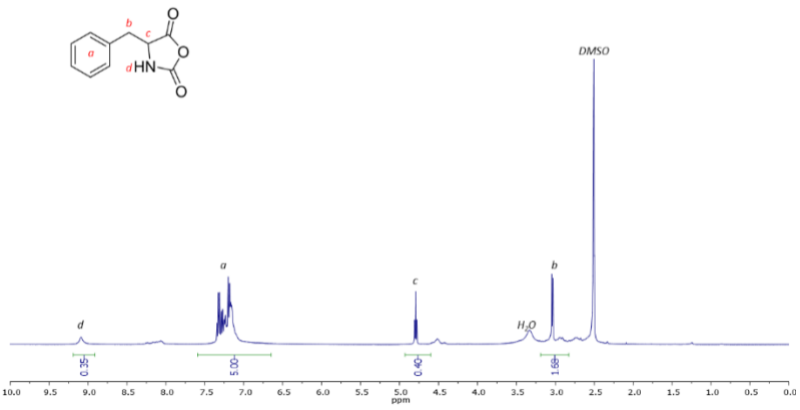

Appendix 17. ^{1}H NMR L-Phenylalanine NCA in DMSO-d_6.

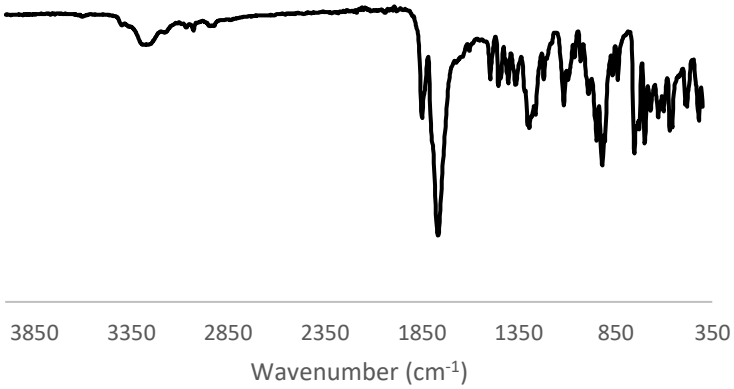

Appendix 18. FTIR spectrum of L-Phenylalanine NCA.

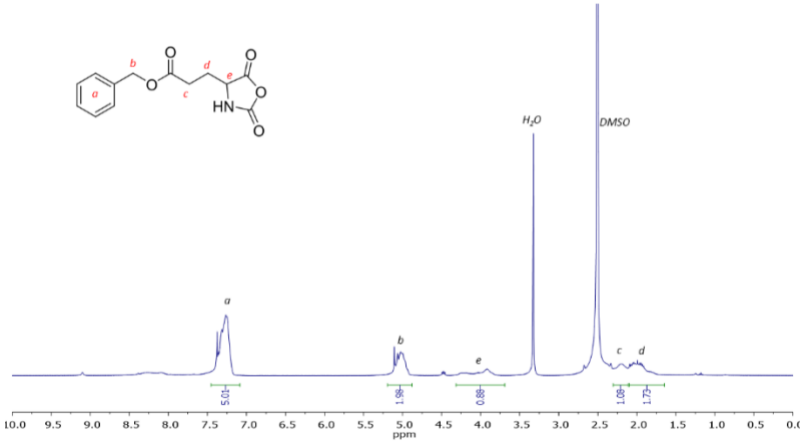

Appendix 19. ^{1}H NMR γ-Benzyl-L-Glutamic Acid NCA in DMSO-d_6.

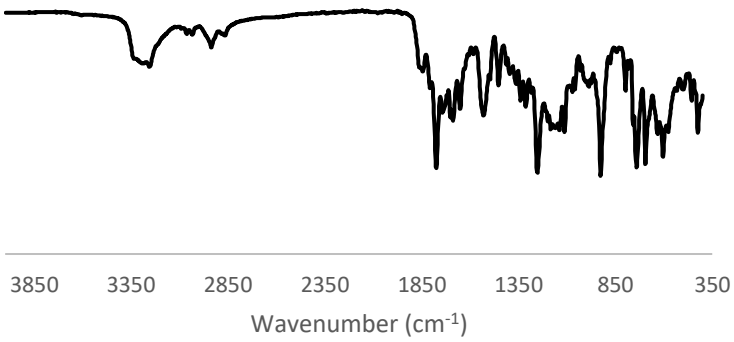

Appendix 20. FTIR spectrum of γ-Benzyl-L-Glutamic Acid NCA.

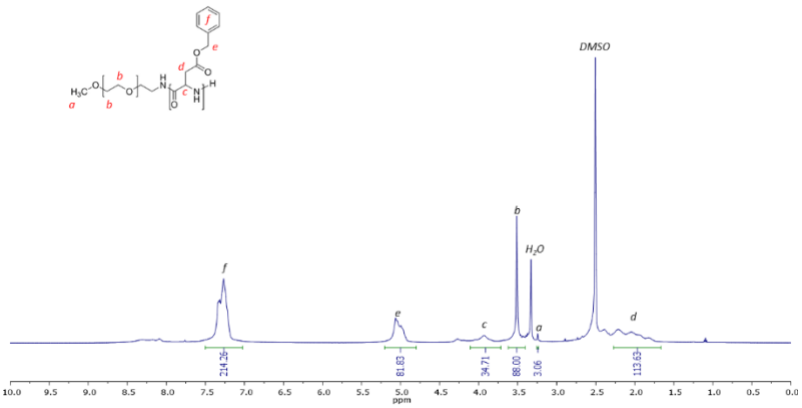

Appendix 21. ^{1}H NMR $mPEG_{22}$-NH-poly(BLGA)$_{43}$ in DMSO-d_6.

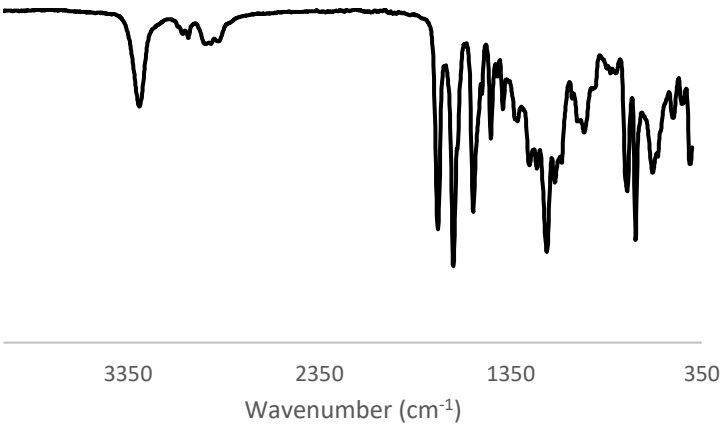

Appendix 22. FTIR $mPEG_{22}$-NH-poly(BLGA)$_{43}$.

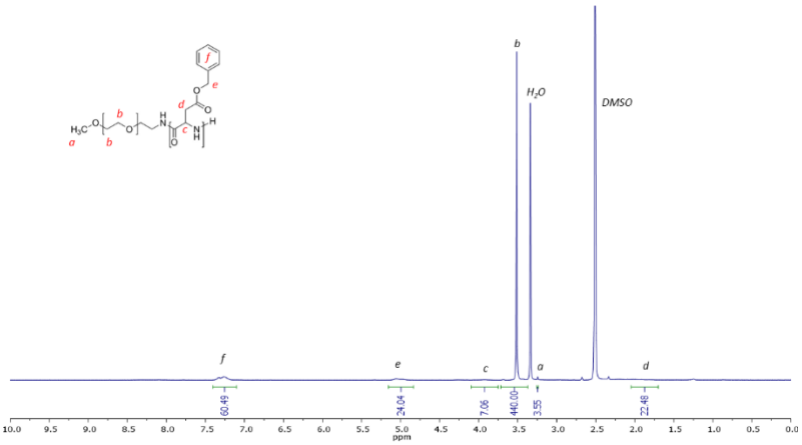

Appendix 23. ^{1}H NMR $mPEG_{113}$-NH-poly(BLGA)$_{12}$ in DMSO-d_6.

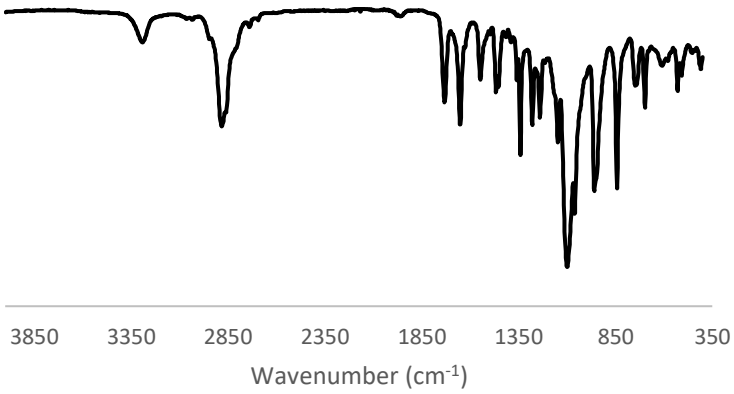

Appendix 24. FTIR $mPEG_{113}$-NH-poly(BLGA)$_{12}$.

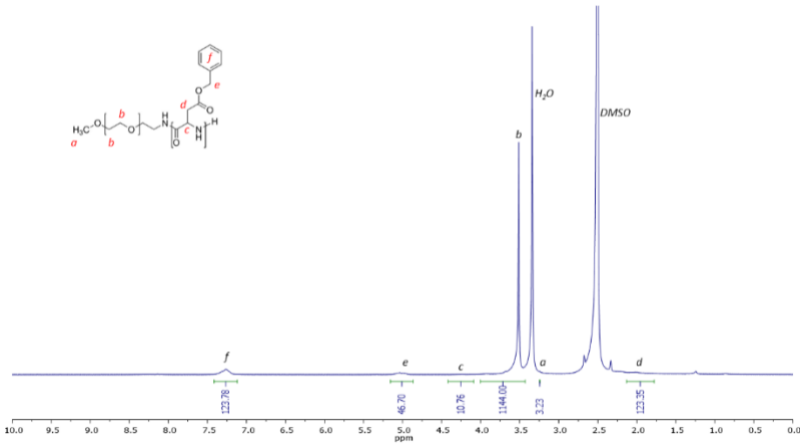

Appendix 25. ^{1}H NMR $mPEG_{295}$-NH-poly(BLGA)$_{25}$ in DMSO-d_6.

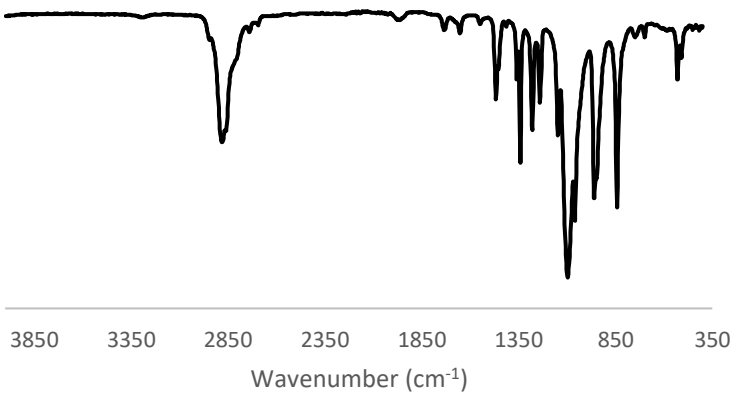

Appendix 26. FTIR $mPEG_{295}$-NH-poly(BLGA)$_{25}$.

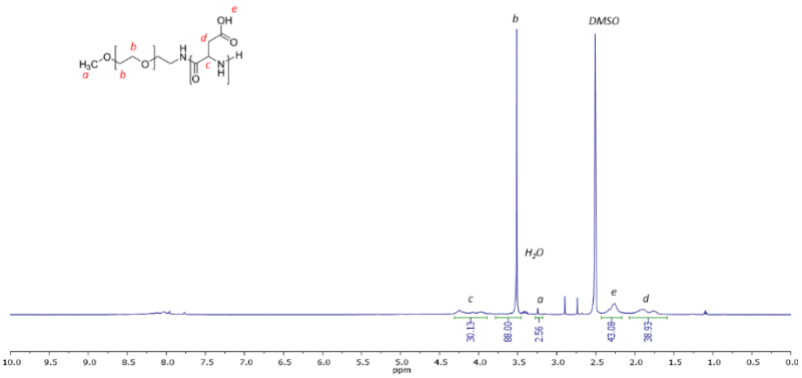

Appendix 27. ^{1}H NMR mPEG$_{22}$-NH-poly(Glu)$_{23}$ in DMSO-d$_6$.

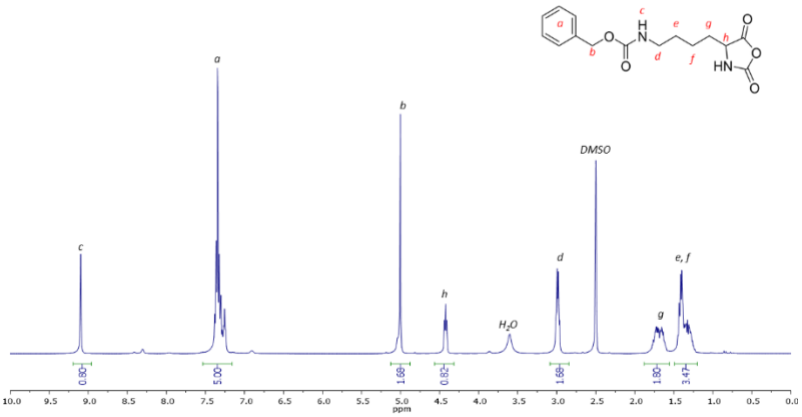

Appendix 28. ^{1}H NMR N-ε-carboxybenzyl-L-Lysine NCA in DMSO-d$_6$.

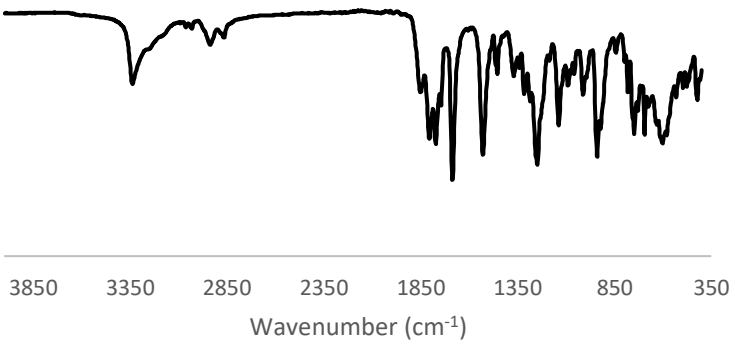

Appendix 29. FTIR spectrum of N-ε-carboxybenzyl-L-Lysine NCA.